CRANFIELD UNIVERSITY

Dimitrios Georgios Varsamis

Development of a fluidic sensor for the detection of herbicides using thylakoid preparations immobilised on magnetic beads to aid regenerability

Cranfield Health

PhD Thesis

CRANFIELD UNIVERSITY

Cranfield Health

PhD Thesis

Academic Year 2008 - 2009

Dimitrios G. Varsamis

Development of a fluidic sensor for the detection of herbicides using thylakoid preparations immobilised on magnetic beads to aid regenerability

Supervisor
Prof. David C. Cullen

Submitted December 2008

This thesis is submitted in partial fulfilment of the requirements for the Degree of Doctor of Philosophy

Abstract

Following the industrial revolution and advances in chemical science, the pollution of the environment with trace organic pollutants has been steadily increasing, which is of concern, due to their effect on the environmental and human health. Tighter legislation that has been introduced in order to minimise the release of harmful pollutants has led to the initiation of monitoring programmes. For example, drinking water suppliers are obliged to systematically monitor drinking water supplied for human consumption for a large range of pollutants. The same applies for waste water treatment facilities. The well-established standard methods of environmental waters analysis require sampling and transportation of samples to the laboratory for detailed measurements. Therefore, the timescale from sampling to reporting is not ideal, as a considerable lag occurs.

There is therefore the potential for the use of *in situ* methods that overcome this issue. As these do not currently exist, a need to address this is identified.

Biosensors are sensing devices that rely on a biologically-derived component as an integral part of their detection mechanism. Biosensors that respond to pollutants could be used for rapid, low cost, field-based pre-screening of water samples.

Herbicides are considered to be the most important class of pesticides used in the E.U. Herbicides can be highly toxic for human and animal health, and increase in the application of herbicides in agriculture during recent decades has resulted in immense pollution of both soil and water. About half of the herbicides used at present in agriculture inhibit the light reactions in photosynthesis, mostly by targeting the Photosystem II (PSII) complex.

A method of detecting certain classes of herbicides is therefore proposed; the photosynthesis-inhibiting herbicides act by binding to PS II, a chlorophyll–protein complex which plays a vital role in photosynthesis, located in the thylakoid membrane of algae, cyanobacteria and higher plants. The inhibition of PS II causes a reduced photoinduced production of hydrogen peroxide, which can be measured by the HRP-mediated luminol chemiluminescence reaction. The design and development of a fluidic sensor unit for the detection of such herbicides, based upon their inhibition of the hydrogen peroxide production, will employ the use of superparamagnetic beads in order to address issues of reuse and regenerability.

The illumination-dependent production of hydrogen peroxide by isolated thylakoids, and its inhibition by herbicides in a concentration-dependent manner, were achieved and measured with the HRP-mediated chemiluminescence reaction with luminol in a cuvette, batch format, allowing for the detection of herbicides down to 6.0×10^{-09}.

The integration of the above reactions has been achieved by designing and constructing a fluidic unit that combines the herbicide-dependent production and the detection of hydrogen peroxide in a single fluidic assay by combining all the individual steps in a compact, portable format, with both HRP and thylakoids covalently coupled on superparamagnetic beads. This addresses issues of regenerability, as the beads are introduced, used and discarded following a measurement, controlled only by magnetic and flow forces. Herbicide detection was achieved to a lower LOD of 5.5×10^{-10} M. The concept development, design and construction of the fluidic unit, as well as results of the detection of herbicides with the batch assay method has been published, in a paper by the author (*Talanta*, 2008, vol. 77, no. 1, pp. 42-47),

Considerable progress has therefore been made towards developing a system that would be suitable for automated, field deployment applications for the detection of the most frequently used classes of herbicides; the lower LOD however is not within the stringent legislated maximum permissible limits set for herbicides measured in water, in European waters.

An immediate step forward would be to achieve the required lower LOD, with the unit's development into a prototype instrument that can be field deployed being the further goal.

Dedicated to my μαμά και μπαμπά

" …when she was a little startled by seeing the Cheshire Cat sitting on a bough of a tree a few yards off.

The Cat only grinned when it saw Alice. It looked good-natured, she thought: still it had *very* long claws and a great many teeth, so she felt that it ought to be treated with respect.

'Cheshire Puss,' she began, rather timidly, as she did not at all know whether it would like the name: however, it only grinned a little wider. 'Come, it's pleased so far,' thought Alice, and she went on.

'Would you tell me, please, which way I ought to go from here?'

'That depends a good deal on where you want to get to,' said the Cat.

'I don't much care where--' said Alice.

'Then it doesn't matter which way you go,' said the Cat.

'--so long as I get *somewhere*,' Alice added as an explanation.

'Oh, you're sure to do that,' said the Cat, 'if you only walk long enough.'

Alice felt that this could not be denied. "

Alice's Adventures in Wonderland (Lewis Carroll, 1865, www.gutenberg.org)

Acknowledgements

Firstly, I would like to express my special thanks to my supervisor Professor Dave Cullen for his support and advice throughout the years.

I also wish to thank all the students and academic and research staff of the former Institute of BioScience and Technology at the former Cranfield University at Silsoe, with whom I shared labs and offices and formed great friendships; far too many people to name, if you are reading this then you ought to know who you are! Special thanks must go to Dr. Louisa Giannoudi, the kindest friend I could have asked for as a fellow student working on the same project.

I also strongly thank the 'support' staff at Cranfield University at Silsoe; the Reception, Security, Canteen, Careers office, Registry, Accommodation office, Library, I.T. Helpdesk and lab technicians and cleaners. The nicest people to be surrounded and helped by.

I thank my work line manager Ms Lucy McCulloch and the team leader Ms Amanda Hutchinson, for offering much in return for so little for so long, by allowing me to take time off to write the thesis when I have been needed so much.

I thank my friend and housemate Ms Karla Berron for putting up with the behavioural changes and the takeover of the study room; my best friend and colleague Mr Yeh Yeau Kuan for the inputting of some references into Refworks, but most importantly for inspiring me to kick-start the writing; and my friend and co-student Mr Derek Annan for the long hours on the phone discussing all thesis and viva related generalities.

I also thank all the medical staff, occupational therapists, massage therapists, physiotherapists and other therapists, for having a go at fixing me in the past 2 years, especially Mr Neville Perrett. Thanks also go to all the fellow RSI sufferers who have brought their stories out in the open online for others to know that no one is alone. Without any of these I would not be writing this sentence.

The recording artists that I have sung along to, thank you for the music. Same goes to the internet radio station "the interweb is trying to kill me" (formerly "culture failure") for providing the soundtrack to my life in front of the laptop.

I also acknowledge the European Union for funding the first two years of the project and Cranfield University for funding the third year.

Finally, to my family, I am eternally grateful for the opportunities given and support in so many ways.

Table of contents

List of figures

List of tables

Abbreviations

ABTS	2,2’-Azino-bis(3-ethylbenzthiazoline-6-sulfonic acid)
Atrazine	2-chloro-4-ethylamino-6-isopropylamino-s-triazine
BSA	Bovine serum albumin
COOH	Carboxyl group
CV	Coefficient of variation
Diuron	3-(3,4-dichlorophenyl)-1,1-dimethylurea
EDC	Ethyl-dimethyl carbodiimide
EDTA	Ethylenediaminetetraacedic acid
ELISA	Enzyme-linked immunosorbent assay
GC-MS	Gas chromatography–mass spectrometry
HCl	Hydrochloric acid
HEPES	N-2-hydroxyethyl piperazine-N'-2-ethane sulfonic acid
HPLC	High-performance liquid chromatography
HRP	Horseradish peroxidase
IR	Infra red
LED	Light Emitting Diode
Lower LOD	Lower limit of detection
Luminol	5-amino-2,3-dihydrophthalazine-1,4-dione
MES	2-Morpholinoethanesulfonic acid
MOPS	4-morpholinepropanesulfonic acid
OD	Optical Density
PBS	Phosphate buffered saline
ppb	Parts per billion
ppm	Parts per million
PSII	Photosystem II
RO	Reverse-osmosis
RSD	Relative standard deviation
SOD	Superoxide dismutase
TRIS	Tris-(hydroxymethyl)aminomethane
UV	Ultraviolet

Chapter 1: Introduction

1.1 Expanded background of the purpose of the work

1.1.1 Environmental pollution by herbicides

The increasing pollution of the natural and built environment with pesticides, endocrine disrupting chemicals and other organic pollutants, and accumulation thereof, is of concern, due to their effect on the environmental and human health.

Langford [1] defines biological impacts of synthetic substances as:

- lethal effects (direct mortalities);
- controlling effects (on growth, reproduction etc);
- directive effects (behavioural responses);
- indirect effects (through effects on other biota or chemistry).

The effects of synthetic substances on organisms are generally toxic in that they interfere with one or more essential processes, resulting in effects ranging from death of the organism (lethal) to changes in sub-cellular structures (sub-lethal). Non-synthetic (naturally occurring) substances can also be present at concentrations that are toxic to organisms (e.g. heavy metals) [2].

The concepts of hazard and risk are widely used in the identification of substances of concern. The hazard associated with a substance is its potential to cause harm and is assessed by collecting data on its properties, such as physico-chemical characteristics, mobility and persistence in environmental media, bioaccumulation and acute and chronic toxicity. Risk is the probability that harm will be caused and requires information on likely environmental concentrations of the substance, derived from known rates of release and dilution factors in the environment. Reliable information on known release rates of many substances is extremely difficult to find and consequently risk

assessments for chemicals already in the environment are not commonly done. Substances on priority lists have been identified primarily in terms of characteristics associated with hazard (persistence, bioaccumulation and toxicity) [2].

Many thousands of chemicals are released into the environment as a result of human activities. For example, the European Inventory of Existing Commercial Chemical Substances (EINECS) [3] contains more than 100,000 chemicals and many of these are likely to be released into the environment to some extent. However, only 61 synthetic substances, or groups of substances, have been identified on priority lists for control [2].

Pesticides introduced in practice since 1945, have spread worldwide as the most significant form of pest control. Their availability on the commercial market reaches a point of thousands of different compounds. Pesticides are chemicals specifically developed and produced for use in the control of agricultural and public health pests, to increase production of food and other products, and to facilitate modern agricultural methods. Antibiotics to control microorganisms are not included. They are usually classified according to the type of pest (fungicides, algicides, herbicides, insecticides, nematicides, and molluscicides) they are used to control. When the word pesticide is used without modification, it implies a material synthesised by humans [4].

Agriculture is the largest user of freshwater resources, using a global average of 70% of all the surface water supplies. Except for the water lost through evaporation and transpiration, the water used in agricultural practices is recycled back to the surface water or groundwater. Agriculture is therefore the main cause of water pollution [5].

Herbicides are considered to be one of the most important classes of pesticides used in the European Union [5]. The application of herbicides in agriculture has increased appreciably during the past few decades, resulting in the massive

pollution of water and soil. About one half of the herbicides used at present in agriculture work by inhibiting the light reactions in photosynthesis, mostly by targeting the Photosystem II (PSII) complex [6]. Worldwide, thousands of tons of photosynthesis-inhibiting herbicides are applied annually. As early as the 1950s, selection for the most effective herbicides took advantage of the fact that some herbicides can inhibit the Hill reaction in isolated chloroplasts [7]. The D1 protein of the PSII reaction centre is the main target of herbicides that inhibit photosynthesis. Photosynthesis-inhibiting herbicides fall into three main groups: phenylureas, triazines and phenols, depending on their chemical structure and binding properties [8]. These compounds are usually absorbed through the roots and then transferred via the xylem to the leaves, although some are directly absorbed by the leaves. These chemicals are quite stable in the soil and are adsorbed by colloids and organic substances on the basis of their ability to exchange cations. Since these herbicides can be highly toxic to humans and animals, their indiscriminate use has serious environmental implications. Consequently, the use of dinoseb was prohibited in the US and in most other countries because of its high toxicity. Atrazine, a possible human carcinogen, has also been banned. The triazine herbicides are among the most commonly detected herbicides in water [9] and are the most persistent. They are transported through pore and ground waters to surface and coastal sea waters [10].

1.1.2 Environmental pollution monitoring: legal frameworks, standard methods, alternative routes

Key E.U. legislation on water quality includes:

- Water Framework Directive (1997),
- Directive on Integrated Pollution Prevention and Control (1996),
- Nitrates Directive (1991),
- Urban Waste Water Treatment Directive (1991),
- Shellfish Waters Directive (1979),
- Dangerous Substances Directive (1976),
- Bathing Waters Directive,
- Drinking Water Directive.

The European Drinking Water Act (1980) does not allow concentrations of herbicides in drinking water to exceed 0.1 μg/l (0.1 ppb) of any individual herbicide and 0.5 μg/l of total herbicides [6]. Thus, in order to meet drinking water standards, concentrations around 0.5 ppb must be readily detectable. Previously, poor evidence on pesticide contamination of waters was documented but with the adoption of the Drinking Water Directive, the drinking water suppliers were obliged to monitor systematically drinking water supplied for human consumption for a large range of pollutants [5].

Therefore, additional, tighter environmental legislation that was introduced in order to minimise the release of harmful pollutants either having immediate or long-term effects, led to the initiation of monitoring programmes.

During 1997 a total number of 1419 sites were monitored for pesticides by the Environment Agency in England and Wales. Considering the 163 individual pesticides analysed in surface water, 58% were detected above 0.1 μg/l on at least one occasion in 1997, while 22% were detected below the 0.1 μg/l level and 20% were never detected. Isoproturon, mecoprop, diuron, atrazine and MCPA exceeded the maximum permissible concentration level most frequently [5].

The standard methods of environmental waters analysis require sampling and transportation of samples to the laboratory for detailed measurements. In this case, skilled personnel are required to perform the sample pre treatment and the rest of the analysis using sophisticated and expensive equipment and consumables. The results from a laboratory analysis are very accurate and provide desirable lower detection limits, in accordance with the legislated limits.

One area where water is routinely monitored for pollutants is in wastewater plants, in order to monitor the effectiveness of the treatment processes. According to U.K. Water Act 2003, wastewater dischargers require permits and according to these permits the limits are set on the amounts of specific

pollutants which can be discharged, as well as a schedule for monitoring and reporting the results. Only standard analytical procedures are allowed to be used providing assurance to government agencies that the results from different laboratories are comparable and well reproduced. Generally, in order to collect the water samples it is necessary first to assess the site where collection is to be undertaken and set a limit of samples that would give sufficient results. Once representative samples are gathered, the next step is the extraction of the analyte from the bulk solution, since most of the analytical methods require the analyte to be in the liquid phase. Some measurements even require separating the analyte from the water entirely.

Although the traditional laboratory methods are both standard and reliable, permitting the determination of several kinds of herbicides simultaneously with high sensitivity, they are time consuming, require expensive equipment, large amounts of organic solvents and the purification of samples prior to assay, thus limiting the number of samples that can be analysed [8; 11]. Full chemical characterisation on all waters is not economically practical [12]. Very importantly, they are not mobile.

A solution would be to have analytical devices that are mobile, i.e. the instrumentation and reagents etc can be transferred easily to the sample, rather than the other way. This would allow for the near-real-time analysis of water samples that would otherwise take days to be analysed. This would be a very important advantage for the related water industries, allowing for appropriate measures to be put in place to rectify / reduce / stabilise the problem sooner. Should the specificity of such field-deployed methods not be as good as that of the standard methods, they could then be used as screening tools, allowing for the selection of water samples to be then further analysed and characterised to be more targeted. They could also be automated, to therefore allow for their 'permanent' (subject to other restriction) deployment in the environment, without the need for an individual to perform the analysis themselves.

The work presented here is therefore attempting to provide new scientific knowledge that will progress the research and development of such field-deployable analytical devices.

1.2 Aims and Objectives

1.2.1 Aims

- The development of a bioassay platform for the detection of trace organic pollutants in water samples, that can be deployed/used in the field, in order to also meet the commercial / regulatory requirements.
- This will be demonstrated by detecting photosynthesis-inhibiting herbicides by measuring their effect on photosynthetic material derived from plant cells.
- The bioassay will be field-deployable and will be addressing issues of reuse and regenerability in a remote working environment.

1.2.2 Objectives

- To demonstrate, given the uncertainty in the literature, the production and chemiluminescence detection of H_2O_2 from illuminated photosynthetic plant material.
- To demonstrate the concentration-dependent inhibition of production of H_2O_2 from illuminated photosynthetic plant material, by photosynthesis-inhibiting herbicides.
- To develop a fluidic unit that can be reused and regenerated by employing the use of magnetic beads to act as the immobilisation support for the bio-recognition elements of the bioassay, allowing for the repeated introduction, use and discardation of the bio-recognition elements.
- To specifically demonstrate a fluidic assay using the principle of the magnetic bead immobilisation, by immobilising HRP on beads that will be used for detection of H_2O_2 using the HRP-mediated luminol chemiluminescence reaction with H_2O_2.

- To transfer the herbicide detection batch assay into the demonstrated fluidic format in order to demonstrate a fluidic assay for the detection of herbicides that can be reused and regenerated, thus allowing for its subsequent development into a field-based system.

Finally,

- To perform the work within the objectives of the funding project, "Assembly and application of Photosystem II-based biosensors for large scale environmental screening of specific herbicides and heavy metals" [13].

1.2.3 Introductory summary on the European project 'Biosensors for Effective Environmental Protection'

The PhD project described in the thesis was part of a European project, titled 'Assembly and Application of Photosystem II-based Biosensors for Large Scale Environmental Screening of Specific Herbicides and Heavy Metals' (short name: 'Biosensors for Effective Environmental Protection', acronym: BEEP). This was part of the Fifth Framework Programme, Project Reference: QLK3-CT-2001-01629.

Objectives

The objective of BEEP was the development of biosensors using Photosystem II (PSII) isolated from photosynthetic organisms to monitor polluting chemicals. This should lead to the set-up of a low cost, easy-to-use apparatus, able to reveal specific herbicides and/or heavy metals, and eventually, a wide range of organic compounds present in industrial and urban effluents, sewage sludge, landfill leak-water, ground water, and irrigation water.

Within the framework of sustainable development, a number of European countries will have to make strong efforts during the coming years to meet the European directives and standards in the areas of environmental monitoring, pollution control, waste management, water and soil quality. This project will contribute to this objective by way of a versatile, low-cost technology with a

presumably lower environmental impact than many traditional techniques for herbicide and heavy metal detection.

A photosystem II based biosensor will avoid costly and often environmentally unsound analyses in two ways:

- biosensors that respond to a range of pollutants can be used for rapid, low cost pre-screening of large numbers of samples to determine samples that will then undergo more detailed analysis. This should avoid the use of large quantities of organic solvents and the need for expensive apparatus to extract herbicide compounds,
- the use of an array of PSII based biosensors that are each highly specific to a given class of pollutant in conjunction with sophisticated data elaboration will enable the user to generate an identikit of the pollutants present in samples.

The project's aims were:

1) The realisation of sensitive and stable biosensors based on isolated Photosystem II for the detection of herbicides and heavy metal.

2) By screening of a large number of photosynthetic organisms and genetic engineering, production of PSII biomediators able to distinguish the various subclasses of herbicides and heavy metals.

3) Realisation of new and sophisticated transduction systems based on printed electrodes, chemiluminescence and fluorescence systems that enhance the sensitivity and specificity of detected signals.

4) Development of miniaturised biosensor prototypes and special software to monitor the information deriving from the mutated PSII biomediators.

5) Practical, on-site application of the biosensors in a mobile unit for environmental screening under real operational conditions, i.e. leak-water from land fills and ground/river waters.

6) Contribution toward spin offs and commercialisation.

The PhD project was part of the Work Programme Three, 'Transduction Systems and Sensor Assembly'. This Work Programme encompassed the realisation of sophisticated and new transduction systems based on: fluorescence, chemiluminescence, amperometric-printed electrodes and alternative systems (optical absorbance of chromophore-quinone).

1.3 Structure of the thesis

Following the introductory chapter, where a review of environmental pollution by herbicides is already given, a review of other relevant literature is reported in Chapter 2, starting with a review of the knowledge and research on sensor technologies. Given the aims and objectives of the work presented, an overview of the photosynthetic process is also given, followed by a review of the prior research on the detection of photosynthesis-inhibiting herbicides as well as an account of the scientific opinion on the production of hydrogen peroxide by photosynthetic material. An introduction to chemiluminescence is presented next, focusing on the luminol chemiluminescence compound, its uses, the involvement of HRP in the catalysis of the reaction, and examples of its use for analytical purposes and specifically for the detection of hydrogen peroxide. A brief account of the use of superparamagnetic beads in fluidic assays with details of examples ends the literature review.

In Chapter 3, the first experimental chapter, the development of a bench-top, batch assay for the detection of H_2O_2 is reported. Given the work to follow in Chapter 4, the development of a standard method to detect H_2O_2, irrespective of its source, was an essential first step, as the HRP-mediated chemiluminescence reaction of luminol with H_2O_2 is the main method used to detect and quantify the results of the rest of the experiments in the thesis.

In Chapter 4, the unsuccessful attempt to effect the production of H_2O_2 by isolated chloroplasts is followed by a detailed account of the successful approach when using isolated thylakoids; this includes varying a number of

experimental parameters to optimise the production. This is followed by reporting on the work performed to cause a concentration-dependent change of the thylakoids' H_2O_2 production after incubation with herbicides.

In Chapter 5, the design and development of the fluidic unit is presented, followed by the development of a fluidic assay for the detection of H_2O_2 using HRP-coated superparamagnetic beads, effectively transferring the batch assay from Chapter 3, as the work performed later would be using the H_2O_2 fluidic assay as the detection method.

In Chapter 6, the transfer of the assay for the detection of photosynthesis-inhibiting herbicides by measuring their effect on the production of H_2O_2 by thylakoids, from batch to fluidic format is presented, using the HRP-coated superparamagnetic beads developed earlier as well as thylakoid-coated superparamagnetic beads. This is followed by the presentation of work on the reuse and stability of the immobilised materials, as well as a report on the matrix effect of real water samples.

A general discussion, conclusions and future work ends the main body of the thesis.

Chapter 2: Literature Review

2.1 Assays, sensors and biosensors for environmental analysis

2.1.1 Definition of sensor, biosensor and categories thereof

The term sensor has been defined as a device or system that responds to a physical or chemical quantity to produce an output that is a measure of that quantity [14]. Chemical sensors are devices that convert concentrations or activities of chemicals into electrical or optical signals related to these quantities [15]. Electrochemical sensors convert the chemical substance being measured into an electrical quantity, such as voltage, current, or charge.

Optical sensors have their optical properties changed by the chemical being measured or by light of a specific wavelength produced by the chemical [15]. Optical sensors detect changes in the properties of light in the ultraviolet, visible and infrared range, which are caused by an interaction between electromagnetic waves and matter. Photonic measurement techniques are being used for their superior sensitivity. A number of different measuring principles have already been applied. These techniques mainly make use of the following optical parameters: absorbance, fluorescence (intensity, decay, polarisation, and energy transfer), bio- and chemiluminescence, phosphorescence, thermoluminescence, light scattering, evanescence, surface plasmon resonance (SPR) [16], refractive index, total internal reflection (TIR), and interferometry [17]. There are also thermal methods for detecting concentrations of substances and major analytical techniques, such as spectroscopy and nuclear magnetic resonance that involve complex instrumentation systems.

Biosensors can be considered as a subgroup of chemical sensors in which a biologically-based mechanism is used for analyte detection [18]. Pietro [19] defines

biosensors as “any discrete sensing device that relies on a biologically derived component as an integral part of its detection mechanism,” although sensors that are used to monitor biological conditions are usually also included. According to the literature [14], a biosensor comprises of two distinct elements: a biological recognition element (e.g. enzymes, whole cells, microorganisms, such as bacteria, fungi, eukaryotic cells, and yeast, cells’ organelles, plant or animal tissue, antibodies and receptors [20]) and, in close contact, a signal transduction element (e.g. optical, acoustic and electrochemical) connected to a data acquisition and processing system. Thus, the signal from the biological element is converted to a quantifiable signal. Therefore, biosensor technologies include biochemical sensors, enzymatic sensors, cellular sensors, sensors for redox reactions, antigen/antibody interactions, and other materials that provide recognition surfaces [21].

Biosensors can be categorised by recognition processes, but they can also be classified by the response mechanism used. The activity of the biological component for a substrate can be monitored by the oxygen consumption, hydrogen peroxide formation, changes in Nicotinamide Adenine Dinucleotide (NADH) concentration, fluorescence, absorption, pH change, conductivity, temperature, mass or others. Thus, the biosensor can be classified in several types according to the transducer: electrochemical (electrodes with amperometry, potentiometry, impedimetry), calorimetric (thermistors or heat sensitive sensors), optical and mass (piezoelectric or surface acoustic wave devices) transducers [22].

2.1.1.1 Microbial biosensors

Microbial biosensors are used largely to monitor environmental chemical contaminants. They are less sensitive to the inhibition by other compounds present in the sample, are more tolerant to the pH variations, temperature and generally have a longer shelflife [22]. In the example of bioluminescent microbial sensors, they comprise essentially of three components. These are as follows:

1. Viable microbial cells (bacteria or yeasts), which have been genetically modified to produce a recombinant organism (e.g. Escherichia coli) that exhibits a number of important traits, e.g. a reporter enzyme such as bacterial luciferase which is induced in the presence of the target analytes (e.g. pesticides).
2. The recombinant organisms are either directly immobilised (e.g. to cellulose nitrate or acetate membrane) or entrapped within a matrix (e.g. agar gel).
3. The recombinant microbial strain carries a bacterial luciferase reporter and a plasmid expressing enzymes that degrade the target chemicals, and the enzyme luciferase is induced in the presence of the contaminant. The luciferase activity is readily measured as light output by a luminometer by adding the substrate luciferin to the test sample.

2.1.1.2 Enzyme biosensors

Problems like selectivity and slow response, characteristic of microbial sensors, can be overcome by the use of enzymes which represent the most commonly used sensing agents, due to their selectivity [20]. Basically, all enzyme sensors work by immobilisation of the enzyme system onto a transducer. Among the enzymes commercially available, the oxidases are used most often. This type of enzyme offers the advantages of being stable, and, in some situations, does not require coenzymes or cofactors [22].

In an analytical process, enzymes are normally used for specific estimation of the corresponding substrates, and, depending on the turnover number of the enzyme, provide a significant amplification system for the sensitive detection of same substrate. In contaminant analysis, both the catalytic conversion of the substrate and the dose-dependent inhibition of an enzymic reaction are important determinants of the contaminant concentration [14].

In contaminant analysis, enzyme biosensors have largely been used for organophosphorus and carbamate pesticide and herbicide analysis. In the case of pesticides, it is largely the inhibition of enzymic activity, in particular acetylcholine esterase (AChE) and butyrylcholine esterase (BChE), that is the

determinant of pesticide concentrations in samples. However, other enzymes have also been used, e.g. tyrosinase and alkaline phosphatase. The analytical set-up is normally based on flow injection analysis (FIA). Generally, the enzymes are bound by covalent or non-specific interactions to a variety of surfaces, which also contain the immobilised substrates in the case of enzyme inhibition-based assays. The reaction of the pesticides in samples with the immobilised enzymes causes inhibition of enzyme activity, depending on the type of pesticide and its concentration. The resultant enzymic product is determined by a number of transduction mechanisms, including change in pH, temperature, fluorescence and potential, measured by amperometry, thermal spectrometry, optical detector and potentiometry, respectively [14].

2.1.1.3 Immunosensors

An immunosensor is a biosensor that uses antibodies as the biological element [14]. The transduction element in the case of immunosensors reported for the detection of chemical and microbial contaminants is largely based on optical, electrochemical and piezoelectric signals. They are a direct descendant of classical uses of antibodies in traditional immunoassays. Therefore, the majority of immunosensors are in essence flow immunoassays. Immunoassays like the enzyme-linked immunosorbent assay (ELISA) have several advantages compared with conventional analysis methods (e.g. GC or HPLC). These are the low costs per sample, the high sample throughput of several hundred samples per day, the easy handling and high sensitivity. Especially for aqueous samples there is only minimal sample preparation necessary and therefore immunoassays are an ideal screening tool, not only in the medical, but also in the environmental field. The extended use of immunosensors is mainly restricted by the time and money consuming development and the lack of a multianalyte capability. Multianalyte detection is achieved by the use of different antibodies for different analytes, immobilised on well-defined, distinct areas [23].

2.1.2 Immobilisation for biosensors

Biological transducers can be immobilised on a solid support in a variety of ways. Physical and chemical methods for immobilisation of the biological component include physical adsorption to surfaces and chemisorption, crosslinking, covalent bonding, entrapment within a polymeric gel, encapsulation in a semiporous capsule and others as use of solid binding matrices [21; 22].

2.1.2.1 Advantages of immobilisation

The immobilisation matrix may function purely as a support. Immobilisation provides several advantages to biosensors. It can improve enzyme stability and preserve its biological activity by providing a non-denaturing environment and preventing the loss of enzyme to the surrounding fluid; this allows for the device to be used multiple times. The polymer matrices used can be designed to control the diffusion of the substrate to the enzyme, and conducting polymers can transduce redox charges from enzyme active sites to electrode surfaces, thus mediating the signal transduction mechanism. Immobilisation is also used to protect enzymes from denaturing proteins and helps avoid extreme pH and chemical microenvironments for the biomolecule. Enzyme stability and maximum activity can be crucial for the performance of biosensors, because destabilisation can result in false biosensor readings [21].

2.1.2.2 Immobilisation methods

The selection of an appropriate immobilisation method depends on the nature of the biological element, the type of the transducer used, the physico-chemical properties of the analyte and the biosensor's operating conditions. The most common methods for immobilisation of biocomponents are adsorption and covalent bonding. A comprehensive review of common methods of immobilisation of proteins onto surfaces or other molecules has been written by Brinkley [24].

Physical adsorption of the biocomponent based on van der Waals attractive forces is the oldest and simplest immobilisation method. In this case, a solution of enzyme, a suspension of cells or a slice of tissue is immobilised by an analyte-permeable membrane, as a thin film covering the transducer. The adsorption method does not require chemical modification of the biological component and it is possible to regenerate the matrix membrane. The advantage of this method is its simplicity and the great variety of beds that could be used. However, loss of adsorbed biological component is possible if changes in pH, ionic strength or temperature occur during use. Entrapping the biological component in matrices such as gels, polymers, pastes or inks, considerably improves its stability and consequently the biosensor performance; therefore it may be essential to use covalent linking [22].

Covalent bonding may be used to achieve the immobilisation of biological components to a membrane matrix or directly onto the surface of the transducer. These methods are based on the reaction between the same terminal functional groups of the protein (not essential for its catalytic activity) and reactive groups on the solid surface of the insoluble bed. Functional groups available in the enzymes or protein mainly originate from the side chain of the amino acid.

2.1.2.3 Materials used for immobilisation

In immobilisation, polymers are normally used to restrict diffusion or to serve as matrices for adsorbing or binding enzymes. A variety of polymers, both synthetic and naturally occurring, have been used for chemical linkages to enzymes or in gelled forms to control diffusion. Some standard microencapsulation techniques that can be used for immobilisation include spray drying, rotary atomisation, coextrusion, fluid bed coating, solvent evaporation, and emulsion and suspension polymerisation. Synthetic polymers used in immobilising enzymes and other biological components include polyacrylamides, poly(maleic anhydrides), poly(meth)acrylic acids, acrylates, poly(vinyl alcohol), Dacron, Nylon and polystyrenes. Natural materials used in

immobilising biological components include agarose, Dextrans, cellulose, glass, collagen, alumina, polysaccharides and polypeptides (compiled from ref. [21]).

2.1.3 Sensors for environmental monitoring

2.1.3.1 Traditional detection methods of herbicides

The most common laboratory-based instrumental methods used to detect herbicides have been summarised as UV spectrometry, liquid chromatography, more recently including HPLC-mass spectrometry (MS) or gas chromatography (GC), capillary electrophoresis or solution-state nuclear magnetic resonance spectroscopy (high resolution-magic angle spinning NMR, HR-MAS NMR) [25]. Common sample preparation methods for instrumental analysis include SPE and SFE, but direct sample introduction has also been reported [26].

2.1.3.2 Biosensors for environmental analyses

It is agreed that the need for detection of toxic chemicals in aquatic and soil environments requires the development of rapid, simple, and low-cost toxicity screening procedures [27]. A review by Patel contains lists of many examples of enzyme biosensors for the analysis of pesticides, herbicides or other chemical contaminants, as well as examples of microbial biosensors and immunosensors reported for chemical contaminants [14]. New tools would be helpful in allowing the simultaneous detection of various analytes ranging from pesticides and their metabolites, to chlorinated solvents and degradation products of detergents. These tools should be reliable, fast and cost-effective as it is necessary to analyse many samples [28].

Pesticides have attracted the greatest interest for environmental biosensors to date. This is because pesticides typically function by means of interacting with a specific biochemical target either as a substrate or as inhibitors. With respect to environmental monitoring, one of the challenges is that a large number of contaminants may be involved, from a variety of related and unrelated chemical

classes. This calls for field analytical methods able to measure a number of compounds without interference by breakdown products or other hazardous co-contaminants [18].

As we strive to better understand and manage risks to human health and ecosystems, the demands on environmental monitoring are increasing. Stricter regulations and a greater public awareness of environmental issues bring requirements to monitor an ever-wider range of analytes in air, water and soil, and to do so with greater frequency and accuracy. Meanwhile, operators are looking to contain the costs of increasingly complex monitoring regimes. In response to these issues, environmental analysts have sought improvements in laboratory-based analytical methods as well as portable solutions that allow sampling and analysis to be undertaken reliably on-site [18].

Immunochemical techniques can be particularly suited for the measurement of organic pollutants (for reviews see references herein [11]). A good correlation has been found between ELISA (enzyme-linked immunosorbent assay) techniques and gas chromatography and mass spectrometry (GC, MS) [28]. However, the typical laboratory-oriented immunoassay format is far from the requirements of automated monitoring systems. Time to achieve results is typically in the range of at least 1 h, and assays require a manual multi-step procedure.

In recent years, immunosensors have been developed for herbicide detection [26]. In contrast to traditional immunoassays, the concept of immunosensors leads to simple immunoanalytical monitoring devices. The general idea is to combine antibodies as recognition elements with an appropriate physico-chemical transducer to achieve an analytical device without the complexity of classical immunoassays.

Within the spectrum of immunochemical techniques, flow immunoassay can be applied when continuous monitoring and high sample throughput are required, also for on-site analysis. Continuous flow systems are easier to automate than

formats using microtitre plates and they can lead to very sensitive detection with rapid results. Either the antibody or the antigen is immobilised on a solid support. Various solid-phase supports are available commercially. The most common materials used are inorganic surfaces and organic polymers in the form of beads, membranes and coils [29]. For example, a flow immunoassay for atrazine using solid phase support with fluorescence has been described [28]. Due to antibodies' individual specificities, it is difficult to use an immunosensor for herbicide monitoring in samples which contain unknown herbicides or several different herbicides [8].

Other techniques have been employed for environmental monitoring [30], including a non-specific electronic nose sensor array for continuous monitoring of water and wastewater quantities of organic pollutants [31; 32]. An optical portable sensor for ammonia has also been developed [33], where a colour change of a dye, in a concentration-dependent manner, which is detected spectrophotometrically.

2.1.4 Ideal characteristics and future improvements of biosensors

The ideal characteristics of a sensor include:

- No hysteresis; the sensor signal should return to baseline after responding to the analyte.
- Signal output should be proportional or bear a simple mathematical relationship to the amount of the analyte in the sample; this is becoming less important because of on-device electronics and integration of complex signal processing options.
- Fast response times; slow response times arising from multiple sensing membranes or sluggish exchange kinetics can seriously limit the range of possible application and prevent use in real-time monitoring situations.
- Good signal-to-noise(S/N) characteristics; the S/N ratio determines the limit of detection; can be improved by using the sensor in flow analysis rather than for steady-state measurements.

- Selectivity; without adequate selectivity, the user can not confidently relate the signal obtained to the target species concentration.
- Sensitivity; sensitivity is defined as the change in signal per unit change in concentration (i.e., the slope of the calibration curve); this determines the ability of the device to discriminate accurately and precisely between small differences in analyte concentration [21].

The analysis of contaminants concerns a number of organisations, including industrial sectors (e.g. agrifood, water and healthcare), regulatory authorities, and food control and environmental agencies. Biosensors form important analytical tools, and instrumentation and kits are already becoming available for use. The major requirements for biosensors are that they are comparable to, or better than, the conventional analytical systems in terms of performance (e.g. reliability, sensitivity, selectivity, specificity and robustness). However, biosensors are expected to fulfil other criteria, e.g. they must be able to provide results in real time, must be simple to use, portable, cost-effective and rugged.

In general, the current generation of biosensors for contaminant analysis have several important limitations, which require addressing if they are to become a significant force in the analytical armoury:

- the sensitivity needs to be improved further;
- the specificity; close consideration should be given to whether the sensor is used for screening purposes or for identification of a specific analyte;
- the response time and longevity need to be further improved; and
- independent validation data on performance characteristics in applications need to be generated, which could subsequently lead to wider acceptance by analysts, in general, and regulatory authorities, in particular [14].

Due to their characteristics, biosensors and related techniques show great promise for environmental monitoring applications. Advances in areas such as toxicity-, bioavailability-, and multi-pollutant screening could widen the potential market and allow for these techniques to become more competitive.

Miniaturisation, reversibility and continuous operation may allow biosensor techniques to be incorporated as detectors in chromatographic systems. Many obstacles still need to be overcome, however, on the road to commercial deployment. Some of these are common to all analytical, field-based methods. They include: the diversity of compounds and the complexity of matrices in environmental samples; the variability in data quality requirements among environmental programmes; and the broad range of possible environmental monitoring applications [18].

Other hurdles are more specific to biosensor technology. Single analyte systems will remain relatively costly to develop, while pre-manufactured biorecognition components have limited shelf and operational lifetimes. Added to this, is the relative complexity of assay format for many potentially portable (but currently laboratory-based) biosensor systems. Key areas for further investigation include improving the sensitivity and selectivity of biosensors as well as overcoming the inherent instability of biological molecules [18].

2.2 Photosynthetic material - based detection of organic trace pollutants

2.2.1 Photosynthesis

2.2.1.1 An introduction

About half of the herbicides used at present in agriculture inhibit the light reactions in photosynthesis, mostly by targeting the Photosystem II (PSII) complex [6].

Photosynthesis is the process by which green plants and certain other organisms use the energy of light to convert carbon dioxide and water into the simple sugar glucose. In so doing, photosynthesis provides the basic energy source for virtually all organisms. An extremely important byproduct of photosynthesis is oxygen, on which most organisms depend.

The overall photosynthetic reaction is:

$6CO_2 + 12H_2O$ + light energy + photosynthetic pigments -------- >

$C_6H_{12}O_6$ (sugar) + $6O_2 + 6H_2O$

Plant photosynthesis occurs in leaves and green stems within specialised cell structures called chloroplasts. One plant leaf is composed of tens of thousands of cells, and each cell contains 40 to 50 chloroplasts. The chloroplast, an oval-shaped structure, is divided by membranes into numerous disk-shaped compartments. These disk-like compartments, called thylakoids, are arranged vertically in the chloroplast in stacks called grana; the grana lie suspended in a fluid known as stroma [34].

Embedded in the membranes of the thylakoids are hundreds of molecules of chlorophyll, a light-trapping pigment required for photosynthesis. Additional light-trapping pigments, enzymes and other molecules needed for photosynthesis are also located within the thylakoid membranes. The pigments and enzymes are arranged in two types of units, Photosystem I and Photosystem II. Because a chloroplast may have dozens of thylakoids, and each thylakoid may contain thousands of photosystems, each chloroplast will contain millions of pigment molecules [34].

Photosystem II (PSII) is a multisubunit complex embedded in the thylakoid membrane of higher plants, algae and cyanobacteria. It contains a large number of cofactors including, chlorophyll, pheophytin, carotenoids, plastoquinone, non-heme iron and manganese, which together trap, transfer and modulate the utilisation of solar energy, to drive the water splitting reaction [35].

2.2.1.2 The role of pigments in photosynthesis

The action spectrum of higher plant photosynthesis includes wavelengths from about 350 nm to 700 nm. About 60% of the sunlight incident on the Earth's surface falls within this photosynthetically active range. Two classes of coloured

compounds, chlorophylls and carotenoids, are responsible for the absorption of light that energises photosynthesis in higher plants. These antenna pigments operate exclusively within the thylakoid membrane, where they are bound to specialised proteins. Chlorophyll is the dominant pigment and occurs in two forms, chlorophyll a and chlorophyll b. Chlorophyll strongly absorbs red and blue light, while scattering most of the incident green light. Carotenoids, which are present in much lower amounts in the thylakoid membrane than chlorophyll, in addition to serving as accessory pigments, they help protect the photosynthetic apparatus from photooxidative damage caused by excess light energy [36; 37].

2.2.1.3 Oxidative stress in plants

Oxidative stress is imposed on cells as a result of one of three factors: 1) an increase in oxidant generation, 2) a decrease in antioxidant protection, or 3) a failure to repair oxidative damage [38].

Various environmental stresses on plants, such as drought, high or low temperature, ultraviolet irradiation (UV), and pollutant gases, suppress CO_2-utilising capacity of chloroplasts, leading to an overflow of light energy which activates dioxygen. The resulting reactive species of oxygen ($^1O_2$, O_2^-, H_2O_2, $\cdot OH$) if not immediately scavenged, oxidise various target molecules to halt photosynthesis (photoinhibition) and promote destructive chain reactions to cell death [39].

When stress-injured leaves are exposed to high light intensities, this leads to production of toxic active oxygen species, including superoxide, hydrogen peroxide (H_2O_2), singlet oxygen and hydroxyl radical. Superoxide is formed by oxygen photoreduction by photosystem I in the chloroplast. Superoxide is then dismutated to H_2O_2. The hydroxyl radical can then be formed by the reaction of H_2O_2 with superoxide. Singlet oxygen is formed by energy transfer from excited triplet state chlorophyll to oxygen. The chloroplast is particularly susceptible to these active oxygen species, whose synthesis is enhanced on exposure to

excess excitation energy. These active oxygen species denature proteins, damage nucleic acids and cause lipid peroxidation.

The D1 protein of photosystem II is particularly susceptible to reactive photoproducts, and its photodamage may be the primary cause of photoinhibition in stressed leaves. Damaged D1 proteins must be excised from the PS-II reaction centres, and replaced with newly synthesized D1 proteins. This repair will be inhibited if protein synthesis is impaired in stressed leaves. Cell death results if H_2O_2 production overwhelms the antioxidative defence mechanisms (catalase, ascorbate peroxidase, monodehydroascorbate reductase, dehydroascorbate reductase, superoxide dismutase, glutathione peroxidase, glutathione reductase and glutathione S-transferase) [40].

2.2.2 Photosynthesis-inhibiting herbicide detection

The most frequently used biosensing systems for monitoring photosynthesis-inhibiting herbicides utilise intact cells of algae, cyanobacteria and diatoms to measure either changes in photocurrent, inhibition of electron transport with artificial mediators, or changes in chlorophyll fluorescence [8]. As an example, damage to the photosynthetic system is immediately identified by a decrease in the fluorescence with a long time constant (delayed fluorescence) and an increase in the immediate fluorescence. The effect of environmental pollution has been studied *in vivo* in leaves and trees and the technique has been used for herbicide detection [41].

One of the advantages in using PSII-based biosensors is the simplicity of the biological transduction, which can be monitored directly without requiring additional markers or transducer molecules. Another advantage is its extreme susceptibility and selectivity towards the binding of some agents. The sensitivity of any PSII-based biosensor is determined by the binding constant of the herbicide. The PSII reaction centre was isolated in 1987 and the isolated complex was found to maintain its herbicide binding ability [8].

During the 1990s there was an increased interest in developing biological sensors to detect low levels of herbicides in water and soil using an isolated PSII complex or reaction centre. Isolated chloroplasts and thylakoids have been widely used in biosensors for herbicide detection. Such biosensors test either the inhibition of the Hill reaction [42], the inhibition of DCPIP photoreduction [43], or changes in chlorophyll fluorescence [44]. Hall and co-workers developed an elegant technique to generate photocurrent using isolated PSII particles immobilised on TiO_2 electrodes in the presence of a quinone as an electron acceptor [45]. They found that this reaction is inhibited by the addition of diuron. In principle, they utilise an electrochemical biosensor based on PSII particles for herbicide detection.

The practical applications of herbicide biosensors based on PSII preparations were earlier limited by their instability, particularly upon illumination. Significant stabilisation of photochemical activity was achieved by the entrapment of cells or PSII-containing subcellular components, e.g. chloroplasts and thylakoids, on either an albumin–glutaraldehyde crosslinked matrix [46; 47] or polyvinylalcohol bearing styrylpyridinium groups [42]. Techniques for immobilisation range from the entrapment of whole cells or isolated membranes or pigment–protein complexes in an agarose, alginate or gelatine matrix, to crosslinking in a glutaraldehyde serum –albumin matrix.

Recently, mutants and adaptable strains of the cyanobacterium Synechocystis sp. PCC6803 have been used in phytotoxicity tests. This approach has been used primarily to study photosynthesis, for example to introduce tolerance (alternative sensitivity) to a variety of stress conditions. Many studies have been successful in verifying the effect of single amino acid modifications on herbicide binding affinity [8]. High affinity binding to the D1 protein is a useful property for the detection of herbicides. Recently, a fluorescence biosensor based on isolated thylakoids from mutants resistant to various herbicide classes was developed [48]. This technology made it possible to distinguish between subclasses of herbicides (e.g. triazines from urea and phenolic type herbicides).

The reaction centres of photosynthetic microorganisms have also been shown to bind herbicides and could potentially be used for the detection of herbicides as part of sensing devices. Recently, isolated D1 protein has been embedded on a working electrode for the potentiometric monitoring of the specific interaction between a protein and an herbicide [26]. Biorecognition systems based on the binding of herbicides to the reaction centre of plants and microorganisms seem to be the most direct method for herbicide detection. However, their stability and sensitivity still needs to be improved. The ELISA approach has been combined with the application of the herbicide-binding D1 protein, allowing mass screening of the herbicide-containing samples [26]. The herbicide binding protein of chloroplasts (D1 protein) is used in ELISA as a substitute for specific antibodies. Among the advantages of this innovation are simplicity of D1 protein preparation, its high stability, and group specificity for the photosynthesis inhibiting herbicides.

2.2.3 Photoinduced production of hydrogen peroxide by photosynthetic material

A group from the Institute of Soil Science and Photosynthesis of the Russian Academy of Sciences has extensively studied the photoinduced production of H_2O_2 in subchloroplast oxygen-evolving PSII particles and isolated complexes of PSII reaction centres using luminol-peroxidase chemiluminescence and pulse photoactivation [49-53]. They have been using luminol-mediated chemiluminescence for the detection of photoinduced production of H_2O_2 at both acceptor and donor sides of PSII. In their experiments, PSII particles from pea leaves, after isolation and further purification steps, were illuminated with saturating flashes of light or continuous illumination. They have found that, inhibitors of PSII, diuron (2 µM) [53] and DCMU [50] inhibit the H_2O_2 production, although no published results indicate a concentration-dependent inhibition.

It has been previously suggested that H_2O_2 is produced in the photosynthetic process by chloroplasts, broken chloroplasts and thylakoids of spinach when exposed to light, in the absence of other electron acceptors [54-56]; however,

newer research tends to discredit the work, as more, but limited, information becomes available about aspects of the processes that take place.

There is a great amount of published work trying to elucidate the photosynthetic process; however, most authors, whatever hypothesis they present in their work based on the research they have performed, add that little is clear about the molecular processes that take place. For example, it is suggested that the decrease in the activity of the photosynthetic light reactions in illuminated thylakoids correlates with the degradation of the protein components of each complex, but the mechanism and regulation of thylakoid protein catabolism are poorly understood [57]. In another published work it was noted that photoinduced production of O_2^- and H_2O_2 was observed during photoinhibition of PSII preparations; however the exact location of the site of photoinduced production of H_2O_2 is obscure [49]. Another journal article author summarises that despite considerable efforts, the detailed mechanism of the water-splitting reaction is still unknown, in particular the structural prerequisites of the catalytic site where water oxidation is supposed to take place [58]. Despite its importance, the reaction centre within PSII that splits water is not fully understood at a molecular level [59], and that the structure of the oxygen evolving complex, as well as the molecular mechanism of water oxidation, is yet to be determined [60]. Authors of another paper suggest that PSII may also produce H_2O_2, but that "controversial" results on the effect of oxygen on photoinhibition indicate that more work is needed to understand the molecular mechanism behind the loss of PSII activity in the light [61].

A review of the literature on the effect of heavy metals on photosynthetic material showcases the inability of the current scientific methods to prove or disprove possible modes of action of pollutants on photosynthesis. Heavy metals affect different components of photosynthetic electron transport chain. Photosystem II appears to be affected by the heavy metals on both oxidising (donor) and reducing (acceptor) side [62]; the overall opinion of the scientific literature however remains very fragmented with no consensus.

For example, several sites have been proposed as a potential target of copper but the exact location of the binding site in PSII is still uncertain [63]. Some authors locate the target of the copper inhibition of PSII on its oxidising site [64; 65], while other studies concluded that copper ions affect the PSII electron transport on the acceptor side [66; 67]. The PSII reaction center has also been considered as the copper binding site [68; 69]. On cadmium, there is agreement that evidence is strong to suggest that it is an inhibitor of the photochemical activity of the chloroplasts, but some studies have concluded that the light reactions of photosynthesis are not sensitive to cadmium [70], while others that they are [71; 72].

2.3 Chemiluminescence and its use for the detection of hydrogen peroxide

2.3.1 Definition of chemiluminescence

Luminescence is the emission of light that does not result from high temperatures (incandescence). In general, luminescence occurs when an atom or molecule is excited into a high energy state, and then decays to the ground state. Since electronic energy levels are quantised, the decay to the ground state is accompanied by the emission of a photon of a specific wavelength. Luminescence is categorised by the mode of excitation that produces the high energy excited state. This excitation energy can be supplied by electromagnetic radiation (photoluminescence also termed as fluorescence and phosphorescence), by heat (pyroluminescence), by frictional forces (triboluminescence), by electron impact (cathodoluminescence), by crystallisation (crystalloluminescence) or by a chemical reaction, in which case it is called chemiluminescence [73]. Fluorescence occurs when an atom or molecule is excited by absorption of a photon into the singlet excited state, which then decays to the ground state. The lifetime of this excited state is very short (on the order of picoseconds), resulting in rapid emission. Some molecules may undergo intersystem crossing where the singlet excited state

becomes a triplet state which has a long lifetime (seconds to hours), resulting in a weak but long-lived glow called phosphorescence [73].

Return of a chemically excited electron to the ground state with emission of a photon is thus called chemiluminescence. The excited molecule can also lose energy by undergoing chemical reactions, by collisional deactivation, internal conversion or inter-system crossing. These radiationless processes are undesirable from an analytical point of view when they compete with chemiluminescence. The fraction of molecules emitting a photon on return to the ground state is the quantum yield (f_{cl}). It is the product of three ratios: $f_{cl}=f_c \cdot f_e \cdot f_f$ where f_c is the fraction of reacting molecules giving an excitable molecule and accounts for the yield of the chemical reaction; f_e is the fraction of such molecules in an electronically excited state and relates to the efficiency of the energy transfer and f_f is the fraction of these excited molecules that return to the ground state by emitting a photon.

2.3.2 Advantages and reviews of chemiluminescence

Since excitation is not required for sample radiation, problems frequently encountered in photoluminescence as light scattering or source instability are absent in chemiluminescence. It has been pointed out that chemiluminescence has a large linear response reaching up to six orders of magnitude, a fast emission of light, especially when it is generated in a single flash, a high stability of several reagents and most of the conjugates (increased stability is often observed after conjugation), and a low consumption of expensive reagents [73]. The short incubation times owing to the high sensitivity generally achieved, the full compatibility with homogeneous or heterogeneous, competitive or not competitive, direct or indirect immunoassays or immunometric assays developed in one step as well as two steps formats and finally the absence of toxicity have also been noted [73]. Kricka and his co-workers have also published several review articles dealing with chemiluminescence [127]. Some of these cover the early developments of chemiluminescence or applications to all fields which can benefit from chemiluminescence while others published regularly up

to 1997 are devoted to recent advances of this method in clinical chemistry. Chemiluminescence has been widely used as detection method in many fields as flow injection analysis, high performance liquid chromatography, capillary electrophoresis and thin layer chromatography [73].

In recent years, several papers dealing with new chemiluminogenic compounds and more than 1500 per year dealing with applications in immunoassays and biomedical research have been published. Although significant improvements in noise reduction and sensitivity, new developments in multianalyte analysis and homogeneous immunoassays, and advances in selectivity of coupling and triggers are expected in the near future. Chemiluminescence has already become an essential tool in medical research as well as in routine analysis [73].

2.3.3 Chemiluminescence compounds

Compounds belonging to five chemical classes: acylhydrazides, acridinium derivatives, dioxetanes, coelenterazines and peroxyoxalic derivatives are currently used. Each of them has advantages counter balanced by drawbacks with the result that none can be definitively preferred to the others. Acylhydrazides, including luminol, are still the most frequently used chemiluminogenic compounds.

Acridinium derivatives have high quantum yields even after easy coupling to proteins. As they do not need catalysts, background signals are low and high sensitivities are frequently obtained. The instantaneous light emission, which has been considered in the past as a disadvantage (measuring problems), allows high rates in automated analysers.

The dioxetanes used for diagnostic applications are enzyme triggered dioxetanes. As for acridinium derivatives, low background signals are observed. Moreover, dioxetanes exhibit a prolonged light emission but they need for a rather long period of time before to reach a constant signal. This last feature represents an unwelcome added incubation time.

Coelenterazine and its analogues are essentially used in association with catalytic proteins as apoaequorin. Used alone, it is a specific luminogenic reagent for superoxide anion.

In the presence of a fluorescer, oxalate derivatives are the most efficient non-biological emitters, with a quantum yield of about 0.25. Fluorescers and oxalates are chosen independently. Efficiency and flexibility are therefore the main advantages of this system. Non-resolved problems of water solubility and stability added to a loss of efficiency in water certainly explain the little success of peroxyoxalate chemiluminescence in immunoassays and biomedical applications.

2.3.4 Luminol chemiluminescence

2.3.4.1 General on luminol chemiluminescence

The first report of luminol chemiluminescence was made by Albrecht in 1928 [74]. Since that time the reaction of luminol and other derivatives of the general hydrazide structure have been studied extensively.

For luminol, the quantum yield, Φ_{cl}, is about 5% in DMSO and about 1% in aqueous systems [73; 75]. Isoluminol shows about 5-10% of that efficiency. The mutagenicity and genotoxicity of chemiluminescence compounds have been tested, to identify potential risks associated with using these chemicals. None of the luminol derivatives tested induced either [76]. Chemiluminescence intensity is proportional to the concentration of luminol, oxidant and catalyst. Therefore, the system can be applied to the determination of luminol, hydrogen peroxide, or the catalyst [77]. As luminol concentration increases, chemiluminescence intensity increases. However, the signals due to peroxide and background chemiluminescence from oxygen are affected similarly. In fact, at high concentrations of luminol, the observed chemiluminescence signal becomes more sensitive to variations in mixing, causing precision to deteriorate.

Concentrations in the range from 0.1 mM to 1 mM luminol are suitable for hydrogen peroxide analysis.

Attaching luminol via the aromatic group to, for example, an analyte is not recommended, as it leads to a large decrease (to 5% of initial) in chemiluminescence due to steric hindrance. However, isoluminol attached via the aromatic group is frequently used as it leads to a large increase in chemiluminescence [78].

Examples of commercial chemiluminescence ELISA kits are the Supersignal® ELISA Femto Maximum Sensitivity Substrate and the SuperSignal® ELISA Pico Chemiluminescent Substrate (both from PIERCE Chemicals), while substrates for detecting HRP-on-antibodies for Western blotting are the BioWest Extended Duration peroxidase substrate (UVP), ECL substrate (Amersham Pharmacia, RPN2108) and the ECL Plus substrate (Amersham Pharmacia, RPN2132).

2.3.4.2 Choice of catalyst/cooxidant; advantages and disadvantages

In aprotic media (dimethylsulphoxide or dimethylformamide), only oxygen and a strong base are required for chemiluminescence [73]. In protic solvents (water, water solvent mixtures or lower alcohols) luminol and hydrogen peroxide will not react to any significant extent unless a third component is present [79]. The third component can function as a catalyst, a cooxidant or both.

An example of a catalyst is peroxidase, since it is unchanged in the overall reaction. Most frequently the enzymes microperoxidase (MPO), horseradish peroxidase (HRP) and catalase, or the substances cytochrome c and haemoglobin are used. Hemin had been the usual catalyst/cooxidant for earlier fundamental studies of luminol chemiluminescence; however, it is not very soluble and is more expensive than other catalysts/cooxidants [73].

An example of a cooxidant is peroxydisulfate. Peroxydisulfate oxidises luminol by two electrons to a diazaquinone, which then reacts with hydrogen peroxide in

a one-to-one reaction yielding chemiluminescence [80]. With peroxydisulfate used as the cooxidant, the chemiluminescence response to peroxide is linear; however, there is background chemiluminescence from peroxydisulfate and luminol that is not sufficiently constant in order to be subtracted.

An example of a catalyst/cooxidant is ferricyanide which oxidises luminol and is reduced to ferrocyanide but is subsequently reoxidised to ferricyanide [80]. Other catalysts of the reactions are ozone, halogens, Fe(III) complexes, Co(II) and Cu(II) ions as well as their complexes [75]. Co(II) and Cu(II) are the most efficient transition metal ions. Both have been investigated as catalysts for hydrogen peroxide determination using luminol [80]; however, problems are encountered. The intensity is proportional to $[H_2O_2]^n$, where n is larger than one. The value of n is quite sensitive to conditions such as pH and luminol concentration.

The use of Co(II) ions as the catalyst of luminol provides the highest sensitivity and stability of reagent, followed by the Cu(II)-catalysed chemiluminescence. However, the use of metal catalysts results in interference from substances that complex the metal ions, while also requiring a high pH. HRP and FRP catalyse the luminol chemiluminescence at a lower pH, therefore being better for coupling to enzymatic reactions, mainly the enzymatic production of H_2O_2. They are also good for coupling to production of H_2O_2 at physiological pH [81]. Superoxide anion, generated by xanthine oxidase (XO) has also been used to oxidise luminol in aqueous solution [75].

2.3.4.3 Reaction mechanism of luminol with HRP

The reaction mechanism followed is shown in Fig. 2.1; initially, an oxidised derivative of the enzyme is formed, HRP-I, which reacts with the anion of luminol ($luminol^O$) to form a half-reduced HRP-II and the radical $luminol^\bullet$. The cycle is completed and the enzyme returns to its native state in a second reaction with a luminol molecule [75]. While the latter step is dependent only on the pH of the system, the initial steps are dependent upon the exact composition of the reacting systems, the nature of the oxidant, additives, buffer,

overall concentration and pH [82]. Since the overall oxidation of luminol to aminophthalate involves the loss of four electrons, it will require two hydrogen peroxide molecules for each luminol [80]. It should be noted that the pH will affect not only the ability of the enzyme to catalyse the chemiluminescence reaction, but also directly affect the ability of luminol to react with H_2O_2 and the kinetics of this reaction, thus altering the speed of the reaction.

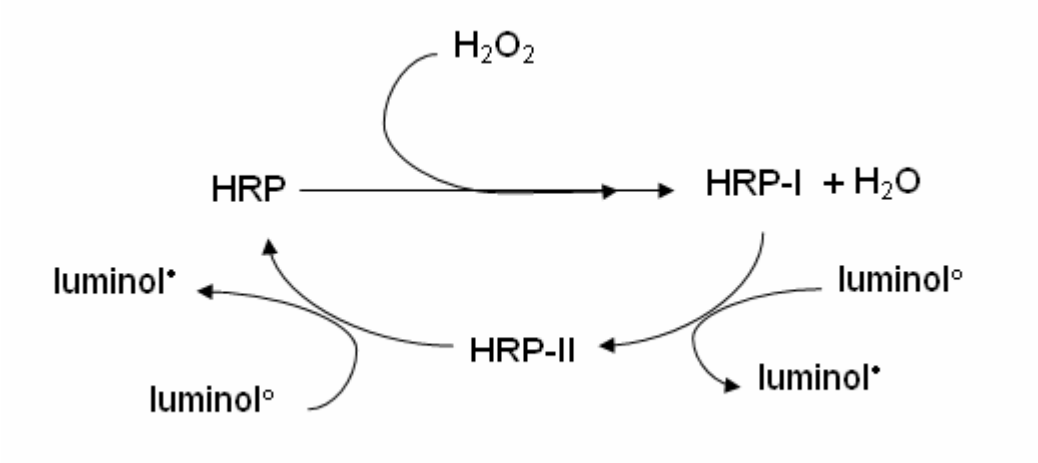

Figure 2.1 Reaction mechanism of the HRP-mediated chemiluminescence reaction of luminol with H_2O_2.

HRP reacts with hydrogen peroxide to form an oxidised HRP (HRP-I) which reacts with the luminol anion to form a half-reduced enzyme (HRP-II) and a luminol radical. The enzyme returns to the reduced form (HRP) by reaction with a second molecule of luminol.

2.3.4.4 Immobilisation of HRP for chemiluminescence assays

Instability of HRP can cause poor assay reproducibility in H_2O_2 assays [83]. The reasons for HRP instability include heat instability of the HRP protein and deficiency of endogenous calcium ion. These problems can be overcome by immobilisation of HRP and supplementation with exogenous calcium ion respectively. Retaining the activity of HRP during an assay is important in order to obtain reproducible results for H_2O_2, using a flow system, because the same HRP is repeatedly used.

Several methods have been developed to immobilise the HRP for use in chemiluminescence sensor, such as cellulose particles, polystyrene tubes and beads [84], polyacrylamide gel [80; 85] and beads [84], magnetic particles [84] and sol-gel [85] in silica and graphite pastes [85] and others.

Generally, its storage stability is good, but there is limited operational stability due to the relatively fast washing out of the HRP into the flow stream [86]. For example, a group has reported immobilising HRP on polyamide membrane and on polyethersulfone membranes [87]. This procedure was repeated 9 times. They observed a drift and instability of the hydrogen peroxide response even within the first 9 runs. At the same time, the background luminescence was increased as the number of assays increased.

2.3.5 Examples of analytical uses of chemiluminescence

The luminol reaction can be the foundation of significantly different analytical determinations. For instance, the reaction could be used to determine:

- luminol itself by holding other variables constant,
- luminol-like derivatives similarly,
- hydrogen peroxide or the progress of reactions that produce H_2O_2,
- the concentrations of metal cations,
- or analytes that effect the concentration of catalysts.

The chemiluminescence reaction provides methods for trace analysis that are attractive because of their high sensitivity. This feature makes chemiluminescence suitable for pollution studies [88].

The use of chemiluminescence as a detection method following traditional analytical separation makes up a significant share of its application in the lab. For example, liquid-phase chemiluminescence has been applied to high-performance liquid chromatography and to capillary electrophoresis. Gas-phase analytical chemiluminescence reactions have in the main been employed with

gas chromatography (GC) to detect trace chemical species or target analytes in complex matrices [89].

In immunoassays, luminol chemiluminescence has been extensively used. Because the oxidation of luminol derivatives has to be catalysed, antigen or antibody labelling with either the catalyst or the luminogenic substrate has been investigated and heterogeneous immunoassays in various formats (direct or indirect detection in competitive or not competitive mode) as well as homogeneous immunoassays have been proposed. In most examples, the antibodies specific to the antigen of interest have HRP immobilised on them, which is quantitatively detected by luminol-H_2O_2 chemiluminescence. An example of an immunoassay for the detection of HRP on antibodies for herbicides with luminol-H_2O_2 has been reported [90]. A chemiluminescence ELISA for pesticides, using chemiluminescence for detection of HRP on antibodies with different specificities towards pesticides immobilised in separate wells has also been described [91]. In attempts to use the specificity of immunoassays out of the lab, flow immunoassays using exactly the same principle have been described. A flow immunoassay for the DDT pesticide has been described, the detection being by the luminol-H_2O_2-HRP chemiluminescence [29], and another for the herbicide 2,4-dichlorophenoxyacetic acid [92]. Isoluminol derivatives that show increased efficiency after coupling, are almost the only tracers to be used in substrate labelled immunoassays. Luminol is more efficient in the free state and is used mostly in enzyme labelled immunoassays [73]. For a comprehensive list of analytical applications of chemiluminescence see a review paper [93].

2.3.6 Chemiluminescence assays for hydrogen peroxide

Development of reliable sensors for H_2O_2 determination is of great importance in both academic and industrial fields. At the same time, a H_2O_2 sensor is often employed as a fundamental detector for various biochemically important substrates which can be converted into H_2O_2 by their oxidases [85]. Hydrogen peroxide is an important component in the oxygen–hydrogen chemical cycle in

natural aquatic systems, being formed as an intermediate in redox processes that transfer oxygen between oxidation states. It is a chemically and biologically labile oxidant that plays a role in a variety of important redox processes occurring within natural waters. In the aquatic environment, H_2O_2 arises from a variety of sources including wet and dry deposition and photochemical reactions involving dissolved organic matter (DOM) [94].

Chemiluminescence is commonly used in the determination of hydrogen peroxide because of its low detection limit and wide dynamic range that can be achieved with relatively simple instrumentation; luminol, lucigenin, bis(2,4,6-trichlorophenyl)oxalate (TCPO) and pyrogallol are mainly used [95].

2.3.6.1 Chemiluminescence assays for enzymatically produced hydrogen peroxide

Great interest of the chemiluminescent reactions in analysis has been the possibility of coupling them with H_2O_2-generating enzyme-catalysed reactions. In this way, the substrates involved in some enzymatic reactions catalysed by specific oxidases can be assayed by chemiluminescent detection. Important examples include the oxidation of glucose by oxygen to gluconolactone and peroxide catalysed by glucose oxidase, the oxidation of uric acid by oxygen to allantoin and hydrogen peroxide catalysed by uricase and the oxidation of cholesterol by oxygen to Δ^4-cholesterone and hydrogen peroxide catalysed by cholesterol oxidase. Such an example in environmental analysis is a flow-injection system for phosphate ion in river water that has been developed [96]. The phosphate ion in the sample reacts in a column with immobilised pyruvate oxidase G and H_2O_2 is produced. This is then detected by luminol-ARP chemiluminescence by a PMT, the LOD being 1 nM. Other examples have been described [73]. In addition, processes generating NADH are amenable to chemiluminescence detection, since NADH reduces molecular oxygen to hydrogen peroxide in the presence of a mediator [80]. In addition to these simple enzymatic reactions generating hydrogen peroxide, multienzymatic systems leading to the production of H_2O_2 can be used for the analysis of a particular

metabolite for which no specific oxidase is available. For example, three consecutive enzymatic reactions are involved in producing peroxide and allowing the chemiluminescent determination of creatinine [17].

2.3.6.2 Examples of direct hydrogen peroxide detection using chemiluminescence

Using a real-time assay for measuring hydrogen peroxide formation, the H_2O_2 release in human HaCaT keratinocytes using the luminol-HRP chemiluminescence reaction has been analysed [97]. An example of the common luminol-HRP reaction for the detection of H_2O_2 in a microsystem has been described [83], where the LOD was 5 pM. The reaction was performed in a flow, with the HRP immobilised. A reagentless biosensor for H_2O_2 with immobilisation of all reagents has also been described. Luminol was electrostatically immobilised on anion exchange resin and packed into a glass tube, while HRP was immobilised in a chitosan membrane which was formed on a glass coil. The two segments were integrated to construct a chemiluminescence flow biosensor. The LOD was $1x10^{-7}$ M [85]. A nonenzymatic H_2O_2 assay that is based on the chemiluminescence reaction of luminol with hypochlorite (NaOCl) has been described [98]. The flash-type luminescence signal (less than 2 s) is linearly dependent on H_2O_2 down to the 10^{-9} M range.

The determination of hydrogen peroxide in rain water is commonly accomplished by a chemiluminescence method which is based on the Cu(II)-catalysed reaction of luminol with hydrogen peroxide [99]. In another example, a FIA with luminol-Co(II) for H_2O_2 in sea water was made, the LOD being 10.6 nM [100]. The well-known liquid phase chemiluminescence reactions based on the luminol or other chemiluminescence reagents in the presence of a catalyst, often suffered from the interference of transition metals (e.g. for luminol: Co, Cu, Fe, Cr and Ni) [99]. A solution that has been applied is the use of EDTA as a masking agent, as it binds with the metal ions; a FIA with luminol- KIO_4 for determination of H_2O_2 has been reported (LOD $3.0x10^{-8}$ M) [101].

Because of the aforementioned problem, different chemiluminescence reactions have also been used; an improved method for the determination of H_2O_2 in natural waters utilising the acridinium ester has been developed [94]. A group has synthesised a new chemiluminescence reagent, DTMC, which reacts with H_2O_2, without the need for substrate and without any interference of metal ions, while the LOD is $4x10^{-8}$ M [95].

2.4 Fluidic sensors and the use of magnetic beads

2.4.1 Microsystems development and fluidic analysis

The application of microtechnology to biotechnology and biosensing has rapidly expanded in recent years in response to recent advances in molecular biology and biochemistry, and microfluidics have become accepted as a means of integrating analytical and synthetic functions in a single device, or lab-on-a-chip [16; 102]. Micromachining techniques consist of microfabrication techniques, mainly developed in semiconductor industries, and other techniques for precision machinery. They are reconstituted based on novel concepts to fabricate miniaturised devices or systems. Especially, the field of miniaturisation of flow type chemical analysis systems attracts increasing interests, due to potential advantages such as high efficiency, reproducibility, low consumption of reagents and samples, fast analysis, parallel processing and multi-functionality. In addition, miniaturisation allows analytical systems to be portable, enhancing their value for field use in environmental monitoring [16].

Flow injection analysis techniques are promising analytical methods because many of the analytical processes required for a measurement can be completed automatically in a flow system. In an FIA system, for example, the introduction of several types of solutions into a flow cell equipped with a suitable detector can be strictly and freely controlled by a computer program and, as a result, a series of processes in an assay could be readily automated. Furthermore, the consumption of reagents and waste solutions in measurements are less than those required for non-flow measurements [103].

Chemiluminescence analysis has some advantages such as sensitivity, ease of use and simple instrumentation, and has been actively investigated for the highly sensitive detection of small amounts of chemical species at ultra-trace levels. Since many chemiluminescence reactions are very fast, they give rise to imprecise measurements as a result of irreproducible mixing of sample and reagents, but the reproducibility and selectivity of the chemiluminescence analysis can be improved by combination with a flow injection method [104].

2.4.2 Superparamagnetic beads and their use in fluidic systems

2.4.2.1 Magnetic beads characterisation

All materials exhibit magnetic properties to some extent at all times, depending on their atomic structure and temperature. Since magnetism originates at the atomic level, from the state of a particular material's electrons, all materials fall into one of five major groups, namely, ferromagnetic, antiferromagnetic, ferrimagnetic, diamagnetic and paramagnetic. Ferromagnetism, antiferromagnetism and ferrimagnetism are ordered states; diamagnetism and paramagnetism are transient states that exist as a result of an applied magnetic field.

- Ferromagnetism

On a microscopic scale, ferromagnetic materials exhibit magnetism even without an applied field. Some, like iron, cobalt and nickel can exhibit strong external magnetic fields under certain conditions.

- Paramagnetism

In the absence of an external magnetic field, the electron energy bands of a paramagnetic material are equally populated with spin 'up' and spin 'down' electrons. Once a magnetic field is applied, there is an imbalance of electrons due to the presence of unfilled bands, and a weak magnetic effect is observed as the net magnetic moments are aligned in the field. Paramagnetic materials lose their magnetic properties immediately when the external magnetic field is removed.

- Ferrimagnetism

Ferrimagnetic materials exhibit characteristics of both ferromagnetic and antiferromagnetic materials. The magnetic moments of the coupled atoms are anti-parallel but unequal in magnitude; therefore there is a net overall magnetisation. The susceptibility is small and positive. The iron oxide materials used in magnetic beads are examples of ferrimagnetic materials. The imbalance in moments is caused by the presence of Fe ions in different oxidation states.

Most of the magnetic particles used in beads have some form of iron oxide. Typically these iron oxide phases are ferrimagnetic, but when particles are manufactured from bulk material, and the diameter of these particles is carefully controlled, a distinctly different magnetic phenomenon is observed. By reducing the particle size to below a critical diameter, the particles become so small that the magnetic moments present in each particle (by virtue of the underlying ferrimagnetism inherent to the material) are constantly being re-oriented by random thermal energy vectors in the system. Thus the particles have a coercivity (ability to resist demagnetisation) of zero and the net magnetic moment of the powder is zero. The bulk powder is thus essentially 'non-magnetic'. However, the particles are still susceptible to applied magnetic fields, and in this regard they are similar to paramagnetic materials. Because of the presence of so many large magnetic moments within the individual powder particles, the susceptibility of the powder is very large, and thus the particles behave like 'super' paramagnets, and usually referred to as superparamagnetic. Removing the applied magnetic field from the particles will instantaneously reduce the overall net magnetic moment of the powder particles back to zero. Thus, the powder has no 'magnetic memory' [105].

2.4.2.2 Uses of superparamagnetic beads

Due to advantages including ease of separation and suitability for automation [106], superparamagnetic beads act as a solid support for a variety of biomagnetic separations such as cell and protein isolation from samples, and detection

thereof. They can be applied to the development of immunoassays and protein applications such as sample preparation, bioassays or the selection of affinity binders [107]. They can also be used for DNA separation and mRNA purification and the highly efficient magnetic separations have therefore also led to improvements in their applications, such as in PCR and in gene detection [108]. They are useful in coupling labile proteins, peptides and functional enzymes for the isolation of a wide variety of targets, e.g. hormones, receptors, disease markers etc [106]. By applying appropriate magnetic fields on the beads, magnetic separators, pumps, filters [109] and manipulation microsystems [110] have been fabricated.

Magnetic beads are often used as solid supports for immunoassay reactions. They feature a large binding surface area per volume and hence a large number of analyte molecules are bound within a small volume, allowing for sensitive detection. Furthermore, incubation times are often shortened significantly as analyte molecules pumped through a beads plug encounter very short diffusion distances to the active surfaces [111].

In conventional test tube based separation assays, magnetic beads are mixed with a sample and the component of interest binds to the biomolecule on the particle surface. The beads are then captured at the bottom of the tube by an external magnet and the supernatant is pipetted off. Multiple washing steps are required for complete separation of bound and unbound sample components [111].

2.4.2.3 Attachment of biological material on superparamagnetic beads

Since paramagnetic beads can be suspended in solution, coating them is an easier manufacturing process than coating classic solid phases, such as microplates or non-magnetic beads. The high surface area provided by submicron particles and the ability to suspend them near the target analyte enable fast reaction times [112].

There are currently several means of attaching biological ligands to microspheres, including adsorption to plain polymeric microspheres, covalent attachment to surface-functionalised microspheres, and attachment to microspheres that are pre-coated with a generic binding protein, such as streptavidin or protein A [113]. Simply adsorbing protein, especially polyclonal IgG, on the surface of polystyrene microspheres is successful more than 95% of the time.

However, covalent attachment has many advantages [114]:

1. Some evidence indicates that one can attach 10–40% more protein covalently than by adsorption.
2. Covalent coupling binds protein more securely, an asset in production of tests or assays that would be influenced by quantities of protein that might leach off the particles over time.
3. The covalent bond is more thermally stable.
4. Covalent coupling conserves costly reagent because it does not require the large excess of protein necessary for crowded adsorption.
5. Covalent attachment at relatively few sites may overcome the issue whereby large, well-adsorbing protein molecules become tightly adsorbed over so wide an area or at so many contact points that they become distorted or denatured.

2.4.2.4 Manipulation of magnetic microbeads

As mentioned previously, by adopting magnetic bead separation techniques [115], the advantages of rapid, efficient and convenient processes can be attained in separating appropriate particles from suspensions. A comprehensive review of recent research on the use of magnetism and magnetic beads in particular in fluidic devices has been published [116].

In conventional magnetic bead separators, rare earth permanent magnets produce a magnetic field [115]. When the magnetic beads suspended in a fluid are subject to the field, forces are generated that cause the particles to migrate and attach to the magnetic poles. After the cancellation of the magnetic field these

separated beads can be re-dispersed in a suspension, achieving the function of a magnetic bead separator.

For microfluidics, a few methods have been reported for the manipulation of magnetic particles [107]. A device with semi-encapsulated spiral electromagnets on a Pyrex glass wafer coupled with microfluidic channels on silicon wafer has been made [115]. As the beads flow in a suspension through the channel, the electromagnets underneath the channel magnetically capture the beads within their magnetic field area.

Another micromagnetic system reported employed microfabricated circuits rather than permanent magnets or electromagnets to generate local magnetic field [110]. Soft lithography was used to fabricate current-carrying circuits that can generate strong local magnetic fields, and manipulate magnetic beads. The magnetic beads suspended in buffer, move towards magnetic field-maxima generated by the current-carrying wires. A similar example is a microelectromagnetic matrix to control the movement of magnetic beads and also a microelectromagnet ring to trap them [117]. The matrix is a multilayer of lithographically patterned conducting wires separated by insulating material, with the ability to trap and move magnetic beads suspended in fluid above the chip.

2.4.2.5 Microsystems employing chemiluminescence and magnetic beads

An example of a microsystem using magnetic beads and electrochemiluminescence has been developed and commercialised [118]. The electrochemiluminescence process follows a conventional immunoreaction step, - a competitive, sandwich or other assay format in which, according to the analyte under measurement, a biotin-labelled antibody, antigen or other complex is incubated with the specific sample analyte in the presence of $(Ru(bpy)_3^{2+}$ labelled binding partner. The complex is captured by the concurrent addition of modified streptavidin-polymer coated magnetic, polystyrene beads. The beads are drawn into a flow-through cell. Under a platinum foil working

electrode lies a moveable permanent magnet. This is raised up to capture the beads on the electrode surface as they are drawn in; there then follows a wash sequence and, prior to measurement, the magnet drops away so as not to influence the photomultiplier tube (PMT) signal detector mounted above the cell. The ECL reaction is initiated by the application of a voltage against a silver/silver chloride reference electrode. Then, everything is washed out.

A generic microfluidic system for biochemical detection using a magnetic bead-based approach for both sampling and manipulating the target molecules has also been constructed [119]. The analytical concept is based on an electrochemical immunoassay. Magnetic beads with anti-antigen antibodies coated on them are used, which are introduced on the electromagnet and held down by the magnetic field. Then, the sample with antigen is injected into the channel. The target antigens are immobilised on the antibodies. Next, secondary antibodies with immobilised enzyme are introduced and incubated. The substrate solution is injected, and the electrochemical detection is performed, with the microelectrodes inside the flow channel, above the magnetic beads. Finally the magnetic beads are released to waste and the device is ready for another immunoassay. The electromagnets and microchannels were fabricated on silicon wafers using micromachining techniques. It should be noted that, from an analytical point, it has not been shown to work yet.

Similar examples include a DNA optical sensor using antibodies immobilised on magnetic beads to capture DNA, where a magnet captures the beads, and chemiluminescence is used for detection of sandwiched DNA [120]; also, the detection hepatitis B antigen in a chemiluminescence assay has been achieved by using antibodies to capture hepatitis B antigen, then captured on magnetic beads and detected by acridinium chemiluminescence [121].

Chapter 3: Bench-top Batch Assay for the Detection of H_2O_2 using HRP-mediated Luminol Chemiluminescence

3.1 Introduction

In order to research the potential light-induced production of hydrogen peroxide by photosynthetic material, with the possibility of inhibition thereof by herbicides, the chemiluminescence detection of hydrogen peroxide was chosen as the detection method, primarily due to its increased sensitivity compared to colorimetric methods.

Chemiluminescent reactions can be classified, according to their reaction kinetics, as either of a slow releasing, "glow" nature, where the emission of light builds slowly and reaches a maximum after a substantial incubation time, typically minutes, or of the "flash" nature, where the mixing of reagent causes the immediate emission of light, typically over milliseconds. An example of glow reactions is that generated by enzyme systems such as HRP using luminol as substrate. A typical flash reaction is generated by acridinium esters. Flash type systems such as the acridinium esters have high or moderate chemiluminescence efficiencies. The chemistry of this type of chemiluminescence light production is well understood. The simple triggering conditions contribute little to the background signal and are an added benefit. They have a wide dynamic range and low temperature dependency. These advantages have led to the use of flash reactions in rapid quantitative detection applications. However, the mixing is of critical importance, photon counting is difficult, as is the engineering of the reaction in a flow system. Glow type systems are excellent for qualitative systems such as identification of proteins on gels, or for quantitative systems if sufficient temperature control can be

maintained; also the signal levels are generally high, and it is easy to engineer the reaction for a flow system [122].

The luminol chemiluminescence reaction is most efficient at high pH. Maximum chemiluminescence is observed in the pH range from 10.4 to 10.8 when using ferricyanide catalysis. Since background chemiluminescence behaves similarly with pH however, the signal-to-background ratio does not decrease nearly as rapidly as the absolute response.

The optimally high pH is a serious limitation to applications of luminol chemiluminescence. One problem is that the luminol reaction and the processes producing hydrogen peroxide cannot occur simultaneously without severe compromises with respect to luminol intensity or the rate of the H_2O_2 production. The differences in pH optima severely limit the possibilities of the approach of performing both reactions simultaneously under one set of conditions, unless a satisfactory compromise can be achieved. Instead, it is necessary to do the two reactions involved in a coupled scheme sequentially, under two sets of conditions. Another problem is that the high pH may accelerate the rate of reaction between hydrogen peroxide and reducing components in biological samples. These reactions consume hydrogen peroxide before it can react with luminol, thus reducing observed chemiluminescence intensity and interfering negatively in analytical procedures [80].

Peroxidase catalysis is promising over the pH range from 7 to 9, since it gives greater chemiluminescence intensity than other catalysts/cooxidants under these conditions. Therefore, for the enzymatically or otherwise generated hydrogen peroxide the application of peroxidases as the biocatalysts of luminol chemiluminescence seems to be more convenient, as they require a weak alkaline reaction medium [123]. For analyses performed at physiological pH, the HRP-luminol-H_2O_2 reaction is the most useful as the optimum is close to pH 8.0 [124].

The role of a buffer is to maintain a constant concentration of hydrogen ions in a reaction. Ideally, a buffer should not influence the reaction, but for some buffers there are undesirable side-effects, e.g. complexing metal ions, enzyme interactions. Buffers are also known to influence light emission in luminescent reactions, and they have been shown to alter the intensity and kinetics of light emission in the chemiluminescent HRP-catalysed oxidation of luminol; in an assay for HRP detection previously described [125], the light emission from the luminol-H_2O_2 assay mixture (blank) was lower in Tris buffer compared to other buffers with pKa's ranging from 6.8 to 9.5. Thus, the optimal buffer for chemiluminescence reaction of luminol is Tris buffer at a pH of 8.0 – 8.5, according to the literature [126].

Based on the above introduction, it was thus decided to employ the luminol-HRP-H_2O_2 chemiluminescence for the assay for the detection of H_2O_2 as the reaction of choice. This would provide the means to detect any probable production of H_2O_2 by photosynthetic material, as well as the inhibition thereof by certain classes of herbicides.

Hence, the standard HRP-mediated luminol chemiluminescence reaction with H_2O_2 required to be developed, as this was envisaged to form the basis of the assay methodology for the detection of photosynthesis-inhibiting herbicides. As H_2O_2 is the substance in the reaction that is of interest to be detected, the work performed on the establishment of a batch, bench-top assay for the detection of H_2O_2 is hereby presented.

3.2 Materials and methods

Trizma, hydrochloric acid (HCl), 5-amino-2,3-dihydrophthalazine-1,4-dione sodium salt (luminol sodium salt), horseradish peroxidase (HRP) (type II, 148 U/mg) and hydrogen peroxide (30% w/w) were purchased from Sigma Chemical Company Ltd. (Gillingham, UK). The Tris-HCl buffer (10mM, pH 8.5) was prepared using deionised, reverse-osmosis (RO) water. Stock solutions of

luminol (30 mM), HRP (150 U/ml) and H_2O_2 (30 μM) were prepared in Tris-HCl buffer, 10 mM, pH 8.5, while for the work presented in Section 3.3.3 the pH was 12. The final solutions of the appropriate concentrations of the reagents were prepared freshly each day, unless stated otherwise.

The sequence of actions that formed a single measurement was:

- 330 μl of different concentrations of luminol in Tris-HCl buffer (10 mM, pH 8.5) and 330 μl of different concentrations of HRP in Tris-HCl buffer (10 mM, pH 8.5) were added in Kartell disposable semi-micro optical polystyrene cuvettes (Thermo Fisher Scientific Ltd., Loughborough, UK), in a time window of 1 hour before the experiment to follow, unless stated otherwise.
- The cuvette with the above 660 μl of the different concentrations of luminol and HRP in Tris-HCl buffer (10 mM, pH 8.5) was placed in the sample holding compartment of a Cary Eclipse fluorescence spectrophotometer (Varian UK Ltd., Oxford, UK). The spectrometer was set up, via the use of its bespoke software, to record the intensity of detected light over 60 seconds.
- Using a PC interface, the spectrometer's detection process was initiated, and 10 seconds later, the sample, an aliquot of Tris-HCl buffer (10 mM, pH 8.5) containing different concentrations of H_2O_2 was forcefully pipetted manually in the cuvette, thus resulting in the chemiluminescence reaction between luminol and H_2O_2, in the presence of HRP.
- At the end of 1 min, the spectrometer would stop recording the intensity of the light detected, and would produce a file containing the light intensity recorded over time, in arbitrary units, collected every 100 ms, over 1 minute. Microsoft Office Excel 2003 was used to further analyse the data.

As the spectrometer's detection sensor (a photomultiplier tube) is very sensitive to light, and, given that the sample holding compartment was not fully closed during the experiment, as a small gap had to be allowed in order to pipette the H_2O_2 sample, it was of outmost importance to ensure that the ambient light achieving to affect the measurement would be maintained at the minimum possible. This was accomplished by covering the top part of the instrument

(where the gap to allow for the pipette to reach the cuvette was found) with a piece of thick, black refuse bag, as well as a piece of black material with a felt-like surface. Most importantly, the experiments were performed in near-complete darkness; the laboratory room ambient light source was switched off (fluorescent tubes), the gap under the door leading to the space outside the laboratory room was sealed with opaque material, and the PC's monitor was set up in a way as to reduce the light intensity emitted by it to the minimum possible, while still allowing the experimenter to distinguish various key graphics on the screen (namely the "start" button and the mouse pointer).

3.3 Results and discussion

3.3.1 Introduction

The results of the literature search and review reveal that it has mainly been of interest to detect and quantify HRP by the use of chemiluminescence [93; 127; 128]. For the purpose of the research described here however, it is hydrogen peroxide that is the reactant of interest. It was therefore important to perform an extensive series of experiments aiming to identify the optimal concentrations of luminol and HRP for the detection of H_2O_2. As mentioned in the Chapter's introduction (Section 3.1), the HRP catalysis of luminol is the most promising in the region of pH between 7 to 9, however, as the pH increases, so does the chemiluminescence signal. In order to investigate the ‘enhancement’ at higher pH, although not ideal from an analytical point for the rest of the work aimed to be performed for this project, H_2O_2 detection measurements were carried out also at a high pH, in order to compare the two sets of conditions.

3.3.2 Bench-top batch assay for the detection of H_2O_2 using HRP-mediated luminol chemiluminescence

In order to identify the wavelength maximum (peak) of the light produced by the reaction and confirm the information available from literature [75; 93] a wavelength

scan was performed (Fig. 3.1). Thus, the wavelength at which the luminol chemiluminescence emits the most light is at 432 nm.

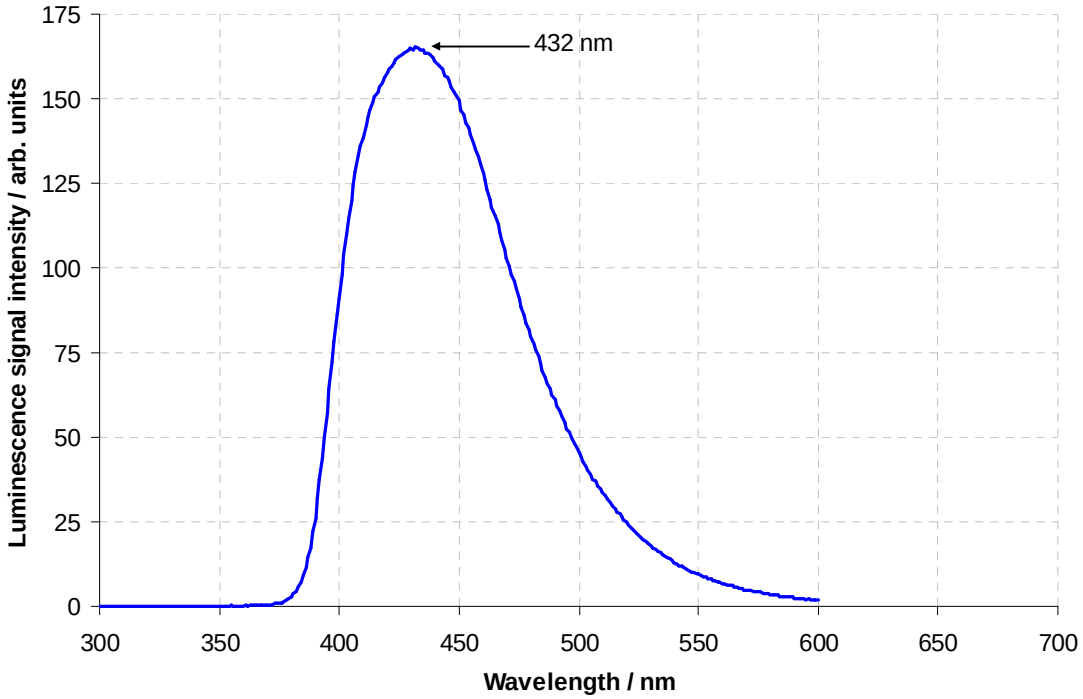

Figure 3.1 Wavelength scan of luminol chemiluminescence.
Chemiluminescence light output detected by the spectrometer, produced by the chemiluminescence reaction of [H_2O_2] = 2 µM, [HRP] = 10 U/ml, [luminol] = 100 µM, in Tris-HCl buffer (10 mM, pH 8.5), over 1 min.

Experiments were performed in order to find the optimal concentrations of the reagents luminol and HRP, for the detection of the lowest concentration of H_2O_2, as well as a wide linear range. For these experiments, the light intensity was measured with the Varian Eclipse spectrophotometer, a large, bench-top detector, with great sensitivity to low light levels, as described in Section 3.2.

Four concentrations of luminol (10 mM, 1 mM, 100 µM, and 50 µM) and five concentrations of HRP (50 U/ml, 20 U/ml, 10 U/ml, 5 U/ml, and 1 U/ml) were tested in all possible combinations (twenty combinations in total) for the detection of H_2O_2. The focus was put on small concentrations of H_2O_2 (1 nM – 1 µM) in order to find the combination of luminol and HRP that allowed for the best detection of H_2O_2; what is more, these concentrations are within the range of H_2O_2 produced by 1 mg of chloroplasts, as suggested by the literature [50; 51].

At higher concentrations of H_2O_2 (in the millimolar region), the reaction acts like a typical glow-type chemiluminescent reaction expanding over minutes. At anything equal to or lower than micromolar concentrations, the result resembles a flash-like spike, typically for a few seconds.

Having identified the peak wavelength at which luminol chemiluminescence is emitted (approximately 432 nm), measurements of light intensity over time were made, at a wavelength of 432 ± 20 nm. Such a large 'window' of detected wavelength was chosen in order to allow the maximum possible light to be detected, and, as the reaction is performed in the dark, any light detected would be more likely to only be from the chemiluminescence reaction. It should be noted that the Varian Spectrometer used does not allow for light of wider wavelength bands to be measured, with 20 nm being the maximum permissible waveband.

The example shown in Fig. 3.2, shows the two methods originally considered and used to interpret the data; one was to measure the light output as such, measuring the maximum, peak output, while the other was to measure the area under the curve, i.e. to add all the data points together, thus integrating the resulting light emission.

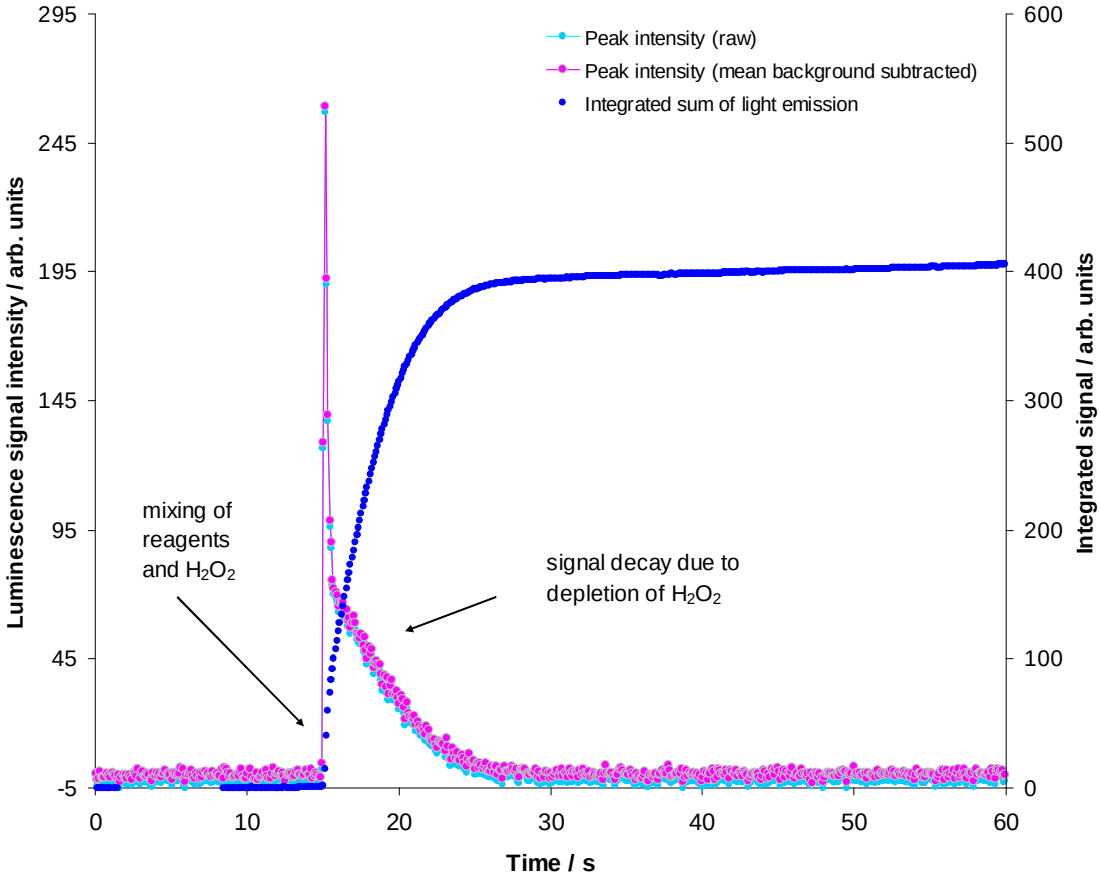

Figure 3.2 Example of graphical analysis of obtained chemiluminescence signal. Chemiluminescence light output detected by the spectrometer, produced by the chemiluminescence reaction of [H_2O_2] = 1 µM, [HRP] = 10 U/ml, [luminol] = 100 µM, in Tris-HCl buffer (10 mM, pH 8.5) in 1 min.

The calculations used to quantify the lower limit of detection (LLOD) were based on the definition of the limit of detection by the International Union of Pure and Applied Chemistry (IUPAC Compendium of Chemical Terminology 2nd Edition, 1997). The limit of detection, expressed as the concentration, c_L, or the quantity, q_L, is derived from the smallest measure, x_L, that can be detected with reasonable certainty for a given analytical procedure. The value of x_L is given by the equation:

$x_L = \bar{x}bi + ksbi$,

$\bar{x}bi$ is the mean of the blank measures,

sbi is the standard deviation of the blank measures, and

k is a numerical factor chosen according to the confidence level desired.

Therefore for a k value of 3, the LOD is the concentration corresponding to a signal 3*s.d. (of the blank) above the mean of the blank.

The LLOD was calculated for all the aforementioned combinations of luminol and HRP and the results are presented in Table 3.1. By comparing all the LLODs, the one that appeared to give the most sensitive detection was the one employing 100 µM luminol and 5 Units/ml HRP, with an LLOD of $9.0x10^{-8}$. For this combination of luminol and HRP further measurements were performed, in order to build a more detailed profile of the detection of H_2O_2, and its graphical representation. Using the same methods of data analysis as shown in Fig. 3.2, the standard curve (Fig. 3.3) and the calibration curve (Fig. 3.4) were drawn for both the maximal light output (peaks), and the integrated light output. The observed LLOD agrees with published literature for similar batch assay development ($18x10^{-8}$ [129], $12x10^{-8}$ [94], $1x10^{-8}$ [130]) and is within range for H_2O_2 production from photosynthetic material. The relative standard deviation was less than 8% from five repeated measurements of a $1x10^{-6}$ H_2O_2 sample.

Table 3.1 Lower limit of H_2O_2 chemiluminescence detection calculated for all combinations of four luminol and five HRP concentrations.

Luminol conc. (M)	**HRP concentration (Units of activity/ml)**				
	50 U/ml	**20 U/ml**	**10 U/ml**	**5 U/ml**	**1 U/ml**
10 mM	$9.3x10^{-7}$	$8.5x10^{-7}$	$8.5x10^{-7}$	$6.7x10^{-7}$	$7.5x10^{-7}$
1 mM	$4.6x10^{-7}$	$5.5x10^{-7}$	$3.1x10^{-7}$	$9.5X10^{-8}$	$5.0x10^{-7}$
100 µM	$1.9x10^{-7}$	$9.9x10^{-8}$	$9.5x10^{-8}$	$9.0x10^{-8}$	$3.5x10^{-7}$
50 µM	$1.1x10^{-6}$	$2.0x10^{-6}$	$6.7x10^{-7}$	$1.0x10^{-7}$	$2.2x10^{-6}$

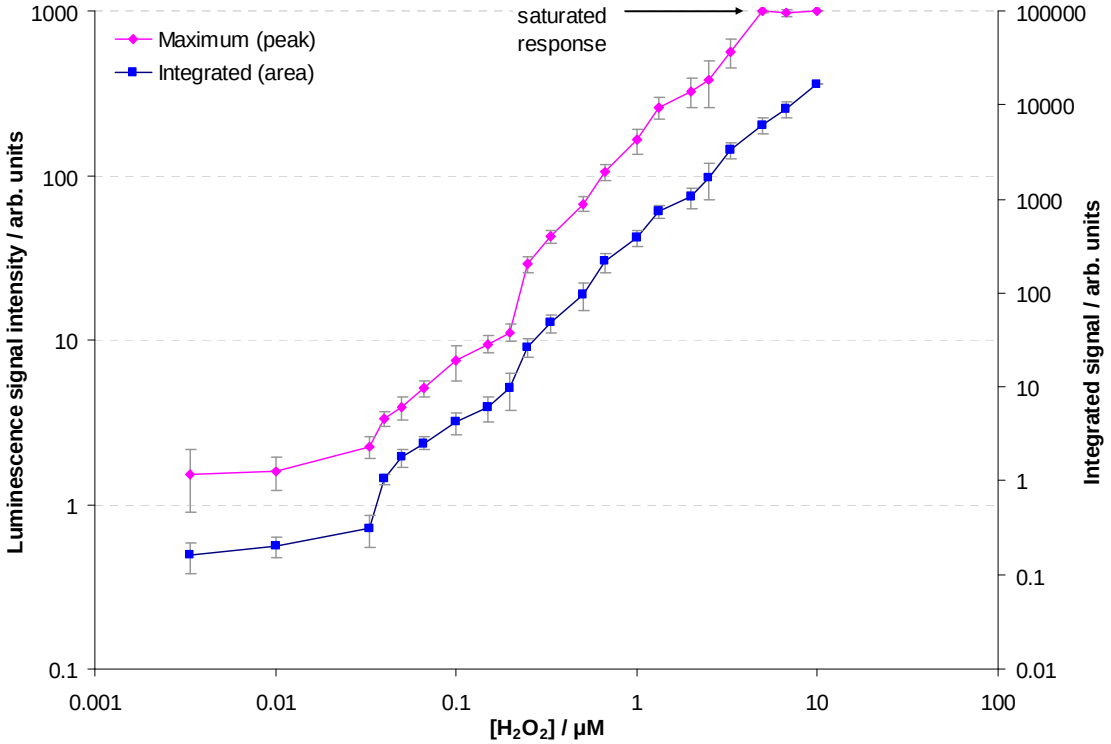

Figure 3.3 Standard curve for the chemiluminescence detection of H_2O_2.
H_2O_2 was assayed by measuring the chemiluminescence light output detected by the spectrometer, produced by the chemiluminescence reaction of [HRP] = 5 U/ml, [luminol] = 100 µM, with different [H_2O_2] = 3.33 nM - 10 µM, in Tris-HCl buffer (10 mM, pH 8.5), in 1 min. Each data point is the average of 5 replicates.

The approach of manually injecting a sample containing the H_2O_2 to be measured in a cuvette is subject to poor precision due to non-reproducible injection [80]. It can however be improved by using a FIA system [104]. Research done with luminol chemiluminescence reaction established a RSD ±13% when sample was manually injected and ±5% when an automatic injector was used. The reproducibility was similar whether total light output or peak light intensity was measured [78]. In the case of the H_2O_2 chemiluminescence detection, the precision of injection of hydrogen peroxide, the volume of hydrogen peroxide and the speed of the injection in association with the size of the assay tube all affect the rate of the chemiluminescence reaction, the quenching of light emission and the precision [128]. This explains the RSD values seen in the results of the standard curve (Fig. 3.3) and generally in all results obtained with the batch assay.

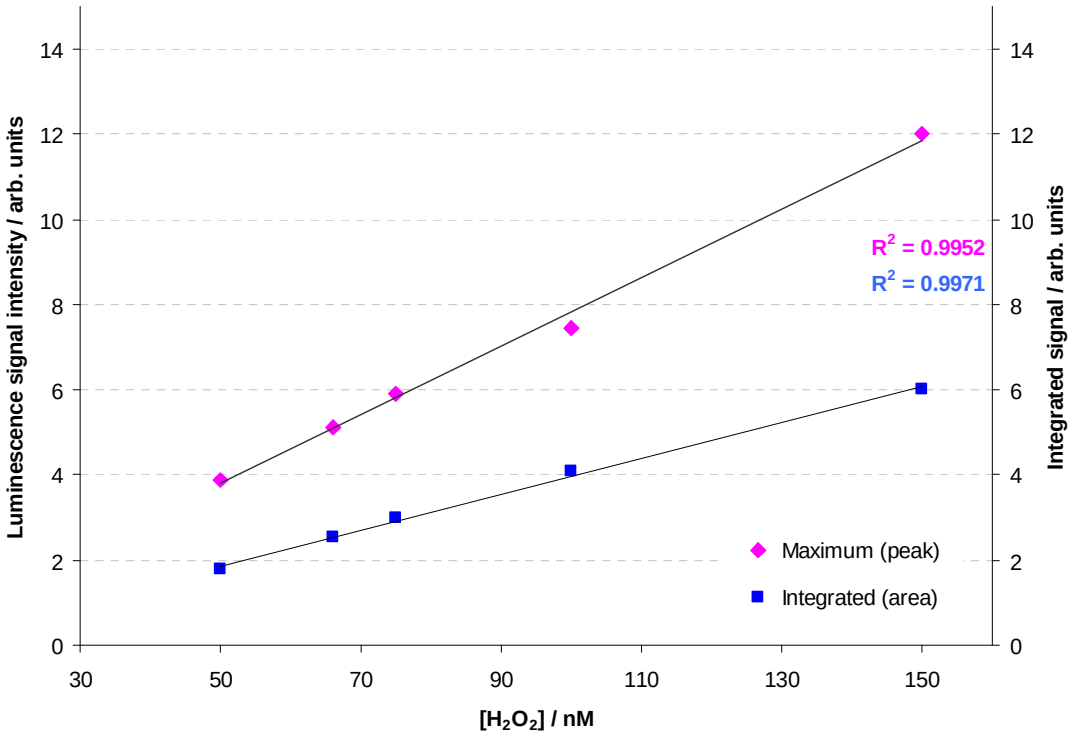

Figure 3.4 Calibration curve for the chemiluminescence detection of H_2O_2.
H_2O_2 was assayed by measuring the chemiluminescence light output detected by the spectrometer, produced by the chemiluminescence reaction of [HRP] = 5 U/ml, [luminol] = 100 µM, with different [H_2O_2], in Tris-HCl buffer (10 mM, pH 8.5), in 1 min. Each data point is the average of 3 replicates.

3.3.3 Investigation into the use of different pH

Luminol is more reactive at high pH according to the literature [124], and confirmation of the potential increase in chemiluminescence signal intensity obtained when doing so was sought. Therefore, the chemiluminescence detection of H_2O_2 was performed at pH 12. As it can be seen in Figure 3.5, the assay with the high pH has a lower H_2O_2 detection range, as well as a higher overall light output. However, as at pH 12 HRP has a half-life of 21 minutes [124] and the fact that the high pH affects irreversibly the activity of HRP, meant that the pH 12 could not be considered further.

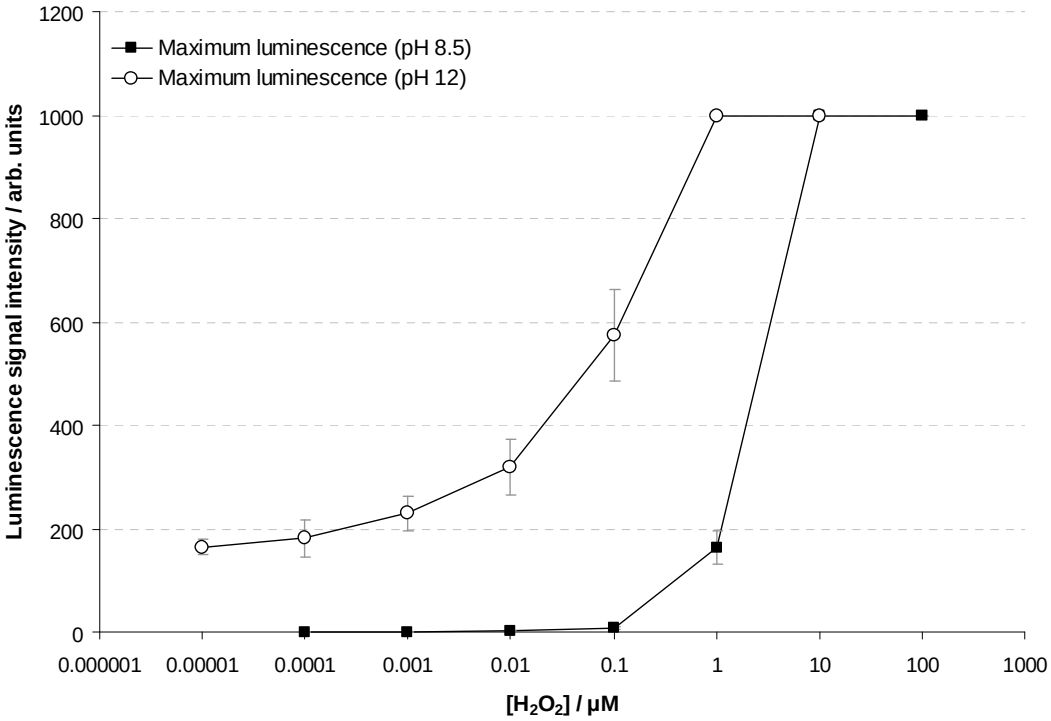

Figure 3.5 Comparison of standard curves of H_2O_2 detection for two different pH values.
Chemiluminescence light output for H_2O_2 detected by the spectrometer, produced by the chemiluminescence reaction of [HRP] = 5 U/ml, [luminol] = 100 µM, in Tris-HCl buffer (10 mM) in 1 min. The pH was 8.5 for ■, and 12 for ○. Each data point is the average of 3 replicates.

3.3.4 Investigation in the effect of varying the bench-top detector's amplification methodology

In order to ensure that the experimental setup was adjusted in an optimal fashion, a series of measurements were performed in order to identify the appropriate level of amplification that the light produced by the chemiluminescence reaction would be receiving by the embedded circuitry of the PMT detector. The bench-top Varian Eclipse spectrometer's proprietary software allows for a user to choose from 3 pre-defined settings of "high", "medium" or "low" PMT voltage, each corresponding to a different level of "gain", i.e. amplification to be applied to the signal produced by the detector in response to the light detected. It should be noted that the sensitivity of the system is not increased as such when the PMT voltage is increased. Figure 3.6 displays the resulting changes of the detector's output values (arbitrary units)

when varying the PMT voltage between the three pre-defined levels. Increasing the amplification of the signal by varying the PMT voltage results in a marked change in the peak signal intensity obtained by a typical chemiluminescence measurement; as it can be seen, the highest concentration of H_2O_2 that the spectrometer can detect is reduced as the PMT voltage increases. What is more, the subsequent H_2O_2 concentrations that can be adequately detected achieve a smoother response with the "medium" voltage setting, compared to the "low" setting. In addition, given the potential focus on the smaller concentrations of H_2O_2 to be detected, in the micromolar region or less, it would not be necessary to allow for millimolar or higher concentrations of H_2O_2 to be adequately detected. Thus, it was decided that no amplification gain would be applied to all subsequent experiments performed with the particular spectrometer, as this would allow for a wider range of detection.

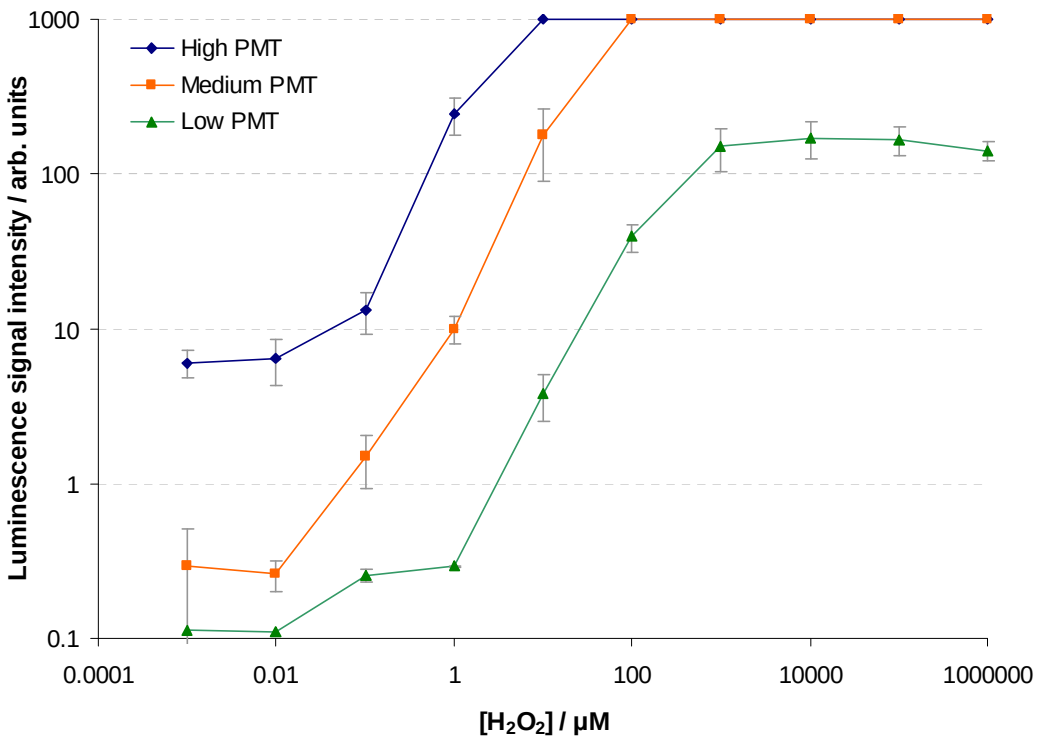

Figure 3.6 Effect of PMT amplification voltage on chemiluminescence H_2O_2 detection.
H_2O_2 detection by the chemiluminescence light output detected by the Varian Eclipse spectrometer with different signal amplification voltages applied. Concentrations: [H_2O_2] = 1 nM -1 M, [HRP] = 5 U/ml, [luminol] = 100 µM, in Tris-HCl buffer (10 mM, pH 8.5). Each data point is the average of 3 replicates.

3.3.5 Investigation in the effect of varying physical parameters of the sample mixing process

In order to optimise the experimental conditions and processes as well as to minimise potential loss of useful signal intensity potentially detected, an investigation into some parameters of the mixing of reagents was performed. As described in more detail in the Materials and Methods of this chapter (Section 3.2), for the cuvette-based assay, for the detection of H_2O_2 using the HRP-mediated luminol chemiluminescence reaction, 330 µl of the sample to be measured were introduced in a cuvette already containing 330 µl of luminol and 330 µl of HRP. This was achieved by expelling the H_2O_2-containing sample, using the common manual pipetting action associated with standard air-displacement pipettes, in the cuvette. The chemiluminescence reaction is initiated the moment the H_2O_2 sample is dispensed in the cuvette containing the rest of the reagents. It has therefore been of great importance to ensure that the dispensing method used was uniform and optimal. The aspiration step of the common pipetting action does not introduce any unreasonable elements of variation; however, the dispensing step can be affected by the type of pipette tip used. Two different pipette tips, of different lengths, were used in the collection and discharge of the sample. It was hypothesised that the length of the pipette tip used could then affect other parameters of the pipetting action and hence introduce variation to the mixing of the reagents. One tip had a length of 3.5 cm (pipette tip "s"), while pipette tip "l" had a length of 5.5 cm.

Another parameter that could vary significantly the flow dynamics of the mixing of the reagents that occurs when dispensing the H_2O_2 sample into the cuvette, is the angle between the pipette tip and the cuvette's inner wall. This is an important parameter that pipette manufacturers usually highlight in pipette manuals [131], suggesting, as good practice, that pipette users dispense the aspirated liquid from the pipette tip into the cuvette indirectly, i.e. against the walls of the cuvette, rather that directly into the centre of the cuvette. It is expected that this is of even greater importance when using a higher than

normal expelling force to the sample, in order to achieve that same greater mixing that will be affecting the reaction dynamics, as is the case in the work presented here. Given the manual nature of the procedure, it was not achievable to keep the angle of pipetting precisely constant to the desired angle, but all care was taken to ensure that discrepancies were kept to a minimum. Two different angles were used while expelling the sample into the cuvette, approximately 35° and 60° between the vertical wall of the cuvette and the tip (Fig. 3.7).

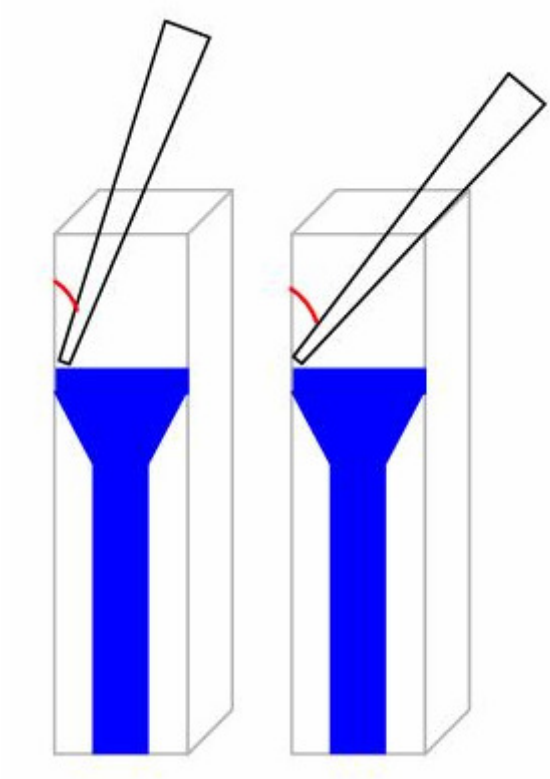

Figure 3.7 Schematic of the different pipetting angles.
Representation of the two different angles between the pipette tip and the cuvette wall employed when releasing the H_2O_2-containing sample in the cuvette containing the luminol and HRP. The left schematic depicts an angle of 35° while the schematic on the right represents the 60° angle, as can be seen by the lengths of the angles' arcs, drawn in red colour.

The length of the pipette tips and the angle in which they were used were assessed combinatorially. The results of altering these two parameters can be seen in Figure 3.8. It is apparent that altering these two experimental method parameters has a significant effect on the performance of the assay for the detection of H_2O_2. Based on the results obtained, it was decided to always

employ the longer pipette tips and dispense the sample with a 60° angle between the tip and the cuvette wall.

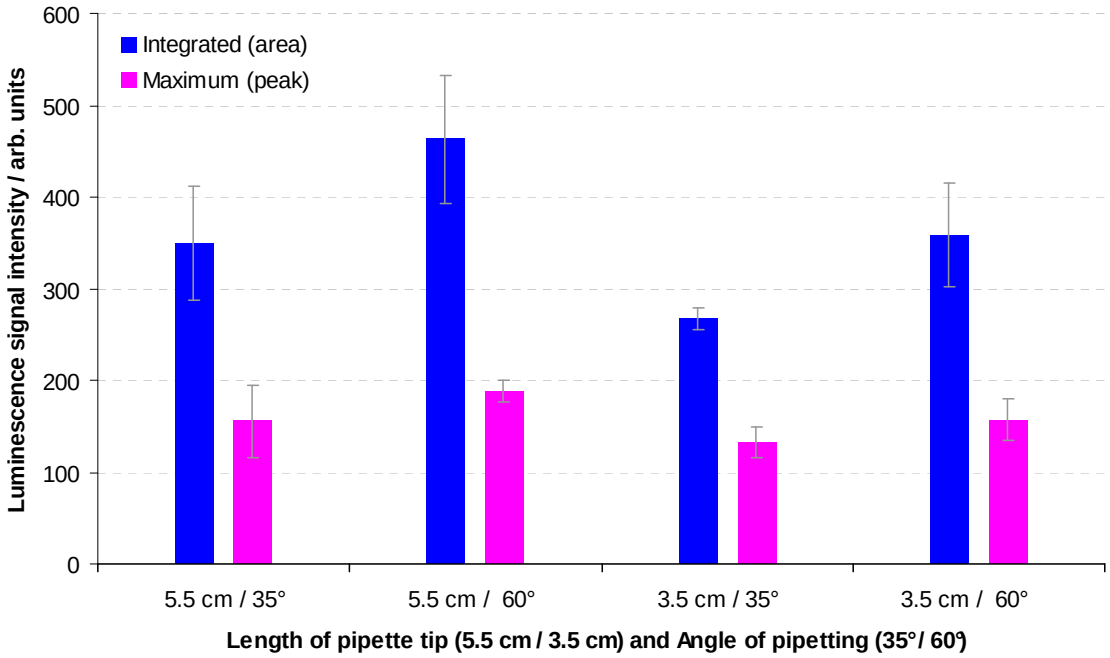

Figure 3.8 Effect of pipetting parameters on the chemiluminescence detection of H_2O_2.
Chemiluminescence light output detected by the spectrometer with different combinations of varying the pipette tip used as well as the angle of dispensing the sample. [H_2O_2] = 1 µM, [HRP] = 5 U/ml, [luminol] = 100 µM, in Tris-HCl buffer (100 mM, pH 8.5). Each data point is the average of 3 replicates.

3.4 General discussion

In Chapter 3, the establishment of the standard chemiluminescence assay for the detection of hydrogen peroxide was described. The concentrations of the reagents (luminol and HRP) were optimised for the most sensitive detection of hydrogen peroxide. It was necessary for instrumentation (PMT gain) as well as other parameters (pipetting) of the batch assay to also be optimised, as the batch, bench-top, manual method employed for the conduct of the experiments introduces methodological parameters that required optimisation and standardisation. This work will form the basis of consequently researching the chemiluminescence detection of the probable production of hydrogen peroxide by photosynthetic material, and inhibition thereof by certain classes of

herbicides. Having established an optimised assay for the detection of standard H_2O_2, the focus can now be placed on the source of the H_2O_2 being replaced by light-induced photosynthesis by-production from photosynthetic material.

Chapter 4: Bench-top Batch Assay for the Detection of Herbicides using HRP-mediated Luminol Chemiluminescence

4.1 Introduction

Having established an optimised HRP-mediated luminol chemiluminescence assay for the detection of standard H_2O_2, the focus was placed on the source of the H_2O_2 being replaced by light-induced production from photosynthetic material.

Although the photosynthetic cycle has not been completely elucidated, it has become an established fact that H_2O_2 is produced at some step of the cycle. Initially, whole chloroplasts were isolated and tested for H_2O_2 production instead of any sub-chloroplast organelles, as the chloroplasts have been shown to fully participate in the whole photosynthetic cycle, and thus potentially produce H_2O_2, and are easier to isolate [8]. Later, isolated thylakoids, a sub-chloroplast organelle, were isolated and tested for H_2O_2 production, and the majority of the work presented in this chapter was performed with thylakoids. Various isolation protocols, for both chloroplasts and thylakoids, were sought in the literature and repeatedly featured protocols were accepted as the standard / optimised.

In order to investigate the ability to effect the production of H_2O_2, isolated chloroplasts and thylakoids were illuminated and then mixed with luminol and HRP in order to detect any produced H_2O_2 (Section 4.2 and 4.3). The production of H_2O_2 was optimised in order to allow for the highest H_2O_2 yields, for a variety of parameters that could potentially be affecting the H_2O_2 production during the illumination step.

The isolated thylakoid preparations were then used further in order to investigate the inhibition of the production of H_2O_2, following their incubation with herbicides (Section 4.4). Ability to report a relationship between herbicide concentration and H_2O_2 produced, in a batch assay format, would form the basis of the project's further direction.

Section 4.5 includes the author's critical review of the effect and relevance of the two standard methods used in plant research to report the 'health' or ability of plants, plant cells, or subcellular organelles to photosynthesise.

4.2 Bench-top batch assay for the detection of H_2O_2 produced by illuminated chloroplasts, using HRP-mediated luminol chemiluminescence

4.2.1 Introduction

A key objective for the successful completion of the work presented in the thesis is the establishment of a causative link between the presence of photosynthesis-inhibiting herbicides in an aqueous sample and a measurable change in a physico-chemical parameter of photosynthetic plant material, when in contact with the sample.

In order to achieve the central aim of detecting herbicides by quantifying their disrupting effect imposed on the photosynthetic ability of plant material, and based on the literature, as reported in Chapter 2, it was initially decided to use chloroplasts isolated from spinach plant leaf cells. There is published research that has utilised whole chloroplasts as, essentially, the biological component that, with an external effect taking place, such as the introduction of a chemical, will alter in morphology or activity, with that change being detected and reported further measured electrochemically, thus forming a biosensor [42-44]. Although the photosynthetic cycle has not been completely elucidated, it has become an established fact that H_2O_2 is produced at some step of the cycle [49]. It has been reported previously that H_2O_2 produced by isolated chloroplasts lamellae has

been detected [132], thus chloroplasts appeared as promising biological elements to be used for the purpose of this project, also being easy to isolate, relatively to other sub-chloroplast organelles.

Therefore, chloroplasts were isolated, and the possible stimulation of H_2O_2 production was examined by illuminating the chloroplasts and measuring any produced H_2O_2 using the HRP-mediated luminol chemiluminescence. A variety of values for parameters of the chloroplasts illumination step were identified in a literature search; the illumination time varied greatly in the literature from milliseconds to minutes, while the distance from the light source was generally kept to the minimum possible allowed from the experimental setups employed. The type of light source used varied greatly depending on the application, with Tungsten filament lamps or halogen lamps in non-miniaturised experiments commonly used, or LEDs for miniaturised setups [49].

4.2.2 Materials and methods

In experiments testing for chemiluminescence signal potentially resulting from H_2O_2 produced by illuminated chloroplasts, the setup and method were kept similar to those used for the standard luminol-HRP-H_2O_2 cuvette assay as described in Section 3.2, apart from the H_2O_2 sample's origin, preparation and illumination steps. More specifically, the 330 µl of a known H_2O_2 concentration sample that was previously pipetted into a cuvette containing 660 µl of luminol and HRP was replaced by 330 µl of an isolated chloroplast-containing aliquot, as the aim of the experiments described in Section 4.2 was to identify and quantify the production of H_2O_2 by chloroplasts.

4.2.2.1 Chloroplast isolation methods

There is a variety of isolation methods; mechanical isolation methods are the most common. These are more likely to succeed for a limited number of species, such as pea and spinach, as opposed to chemical and enzymatic permeabilisation of cells [133]. The age of the plant material is an important factor

in determining the yield of the desired organelles; the yield decreases rapidly with the age of the plant, as organelles aggregate into sticky lumps, which is the most serious problem during organelle isolation. Hence leaves of baby spinach plants were used in order to isolate the chloroplasts [134].

Chloroplast preparations, as used in experiments described in Section 4.2, were prepared using two different protocols, Chloroplast Isolation Protocol 1 and 2, coded as Ch0a and Ch0b. These were identified as common chloroplast isolation protocols used in the literature. Full step-by-step descriptions follow.

4.2.2.1.1 Chloroplast isolation protocol 1 (Ch0a)

Chloroplast isolation was performed using a modification of a protocol described previously [26]. One hundred grams (fresh weight) of fresh baby spinach leaves (Tesco Stores Ltd., Cheshunt, Hertfordshire, UK, Bedford Branch) were washed with distilled water, dried on filter paper and homogenised in a blender, in 300 ml of extraction buffer (0.35 M sucrose, 50 mM Tris-HCl, 10 mM NaCl, pH 8.0). The homogenate was filtered through 4 layers of cheese-cloth and through sieves with a pore diameter 100 μm. Centrifugation was performed for 10 min at 2000 g at 4℃ (Model J2-21 centrifuge, Beckman, German y). The pellet was resuspended in extraction buffer. The final preparation was divided in 200 μl aliquots in Eppendorf tubes, immersed in liquid nitrogen, and then stored at -80℃. The buffers were at 4℃, the room temperature was 15℃, and the ambient light was kept at the bare minimum necessary to conduct the work. The isolation was carried out post-sunset, in order to minimise the ambient light in the otherwise well-lit area of the centrifuge. All chemicals were from Sigma Chemical Company Ltd. (Gillingham, UK).

4.2.2.1.2 Chloroplast isolation protocol 2 (Ch0b)

Chloroplast isolation was performed using a modification based on two variations of the same protocol, as described in [135] and in [136]. Thirty five grams (fresh weight) of fresh baby spinach leaves (Tesco Stores Ltd., Cheshunt, Hertfordshire, UK, Bedford Branch) were washed with distilled water, dried on

filter paper and homogenised in a blender, in 100 ml of a partially frozen slurry of buffer (0.4 M sorbitol, 25 mM tris(hydroxymethyl)-methylglycin-NaOH, pH 8). The homogenate was filtered through 10 layers of muslin with an added 2 cm layer of cotton wool. The filtrate was centrifuged at 2500 g for 1 min at 4℃ (Model J2-21 centrifuge, Beckman, Germany). The supernatant was discarded and the pellet was resuspended in same buffer. The final preparation was divided in 200 µl aliquots in Eppendorf tubes, immersed in liquid nitrogen, and then stored at -80℃. The buffers were at 4℃, the ro om temperature was 15℃, and the ambient light was kept at the bare minimum necessary to conduct the work. The isolation was carried out post-sunset, in order to minimise the ambient light in the otherwise well-lit area of the centrifuge. All chemicals were from Sigma Chemical Company Ltd. (Gillingham, UK).

4.2.2.2 Chloroplast illumination and chemiluminescence H_2O_2 detection methodology

Trizma, hydrochloric acid (HCl), 5-amino-2,3-dihydrophthalazine-1,4-dione sodium salt (luminol sodium salt), HRP (type II, 148 U/mg), MES, NaOH, sucrose and hydrogen peroxide (H_2O_2) (30% w/w) were purchased from Sigma Chemical Company Ltd. (Gillingham, UK). The Tris-HCl buffer (10 mM, pH 8.5) was prepared using reverse-osmosis (RO) water. Buffer "A2" was prepared with 0.4 M sucrose in 10 mM Tris-HCl, pH 8.5. Buffer "B1" was 10 mM MES-NaOH, pH 7.0, and buffer "B2" was prepared with the addition of 0.4 M sucrose in buffer "B1". Stock solutions of luminol (30 mM), HRP (150 U/ml) and H_2O_2 (30 µM) were prepared in Tris-HCl buffer, 10 mM, pH 8.5, unless otherwise stated. The final solutions of the appropriate concentrations of the reagents were prepared freshly each day, unless stated otherwise.

The experiments described in the current section, Section 4.2, were based on the HRP-mediated luminol chemiluminescence reaction in cuvettes using a bench-top spectrometer, with the H_2O_2 required for the reaction being provided by illuminated isolated chloroplast samples. It is therefore a variation of the experimental process of detecting known H_2O_2 samples using

chemiluminescence, as described in Section 3.2. The sequence of actions that formed a single measurement was based on that described in Section 3.2, with the crucial illumination of the sample as an added step, due to the different nature of the sample itself.

The steps thus followed are:

- 330 µl of luminol (100 µM) in Tris-HCl buffer (10 mM, pH 8.5) and 330 µl of HRP (5 Units/ml) in Tris-HCl buffer (10 mM, pH 8.5) were added in a Kartell disposable semi-micro optical polystyrene cuvette (Thermo Fisher Scientific Ltd., Loughborough, UK), in a time window of 1 hour before the experiment to follow.
- The cuvette with 660 µl of luminol and HRP in Tris-HCl buffer (10 mM, pH 8.5, unless otherwise stated) was placed in the sample holding compartment of a Cary Eclipse fluorescence spectrophotometer (Varian UK Ltd., Oxford, UK). The spectrometer was set up, via the use of its bespoke software, to record the intensity of detected light over 60 seconds.
- In order to induce the production of H_2O_2 by the chloroplasts, the sample illumination step was undertaken:
    - The previously isolated chloroplast preparations were diluted in a suitable buffer in order to form the measuring sample (three different buffers and three different dilutions tested).
    - A 330 µl diluted sample was aspirated in a pipette tip attached to an air-displacement pipette.
    - The pipette was placed 10 cm underneath a JC12V20W halogen lamp (20 watts, 350 lumens)(EiKO Ltd. Kansas, USA), with a borosilicate Pyrex glass Petri dish (SciLabware Ltd, Stone UK) containing water in between the pipette tip containing the sample and the light source (Fig. 4.1).
    - The light source was powered and illumination took place, for a variety of duration of time (10 – 120 s).
    - When the designated illumination time ended, the light source was switched off.

- Using a PC interface, the spectrometer's detection process was initiated the moment the illumination ended, and 10 seconds later the aliquot containing the previously illuminated chloroplast sample was forcefully pipetted manually in the cuvette, thus resulting in the initiation of any potential chemiluminescence reaction between luminol and previously produced H_2O_2, in the presence of HRP.
- At the end of 1 min, the spectrometer would stop recording the intensity of the light detected, and would produce a file containing the light intensity recorded over time, in arbitrary units, every 100 ms, over 1 minute. Microsoft Office Excel 2003 was used to further analyse the data.

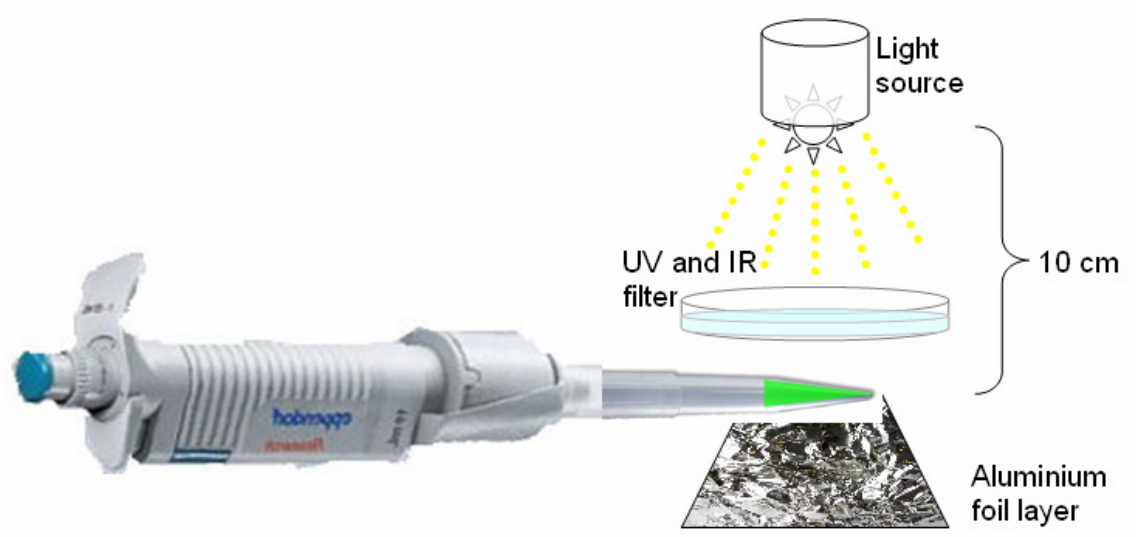

Figure 4.1 Schematic representation of the experimental setup for the illumination of chloroplasts by a halogen lamp.

The chloroplast sample is contained within the pipette tip, in order to allow for the fast transfer of the sample post-illumination to the cuvette with the HRP and luminol. Not to scale.

It should be noted that during the manipulation of the chloroplasts, the ambient light was restricted using the same methods employed in the general chemiluminescence assay, described in the standard chemiluminescence assay Materials and Methods (Section 3.2).

4.2.3 Results and discussion

Using the isolation procedures outlined in the Materials and Methods (Section 4.2.2.1), two different chloroplast preparations were obtained, coded Ch0a and Ch0b. Using these, a multitude of measurements was made with the aim to achieve, and optimise, the production of H_2O_2 by chloroplasts following illumination, and detection thereof. Some parameters were therefore altered between experiments, aiming to identify the optimal conditions for achieving an H_2O_2 production from chloroplasts.

4.2.3.1 Effect of different buffers on H_2O_2 production by chloroplasts

Different buffers were used to dilute the concentrated chloroplast preparations to the desired chlorophyll content concentration, prior to the illumination:

- Buffer "A1": 10 mM Tris-HCl, pH 8.5,
- Buffer "A2": 0.4 M sucrose, 10 mM Tris-HCl, pH 8.5,
- Buffer "B1": 10 mM MES-NaOH, pH 7.0,
- Buffer "B2": 0.4 M sucrose, 10 mM MES-NaOH, pH 7.0.

This was an attempt to investigate not only the effect of different buffers with different pH on the production of hydrogen peroxide, but also importantly of different osmolarities. Both isolation protocols require the chloroplasts to be stored in buffers with a high concentration of a sugar, in order to achieve the osmotic balance between the internal and external environments of a chloroplast's wall. This balance therefore removes the osmotic forces that would otherwise cause the chloroplasts to swell or loose volume, depending on the osmolarity in relation to the external environment. This effect is common to most biological membranes, as the osmotic forces are a means of allowing for intra-extra membrane communication, exchange of analytes etc.

The results of using the different dilution buffers on the production of H_2O_2 by the two different chloroplast preparations, as measured by the chemiluminescence detection of any produced H_2O_2, are presented in Table

4.1. As it can be seen from the results presented, no chemiluminescence signal was obtained, suggesting that no H_2O_2 was produced by the chloroplasts or successfully detected following the production.

Table 4.1 Peak signal intensity (background subtracted) obtained from the HRP-mediated luminol chemiluminescence with H_2O_2 provided by illuminated chloroplasts diluted in different buffers.

	Chemiluminescence signal intensity	
Buffer	**Chloroplasts Ch0a**	**Chloroplasts Ch0b**
Buffer "A1"	None detected	None detected
Buffer "A2"	None detected	None detected
Buffer "B1"	None detected	None detected
Buffer "B2"	None detected	None detected

The signal intensities presented, detected by a bench-top spectrophotometer, resulted from the production of light by the cuvette-based chemiluminescence reaction of luminol, HRP and H_2O_2. [HRP] = 5 U/ml, [luminol] = 100 µM, in Tris-HCl buffer (10 mM, pH 8.5). Any H_2O_2 present was previously produced by illuminating the two different preparations of chloroplasts with a halogen lamp (20 watts, 350 lumens) at a distance of 10 cm for 1 min, while aspirated in a semi-transparent pipette tip. The chloroplast preparations were diluted in the following buffers: buffer "A1" (10 mM Tris-HCl buffer, adjusted to pH 8.5), buffer "A2" (0.4 M sucrose, 10 mM Tris-HCl buffer, adjusted to pH 8.5), buffer "B1" (10 mM MES, brought to pH 7.0 with NaOH) and buffer "B2" (0.4 M sucrose, 10 mM MES, brought to pH 7.0 with NaOH). Chloroplasts were diluted to achieve a chlorophyll content of 0.1 mg/ml. Average values shown are the results of 3 replicates.

4.2.3.2 Effect of different dilution factors on H_2O_2 production by chloroplasts

In order to initiate the process of potentially identifying the quantity of chloroplasts that would produce a high H_2O_2 concentration with respect to the absorbance of light inherent to the chloroplasts due to their colour and non-transparency, i.e. optical density, the following investigation was performed.

Various dilutions of the isolated chloroplasts were tested for the illumination-induced production of H_2O_2:

- Dilution A: Adjusted by volume to chlorophyll content 0.284 mg/ml,

- Dilution B: Adjusted by volume to chlorophyll content 0.05 mg/ml,
- Dilution C: Adjusted by volume to chlorophyll content 0.1 mg/ml,
- Dilution D: Adjusted by volume to chlorophyll content 0.5 mg/ml.

The results of using the different dilution factors on the production of H_2O_2 by the two different chloroplast preparations, as measured by the chemiluminescence detection of any produced H_2O_2, are presented in Table 4.2. As it can be seen from the results presented, no chemiluminescence signal was obtained, suggesting that no H_2O_2 was produced by the chloroplasts or successfully detected following the production.

Table 4.2 Peak signal intensity (background subtracted) obtained from the HRP-mediated luminol chemiluminescence with H_2O_2 provided by illuminated chloroplasts diluted in different degrees.

Chloroplast concentration	Chemiluminescence signal intensity	
	Chloroplasts Ch0a	Chloroplasts Ch0b
Dilution A	None detected	None detected
Dilution B	None detected	None detected
Dilution C	None detected	None detected
Dilution D	None detected	None detected

The signal intensities presented, detected by a bench-top spectrophotometer, resulted from the production of light by the cuvette-based chemiluminescence reaction of luminol, HRP and H_2O_2. [HRP] = 5 U/ml, [luminol] = 100 µM, in Tris-HCl buffer (10 mM, pH 8.5). Any H_2O_2 present was previously produced by illuminating the two different preparations of chloroplasts with a halogen lamp (20 watts, 350 lumens) at a distance of 10 cm for 1 min, while aspirated in a semi-transparent pipette tip. The chloroplast preparations were diluted in buffer "A2" (0.4 M sucrose, 10 mM Tris-HCl buffer, adjusted to pH 8.5), in four different dilutions (A: [chlorophyll] = 0.284 mg/ml, B: [chlorophyll] = 0.05 mg/ml, C: [chlorophyll] = 0.1 mg/ml and D: [chlorophyll] = 0.5 mg/ml. Average values shown are the results of 3 replicates.

4.2.3.3 Effect of different illumination times on H_2O_2 production by chloroplasts

It was expected that varying the duration of the illumination process would be affecting the amount of H_2O_2 produced by chloroplasts. Therefore, during the

step of the illumination of chloroplasts, different durations of illumination were employed:

- 10 s
- 20 s
- 60 s
- 120 s.

The results of using the different illumination times on the production of H_2O_2 by the two different chloroplast preparations, as measured by the chemiluminescence detection of any produced H_2O_2, are presented in Table 4.3. As it can be seen from the results presented, no chemiluminescence signal was obtained, suggesting that no H_2O_2 was produced by the chloroplasts or successfully detected following the production.

Table 4.3 Peak signal intensity (background subtracted) obtained from the HRP-mediated luminol chemiluminescence with H_2O_2 provided by illuminated chloroplasts illuminated for different times.

Illumination duration	Chemiluminescence signal intensity	
	Chloroplasts Ch0a	Chloroplasts Ch0b
10 s	None detected	None detected
20 s	None detected	None detected
60 s	None detected	None detected
120 s	None detected	None detected

The signal intensities presented, detected by a bench-top spectrophotometer, resulted from the production of light by the cuvette-based chemiluminescence reaction of luminol, HRP and H_2O_2. [HRP] = 5 U/ml, [luminol] = 100 µM, in Tris-HCl buffer (10 mM, pH 8.5). Any H_2O_2 present was previously produced by illuminating the two different preparations of chloroplasts with a halogen lamp (20 watts, 350 lumens) at a distance of 10 cm, while aspirated in a semi-transparent pipette tip. The chloroplast preparations were diluted in buffer "A2" (0.4 M sucrose, 10 mM Tris-HCl buffer, adjusted to pH 8.5), with a [chlorophyll] = 0.1 mg/ml. The illumination duration was varied between 10 – 120 s. Average values shown are the results of 3 replicates.

4.2.3.4 Effect of the addition of H_2O_2 'spikes' to chemiluminescence signal

Following the inability to detect a chloroplast-derived H_2O_2 chemiluminescence signal, measurements were taken when illuminated as well as non-illuminated chloroplasts were spiked with known H_2O_2 concentrations, in order to observe whether the chemiluminescence reaction that was expected to be taking place with the added H_2O_2 would be detected. It was observed that adding known concentrations of H_2O_2 (0.1 µM - 10 µM) in the final chloroplast sample, even when omitting the illumination step, did not produce any chemiluminescence signal; results are presented in Table 4.4.

Table 4.4 Signal intensity (background subtracted) obtained from the HRP-mediated luminol chemiluminescence with H_2O_2 provided by illuminated chloroplasts illuminated with added H_2O_2 in sample.

Added H_2O_2 (µM)	Chemiluminescence signal intensity			
	Chloroplasts Ch0a		Chloroplasts Ch0b	
	Illuminated	Non- Illuminated	Illuminated	Non- Illuminated
0.1	N/D	N/D	N/D	N/D
1	N/D	N/D	N/D	N/D
10	N/D	N/D	N/D	N/D

The signal intensities presented, detected by a bench-top spectrophotometer, resulted from the production of light by the cuvette-based chemiluminescence reaction of luminol, HRP and H_2O_2. [HRP] = 5 U/ml, [luminol] = 100 µM, in Tris-HCl buffer (10 mM, pH 8.5). The H_2O_2 present was an added 'spike' of known H_2O_2 samples of 0.1 – 10 µM (final concentration) in the Non-illuminated samples, or potentially also from the chloroplasts in the case of the illuminated samples. The chloroplast preparations were diluted in buffer "A2" (0.4 M sucrose, 10 mM Tris-HCl buffer, adjusted to pH 8.5), with a [chlorophyll] = 0.1 mg/ml. Average values shown are the results of 3 replicates. N/D: None detected.

Absorption of the blue light produced during luminol chemiluminescence by chloroplasts was considered as a possible inhibiting factor. An absorbance scan of a chloroplast sample does reveal that a peak of absorbance lies in the region very close to the peak obtained from the chemiluminescence of luminol (Fig. 4.2), thus making the hypothesis plausible.

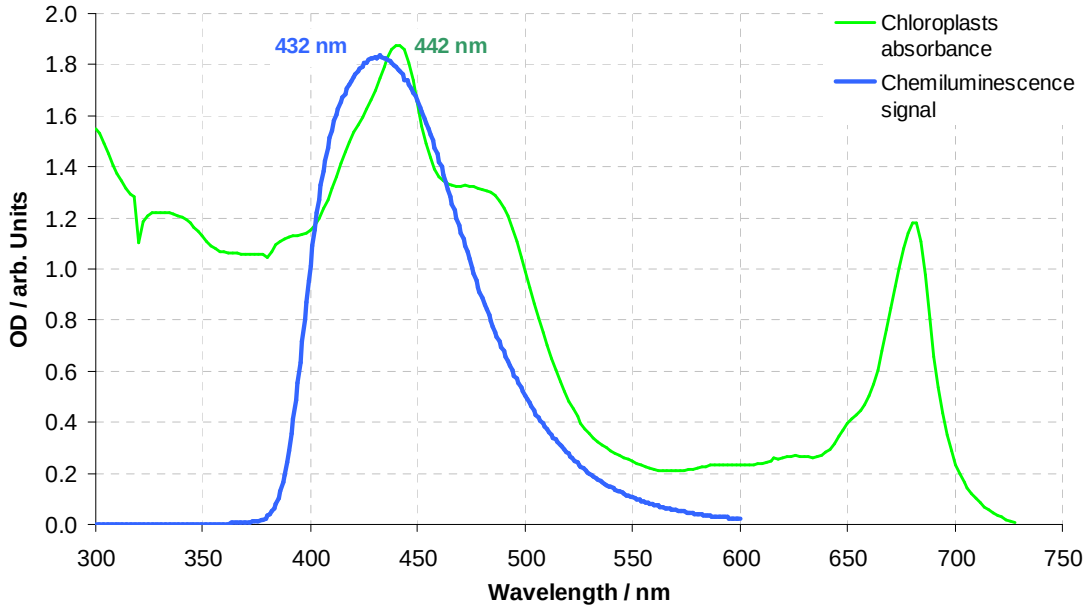

Figure 4.2 Absorbance scan of a chloroplast sample.

The chlorophyll content of the chloroplasts sample was 0.2837 mg/ml. The blue trace represents the luminol chemiluminescence signal spectrum distribution.

However, repeating the measurements presented in Table 4.4 having removed by centrifugation the chloroplasts following the addition of the H_2O_2 spikes but prior to the chemiluminescence assay gave no signal. The same absence of signal was observed when the centrifuged chloroplasts' supernatant was then spiked with H_2O_2, following the centrifugation step.

Osmotically breaking up the chloroplasts post-illumination, and thus releasing their content, and then measuring the chemiluminescence signal achieved and detected using the standard methodology still failed to produce any chemiluminescence signal.

4.2.4 Conclusions

As it can be seen from the results presented in Section 4.2.3, no chemiluminescence signal was detected following the illumination of isolated chloroplasts, under a variety of different conditions. More importantly, the results presented in Section 4.2.3.4 suggest that it is likely that the

chemiluminescence response is influenced not by quenching of the light emission, but by elimination of the H_2O_2. It has been found that this affects added H_2O_2, and therefore possibly any H_2O_2 produced by the chloroplasts as well. It appears to be an effect inherent in the chloroplasts preparations, not necessarily within the chloroplasts however, as the scavenging / quenching of added H_2O_2 is observed when using the chloroplasts preparations' supernatant as well as when the chloroplasts are osmotically broken. A final remark is that a catalase-type activity is present in the chloroplast preparations. In the literature review (Section 2.2.1.3) it is explained in detail that under normal or stress conditions, plant cells (and animal cells) use complex means to remove H_2O_2 and every other type of radical oxygen species that is produced. Catalase is an enzyme present in the cells of plants, animals and aerobic bacteria. It promotes the conversion of hydrogen peroxide to water and molecular oxygen:

$2H_2O_2$ to $2H_2O + O_2$

Catalase also uses hydrogen peroxide to oxidise toxins including phenols, formic acid, formaldehyde and alcohols.

$H_2O_2 + RH_2$ to $2H_2O + R$

In order to achieve the production of H_2O_2 by photosynthetic plant material, alternative preparations would therefore have to be considered.

4.3 Bench-top batch assay for the detection of H_2O_2 produced by illuminated thylakoids using HRP-mediated luminol chemiluminescence

4.3.1 Introduction

Following the inability to obtain any detection of H_2O_2 produced by chloroplasts, it became necessary to find alternative means of obtaining a chemiluminescence signal produced by organelles that take part in the photosynthetic oxygen evolution. On the next lower 'level' of organisational complexity and completeness of structural organisation is the thylakoid, as graphically displayed in Fig. 4.3a and a photograph of a chloroplast with clearly

visible the stacks of thylakoids within, in Fig. 4.3b. Thylakoids have been used in the literature as the photosynthetic material of choice for H_2O_2 production studies [49], suggesting that catalase-like activity is not found in isolated thylakoids. Also, thylakoids are able to take part in the key photosynthetic oxygen evolution stages [37; 54; 137].

A review of the literature revealed some isolation protocols that featured repeatedly as the preferred isolation methods in many different peer-reviewed published research papers by a variety of groups [8; 9; 46-48; 48; 134; 138-147]. Based on these, and in order to optimise the isolation procedure, three distinctively different isolation protocols were tested, with two further variations of two of these protocols. All five different isolated thylakoid preparations were then tested for H_2O_2 production by illuminating them and then using the HRP-mediated luminol chemiluminescence reaction, in exactly the same way as in Section 4.2 with the chloroplasts. The effect, and optimisation, of a multitude of different experimental parameters were investigated; the results of these investigations make up the sub-sections under Section 4.3.3.

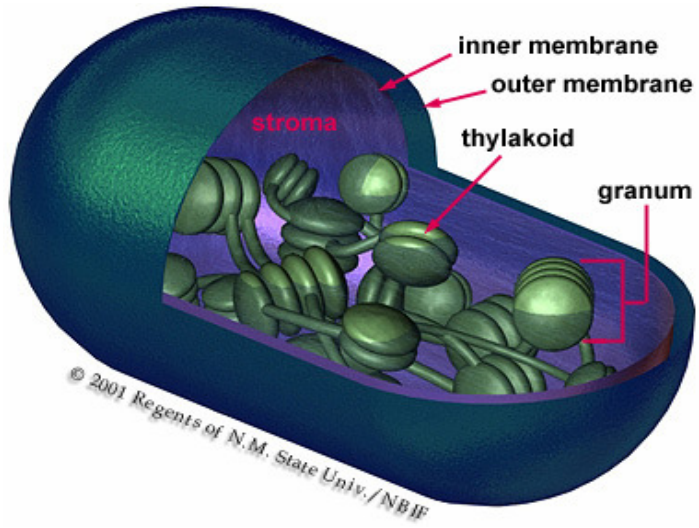

Figure 4.3a: Schematic representation of a chloroplast and the thylakoids within.

Figure 4.3b: Chloroplast cross-section, showing clearly the stacks of thylakoid disks. Photograph by A.D. Greenwood, then at Dept. of Botany, Imperial College London, circa early 1970s; scan by Dr. J. Nield. With permission.

Figure 4.3 Schematic and photographic representation of a chloroplast and the thylakoids within.

4.3.2 Materials and methods

In experiments testing for chemiluminescence signal potentially resulting from H_2O_2 produced by thylakoids, the setup and method were kept similar to the standard luminol-HRP-H_2O_2 cuvette assay as described in Section 3.2, apart from the H_2O_2 sample's origin, preparation and illumination steps. More specifically, the 330 µl of a known H_2O_2 concentration sample that was previously pipetted into a cuvette with 660 µl of luminol and HRP, was replaced by 330 µl of an isolated thylakoid-containing aliquot, as the aim of the experiments described in Section 4.3 was to identify and quantify the production of H_2O_2 by thylakoids.

4.3.2.1 Thylakoid isolation methods

Thylakoid preparations, as used in experiments described in Section 4.3, were made using five different protocols or variations thereof (Thylakoid Isolation Protocol 1, 2, 3, 4 and 5). Full step-by-step descriptions follow.

4.3.2.1.1 Thylakoid isolation protocol 1 (Ch1)

Thylakoid isolation was performed using a modification of a protocol described previously [148]. One hundred grams (fresh weight) of fresh baby spinach leaves (Tesco Stores Ltd., Cheshunt, Hertfordshire, UK, Bedford Branch) were washed with distilled water and homogenised in a blender, in 300 ml of extraction buffer (0.3 M mannitol, 30 mM tetrasodium pyrophosphate, 2 mM ethylenediaminetetraacedic acid (EDTA), 0.1% bovine serum albumin (BSA), pH 7.9). The homogenate was filtrated through sieves with a pore diameter of 100 µm. Centrifugation was performed for 1 min at 600 g at 4℃ (Model J2-21 centrifuge, Beckman, Germany). The pellet was resuspended in the rinsing buffer (0.3 M mannitol, 2 mM 4-morpholinepropanesulfonic acid (MOPS), 2 mM ethylene-diaminetetraacedic acid (EDTA), 0.1% bovine serum albumin (BSA), pH 7.9). The mixture was centrifuged for 1 min at 2000 g at 4℃. The pellet was resuspended in 100 ml of distilled water in order to disrupt the chloroplasts. The obtained thylakoid membranes were stirred for 10 s, and placed in the rinsing

buffer and further centrifuged for 2 min at 2000 g. The pellet was resuspended in the rinsing buffer. The final preparation was divided in 200 µl aliquots in Eppendorf tubes, immersed in liquid nitrogen, and then stored at -80℃. The buffers were at 4℃, the room temperature was 15℃, and the ambient light was kept at the bare minimum. The isolation was carried out post-sunset, in order to minimise the ambient light in the well-lit area of the centrifuge. All chemicals were from Sigma Chemical Company Ltd. (Gillingham, UK).

4.3.2.1.2 Thylakoid isolation protocol 2 (Ch2)

Thylakoid isolation was performed using a modification / combination of subsequent steps of protocols described previously in [135], [149] and [136]. One hundred grams (fresh weight) of fresh baby spinach leaves (Tesco Stores Ltd., Cheshunt, Hertfordshire, UK, Bedford Branch) were washed with distilled water, dried on filter paper and homogenised in a blender, in 300 ml of a partially frozen slurry of buffer No1 (0.33 M sorbitol, 0.02 mM $MgCl_2$, 20 mM MES, brought to pH 6.5 with NaOH). The homogenate was filtered through 2 layers of cheese cloth with an added 2 cm layer of cotton wool. The filtrate was centrifuged at 2200 g for 60 s at 4℃ (Model J2-21 centrifuge Beckman, Germany). The supernatant and the soft pellet were discarded and the pellet was resuspended in 250 ml of buffer No2 (0.33 M sorbitol, 0.5 mM Tris base, brought to pH 7.5 with HCl), and then centrifuged at 2200 g for 60 s. The supernatant and the soft pellet were discarded and the pellet was resuspended in a small volume (25 ml) of buffer No3 (0.33 M sorbitol, 1 mM KCl, 1 mM Magnesium acetate tetrahydrate, 0.5 mM Tris base, brought to pH 7.5 with HCl). The suspension was then incubated in a large volume (225 ml) of hypotonic medium, buffer No4 (5 mM $MgCl_2$) for 60 s, followed by the addition of an equal volume of buffer No5 (0.66 M sorbitol, 5 mM $MgCl_2$, 40 mM MES, brought to pH 6.5 with NaOH). The suspension was then centrifuged at 3000 g for 4 min. The pellet was resuspended in the final buffer (5 mM $MgCl_2$, 15 mM NaCl, 2 mM MES, brought to pH 6.9 with NaOH). The final preparation was divided in 200 µl aliquots in Eppendorf tubes, immersed in liquid nitrogen, and then stored at -80℃. The buffers were at 4℃, the room temperature was 15℃,

and the ambient light was kept at the bare minimum. The isolation was carried out post-sunset, in order to minimise the ambient light in the well-lit area of the centrifuge. All chemicals were from Sigma Chemical Company Ltd. (Gillingham, UK).

4.3.2.1.3 Thylakoid isolation protocol 3 (Ch3)

The thylakoid isolation was performed using the same protocol employed in the thylakoid isolation protocol 2, with a few changes; the first centrifugation step lasted 4 min, instead of 1 min, the second centrifugation step lasted 4 min, instead of 1 min and the third centrifugation step lasted 10 min instead of 4 min. All other details of steps taken were kept the same.

4.3.2.1.4 Thylakoid isolation protocol 4 (Ch4)

Thylakoid isolation was performed using a modification of a protocol described previously [150]. Fifty grams (fresh weight) of fresh baby spinach leaves (Tesco Stores Ltd., Cheshunt, Hertfordshire, UK, Bedford Branch) were washed with distilled water and homogenised in a blender, in 250 ml of buffer No1 (5 mM $MgCl_2$, 0.3 M sucrose, 1 mM EDTA, 1 mM PMSF (phenylmethylsulfonylfluoride), 20 mM Tricine, adjusted to pH 7.8 with NaOH). The homogenate was filtrated through 4 layers of cheesecloth. Centrifugation was performed for 2 min at 700 g at 4℃ (Model J2-21 centrifuge, Beckman, Germany) and the pellet was discarded. Another centrifugation was performed for 20 min at 7500 g, 4℃ and the supernatant was discarded. The pellet was suspended with 200 ml buffer No2 (5 mM $MgCl_2$, 70 mM sucrose, 1 mM PMSF (phenylmethylsulfonylfluoride), 20 mM Tricine, adjusted to pH 7.8 with NaOH). After another centrifugation for 20 min, at 7500 g, 4℃, the supernatant was discarded. The pellet was suspended with minimum quantity of buffer No2, divided in 200 µl aliquots in Eppendorf tubes, immersed in liquid nitrogen, and then stored at -80℃. The buffers were at 4℃, the room temperature was 15℃, a nd the ambient light was kept at the bare minimum. The isolation was carried out post-sunset, in order to minimise the ambient light in the well-lit area of the centrifuge. All chemicals were from Sigma Chemical Company Ltd. (Gillingham, UK).

4.3.2.1.5 Thylakoid isolation protocol 5 (Ch5)

The thylakoid isolation was performed using the same protocol employed in the thylakoid isolation protocol 4, with one change: the protease inhibitor PMSF was not included in buffer No1 or buffer No2.

4.3.2.2 Thylakoid illumination and chemiluminescence H_2O_2 detection methodology

Basic chemicals and reagents used (luminol, HRP and preparations thereof) were the same as described in 4.2.2.2. The additional buffers prepared, used in 4.3.3.3, were buffer B (5 mM $MgCl_2$, 15 mM NaCl, 2 mM MES, brought to pH 6.9 with NaOH), buffer C (5 mM $MgCl_2$, 70 mM sucrose, 1 mM PMSF, 20 mM Tricine, adjusted to pH 7.8 with NaOH) and buffer D (5 mM $MgCl_2$, 70 mM sucrose, 20 mM Tricine, adjusted to pH 7.8 with NaOH). The pipette tips used in Section 4.3.3.5 were the Fisherbrand 'Blue' and 'Natural' polypropylene 200 µl to 1,000 µl tips (Thermo Fisher Scientific Ltd., Loughborough, UK).

The experiments described in the current section, 4.3, were based on the HRP-mediated luminol chemiluminescence reaction in cuvettes using a bench-top spectrometer, with the H_2O_2 required for the reaction being provided by illuminated isolated thylakoid-containing samples. It is therefore a variation of the experimental process of detecting known H_2O_2 samples using chemiluminescence, as described in Section 3.2. The sequence of actions that formed a single measurement was based on that described in Section 3.2, with the crucial illumination of the sample as an added step.

The steps thus followed are:

- 330 µl of luminol (100 µM) in Tris-HCl buffer (10 mM, pH 8.5) and 330 µl of HRP (5 Units/ml) in Tris-HCl buffer (10 mM, pH 8.5) were added in a Kartell disposable semi-micro optical polystyrene cuvette (Thermo Fisher Scientific Ltd., Loughborough, UK), in a time window of 1 hour before the experiment to follow.

- The cuvette with 660 µl of luminol and HRP in Tris-HCl buffer (10 mM, pH 8.5, unless otherwise stated) was placed in the sample holding compartment of a Cary Eclipse fluorescence spectrophotometer (Varian UK Ltd., Oxford, UK). The spectrometer was set up, via the use of its bespoke software, to record the intensity of detected light over 60 seconds.
- In order to induce the production of H_2O_2 by the thylakoids, the sample illumination step was undertaken:
    - The previously isolated thylakoid preparation was diluted in a desired buffer in order to form the measuring sample.
    - A 330 µl diluted sample was aspirated in a pipette tip attached to an air-displacement pipette.
    - The pipette was placed in close proximity to the light source, with the exact distance varying depending on the source.
    - The light source was powered and illumination took place, for the desired duration of time.
    - When the designated illumination time ended, the light source was switched off.
- Using a PC interface, the spectrometer's detection process was initiated the moment the illumination ended, and 10 seconds later the aliquot containing the previously illuminated chloroplast sample was forcefully pipetted manually in the cuvette, thus resulting in the initiation of any potential chemiluminescence reaction between luminol and H_2O_2, in the presence of HRP.
- At the end of 1 min, the spectrometer would stop recording the intensity of the light detected, and would produce a file containing the light intensity recorded over time, in arbitrary units, every 100 ms, over 1 minute. Microsoft Office Excel 2003 was used to further analyse the data.

The illumination step was performed using alternative light sources, or variations thereof. The different light sources used to illuminate the thylakoids were:

- The JC12V20W halogen lamp (20 watts, 350 lumens)(EiKO Ltd. Kansas, USA)
- The above lamp but covered with semi-transparent coloured sheets, normally used in light engineering (LEF-64SET, Farnell Ltd, Leeds, UK)
- A laser-diode light source (630-680 nm, rated output wattage: 1 mW) (source and make unknown).

When the JC12V20W halogen lamp was employed, with or without the coloured filters, the experimental setup used was as portrayed in Fig. 4.4. The pipette was placed 10 cm underneath the lamp, with a borosilicate Pyrex glass Petri dish (SciLabware Ltd, Stone UK) containing water in between the pipette tip containing the sample, and the light source.

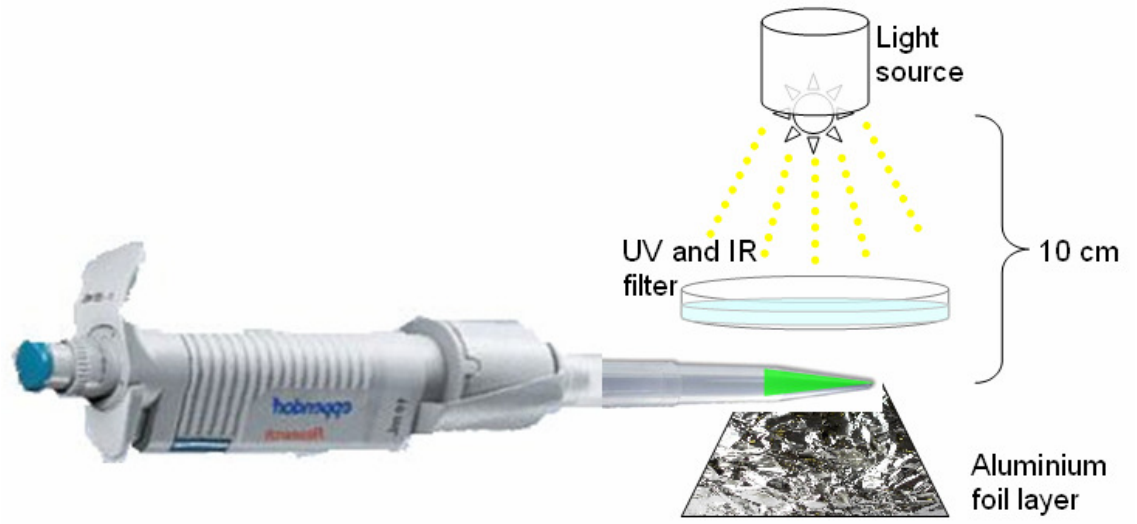

Figure 4.4 Schematic representation of the experimental setup for the illumination of thylakoids by a halogen lamp step.

The thylakoid sample is contained within the pipette tip, in order to allow for the fast transfer of the sample post-illumination to the cuvette with the HRP and luminol. Not to scale.

When the laser diode was used to illuminate the thylakoid preparation, the set-up could not be kept the same as with the halogen light source, but had to be re-designed, due to the limited spread of light inherent in laser technology. The

chosen setup during the illumination with the laser light source can be seen in Figure 4.5.

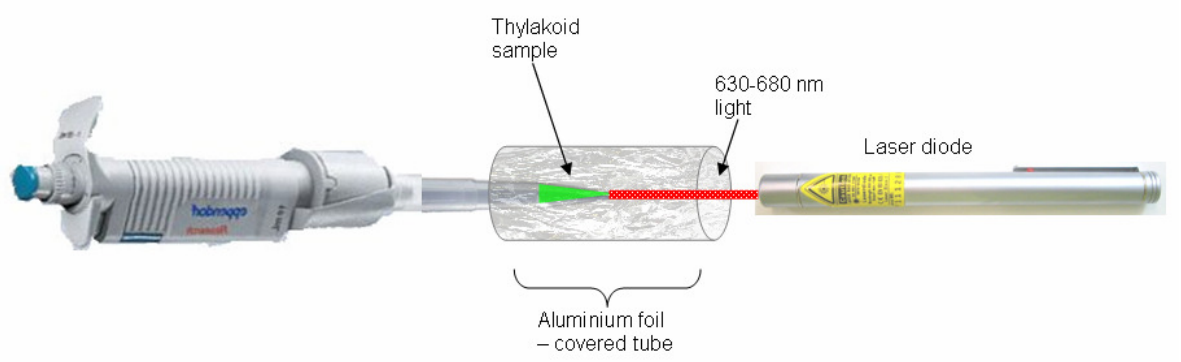

Figure 4.5 Schematic representation of the experimental setup for the illumination of thylakoids by a laser diode.

The thylakoid sample is contained within the pipette tip, in order to allow for the fast transfer of the sample post-illumination to the cuvette with the HRP and luminol. Not to scale.

It should be noted that during the manipulation of the thylakoids, the ambient light was restricted using the same methods employed in the general chemiluminescence assay, described in the standard chemiluminescence assay Materials and Methods (Section 3.2).

4.3.3 Results and discussion

Using the experimental procedure outlined in the Materials and Methods, five different thylakoid preparations were obtained by using the five different isolation protocols; the resulting thylakoid preparations were code-named Ch1, Ch2, Ch3, Ch4 and Ch5.

According to Whatley [151], three different properties of light may separately affect the metabolism and development of a plant: its spectral quality, its intensity and its duration. The response produced depends initially on the receptive pigment, which determines the wavelengths of light which are absorbed, and secondarily

on the intensity and duration of illumination. It was therefore decided to investigate these parameters.

Using the five different thylakoid preparations, a multitude of measurements was made with the aim to achieve, and optimise, the production of H_2O_2 by thylakoids following illumination, and detection thereof. Some parameters were therefore investigated and altered between experiments, aiming to identify the optimal. These parameters were:

- the illumination time
- the amount of thylakoids being illuminated, as represented by the chlorophyll concentration
- the buffer used during the illumination
- the distance between the light source and the thylakoids
- the pipette tip used to hold the thylakoids during the illumination and
- the light source used to illuminate the thylakoids.

The results presented below show the H_2O_2 production yields from the different thylakoid preparations, when altering one key parameter, while keeping the other experimental parameters constant or optimised.

4.3.3.1 Investigation of the effect of different illumination times on the H_2O_2 production by thylakoids

It was important to examine the effect of changing the illumination time on the production of H_2O_2 by the different thylakoid samples. A wide range of times from 0 to 15 min was investigated in order to identify any patterns. Therefore, samples of all five different thylakoid preparations were illuminated, keeping all experimental parameters constant, apart from the length of time that the illumination took place, before detecting the production of H_2O_2, using the standard chemiluminescence reaction. The results obtained can be seen in Figure 4.6.

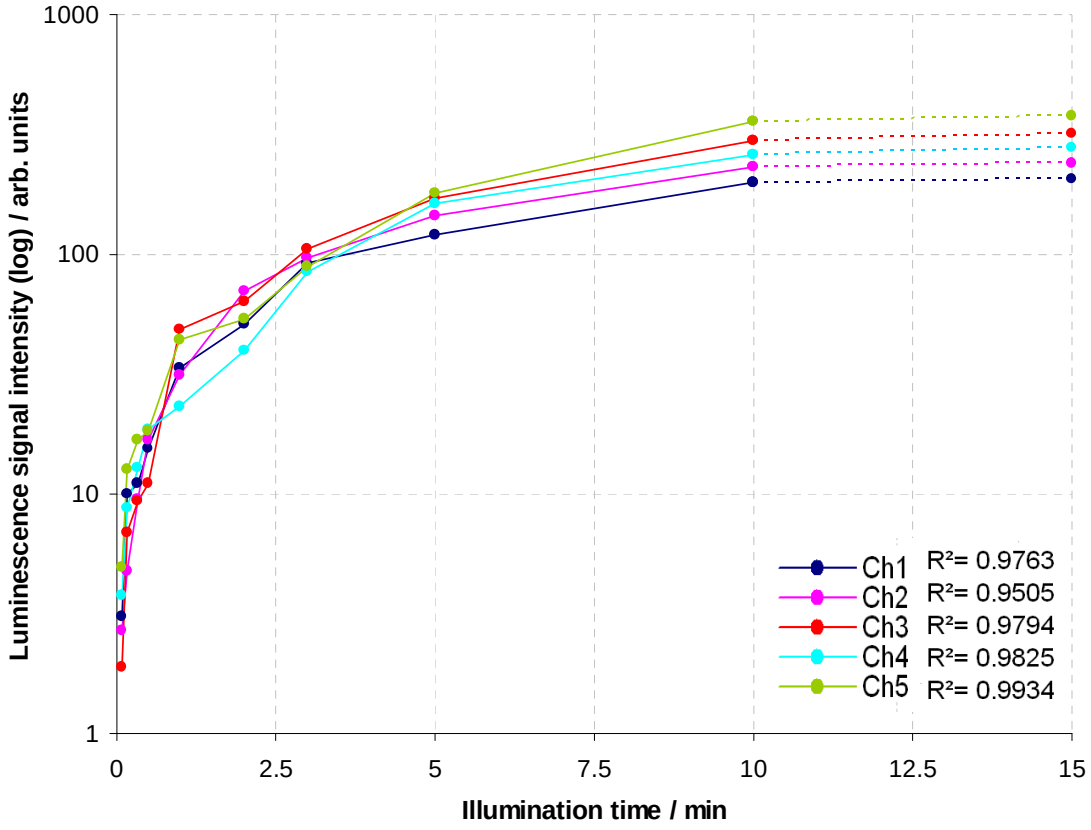

Figure 4.6 Effect of illumination time on the production of H_2O_2 by different thylakoid preparations.

The luminescence signal, detected by a bench-top spectrophotometer, resulted from the production of light by the cuvette-based chemiluminescence reaction of luminol, HRP and H_2O_2. [HRP] = 5 U/ml, [luminol] = 100 µM, in Tris-HCl buffer (10 mM, pH 8.5). The H_2O_2 was previously produced by illuminating diluted thylakoid preparations with an un-filtered halogen lamp (20 watts, 350 lumens) at a distance of 10 cm while aspirated in a pipette tip, for an illumination time of 0 – 15 min. The Ch1 thylakoid preparation ([chlorophyll] = 284 µg/ml) and the Ch3 thylakoid preparation ([chlorophyll] = 237 µg/ml) were diluted in buffer B (5 mM $MgCl_2$, 15 mM NaCl, 2 mM MES, brought to pH 6.9 with NaOH). The Ch2 thylakoid preparation ([chlorophyll] = 171 µg/ml), the Ch4 thylakoid preparation ([chlorophyll] = 131 µg/ml) and the Ch5 thylakoid preparation ([chlorophyll] = 64 µg/ml) were diluted in buffer A (10 mM Tris-HCl buffer, adjusted to pH 8.5). Average values and the SDs shown are the results of 3 replicates. The R^2 values have been calculated only for the time period 0-10 min.

It is known, that, the greater the duration of illumination the more photosynthesis will, in general, be accomplished, under normal physiological conditions [151]. It can be observed from the results, that, increasing the length of illumination time resulted in an increase of H_2O_2 being produced, although, after 10 minutes of illumination, there appears to be no more H_2O_2 being produced.

This could be the result of, at some point in time between 10 and 15 min, the rate of H_2O_2 production being reduced to zero, or it could be that H_2O_2 quenching is taking place. It is known from the literature [152] that increased illumination time results in degradation of thylakoids and other sub-chloroplast particles. What is more, H_2O_2 photoproduction by spinach thylakoids has been shown to cease after approximately 10 minutes of continuous illumination in isolated thylakoids (17 µg chlorophyll / cm^3), illuminated by white light (200 W / m^2). The generation of highly active oxygen species during electron transport, and resulting thylakoid inactivation, has been suggested as the cause [137].

In order to therefore ensure the integrity of thylakoids, particularly for the purpose of the detection of herbicides in later experiments, it was decided not to extend the illumination time longer than 10 min, as the production of H_2O_2 would not be reliably correlated to the effect of herbicides, as other physiological processes may be affecting the production.

As it can be seen, the increase of H_2O_2 production over time differed for the different thylakoid preparations. The relationship is linear, with the R^2 values very close to 1 for the first 10 minutes of illumination.

4.3.3.2 Investigation of the effect of different chlorophyll concentrations on the H_2O_2 production by thylakoids

The production of H_2O_2 by the different thylakoid preparations was tested over a range of dilutions, in order to identify the optimal thylakoid concentration for each different thylakoid preparation, as well as to then also identify the overall better performing thylakoid preparation against the other preparations. The chlorophyll concentration was used as the indirect descriptor parameter to characterise the different final amounts of thylakoids tested, expressed in µg/ml. Different dilutions of the five different thylakoid preparations were illuminated in order to induce the production of H_2O_2, which was then detected using the HRP-mediated luminol chemiluminescence reaction. All steps were conducted

using the standard operating procedure as described in the Methods (Section 4.3.2.2). The results can be seen in Fig. 4.7 below.

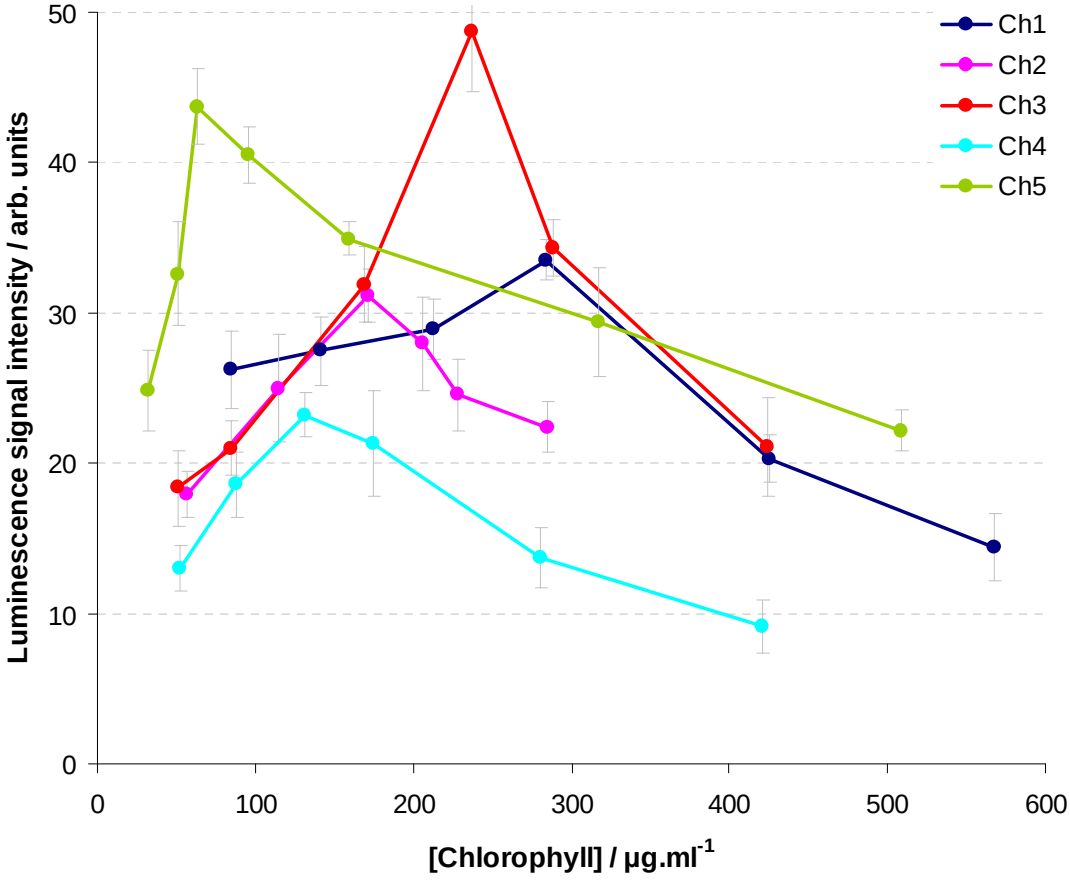

Figure 4.7 Effect of thylakoid concentration (reported as chlorophyll concentration) used during the illumination of different thylakoid preparations on the production and detection of H_2O_2.

The luminescence signal, detected by a bench-top spectrophotometer, resulted from the production of light by the cuvette-based chemiluminescence reaction of luminol, HRP and H_2O_2. [HRP] = 5 U.ml-1, [luminol] = 100 µM, in Tris-HCl buffer (10 mM, pH 8.5). The H_2O_2 was previously produced by illuminating different dilutions of thylakoid preparations with an un-filtered halogen lamp (20 watts, 350 lumens) at a distance of 10 cm for 1 min, while aspirated in a 'white' semi-transparent pipette tip. The thylakoid preparations were diluted in the following buffers: Ch1 thylakoid preparation and the Ch3 thylakoid preparation were diluted in buffer B (5 mM $MgCl_2$, 15 mM NaCl, 2 mM MES, brought to pH 6.9 with NaOH). The Ch2 thylakoid preparation, the Ch4 thylakoid preparation and the Ch5 thylakoid preparation were diluted in buffer A (10 mM Tris-HCl buffer, adjusted to pH 8.5). Average values and the SDs shown are the results of 3 replicates.

While keeping other experimental parameters constant or optimised, it can be seen that, for all different thylakoid preparations, varying the amount of thylakoids illuminated resulted in varying amounts of H_2O_2 being produced and/or detected. The different thylakoid preparations did behave differently, but no differences in H_2O_2 production of the order of $x10^1$ or more were observed; the difference between the lowest (Ch4) and highest (Ch3) maxima was only approximately two-fold, from about 25 a.u. to 50 a.u. This suggests that the isolation protocols employed for all different thylakoid preparations have been relatively optimised throughout the many decades of their use by scientists, and thus resulting in relatively non-discriminatory formulations.

For each thylakoid preparation separately, it can be seen that increasing the amount of thylakoids illuminated did also result in an increase of H_2O_2 being produced and detected up to a point, while further increase of the thylakoid concentration seemingly resulted in a decrease of the H_2O_2 being produced and detected. This was observed independently for all five different thylakoid preparations, with the concentration of chlorophyll where the decrease in chemiluminescence signal starts, being different for each thylakoid preparation.

As each measurement employs two main stages (the illumination, and thus production of H_2O_2) and the chemiluminescence detection of produced H_2O_2, the decrease in signal could be attributed to either of those two stages. There is little knowledge that could be gained on the characteristics of the production of H_2O_2 by the thylakoids, and specifically how varying the concentration of thylakoids affects the said production, particularly how and why increasing the thylakoid concentration may affect negatively the H_2O_2 production, without the use of equipment, skills and knowledge that were not readily present when the work was taking place. Focus was therefore placed on the second stage of a measurement, namely the chemiluminescence detection of the produced H_2O_2.

With the second stage of a measurement being the H_2O_2 detection after its production by illuminated thylakoids, it was considered a possibility that the

reduction in chemiluminescence signal could be associated with the detection of H_2O_2 instead. It is likely, that an increase in the concentration of thylakoids while the chemiluminescence light production is taking place in the cuvette, also results in an increase of the absorption due to the thylakoids in the sample that is higher than the increased H_2O_2 production due to same increased thylakoid concentration.

As it can be seen from Fig. 4.8, thylakoid preparations do absorb a significant amount of light in the blue region. That is because chlorophyll absorbs most of the red and blue part of the spectrum and transmits the green, and hence appears green. As luminol chemiluminescence peaks at approx 432 nm, the blue light emitted during the H_2O_2 detection falls within one of the absorbance peaks of the thylakoid samples.

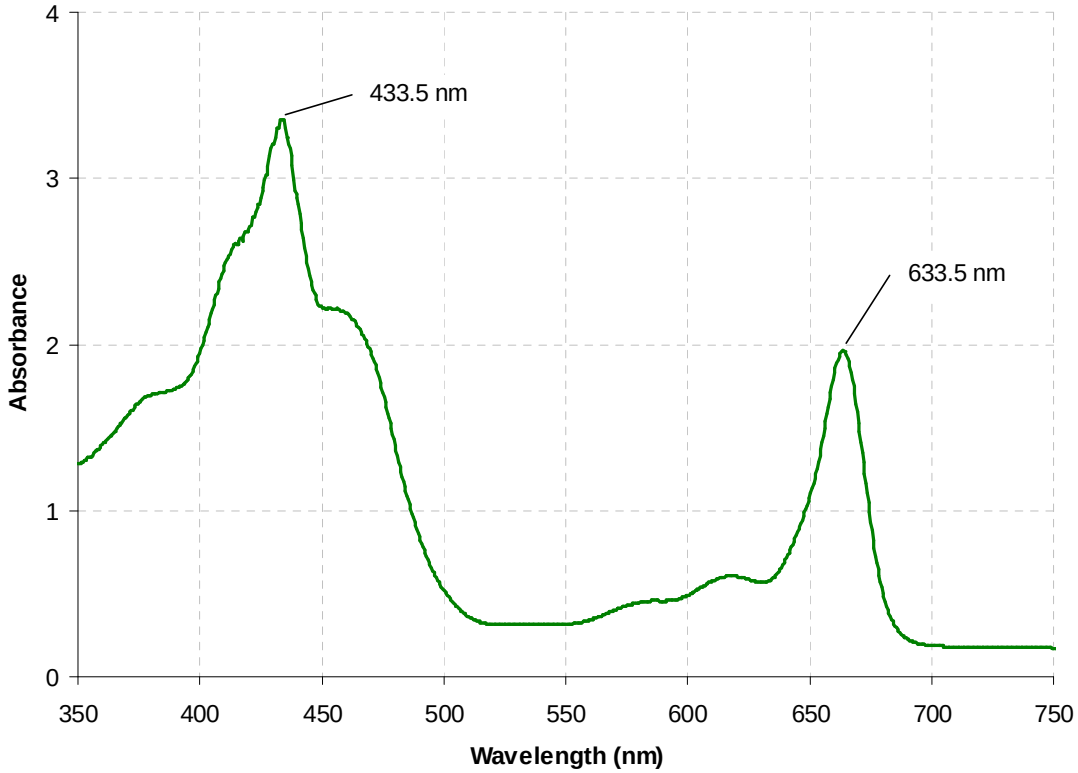

Figure 4.8 Wavelength absorbance scan of a thylakoid sample (chlorophyll content 0.4 mg/ml).

In order to investigate this possibility, measurements were made with known concentrations of H_2O_2 being 'spiked' with illuminated and non-illuminated thylakoid preparations. The results of these measurements can be seen in Figure 4.9.

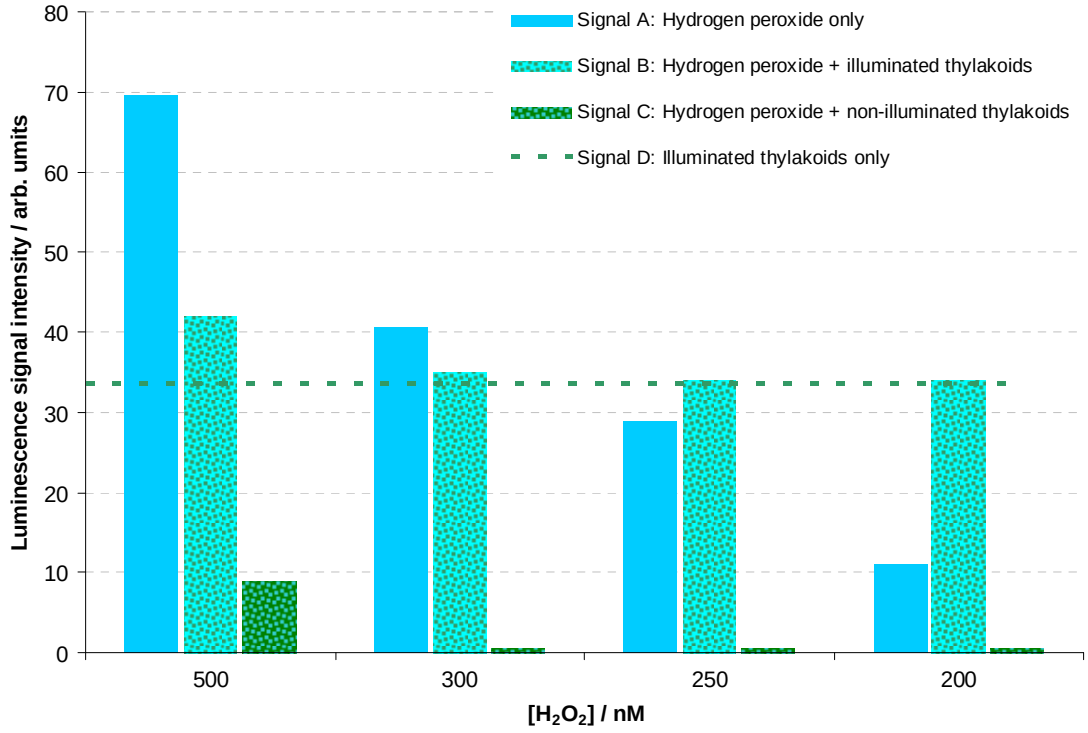

Figure 4.9 Effect of thylakoid absorption on the detectability of H_2O_2 from a standard sample or resulting from the illumination of thylakoids.

Signal A: light intensity output from the cuvette-based chemiluminescence reaction of known H_2O_2 sample ([H_2O_2] = 200 – 500 nM) with luminol and HRP ([HRP] = 5 U.ml-1, [luminol] = 100 µM, detected by a bench-top spectrophotometer.
Signal B: light intensity output from the cuvette-based chemiluminescence reaction of known H_2O_2 sample ([H_2O_2] = 200 – 500 nM) with luminol and HRP ([HRP] = 5 U.ml-1, [luminol] = 100 µM, detected by a bench-top spectrophotometer, in the presence of illuminated thylakoids (Ch1, [chlorophyll] = 284 $\mu g.ml^{-1}$). The Ch1 thylakoid preparation was illuminated with an un-filtered halogen lamp (20 watts, 350 lumens) at a distance of 10 cm for 1 min, while aspirated in a 'white' semi-transparent pipette tip.
Signal C: light intensity output from the cuvette-based chemiluminescence reaction of known H_2O_2 sample ([H_2O_2] = 200 – 500 nM) with luminol and HRP ([HRP] = 5 U.ml-1, [luminol] = 100 µM, detected by a bench-top spectrophotometer, in the presence of non-illuminated thylakoids (Ch1, [chlorophyll] = 284 $\mu g.ml^{-1}$)
Signal D: light intensity output from the cuvette-based chemiluminescence reaction of luminol, HRP and H_2O_2. [HRP] = 5 U.ml-1, [luminol] = 100 µM, in Tris-HCl buffer. The H_2O_2 was previously produced by illuminating diluted thylakoid preparation (Ch1 [chlorophyll] = 284 $\mu g.ml^{-1}$) with an un-filtered halogen lamp (20 watts, 350 lumens) at a distance of 10 cm for 1 min, while aspirated in a 'white' semi-transparent pipette tip. All reagents and samples used were made in Tris-HCl buffer (10 mM, pH 8.5).

From the results presented in Figure 4.9, it can be observed that the thylakoids' pigmentation and density did indeed result in absorption of the chemiluminescence-derived light, therefore not allowing some of it to be detected. A 500 nanomolar H_2O_2 sample, which on its own gave a chemiluminescence signal of approximately 70 arbitrary units (signal A on graph), when mixed with a non-illuminated thylakoid sample equivalent to a chlorophyll concentration of approx. 284 µg/ml, was reduced to giving a chemiluminescence signal of only 10 units (signal C). When the same thylakoid sample was illuminated for 1 min without any added H_2O_2, it gave a signal of 34 units (signal D), while when illuminated with the same 500 nM H_2O_2 sample, the signal rose to about 42 units (signal B). Signal B appears to be the equivalent of adding signals C and D, which seems logical, as it is essentially a combination of the two experiments (result of the known H_2O_2 sample in the presence of thylakoids [signal C], and result of illuminating those same thylakoids [signal D]).

For lower concentrations of known H_2O_2, which resulted, on their own, in lower chemiluminescence signals, the addition of same non-illuminated thylakoid sample resulted in complete inhibition of the chemiluminescence signal, by 'masking' it, due to absorption. However, when the same thylakoid sample was illuminated, it gave almost the same chemiluminescence signal of about 34 units with or without the presence of those smaller (300 nM or less) H_2O_2 samples. What this suggests is that a sample of Ch1 isolated thylakoids, diluted to a concentration of 284 µg/ml chlorophyll, produces, after illumination for 1 min, the equivalent of 1.2 µM H_2O_2. This is based on the observation that the H_2O_2 sample of 500 nM giving a chemiluminescence signal of 70 units (signal A) fell to 10 units when adding that same amount of thylakoids (signal C); therefore for a signal (D) of 33.5 units suffering from the same absorption effect, the equivalent amount of un-absorbed H_2O_2 ought to have been in the 1.2 micromolar region. This is also supported by the fact that, for smaller concentrations of H_2O_2 being tested with illuminated thylakoids, the signal (B) obtained is almost constant, suggesting that it is primarily resulting from the

thylakoids-produced H_2O_2, and that this is not near the 500 nM concentration, but larger enough in order for its signal not be masked due to the absorption by the thylakoids.

4.3.3.3 Investigation of the effect of different buffers on the H_2O_2 production by thylakoids

As described in the isolation protocols (Section 4.3.2.1), different buffers have been described as suitable for dilution and storage of the thylakoids in published protocols. In each protocol, the suggested 'final' storage and usage buffer has been chosen due to its perceived superiority over others that may have been tested by the scientists that established the isolation protocols. It was therefore decided to test these buffers, for all five different thylakoid preparations, by using them as the dilution buffer used to dilute the thylakoids to the desired final chlorophyll concentration in the 330 µl sample that would be illuminated and then tested for H_2O_2 in the HRP-mediated luminol chemiluminescence cuvette assay. Therefore, four different buffers were used to dilute the five different thylakoid preparations: buffer A (10 mM Tris-HCl buffer, adjusted to pH 8.5), buffer B (5 mM $MgCl_2$, 15 mM NaCl, 2 mM MES, brought to pH 6.9 with NaOH), buffer C (5 mM $MgCl_2$, 70 mM sucrose, 1 mM PMSF, 20 mM Tricine, adjusted to pH 7.8 with NaOH) and buffer D (5 mM $MgCl_2$, 70 mM sucrose, 20 mM Tricine, adjusted to pH 7.8 with NaOH). Each different thylakoid preparation diluted in each of the four buffers was illuminated using the standard illumination protocol and then tested for H_2O_2 production using the standard chemiluminescence reaction protocol described in the Methods. The results can be seen in Figure 4.10.

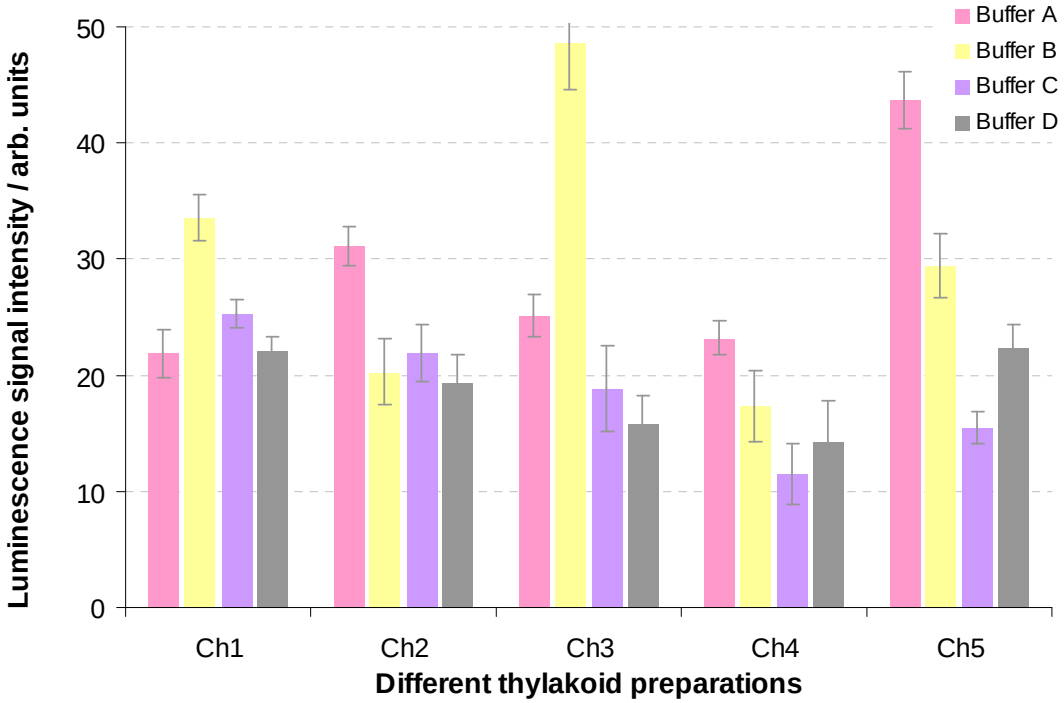

Figure 4.10 Effect of buffer used during the illumination of different thylakoid preparations on the production and detection of H_2O_2.

The luminescence signal, detected by a bench-top spectrophotometer, resulted from the production of light by the cuvette-based chemiluminescence reaction of luminol, HRP and H_2O_2. [HRP] = 5 U.ml-1, [luminol] = 100 µM, in Tris-HCl buffer (10 mM, pH 8.5). The H_2O_2 was previously produced by illuminating diluted thylakoid preparations with an un-filtered halogen lamp (20 watts, 350 lumens) at a distance of 10 cm for 1 min, while aspirated in a 'white' semi-transparent pipette tip. The thylakoid preparations were diluted as following: Ch1 [chlorophyll] = 284 µg.ml^{-1}, Ch2 [chlorophyll] = 171 µg.ml^{-1}, Ch3 [chlorophyll] = 237 µg.ml^{-1}, Ch4 [chlorophyll] = 131 µg.ml^{-1} and Ch5 [chlorophyll] = 64 µg.ml^{-1}. Average values and the SDs shown are the results of 3 replicates.

In order to compensate for the effect the varying pH would have on the chemiluminescence reaction that would be taking place post-illumination, thereby altering the H_2O_2 detection per say, it was initially decided to repeat the measurements with all four buffers with their pHs adjusted to 8.5, the standard chemiluminescence reaction pH, and then to factor in the effect of this to the measurements when the four different buffers were used in their assigned pH (6.9 – 8.5). This method however, would have introduced an added complication, as it would be altering not only the desired parameter, the pH of the chemiluminescence reaction, but also the pH during the thylakoid

illumination, thus making the results incomparable. Instead, it was decided to therefore repeat the standard HRP-mediated luminol chemiluminescence reaction with H_2O_2 at the pH 7.8 and 6.9, and then calculate the proportional change in signal effected by the change in pH alone, and apply this proportion as a factor to the signal resulting by the chemiluminescence detection of the H_2O_2 produced by the thylakoids when diluted in the buffers with the varying pHs.

As it can be seen from the graph, the thylakoid preparations reacted differently to the four buffers tested. The results demonstrate no association between the use of the buffer suggested in each protocol and the H_2O_2 production by the thylakoids. Having adjusted the results solely for the difference in pH that using the Buffers B, C or D effect during the chemiluminescence detection, it can be seen from the graph that for thylakoid preparations Ch1 and Ch3, the buffer effecting the highest production of H_2O_2 during illumination is Buffer B, while for the other three thylakoid preparations, Buffer A effects the highest yield. Therefore, the specific buffers were used when using the thylakoid preparations for other experiments.

4.3.3.4 Investigation of the effect of the distance of illumination on the H_2O_2 production by thylakoids

As mentioned in the introduction of the Results, (Section 4.3.3), the intensity of the light used to illuminate a plant is a property that affects the plant's response to the light stimulus. The intensity of light markedly affects the rate of the oxygen photosynthetic evolution in photosynthesis. There is a linear relationship over a wide range up to a saturating light intensity, at which point other factors become rate-limiting [151; 153].

Therefore, an investigation was conducted on the effect of different distances from the light source on the H_2O_2 production by thylakoids, as, increasing the distance between the light source and the thylakoids, reduces the intensity of light that reaches the sample. The results of the experiment can be seen in

Figure 4.11. As expected, increasing the distance between source and sample, and therefore reducing the energy available to the thylakoids, resulted in an associated reduction of the H_2O_2 being produced during the illumination.

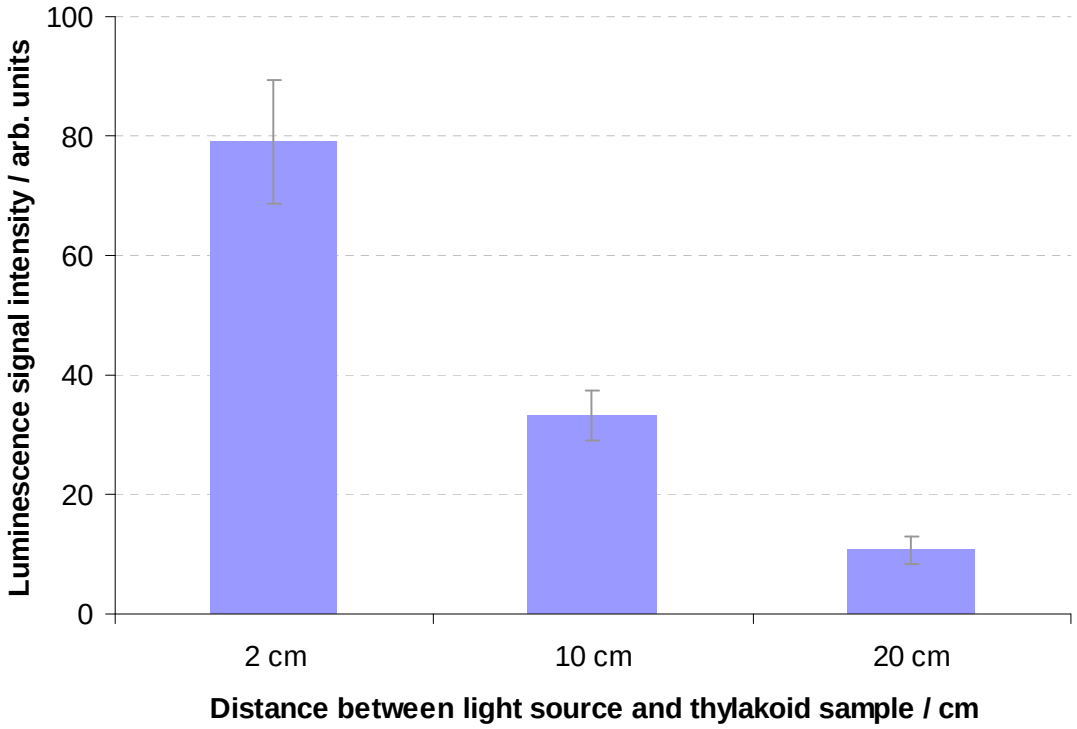

Figure 4.11 Effect of distance between the light source and the illuminated thylakoid sample on the production of H_2O_2.

The luminescence signal, detected by a bench-top spectrophotometer, resulted from the production of light by the cuvette-based chemiluminescence reaction of luminol, HRP and H_2O_2. [HRP] = 5 U.ml-1, [luminol] = 100 µM, in Tris-HCl buffer (10 mM, pH 8.5). The H_2O_2 was previously produced by illuminating diluted thylakoid samples with an un-filtered halogen lamp (20 watts, 350 lumens) at a varying distance of 20, 10 and 2 cm for 1 min, while aspirated in a 'white' semi-transparent pipette tip. The thylakoid preparation Ch1 [chlorophyll] = 284 µg.ml^{-1}, was diluted in buffer B (5 mM $MgCl_2$, 15 mM NaCl, 2 mM MES, brought to pH 6.9 with NaOH). Average values and the SDs shown are the results of 3 replicates.

4.3.3.5 Investigation of the effect of different pipette tips on the H_2O_2 production by thylakoids

As described in the thylakoid illumination and chemiluminescence H_2O_2 detection methodology (Section 4.3.2.2), the experimental procedure required

the positioning of the 330 µl thylakoid sample in a pipette tip fitted on an air-displacement pipette for the illumination step, in order to allow for the fast and easy transition from the illumination step to the measurement of the H_2O_2 produced during the illumination. The possibility of the pipette tips affecting the spectral quality of light reaching the thylakoids was considered, and thus investigated.

The two pipette tips commonly used interchangeably in the facilities of this work taking place (Fig. 4.12) were used in order to identify the preferred product. For all five different thylakoid preparations, each with different chlorophyll amounts and therefore responses to excitation by light, the same measurements were made with the thylakoid sample being illuminated while aspirated within the 'blue'-tinted semi-clear pipette tips and in the 'white'-tinted semi-clear tips.

Figure 4.12 Photographs of the two different pipette tips used as sample containers during the illumination of the samples.

The thylakoid aliquots were aspirated into the tip, and then illuminated through the pipette tip. Top: 'white'-tinted semi-clear tip; bottom: 'blue'-tinted semi-clear pipette tip. Both types pictured are made of polypropylene, with a capacity of 200 µl to 1,000 µl (Thermo Fisher Scientific Ltd., Loughborough, UK.

Briefly, the measurements performed consisted of illuminating thylakoid samples while aspirated in the different pipette tips, and then measuring the H_2O_2 produced using the chemiluminescence reaction. All parameters of the measurements were kept constant, apart from the tips, and as described in the standard experimental procedure in Section 4.3.2.2. The results can be seen in Fig. 4.13.

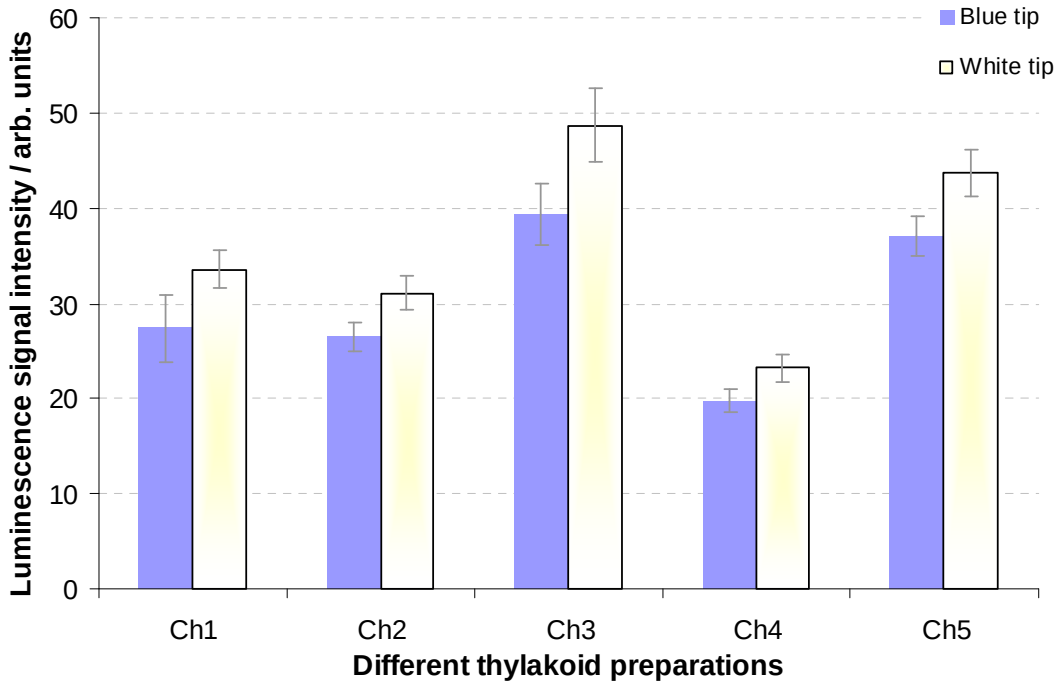

Figure 4.13 Effect of pipette tip light absorption and transmittance on the production of H_2O_2 by different thylakoid preparations.

The luminescence signal, detected by a bench-top spectrophotometer, resulted from the production of light by the cuvette-based chemiluminescence reaction of luminol, HRP and H_2O_2. [HRP] = 5 U.ml-1, [luminol] = 100 µM, in Tris-HCl buffer (10 mM, pH 8.5). The H_2O_2 was previously produced by illuminating diluted thylakoid preparations with an un-filtered halogen lamp (20 watts, 350 lumens) at a distance of 10 cm for 1 min, while aspirated in two different pipette tips tested. The Ch1 thylakoid preparation ([chlorophyll] = 284 µg.ml^{-1}) and the Ch3 thylakoid preparation ([chlorophyll] = 237 µg.ml^{-1}) were diluted in buffer B (5 mM $MgCl_2$, 15 mM NaCl, 2 mM MES, brought to pH 6.9 with NaOH). The Ch2 thylakoid preparation ([chlorophyll] = 171 µg.ml^{-1}), the Ch4 thylakoid preparation ([chlorophyll] = 131 µg.ml^{-1}) and the Ch5 thylakoid preparation ([chlorophyll] = 64 µg.ml^{-1}) were diluted in buffer A (10 mM Tris-HCl buffer, adjusted to pH 8.5). Average values and the SDs shown are the results of 3 replicates.

As it can be seen from the results, it was observed that, for all thylakoid preparations, the H_2O_2 produced by the thylakoids when illuminated through the 'white' tips was consistently higher, when compared to the amount of H_2O_2 produced by thylakoids when illuminated while aspirated in the 'blue' tips. As all other experimental details were kept the same, this difference can be attributed to the effect the 'blue' tip has on the spectral qualities of the light that is transmitted through the tip to the sample. This is probably a combination of the overall reduction in intensity of the light, due to increased absorbance, as well

as due to a shift in the wavelengths that are allowed to be transmitted through the pipette tip to the sample. Hence, all measurements were made with the 'white' pipette tips.

4.3.3.6 Investigation of the effect of different light sources on the H_2O_2 production by thylakoids

It was discovered from key literature that halogen lamps have been widely used for the illumination of photosynthetic material and whole plants [153]. What is more, most fluidic sensors using some isolated and immobilised photosynthetic material, usually employ red light to excite the material [9; 48; 154]. Therefore, a halogen lamp was used as the main light source throughout the work presented in Chapter 4, emitting at the whole of visible spectrum; this was fitted with optical filters to modulate wavelengths of different wavebands. Also a red laser diode was used, providing only red light, which, as mentioned, is the one most frequently used according to literature.

4.3.3.6.1 Characterisation of the light sources; light intensity and other parameters

Incandescent lamps radiate visible light by thermal radiation generated from tungsten filaments heated to a high temperature by an electric current. The energy distribution is continuous, but the intensity of red light is higher than that of blue light [153]. Tungsten incandescent lamps are thermal radiators that emit a continuous spectrum of light extending from about 300 nanometers, in the ultraviolet region, to about 1400 nanometers, in the near infrared region. Halogen bulbs, a high-performance version of the incandescent tungsten lamp, typically contain traces of iodine or bromine in the fill gas, which return evaporated tungsten to the filament far more efficiently than lamps made with other gases [155].

The filters, used to modulate the light emitted from the halogen light source, are categorised as absorption filters; they selectively transmit some portions of the

incident white light spectrum, but absorb other wavelengths. More specifically, they are categorised as colour correction or compensation filters; they consist of colloidal carbon mixed with suitable dyes and dispersed in gelatin to achieve the desired spectral characteristics. Colour correction filters differ from colour balancing and conversion filters in that they control colour by attenuating principally the red, green, and/or blue regions of the visible light spectrum rather than fine-tuning overall spectral performance, thus they do not possess band-pass or other similar properties.

The light intensity profile over a wide light spectrum was measured for the light sources, in order to gain insight into the intensity of light that should be expected from each source, as well as a more specific understanding of the effect of the different absorption filters on the spectral characteristics of the halogen lamp. This is also very important due to the characteristics of photosynthesis, and its components, especially the chlorophylls and other pigments, as described elsewhere (Section 2.2.1).

The light intensity spectral distribution wavelength scan of different light sources was performed by placing an optical fibre, connected to a spectrometer, in the area directly underneath the halogen lamp, facing towards the source, at a distance of 10 cm. For the laser diode, the laser beam was focused directly in the fibre's opening. The results are presented in Figure 4.14.

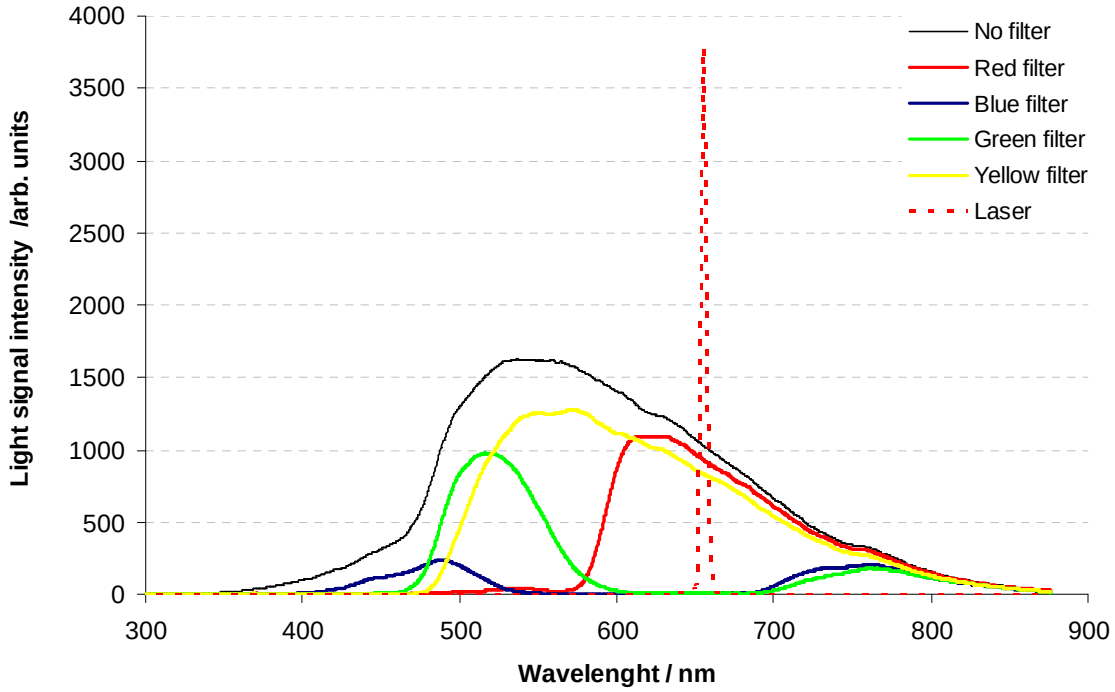

Figure 4.14 Light intensity spectral distribution wavelength scan of different light sources used to illuminate the thylakoid preparations.

All traces, apart from the 'laser' refer to the JC12V20W halogen lamp (output: 20 W), without a filter ('No filter') or with a coloured, semi-transparent sheet of various colours. The laser light source was a laser photodiode (output: 1 mW).

As it can be seen from Fig. 4.14, the different filters resulted in very different outputs, both in spectral quality (wavelength) and quantity (intensity). What is more, a portion of all wavelengths are hindered by the use of the filters. This effect is common to most filters; this type of unwanted absorption is termed secondary absorption. If the filters were of the highest quality, the plots in Fig. 4.14 would have very sharp peaks centred in specific wavelength regions, and near-maximum absorption at the rest of the wavelengths [156]. For example, the red filter blocked most of the light of less that approximately 600 nm; in other words, the light emitted from the source in the violet, blue, green and yellow bands, while the green filter blocked most light of orange and violet wavelength bands, while allowing light of the green and some blue and red wavelengths. The laser diode has a distinctively coherent, collimated and near-monochromatic light output, peaking at 655 nm. Overall, it appears that most filters did not absorb light of the unwanted wavelengths perfectly; that can be

said for the blue, green and yellow filters, where there are clear but small peaks in the red region, for the blue and green filters, and an overall non-absorbance for the yellow.

Based on the light intensity output over the whole visible light spectrum and beyond, as displayed in Fig. 4.14 above, the 'total light output' of the halogen lamp light source, with and without the optical absorption filters, as well as of the laser source was measured, by calculating the sum of all the data points over the aforementioned spectrum. The results can be seen in Figure 4.15.

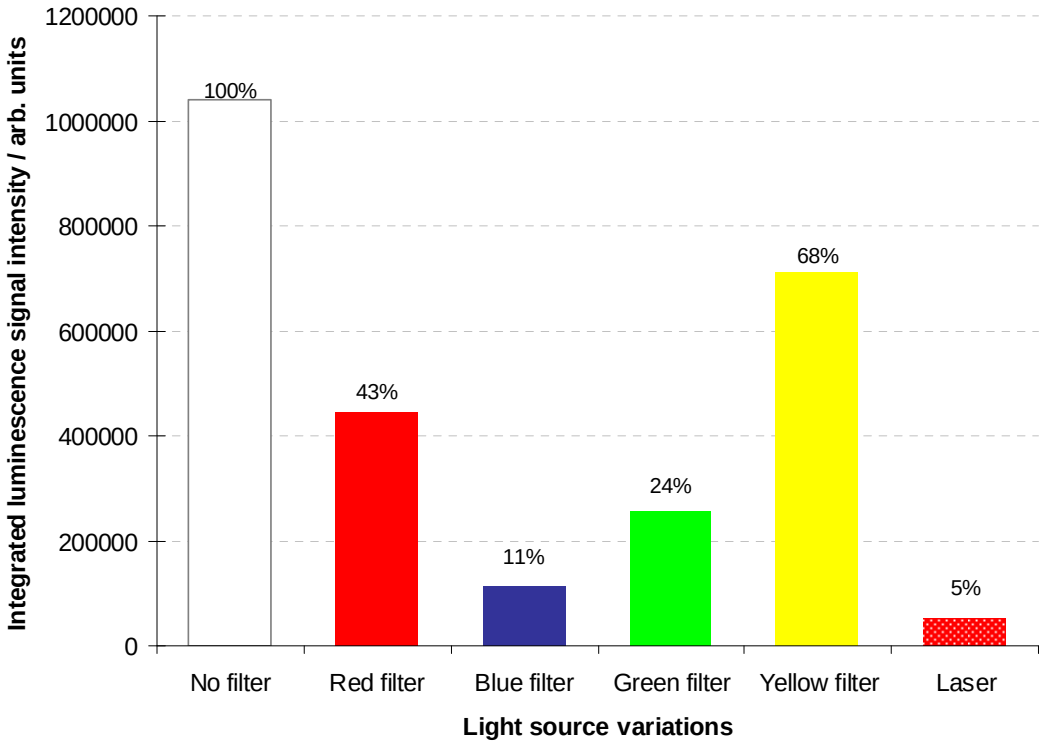

Figure 4.15 The sums of total light output achieved by the two different sources, halogen lamp and laser diode, over the whole spectrum between 300 and 870 nm.

For the halogen lamp, the total light output was calculated when used on its own, as well as with the optical absorption filters (Red, Blue, Green, Yellow), that changed its spectral qualities. The percentage above each column depicts the proportion of 'total light output' each light source achieved in comparison to the un-filtered halogen lamp (left-most column).

It was important to calculate a means of comparing the light output of all the different light sources, as the wavelengths over which they produced light (or allowed to pass, in the case of the optical filters) varied greatly, and, as the filters were essentially attenuating the original, 'no filter' light output, it was expected that the 'total light output' achieved when using the filters would only be a proportion of the original, non-filtered light of the halogen lamp source. It was also important to calculate the same for the laser diode, which, given the nature of laser light, emits at very discreet bandwidth, compared to any other light source, as also seen from Figure 4.14. The 'total light output' produced by each source was also calculated as a proportion of the 'total light output' produced by the halogen lamp without a filter, which thus served as the 'standard' against which the other sources were compared to.

4.3.3.6.2 Effect of dual UV and IR filter on light intensity profile of light source

Simple methods have been employed in photosynthesis applied research in order to minimise the harmful effect of undesirable wavelengths of radiation. Some reported include employing a glass filter intercepting the pathway of the light arriving to the sample from the source in order to reduce UV (glass stops 70% of UV-B rays) [61], or the use of a water layer between the light source and the sample [157], as water absorbs IR wavelength to varying degrees [158]. In order to minimise UV/IR wavelengths and importantly heat, a borosilicate Pyrex glass Petri dish (SciLabware Limited, Stone UK) was used as the container in which water of 1 cm thickness was contained, placed in between the light source and the illuminated thylakoid sample, hence together acting as a dual UV and IR filter, as used similarly by others [49; 134; 145].

The effect this dual UV and IR filter had on the intensity of light arriving to the thylakoid sample over a broad wavelength was investigated. As it can be seen from Figure 4.16, over the wavelengths 175 nm to 875 nm, no reduction in the intensity of light available to the illuminated thylakoids was observed. This includes the near infra-red wavelengths (770 – 1400 nm), as well as all UV-A (315 – 400 nm) and UV-B (280 – 315 nm) light, as well as some of the UV-C

light (100 – 280 nm). It is therefore not an observation that the filter has attenuated any wavelengths of optical radiation that it was possible to measure using the available instrumentation. It was nevertheless decided to employ the setup for all experiments that employed this light source.

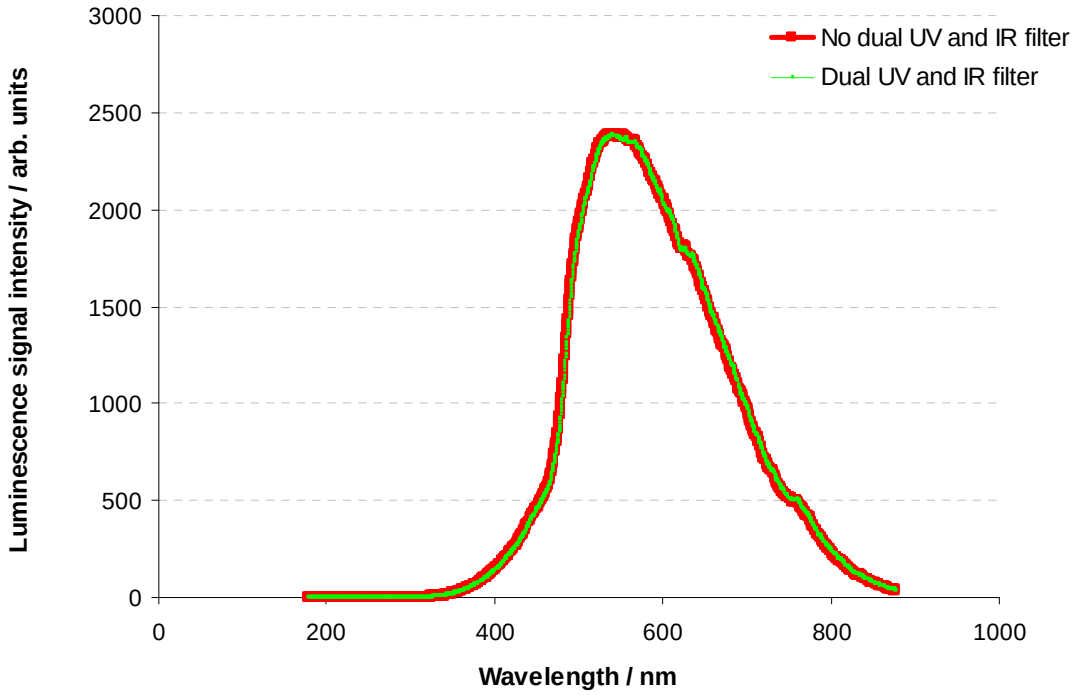

Figure 4.16 Light intensity spectral distribution wavelength scan of halogen lamp light source with and without a borosilicate Pyrex glass Petri dish filled with water acting as a UV and IR filter between the light source and the detector.

4.3.3.6.3 Effect of different light sources on the H_2O_2 production by thylakoids

It was considered of paramount importance to examine the effect of different light sources used for the illumination step, on the thylakoids. The halogen lamp, un-filtered or with a filter, as well as the laser diode, were used to illuminate the thylakoids. The results of the chemiluminescence detection of the produced H_2O_2 can be seen in Figure 4.17, for each of the five different thylakoid preparations. For the four filters (red, blue, green and yellow) and the laser diode used, superimposed on the 'opaque' columns, which are the experimentally obtained H_2O_2 values, are the expected values, visualised as

semi-transparent columns. The expected, theoretical values were calculated from the results presented in Section 4.3.3.6.1, where the spectral distribution of light produced by the filtered lamp and the laser diode as well as their intensity over the spectrum, were calculated, summed and then compared to that of the halogen lamp without a filter, as presented in percentages in Fig. 4.15. They therefore represent the amount of H_2O_2 that would be produced and detected if the spectral quality of different lights did not affect the said production, but if only the overall intensity did so.

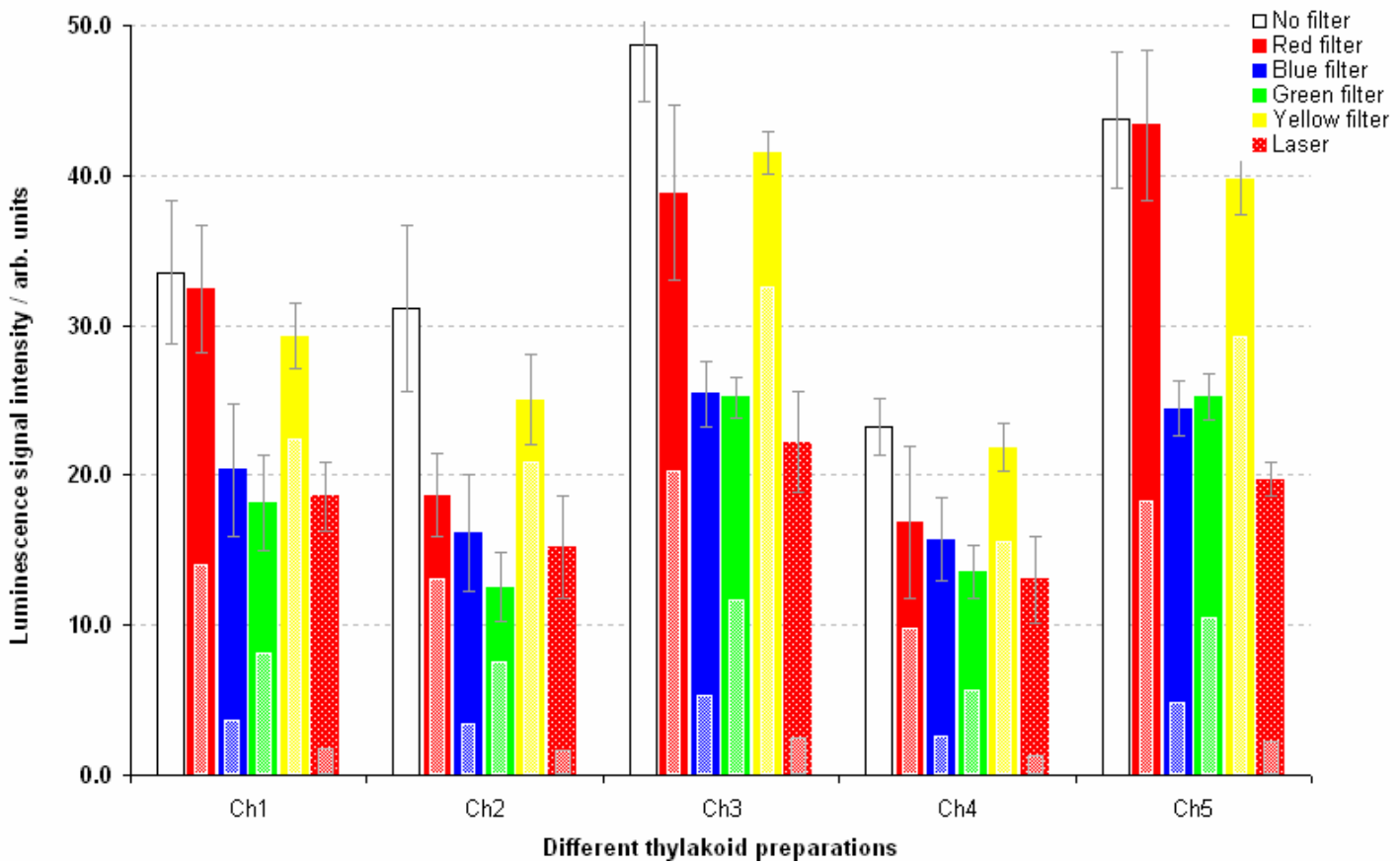

Figure 4.17 Effect of light source used for the illumination step on the production of H_2O_2 by different thylakoid preparations.

The luminescence signal, detected by a bench-top spectrophotometer, resulted from the production of light by the cuvette-based chemiluminescence reaction of luminol, HRP and H_2O_2. [HRP] = 5 U.ml-1, [luminol] = 100 µM, in Tris-HCl buffer (10 mM, pH 8.5). The H_2O_2 was previously produced by illuminating diluted thylakoid preparations with an un-filtered halogen lamp, as well as filtered versions of the lamp, and a laser source, at a distance of 10 cm for 1 min. The Ch1 thylakoid preparation ([chlorophyll] = 284 µg.ml^{-1}) and the Ch3 thylakoid preparation ([chlorophyll] = 237 µg.ml^{-1}) were diluted in buffer B (5 mM $MgCl_2$, 15 mM NaCl, 2 mM MES, brought to pH 6.9 with NaOH). The Ch2 thylakoid preparation ([chlorophyll] = 171 µg.ml^{-1}), the Ch4 thylakoid preparation ([chlorophyll] = 131 µg.ml^{-1}) and the Ch5 thylakoid preparation ([chlorophyll] = 64 µg.ml^{-1}) were diluted in buffer A (10 mM Tris-HCl buffer, adjusted to pH 8.5). Average values and the SDs shown are the results of 3 replicates.

As it can be seen, altering the light sources or variations thereof did have a clear effect on the amount of H_2O_2 produced by the illuminated thylakoids. The unfiltered halogen lamp provided the optimal illumination conditions for the highest H_2O_2 production by all different thylakoid preparations. Had the effect been only due to the differences in overall light intensity, and not wavelength characteristics of the light produced by each light source, the H_2O_2 production would have varied even more than that achieved.

This is visually highlighted by the semi-transparent columns superimposed over the actual results of chemiluminescence signal obtained following the illumination by each light source. The semi-transparent columns represent the expected chemiluminescence signal to be achieved by each variation of the halogen lamp and the laser diode, based on the proportion each of those light sources' 'total light output' constituted of the un-filtered halogen lamp's 'total light output', previously reported as percentages in Figure 4.15.

The actual results obtained thus highlight the effect the different spectral distributions have on the production of H_2O_2. Table 4.5 presents a summary of the expected H_2O_2 production obtained by illumination with the different filters and the laser diode, as well as the results obtained, compared to the expected values, all expressed as percentages of the experimental values obtained with the un-filtered halogen lamp, which therefore is used as the 'standard'.

Firstly, it is noted that the different thylakoid preparations performed and behaved differently under the same illumination wavelength qualities. This is seen in the table under the heading "**H_2O_2 produced, as proportion of H_2O_2 production with un-filtered lamp**", by comparing vertically the percentage values for the 5 different preparations, under a filtered version of the halogen lamp. This suggests that, irrespective of the actual peak chemiluminescence signal detected, and therefore H_2O_2 produced under each filtered illumination, i.e. when instead observing the performance, for each preparation, under the

different filters, in relation to the values set as the standard (100%), there is qualities of the thylakoids that differ from preparation to preparation, and these qualities affect the utilisation of specific wavelengths of light. It is suggested that the different pigments in thylakoids, which utilise different wavelengths of light differently, account for these differences.

Table 4.5 Summary of H_2O_2 detection for the different thylakoid preparations, with the different illumination sources and set-ups.

	No filter	Red filter	Blue filter	Green filter	Yellowfilter	Laser
Expected H_2O_2 production as proportion of un-filtered halogen lamp production, based on light intensity sum						
	100%	43%	11%	24%	68%	5%
H_2O_2 produced, as proportion of H_2O_2 production with un-filtered lamp						
Ch1	100%	97%	61%	54%	87%	55%
Ch2	100%	60%	52%	40%	80%	49%
Ch3	100%	80%	52%	52%	85%	46%
Ch4	100%	73%	68%	58%	94%	56%
Ch5	100%	99%	56%	58%	91%	45%
Average H_2O_2 produced, as proportion of H_2O_2 production with un-filtered lamp						
	100%	82%	58%	52%	88%	50%
Absolute increase of observed H_2O_2 production against the expected						
Ch1		227%	554%	221%	128%	1091%
Ch2		141%	474%	164%	118%	960%
Ch3		187%	476%	211%	125%	898%
Ch4		171%	616%	239%	138%	1103%
Ch5		233%	510%	236%	133%	887%
Average absolute increase of observed H_2O_2 production against the expected						
		192%	526%	214%	128%	988%
Average relative increase of observed H_2O_2 production against the expected						
		92%	426%	114%	28%	888%

As it can be seen from Table 4.5, when comparing the first numerical row (the expected results) to the last row, for each filter, there was a significant increase in the amount of H_2O_2 produced (average of 5 preparations), compared to what would have been obtained if only the intensity of the light had an effect on the H_2O_2 production. For example, when employing the blue filter, the average

H_2O_2 produced was 58% that of the un-filtered light, while the expected proportion ought to have been only 11%, based on the light intensity per say; as light of the blue region of the spectrum is highly effective however, and thus desirable, for the photosynthetic processes, the 4-fold (426%) increase observed can be thus explained. The very high difference observed between the expected and achieved H_2O_2 production with the laser diode can again be partly attributed to the usefulness of the region of light emitted by the source (655 nm). However, another reason is the fact that laser light is collimated, and thus, when shone directly onto the thylakoid sample, as illustrated in Fig. 4.5, there is minimal loss due to dispersion, refraction or other lossy behaviour that is observed with the light produced from the halogen lamp.

The efficiency of plant photosynthesis is not the same throughout the 400 to 700 nm waveband. Just as the human eye has visual curves (further information on the differences between photometry and radiometry in Section 6.3.3.2), plants have sensitivity curves over a wide range. Plants select effective wavelengths from white light and utilise them accordingly [153].

Hence, as green light does not correspond to the energy needed for any of the various electronic transitions possible in the chlorophyll molecule, chlorophyll cannot therefore absorb green light [151]. The spectral quality of light is of great importance; an intense source of monochromatic green light at 530 nm would not be absorbed significantly by pure chlorophyll in solution, so would not be expected to be effective in photosynthesis. However, action spectrums for photosynthesis show that green light is nevertheless effective, though the main peaks are in the blue and red wavelength bands. The usefulness of green light appears to be due to the absorption of light by the carotenoids which normally accompany the chlorophylls in thylakoids; the additional absorbed light is transferred by resonance transfer to yield excited electrons, equivalent to those produced by direct red light absorption into the antennae systems. This situation may be approached in woodland, where the canopy absorbs blue and red light preferentially and transmits the green, i.e. the understorey plants get greener

light. This energy transfer has important implications for the successful growth of understorey plants in forests, which are therefore at a less disadvantage that might be expected.

An action spectrum of photosynthesis is a graph of the relative effectiveness of light of different wavelengths needed to bring about a biological response, for example oxygen evolution in photosynthesis [151], presented in Fig. 4.18. The photosynthesis action spectrum has a large peak composed of two peaks at about 675 and 625 nm in the red light region, and a smaller peak between 440 and 450 nm in the blue. As it can be seen, red light has the strongest action and blue light a weaker action.

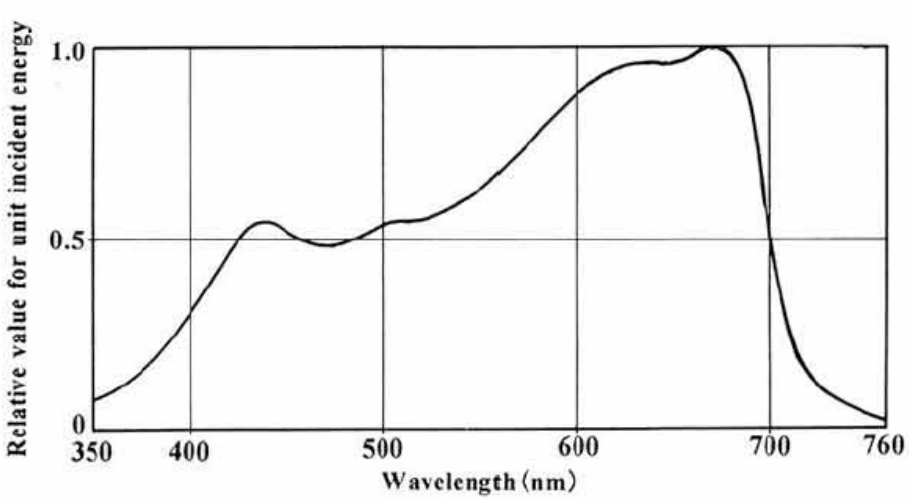

Figure 4.18 Average values for photosynthesis action spectra from different plant species.
From [153].

It is red light that is both best absorbed by chlorophyll and results in maximal photosynthesis [153], as it can also be deducted from the wavelength absorbance scan of thylakoids (Fig. 4.8) and Fig 4.18. This is probably the reason why red light has been so extensively, almost exclusively, used in recent biosensors utilising plant material [8; 9; 48; 142; 154; 159]. The fact that green light does also effect the photosynthetic oxygen evolution appears however to have often been disregarded, instead focusing on the fact that chlorophyll does not absorb and

therefore utilise it. Clearly however, the results obtained by illuminating the thylakoids with 'green' light support the fact that green light is useful and actually utilised in photosynthesis. Table 4.6 highlights this fact; as it can be seen, a third of the photosynthesis is actioned by green light, just as green light responds to about a third of the light provided by a typical incandescent lamp.

Table 4.6 Photosynthesis action spectrum distribution, and spectrum distribution for incandescent lamps.

	Blue light (400-500 nm) (%)	Green light (500-600 nm) (%)	Red light (600-700 nm) (%)
Photosynthesis action spectrum	23.5	32.0	44.5
Incandescent lamp	12.3	33.3	54.4

Reproduced from [153].

4.3.4 Conclusions

Following the unsuccessful attempt to effect the production of H_2O_2 from illuminated chloroplasts, attempting to do so by using sub-chloroplast organelles, the thylakoids, was successful. This was measured with the HRP-mediated chemiluminescence reaction of luminol with the produced H_2O_2.

Five different isolation protocols were used and, following a series of investigations into their performance, as far as H_2O_2 production is concerned, by altering a variety of external parameters (illumination time, illumination distance, illumination source, buffer) and a thylakoid-specific parameter (individual preparation's chlorophyll concentration), all five preparations were optimised for use.

There was variation in the maximum production of H_2O_2 achieved by each preparation, but none that would allow for the definitive selection of a preparation that would be clearly the one to proceed further with the experiments described in Section 4.4 for the investigation of the potential inhibition of the aforementioned H_2O_2 production if effected (by illumination)

after an incubation of the thylakoids with photosynthesis-inhibiting herbicides. Preparation Ch5 allowed for the highest production of H_2O_2 after a 10 min illumination, while also containing the least amount of thylakoids (as measured by the chlorophyll concentration), but this would not necessary also be translated in the lowest LOD for herbicides.

As it is a cuvette-based batch method, with the isolated thylakoids in suspension, the chemiluminescence signal intensity resulting from the H_2O_2 effectively underreported the amount of H_2O_2 produced, due to the sample's optical density.

The experimental conditions, optimal for the highest production of H_2O_2 are:

- Illumination source: 20 W halogen lamp, full spectrum
- Illumination time: 10 min
- Illumination distance: 10 cm
- Buffer: thylakoid preparation specific
- Chlorophyll concentration: thylakoid preparation specific

It is surprising that Ch5 thylakoid preparation produced much better H_2O_2 yields than Ch4, as the only difference in the protocols was the absence of PMSF in the Ch5 protocol. It should be noted that, normally, PMSF is added in extraction / isolation buffers in order to inhibit plant proteinases, which degrade plant organelles [139; 160].

4.4 Batch assay for the detection of herbicides, by measuring the illuminated thylakoids' H_2O_2 production inhibition

4.4.1 Introduction

The successful production of H_2O_2 by illuminated thylakoids, as presented in Section 4.3, was an important accomplishment in the overall progress of this work. Following this, the next important milestone to be achieved was the development of an assay for the detection of herbicides, based on the H_2O_2

production by thylakoids. As described in the literature review (Section 2.2.2), many biosensors have been developed using as the basis of their working method the inhibition of photosynthesis by specific classes of herbicides, albeit using different parameters affected by this inhibition as the affected variable, changes of which are then correlated to the concentration of the herbicide bringing about that change. This may be an increase in fluorescence, or a decrease of current in an electrochemical signal detection etc.

Therefore, building upon the work on producing of H_2O_2 by thylakoids in the absence of herbicides, it was thus decided to extend the experimental methods used in Section 4.4 with the additional step of the incubation of thylakoids with herbicides, prior to the illumination, during which the H_2O_2 is normally produced, and the subsequent chemiluminescence analysis of the sample, for the detection of said H_2O_2. The herbicides tested were: atrazine, diuron, propanil, 2,4-D, paraquat and acifluorfen. Atrazine, diuron and propanil are photosynthesis-inhibiting herbicides, while the remaining three employ other modes of action. Three photosynthesis-inhibiting herbicides were chosen, each representing a main family of herbicides, the triazines, the ureas and the amides. The specific photosynthesis-inhibiting herbicides were chosen due to their frequent use as herbicides of choice for studies presenting assays for these classes of herbicides [8; 9; 48; 142; 154; 159]. Atrazine and diuron are also amongst the most widely used herbicides in agriculture, and they are also amongst the herbicides that are most frequently found in excess of the E.U. maximum permissible amount of 0.1 µg/l. 2,4-D, paraquat and acifluorfen were chosen as commonly found herbicides, and were included in the study in order to ascertain the selectivity of the developed assay for photosynthesis-inhibiting herbicides and to identify potential unwanted effects on the assay due to their modes of action.

Before reporting the results of incubating isolated thylakoids with the herbicides, a report of the mode of action and usage is given for each of the six herbicides.

4.4.1.1 Biochemical mode of action of selected herbicides

4.4.1.1.1 Method of action of photosynthesis-inhibiting herbicides

Triazines and ureas are well-known herbicides that specifically fix to the Q_B binding site of PSII with high affinity. This blocks the photosynthetic electron flow. The principal mode of action of ureas, triazines and other similar herbicides is to disrupt the light reaction of photosynthesis (Fig. 4.19). PSII is responsible for the production of oxygen and supplies electrons, which move, via a chloroplastic electron transport system, to a positive moiety formed on excitation of PS I. PS I produces the high-energy electrons that ultimately reduce $NADP^+$ to NADPH, with the latter then responsible for the reduction of carbon dioxide to sugar. These classes of herbicides interfere with the photosynthetic process at the Q_B binding site of PSII as well as a probable secondary location probably in PS I [161-163]. Urea and triazine inhibition of oxygen evolution is reversible, and can be removed by washing [164].

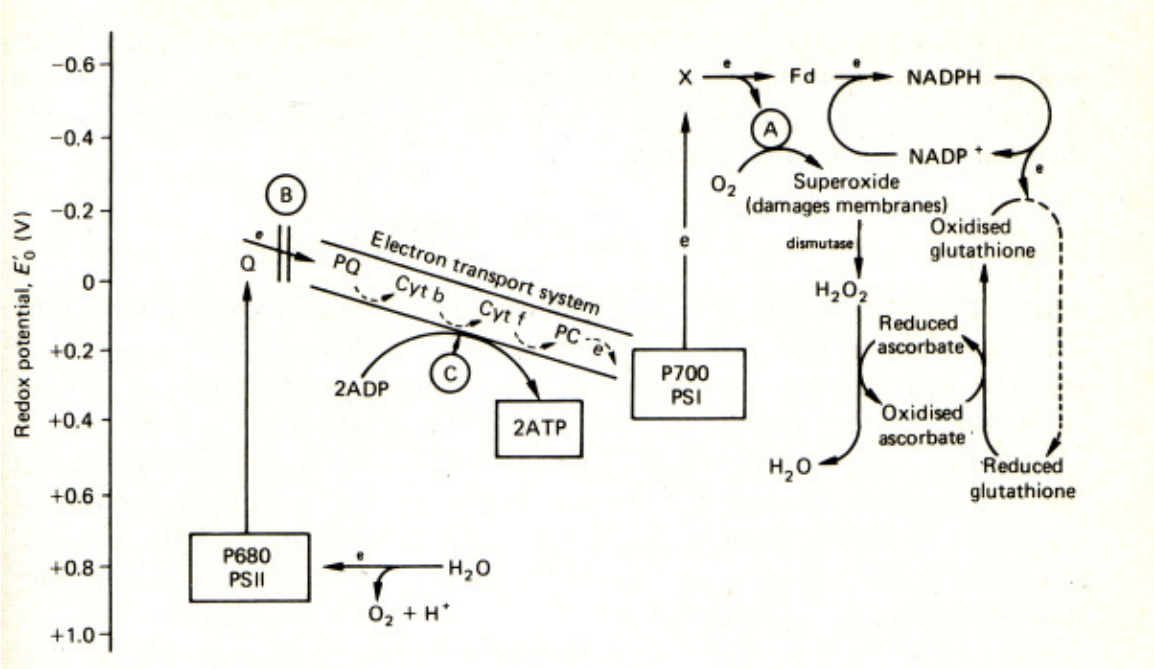

Figure 4.19 Light reactions of photosynthesis and sites of action of certain classes of herbicides.

PQ, plastoquinone; Cyt b, cytochrome b; PC, plastocyanin; PS, photosystems I and II; Q, X, electron acceptors; A, site of electron deflection by quaternary ammonium compounds; B, primary site of action of triazines and ureas; C, site of action of uncouplers such as phenols. With permission, from [165]

4.4.1.1.2 Atrazine characteristics

Atrazine (2-Chloro-4-ethylamino-6-isopropylamino-1,3,5-triazine) belongs to the class of triazine compounds. A wide range of triazines have been synthesised over time to control annual and broadleaved weeds in a variety of crops as well as in non-cropped land. They are effective, at low dosages, in killing broad-leaved weeds in corn and other crops and they can be used in high dosages as soil sterilants. In general, these herbicides are applied in pre- or post-emergence and they are absorbed by the roots or by the foliage, respectively. In some cases, they are used in combination with other herbicides to broaden the spectrum of activity. These compounds have an appreciable persistence in soil [10].

4.4.1.1.3 Diuron characteristics

Diuron (3-(3,4-Dichlorophenyl)-1,1-dimethylurea) is a urea herbicide. Urea is the amide of carbonic acid. Phenylureas belong to a numerous group of substituted ureas directly applied to soil in pre-emergence to control annual grasses in various crops [10]. It binds to a critical site in the Photosystem II region of chloroplasts, shutting down CO_2 fixation and energy production. Indirect production of reactive lipid peroxides contributes to a loss of membrane integrity and organelle function [161-163].

4.4.1.1.4 Propanil characteristics

Propanil (3',4'-Dichloropropionanilide) is an amide herbicide. In general, the amides are photosynthesis inhibitors. These chloroacetamides are effective pre-emergence herbicides for annual grasses and annual broad-leaved weeds but they also have foliar contact activity. In general, these compounds are soil applied and used in various horticultural crops, such as maize, soybean, and sugarcane. They are normally absorbed by shoots and roots and they are, in general, non-persistent compounds in soil [10]. At low concentrations propanil is a strong inhibitor of photosynthetic electrons, at a site near plastoquinone. At

higher concentrations it attacks chloroplasts and other cell membranes and at 1 mM it uncouples oxidation from phosphorylation [165; 166].

4.4.1.1.5 2,4-D characteristics

2,4-D (2,4-Dichlorophenoxyacetic acid) is a chlorinated phenoxyacetic acid compound, discovered during the Second World War [10]. It disrupts normal cell growth, acting as a growth hormone, similar to natural auxins. The term 'auxins' applies to compounds which are able to stimulate the growth of plant tissue [167]. It stimulates the growth of old cells and the rapid expansion of new cells. The rapid growth in cell size without normal cell division effectively crushes the plant's water and nutrient transport system [161; 162; 165].

4.4.1.1.6 Paraquat characteristics

Paraquat (1,1′-Dimethyl-4,4′-bipyridinium dichloride hydrate or methyl viologen dichloride) is a broad spectrum herbicide absorbed by leaves, but is not translocated in sufficient quantities to kill the roots of perennial weeds. It has a quaternary ammonium structure and is rapidly adsorbed and inactivated in soil. Therefore, it is not effective as a pre-emergence herbicide [10]. Paraquat is a quaternary ammonium (bipyridinium) herbicide. In the presence of light, it is reduced to a stable free radical, which then causes toxic effects to the plant [166]. At high light intensities, paraquat acts as a contact poison when applied on leaves, while in low light, some translocation can occur. Even in the dark the plant dies after some days, but the dramatic toxic effects require the presence of light, oxygen and photosynthetic tissue. Although the importance of light makes the light reactions of photosynthesis an obvious candidate as the primary candidate of paraquat, it does not inhibit the Hill reaction in isolated chloroplasts [165].

In 1937 Hill found that the isolated chloroplasts upon illumination were unable to reduce carbon dioxide, but able to remove electrons from water and pass them to a suitable artificial electron acceptor [168]. As a result, water evolves, while the artificial electron acceptor is reduced. There are numerous electron acceptors

that can replace carbon dioxide in the Hill reaction, amongst them being methyl viologen, used since the 1930's as a redox indicator (by Hill and others), only to be discovered in 1955 as an herbicide named paraquat. Paraquat inhibits the reduction of $NADP^+$ and therefore prevents the reduction of carbon dioxide in the photosynthetic carbon cycle [165], as it replaces ferredoxin as electron acceptor in PSI. After the reduction, paraquat is automatically reoxidised by oxygen to form superoxides. Therefore its primary action is the generation of free radicals [4].

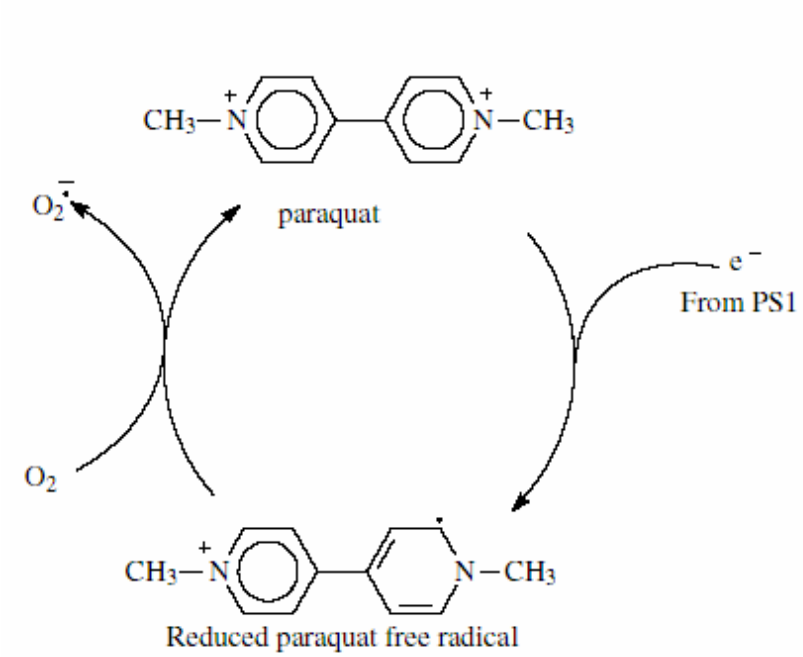

Figure 4.20 The mode of action of paraquat by its redox cycle.
With permission from [4]

Many other natural processes form superoxide radicals, and the cells have efficient enzymes called superoxide dismutases (SOD) that detoxify the superoxide radicals. However, the detoxification is not complete because another very reactive substance, namely, hydrogen peroxide, is produced from it. Hydrogen peroxide must then be reduced to water by reduced ascorbic acid, catalases or glutathione peroxidases. If this does not happen fast enough, H_2O_2 may react further, producing the extremely reactive hydroxyl radical [4]. However, in the presence of paraquat, the production of superoxide is greatly enhanced,

all available reduced ascorbic acid is oxidised and thereafter H_2O_2 accumulates [165].

4.4.1.1.7 Acifluorfen characteristics

Acifluorfen is a phenolic herbicide. These compounds are used in post-emergence and frequently applied in combination with other herbicides to extend the spectrum of weed species to be controlled [10]. Its effective usage is dependent on the presence of light. The primary effect of phenolic herbicides on weeds is to disrupt cellular and sub-cellular lipoprotein membranes, so that they lose their selective permeability, leak their contents, thus causing cell death, leaf bleaching [169] and cause the plant to die. More specifically, acifluorfen interferes with a wide range of biochemical processes in plants and plant cell organelles; it destabilises lipoprotein membranes, inhibits the Hill reaction in isolated chloroplasts, affects the mitochondrial electron transport and inhibits the synthesis of proteins. It also interferes with the photosynthetic reduction of carbon dioxide by inhibiting the reduction of $NADP^+$. Interference with electron transport in illuminated chloroplasts probably leads to the formation of singlet oxygen or other oxidants, which are known to cause peroxidation of membrane lipids with disruption of function and leakage of contents [162; 165]. Light is essential for the activation of the disruption process, although the specific role light plays in its activation is uncertain, with many conflicting theories [165; 170; 171].

4.4.2 Materials and methods

Basic chemicals and reagents used (luminol, HRP and preparations thereof) were the same as described in Section 4.3.2.2. The six herbicides used were all from the PESTANAL® range, analytical standard grade from Sigma Chemical Company Ltd. (Gillingham, UK). The herbicides were diluted in a variety of concentrations, all in Tris-HCl buffer (10 mM, pH 8.5). The following information sources were used in order to identify the appropriate method (solvent and concentration) to solubilise each herbicide used: [4; 7; 163; 165; 172; 173].

The experiments described in Section 4.4.3 were HRP-mediated luminol chemiluminescence reactions with H_2O_2, in cuvettes, using a bench-top spectrometer, with the H_2O_2 required for the reaction being provided by illuminated isolated thylakoid preparations, while potentially inhibited by herbicides, during an incubation period prior to the illumination. It is therefore a variation of the experimental process used in Section 4.3.3. The sequence of actions that formed a single measurement was based on that described in Section 4.3.2.2, with the main difference being that, prior to the illumination step, the thylakoid sample was mixed with a herbicide sample, incubated, and only then illuminated. These measurements were repeated for the different herbicides, with the five different thylakoid preparations, while also altering the incubation time.

More specifically, the luminescence signal, detected by a Varian bench-top spectrophotometer, resulted from the production of light by the cuvette-based chemiluminescence reaction of luminol, HRP and H_2O_2. [HRP] = 5 U.ml-1, [luminol] = 100 µM, in Tris-HCl buffer (10 mM, pH 8.5). The H_2O_2 was previously produced by illuminating diluted thylakoid preparations with an un-filtered halogen lamp (20 watts, 350 lumens) at a distance of 10 cm for 5 min. Prior to the illumination, the thylakoid sample was incubated with different concentrations of the different herbicides for different lengths of time.

The Ch1 thylakoid preparation ([chlorophyll] = 284 $\mu g.ml^{-1}$) and the Ch3 thylakoid preparation ([chlorophyll] = 237 $\mu g.ml^{-1}$) were diluted in buffer B (5 mM $MgCl_2$, 15 mM NaCl, 2 mM MES, brought to pH 6.9 with NaOH). The Ch2 thylakoid preparation ([chlorophyll] = 171 $\mu g.ml^{-1}$), the Ch4 thylakoid preparation ([chlorophyll] = 131 $\mu g.ml^{-1}$) and the Ch5 thylakoid preparation ([chlorophyll] = 64 $\mu g.ml^{-1}$) were diluted in buffer A (10 mM Tris-HCl buffer, adjusted to pH 8.5).

The calculations used to quantify the lower limit of detection (LLOD) were based on the definition of the limit of detection by the International Union of Pure and Applied Chemistry (IUPAC Compendium of Chemical Terminology 2nd Edition,

1997), as described in Section 3.3.2. For a k value of 3, the LOD is the concentration corresponding to a signal 3*s.d. (of the blank) above the mean of the blank. As the assays performed aim to detect herbicides based on their inhibition of a signal, rather than an increase, this means that the signal obtained by a 'blank' sample is the highest achievable, with therefore the (lower) LOD being calculated by subtracting, rather than adding the signal obtained by 3*s.d. (of the blank).

4.4.3 Results and discussion

4.4.3.1 Chemiluminescence batch assay for atrazine

Samples of the five different thylakoid preparations, at the optimal chlorophyll concentrations as identified in Section 4.3.3.2, were incubated with samples of different atrazine concentrations ($1x10^{-4}$ – $1x10^{-8}$ M) for different lengths of time (1 – 15 min) and then illuminated for 5 min. The individual results were plotted for all different combinations, and can be found in Appendix I. From these, it can be seen that the longer incubation times resulted in a more distinct effect (reduction) on the H_2O_2 production, although the rate of inhibition fell considerably with incubation times longer than 10 min; thus the 10 min incubation time was chosen as the optimal. That would help detect lower concentrations of atrazine, as it was expected that, with the increased incubation time, a detectable reduction in H_2O_2 production, and therefore chemiluminescence signal, would be achieved by lower herbicide concentrations.

A summary of the chemiluminescence signal of the H_2O_2 produced and detected for the different atrazine concentrations and the different thylakoid preparations, with the 10 min incubation time, is seen in Fig. 4.21.

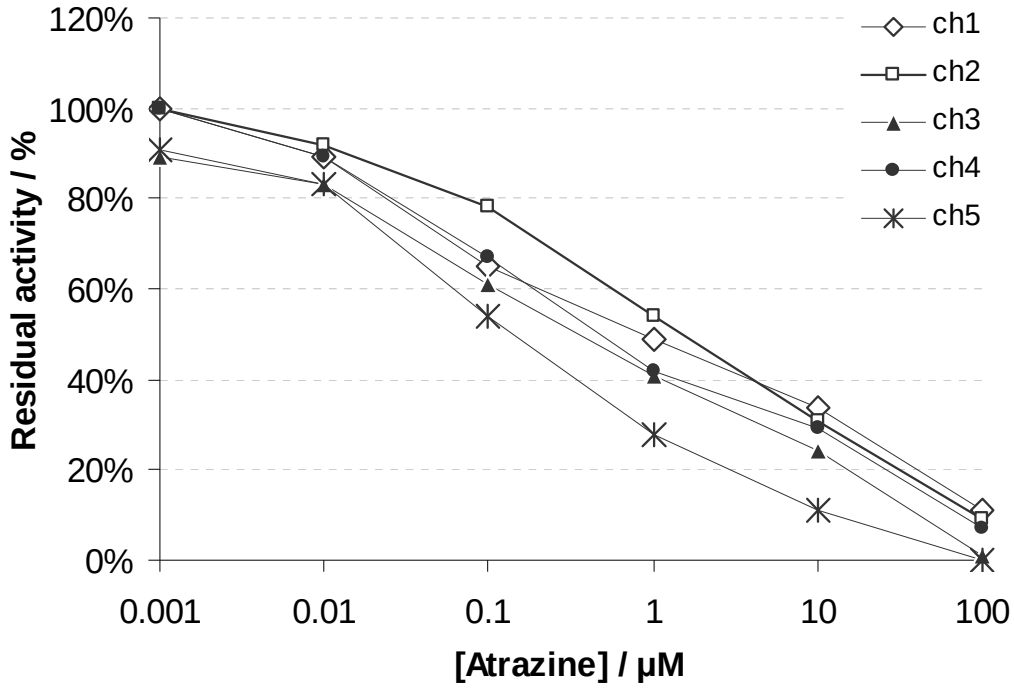

Figure 4.21 Standard curves of the inhibition of H_2O_2 production of five different thylakoid preparations (Ch1 – Ch5) by atrazine, measured by HRP-mediated luminol chemiluminescence, following a 10 min incubation and a 5 min illumination step.

Based on the results obtained, the LLODs for the different thylakoid preparations were calculated, shown in Table 4.7.

For all thylakoid preparations, the upper LOD of atrazine is around the region of $1x10^{-4}$ M. It is therefore evident that the detection range is quite wide, mainly 4 orders of magnitude. This is believed to be due to the high concentration of thylakoids, and therefore binding sites for the atrazine molecules. It is therefore believed that, for the same reason, the lower LODs achieved can inherently not be very low, as a small concentration of atrazine will make too small a change in the total amount of H_2O_2 produced to be satisfactorily detected, especially as the effect of atrazine is not an increase or presence of signal, in which case the detector's LOD and background signal would be the only limiting factors, but the inhibition of a maximum signal already present.

Table 4.7 Limits of detection of atrazine, obtained with the five different thylakoid preparations.

Thylakoid	LLOD (M)
Ch1	1.0×10^{-08}
Ch2	2.5×10^{-07}
Ch3	6.7×10^{-08}
Ch4	3.9×10^{-08}
Ch5	6.0×10^{-09}

As it can be seen from Table 4.7, the thylakoid preparation Ch5 was thus identified as the one allowing for the most sensitive detection of atrazine. More measurements were therefore made with Ch5, in order to obtain a more detailed profile of the effect of atrazine on the H_2O_2 production by thylakoids. The results can be seen in Fig. 4.22.

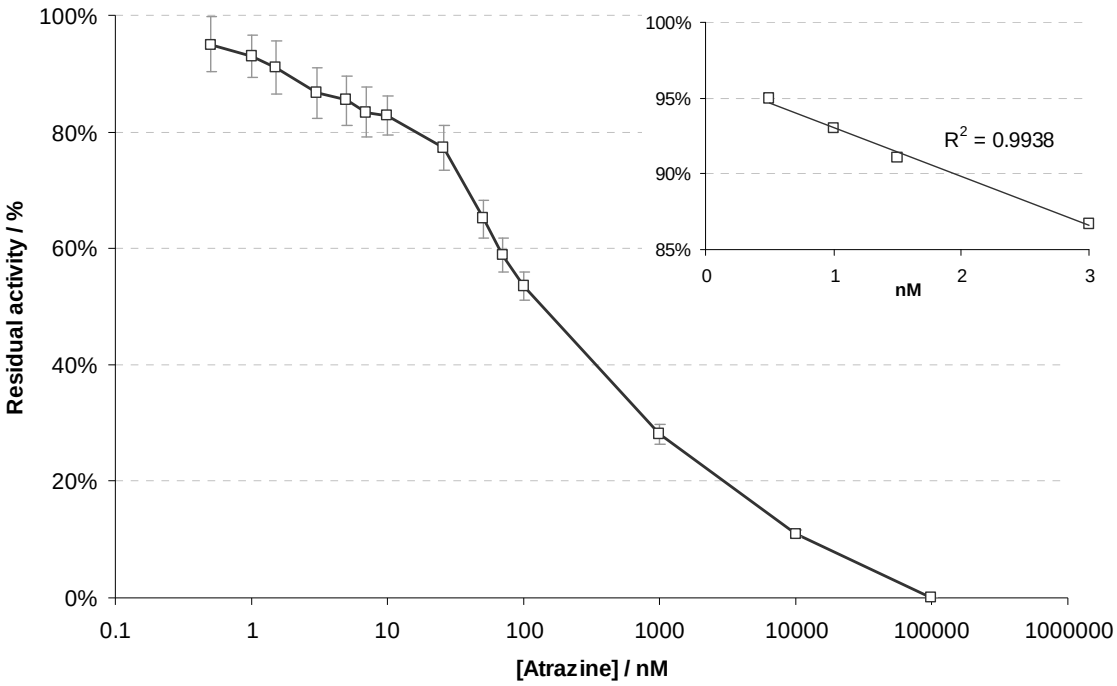

Figure 4.22 Calibration curve for the detection of atrazine, using the bench-top batch assay with Ch5 thylakoids in suspension. Inset: linear range.

The concentration of atrazine that equals 0.1 µg/l, which is the maximum permissible amount of an individual herbicide in drinking and other waters in the E.U., is $4.6x10^{-10}$ M. Therefore, the current bench-top batch assay developed for the detection of photosynthesis-inhibiting herbicides does not reach the desired limit of detection for atrazine.

4.4.3.2 Chemiluminescence batch assay for diuron

Samples of the five different thylakoid preparations, at the optimal chlorophyll concentrations as identified in Section 4.3.3.2, were incubated with samples of different diuron concentrations ($1x10^{-4}$ – $1x10^{-8}$ M) for different lengths of time (1 – 15 min) and then illuminated for 5 min. The individual results were plotted for all different combinations, and can be found in Appendix I. From these, it can be seen that the longer incubation times resulted in a more distinct effect (reduction) on the H_2O_2 production, although the rate of inhibition fell considerably with incubation times longer than 10 min; thus the 10 min incubation time was chosen as the optimal. That would help detect lower concentrations of diuron, as it was expected that, with the increased incubation time, a detectable reduction in H_2O_2 production, and therefore chemiluminescence signal, would be achieved by lower herbicide concentrations.

A summary of the chemiluminescence signal of the H_2O_2 produced and detected for the different diuron concentrations and the different thylakoid preparations, with the 10 min incubation time, is seen in Fig. 4.23.

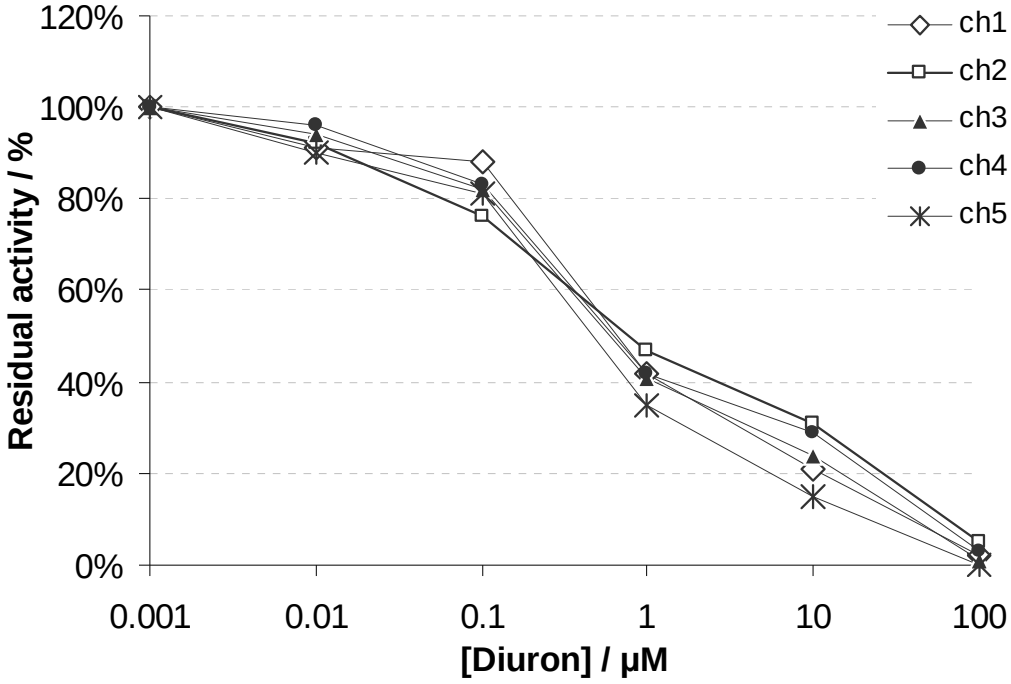

Figure 4.23 Standard curves of the inhibition of H_2O_2 production of five different thylakoid preparations (Ch1 – Ch5) by diuron, measured by HRP-mediated luminol chemiluminescence, following a 10 min incubation and a 5 min illumination step.

Based on the results obtained, the LLODs for the different thylakoid preparations were calculated, shown in Table 4.8. Compared to the LODs for atrazine (Table 4.7), it can be seen that a less sensitive detection of diuron was achieved.

Table 4.8 Limits of detection of diuron, obtained with the five different thylakoid preparations.

Thylakoid	LLOD (M)
Ch1	1.0×10^{-07}
Ch2	1.6×10^{-07}
Ch3	9.4×10^{-08}
Ch4	1.2×10^{-07}
Ch5	8.0×10^{-08}

For all thylakoid preparations, the upper LOD of diuron is around the region of $1x10^{-4}$ M. It is therefore evident that the detection range is relatively wide, 3-4 orders of magnitude, but narrower than that achieved for atrazine.

As it can be seen from Table 4.8, the thylakoid preparation Ch5 was thus identified as the one allowing for the most sensitive detection of diuron. More measurements were therefore made with Ch5, in order to obtain a more detailed profile of the effect of diuron on the H_2O_2 production by thylakoids. The results can be seen in Fig. 4.24.

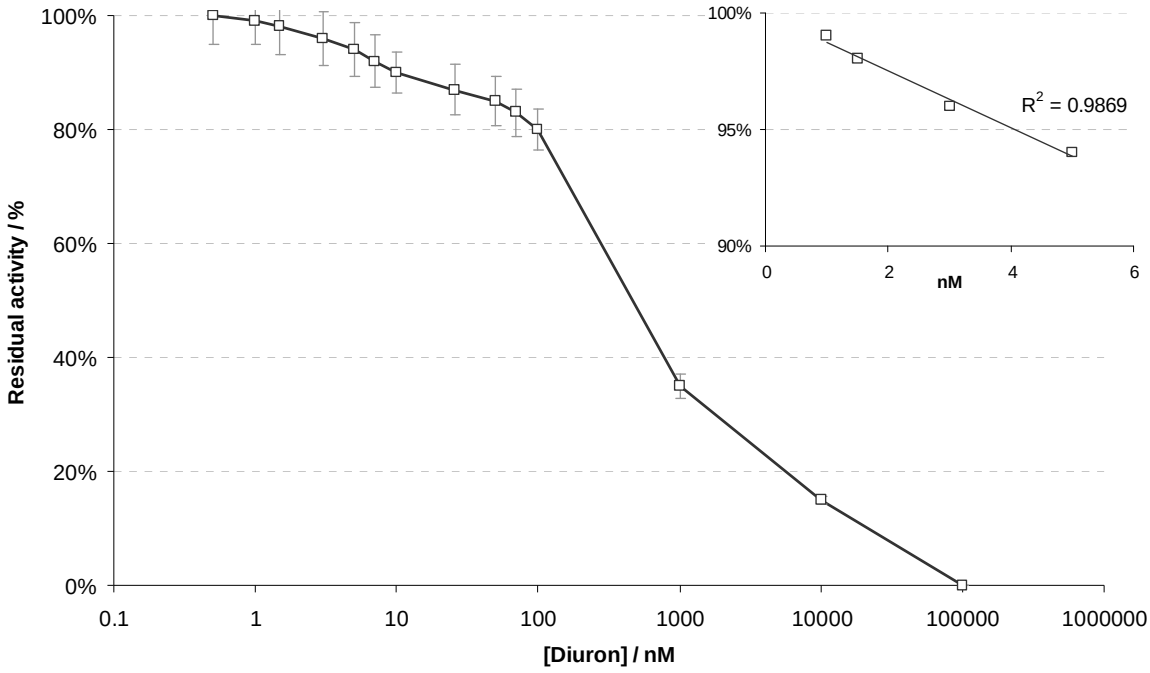

Figure 4.24 Calibration curve for the detection of diuron, using the bench-top batch assay with Ch5 thylakoids in suspension. Inset: linear range.

The concentration of diuron that equals 0.1 µg/l, which is the maximum permissible amount of an individual herbicide in drinking and other waters in the E.U., is $4.3x10^{-10}$ M. Therefore, the current bench-top batch assay developed for the detection of photosynthesis-inhibiting herbicides does not reach the desired limit of detection for diuron.

4.4.3.3 Chemiluminescence batch assay for propanil

Samples of the five different thylakoid preparations, at the optimal chlorophyll concentrations as identified in Section 4.3.3.2, were incubated with samples of different propanil concentrations ($1x10^{-4}$ – $1x10^{-8}$ M) for different lengths of time (1 – 10 min) and then illuminated for 5 min. The individual results were plotted for all different combinations, and can be found in Appendix I. From these, it can be seen that the longer incubation times resulted in a more distinct reduction of the H_2O_2 production, for the lower concentrations of propanil assayed, while the higher concentrations resulted initially in a decrease of the H_2O_2 production, followed by an increase, after an incubation of 5 min or so.

A summary of the chemiluminescence signal of the H_2O_2 produced and detected for the different propanil concentrations and the different thylakoid preparations, with the 10 min incubation time, is seen below in Fig. 4.25.

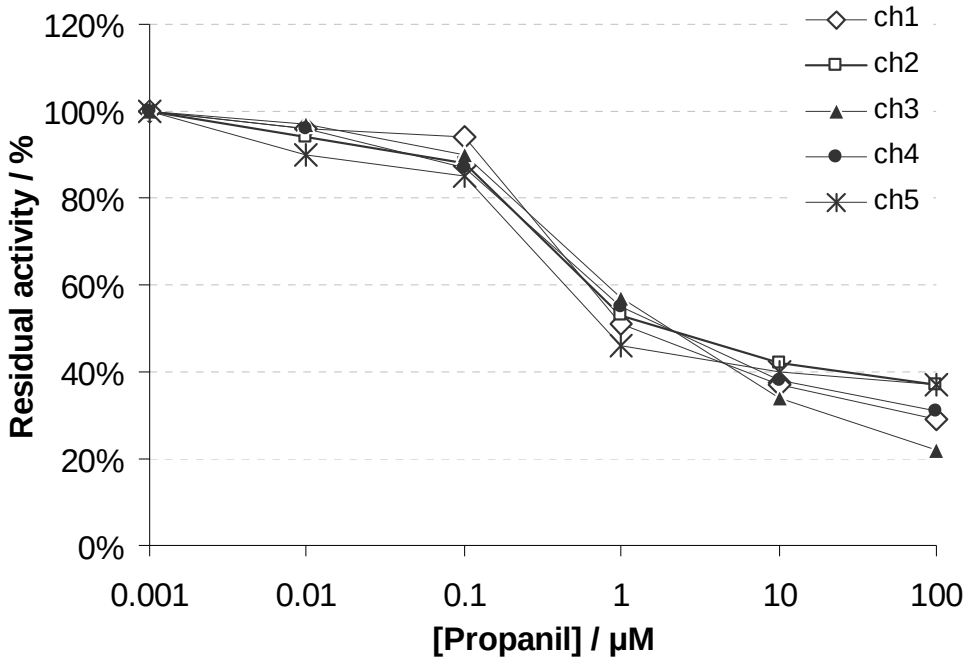

Figure 4.25 Standard curves of the inhibition of H_2O_2 production of five different thylakoid preparations (Ch1 – Ch5) by propanil, measured by HRP-mediated luminol chemiluminescence, following a 10 min incubation and then a 5 min illumination step.

Based on the results obtained, the LLODs for the different thylakoid preparations were calculated, shown in Table 4.9.

As it can be seen from Table 4.9, the thylakoid preparation Ch5 was thus identified as the one allowing for the most sensitive detection of propanil. More measurements were therefore made with Ch5, in order to obtain a more detailed profile of the effect of propanil on the H_2O_2 production by thylakoids. The results can be seen in Fig. 4.26.

Table 4.9 Limits of detection of propanil, obtained with the five different thylakoid preparations.

Thylakoid	LLOD (M)
Ch1	2.3×10^{-07}
Ch2	5.4×10^{-07}
Ch3	2.9×10^{-07}
Ch4	2.4×10^{-07}
Ch5	1.4×10^{-07}

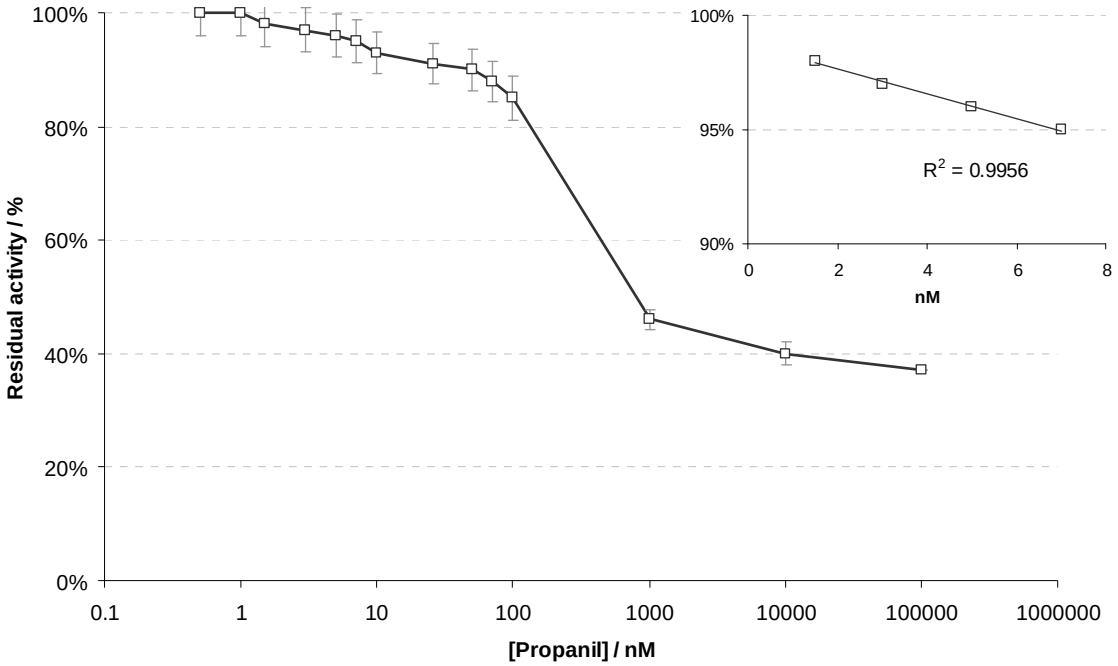

Figure 4.26 Calibration curve for the detection of propanil, using the bench-top batch assay with Ch5 thylakoids in suspension. Inset: linear range.

As it can be seen from Figures 4.25 and 4.26, the inhibitory effect of propanil on the production of H_2O_2 by thylakoids could be interpreted as having a distinctively sigmoidal shape when plotted. However, when examined in conjunction with the detailed time-concentration results found in Appendix I, it is clear that, for the higher concentrations of propanil, as the incubation time increases, the inhibitory effect they have on the H_2O_2 production and thus chemiluminescence signal appears to be decreasing, thus leading to an increase in chemiluminescence signal.

Therefore, for propanil, the upper LOD cannot be calculated with the limited set of measurements that have been taken, but, more importantly, due to the fact that, as the concentration of propanil in a sample increases, the inhibitory effect on the thylakoids' H_2O_2 production over time appears to be decreasing, in contrast with the effect smaller concentrations of propanil have. This is in direct contrast to the behaviour of atrazine and diuron, where increased

concentrations and increased incubation time both result in a decrease of the H_2O_2 production, and thus chemiluminescence signal obtained.

Such behaviour, although unexpected due to propanil's classification as a photosynthesis-inhibiting herbicide, is explained in the literature; as mentioned in Section 4.4.1.1.4, at low concentrations, propanil is a strong inhibitor of photosynthetic electrons, at a site near plastoquinone. At higher concentrations it attacks chloroplasts and other cell membranes and at 1 mM it uncouples oxidation from phosphorylation [165; 166]. However, no research literature could be found confirming the above.

The concentration of propanil that equals 0.1 µg/l, which is the maximum permissible amount of an individual herbicide in drinking and other waters in the E.U., is $4.6x10^{-10}$ M. Therefore, the current bench-top batch assay developed for the detection of photosynthesis-inhibiting herbicides does not reach the desired limit of detection for propanil.

4.4.3.4 Chemiluminescence batch assay for 2,4-D

Samples of the Ch5 thylakoid preparation, at the optimal chlorophyll concentration as identified in Section 4.3.3.2, were incubated with samples of different 2,4-D concentrations ($1x10^{-4}$ – $1x10^{-7}$ M) for different lengths of time (1 – 15 min) and then illuminated for 5 min. The chemiluminescence signals of the H_2O_2 produced and detected for the different 2,4-D concentrations with the different incubation times, are seen below in Fig. 4.27.

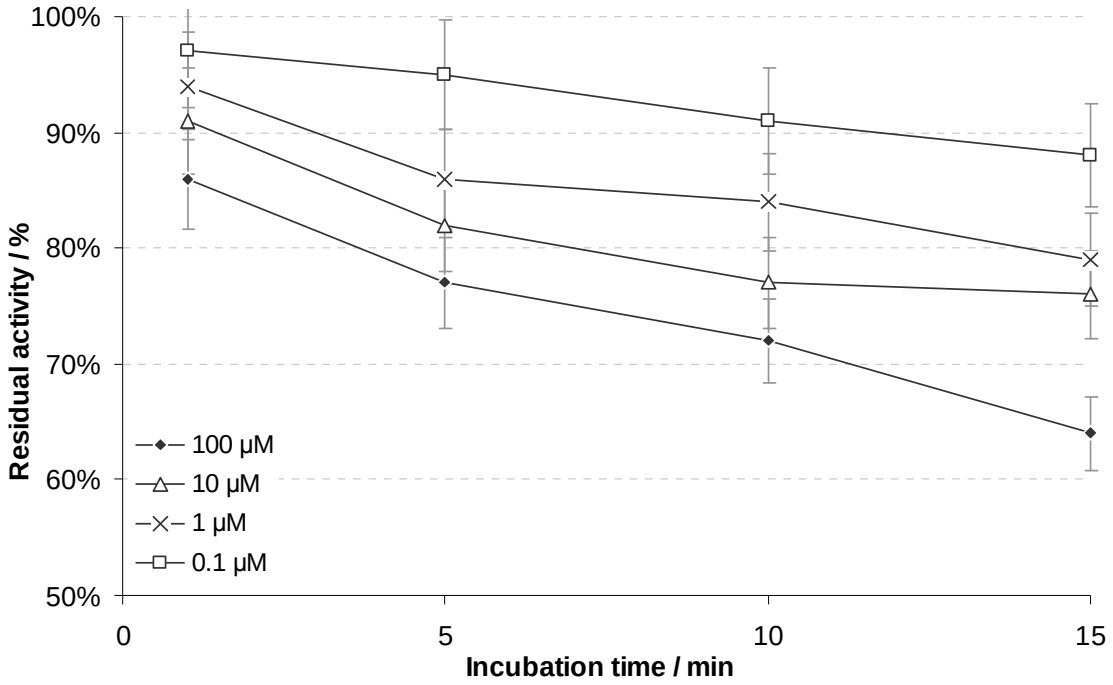

Figure 4.27 Effect of 2,4-D concentrations, measured over time, on the H_2O_2 production of the Ch5 thylakoid preparation, following a 5 min illumination step, measured by HRP-mediated luminol chemiluminescence.

In Fig. 4.27, it can be seen that 2,4-D had an inhibitory effect on the production of H_2O_2 by the Ch5 thylakoids, which was more pronounced over longer incubation periods. The inhibition is not comparable to that effected by the photosynthesis-inhibiting herbicides, but nonetheless it was not an expected result, as 2,4-D acts by inhibiting certain biochemical pathways that are irrelevant to the plants' ability to photosynthesise (Section 4.4.1.1.5). No mention in literature of experiments on the effect of 2,4-D on isolated thylakoids or PSII could be retrieved.

4.4.3.5 Chemiluminescence batch assay for paraquat

Samples of the five different thylakoid preparations, at the optimal chlorophyll concentrations as identified in Section 4.3.3.2, were incubated with samples of different paraquat concentrations ($1x10^{-4}$ – $1x10^{-7}$ M) for different lengths of time (1 – 15 min) and then illuminated for 5 min. The individual results were plotted for all different combinations, and can be found in Fig. 4.28.

a) Thylakoid preparation Ch1

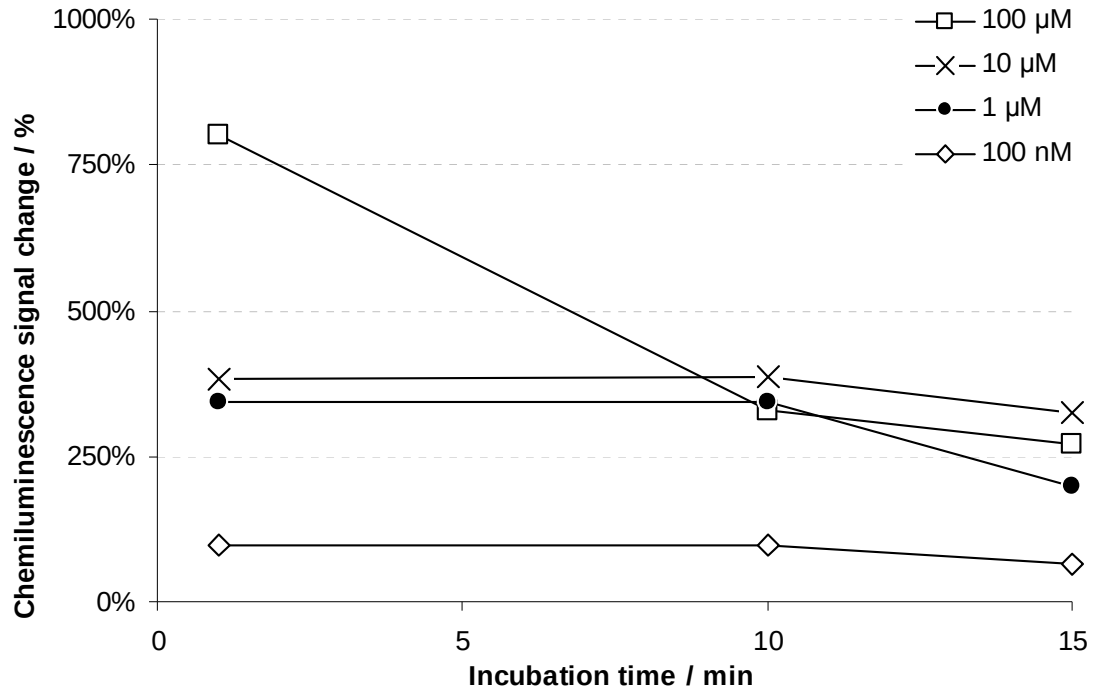

b) Thylakoid preparation Ch2

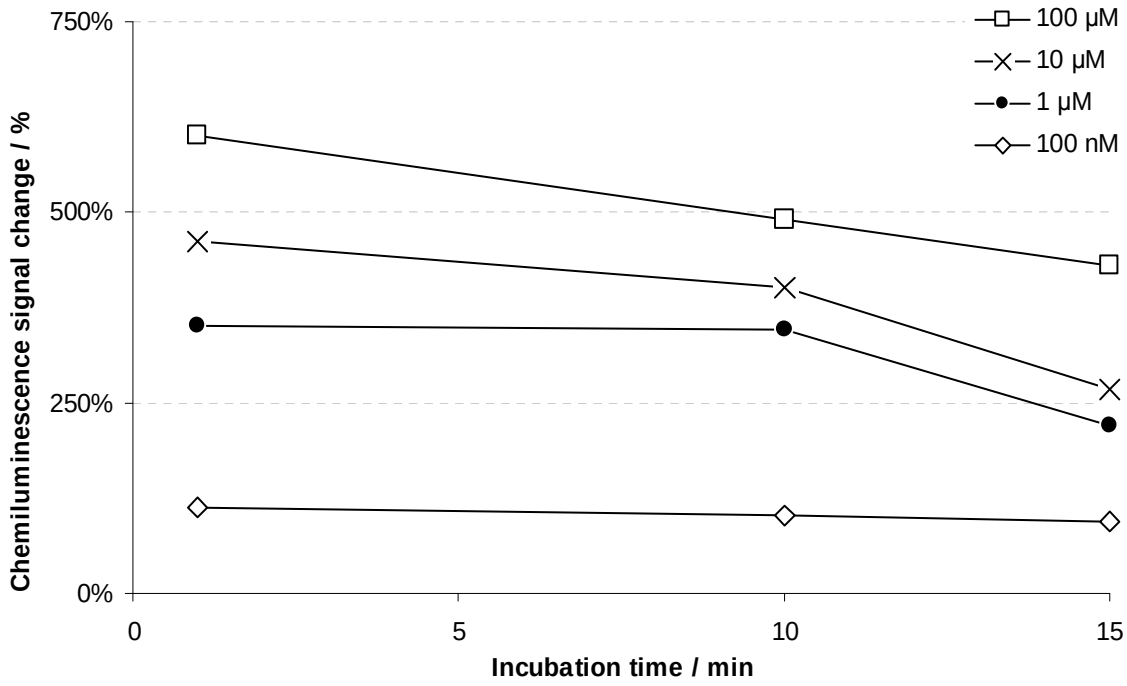

c) Thylakoid preparation Ch3

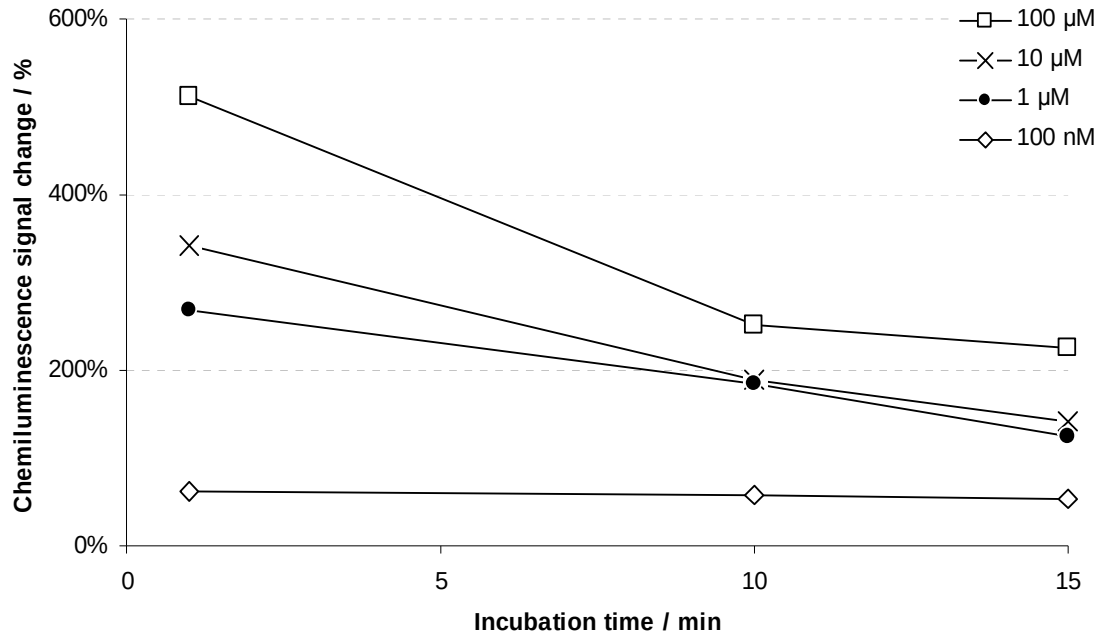

d) Thylakoid preparation Ch4

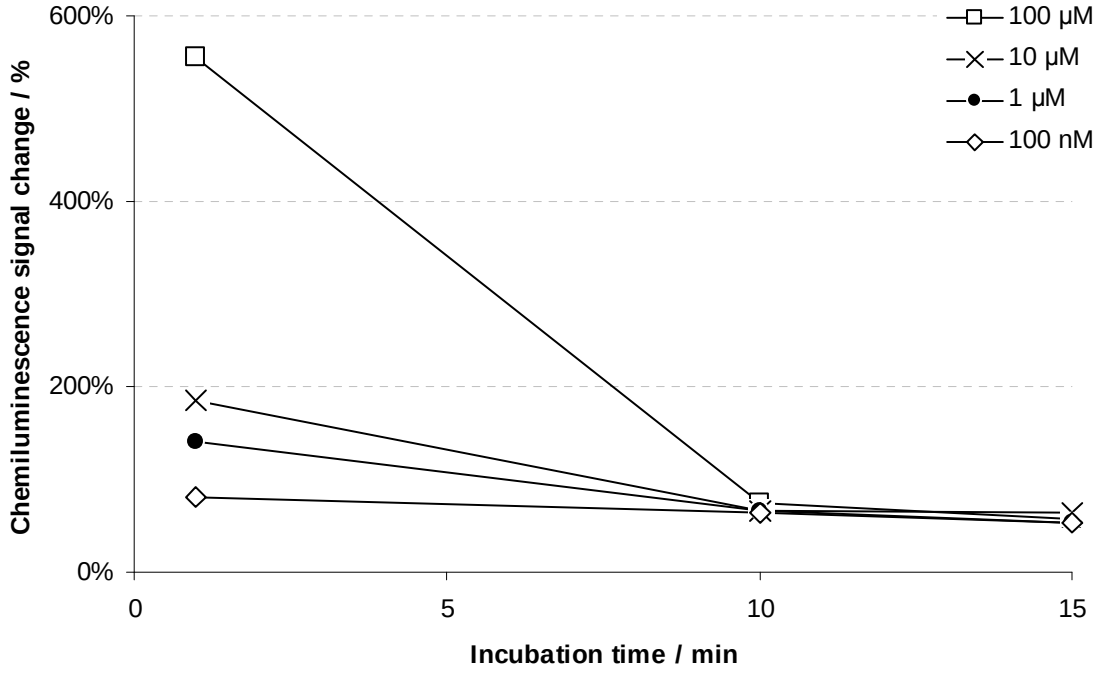

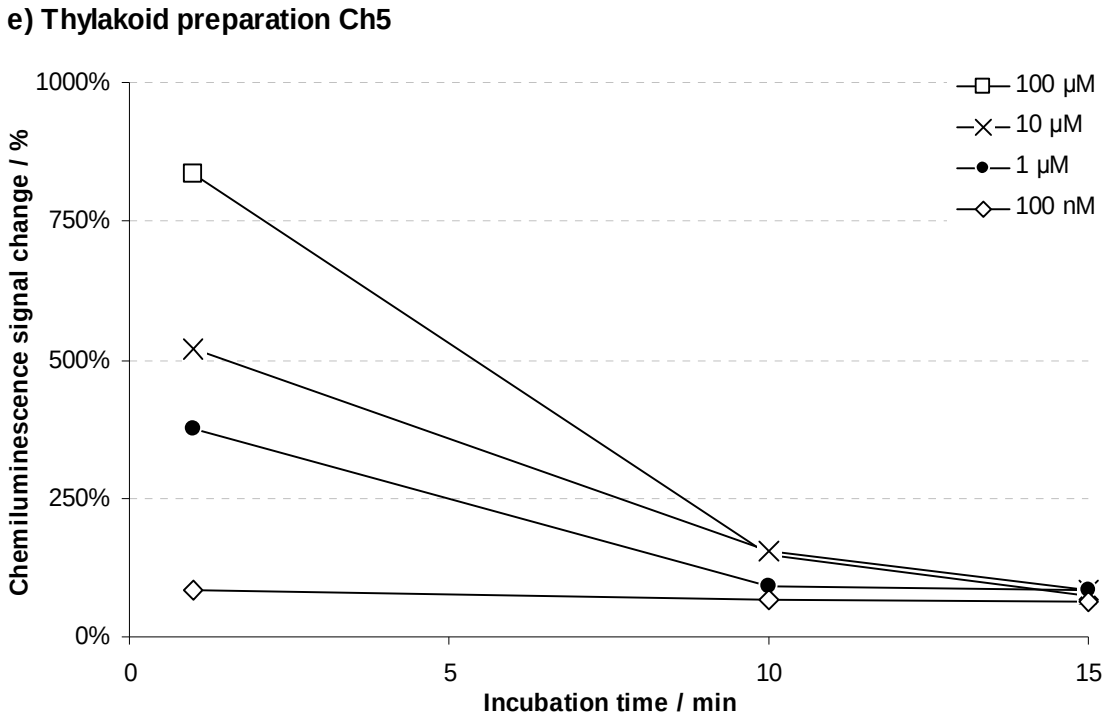

Figure 4.28 Effect (a–e) Effect of paraquat on chemiluminescence signal due to H_2O_2 obtained from five isolated thylakoid preparations, over different incubation times, followed by a 5 min illumination step.

The Y-axis represents the percentile change of the chemiluminescence signal, and therefore H_2O_2 concentration produced during the illumination step, observed following the incubation for different periods of time of the thylakoids with paraquat, compared to the 'base' signal, which is assigned the 100% mark, obtained from the thylakoids when illuminated but not previously incubated with paraquat. Each graph (a-e) presents the results obtained with a different thylakoid preparation (thylakoid preparations Ch1 – Ch5 respectively).

As it can be seen, for all five different thylakoid preparations, paraquat had a distinctively different effect on the expected H_2O_2 produced by thylakoids following illumination, compared to the photosynthesis-inhibiting herbicides. For most concentrations of paraquat, there was a large increase in chemiluminescence signal observed, and hence possibly H_2O_2 produced by the thylakoids, when compared to the signal that was achievable by the thylakoids following the illumination without a herbicide incubation step. The very high chemiluminescence signals obtained following a 1 minute incubation of the thylakoids with paraquat did then fall over time, suggesting that, the very large

amounts of H_2O_2 produced during the period up to 1 min, were then somehow removed.

As explained in detail in Section 4.4.1.1.6, in the presence of light, paraquat is reduced to a stable free radical, which then causes toxic effects to the plant [166]. The dramatic toxic effects of paraquat require the presence of light, oxygen and photosynthetic tissue. Although the importance of light makes the light reactions of photosynthesis an obvious candidate as the primary candidate of paraquat, it does not inhibit the Hill reaction in isolated chloroplasts [165]. Therefore its primary action is the generation of free radicals, including hydrogen peroxide [4]. Hydrogen peroxide must then be reduced to water by reduced ascorbic acid, catalases or glutathione peroxidases, and there are such processes in place within the plant cells. In the presence of paraquat, the production of hydrogen peroxide is greatly enhanced and it then accumulates [165].

It is therefore suggested, that, the observed decrease, over time, of the concentration of H_2O_2 that is produced during the initial contact of paraquat with the thylakoids is the result of the H_2O_2-reducing facilities of the thylakoids coming into action, after a delay. This was also supported by simple measurements made, whereby the addition of catalase in thylakoid samples that were being incubated with paraquat caused the elimination of any H_2O_2 signal being detected by chemiluminescence; this is in accordance with the literature [169], whereas it is suggested that the inhibition caused by paraquat is reduced if O^{-}_2 or H_2O_2 scavenging enzymes and quenching systems are added to plant photosynthetic material. Of course, as it is the production of H_2O_2 by thylakoids that is of analytical interest for this work, the use of catalase therefore inhibits all desired H_2O_2 as well as this produced the effect of paraquat.

As the incubation of the thylakoids with paraquat did not result in a meaningful inhibition of their H_2O_2-producing capacity, no further measurements were made, and there are no dose-response curves obtained to plot that would be classified as a calibration curve for the detection of paraquat based on the

inhibition of H_2O_2 production by the thylakoids, and hence reduction of the chemiluminescence signal. It is important however to acknowledge the effect paraquat has on the photosynthetic material itself, as it leads to the exact opposite result than the photosynthesis-inhibiting herbicides do (i.e. production of H_2O_2 rather than inhibition).

4.4.3.6 Chemiluminescence batch assay for acifluorfen

Samples of the five different thylakoid preparations, at the optimal chlorophyll concentrations as identified in Section 4.3.3.2, were incubated with samples of different acifluorfen concentrations ($1x10^{-4}$ – $1x10^{-7}$ M) for different lengths of time (1 – 15 min) and then illuminated for 5 min. The individual results were plotted for all different combinations, and can be found in Fig. 4.29.

a) Thylakoid preparation Ch1

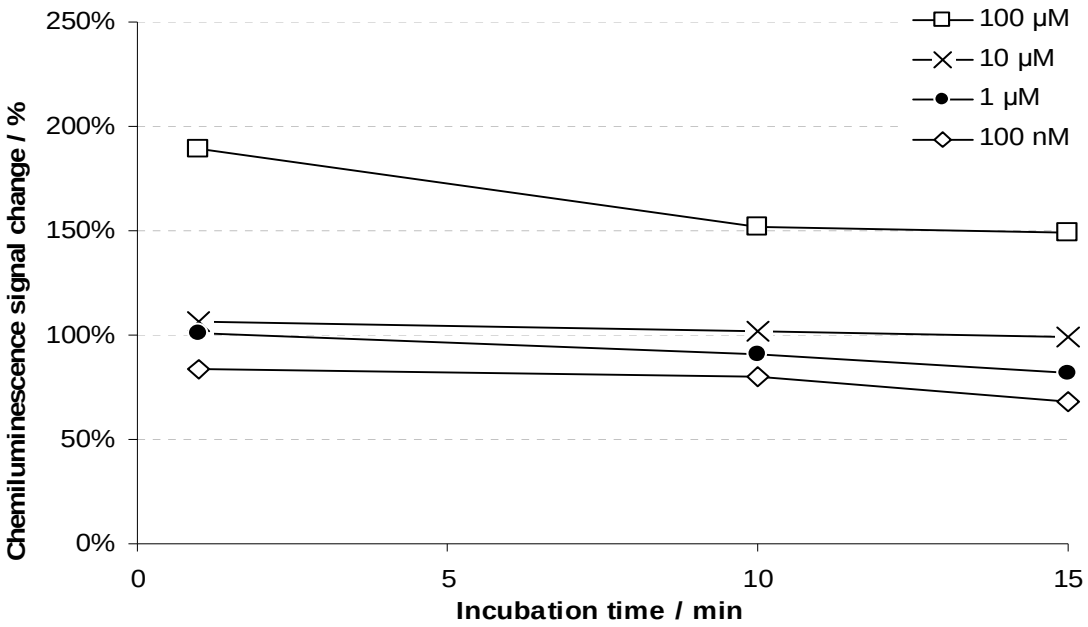

b) Thylakoid preparation Ch2

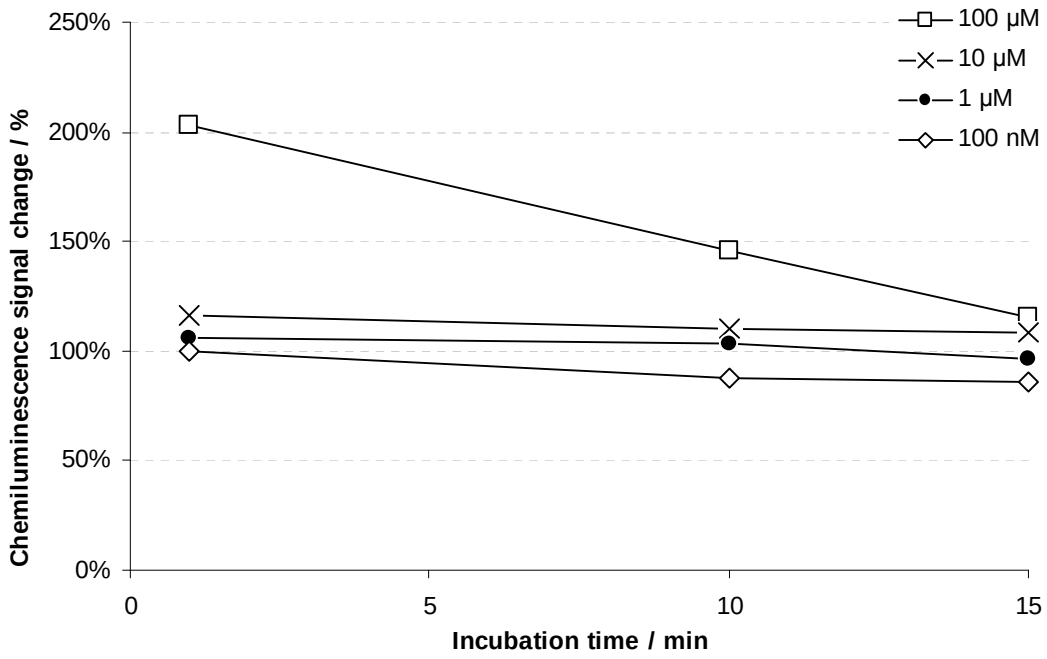

c) Thylakoid preparation Ch3

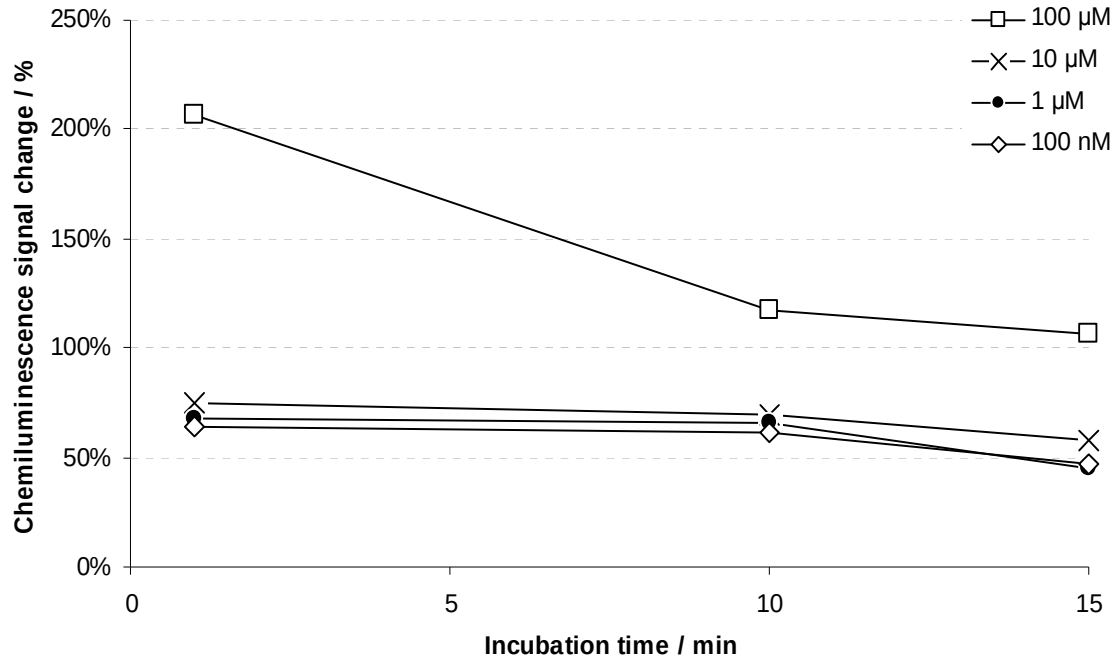

d) Thylakoid preparation Ch4

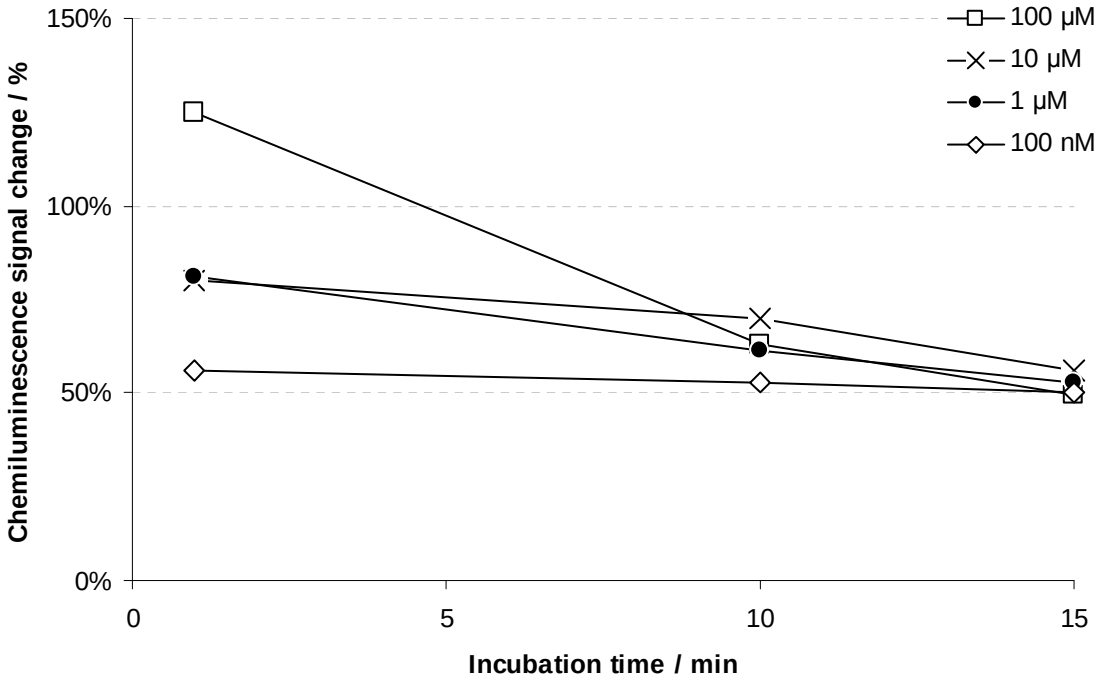

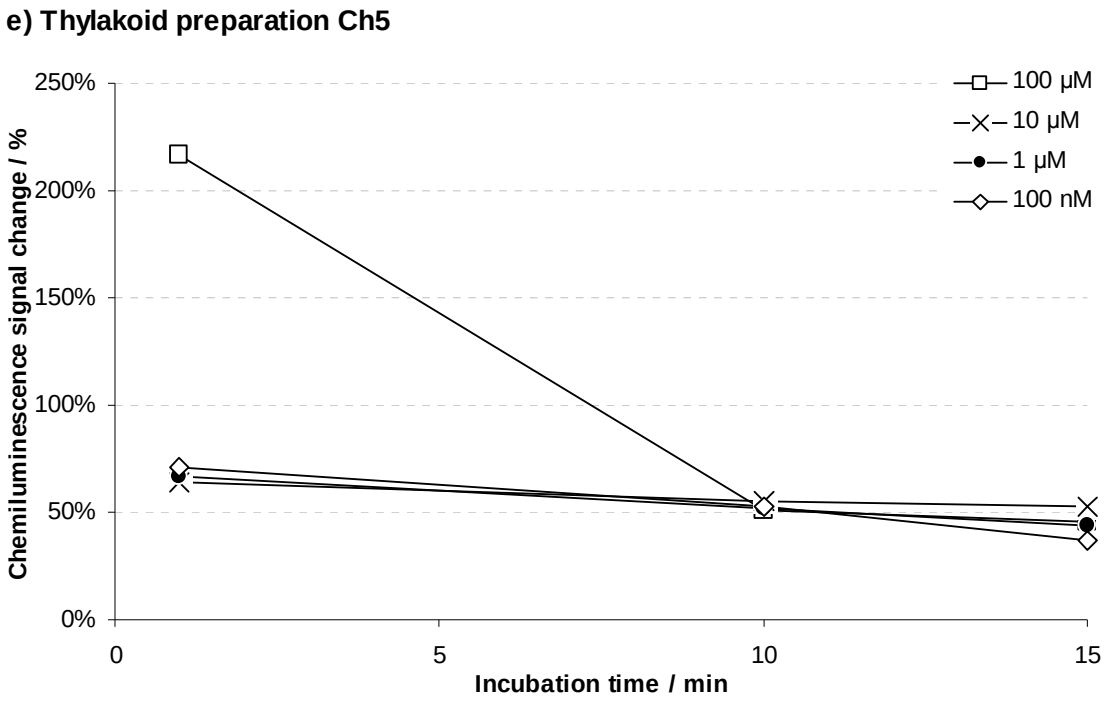

Figure 4.29 Effect (a–e) of acifluorfen on chemiluminescence signal due to H_2O_2 obtained from five isolated thylakoid preparations, over different incubation times, followed by a 5 min illumination step.

The Y-axis represents the percentile change of the chemiluminescence signal, and therefore H_2O_2 concentration produced during the illumination step, observed following the incubation for different periods of time of the thylakoids with acifluorfen, compared to the 'base' signal, which is assigned the 100% mark, obtained from the thylakoids when illuminated but not previously incubated with acifluorfen. Each graph (a-e) presents the results obtained with a different thylakoid preparation (thylakoid preparations Ch1 – Ch5 respectively).

As it can be seen, for all five different thylakoid preparations, the highest concentration of acifluorfen tested had a distinctively different effect on the expected H_2O_2 produced by thylakoids following illumination, compared to the photosynthesis-inhibiting herbicides. The increase in chemiluminescence signal observed, when compared to the signal that was achievable by the thylakoids following the illumination without a herbicide incubation step, did then fall over time. What is more, the effect of acifluorfen on the thylakoids appears not to be as strong as with paraquat, as the only concentration that effected a large increase of the H_2O_2 produced was the $1x10^{-4}$ M, which then fell over time,

suggesting that, the higher than expected amount of H_2O_2 produced during the period up to 1 min, was then somehow removed.

As explained in detail in Section 4.4.1.1.7, acifluorfen interferes with a wide range of biochemical processes in plants and plant cell organelles, including inhibiting the Hill reaction in isolated chloroplasts. Interference with electron transport in illuminated chloroplasts probably leads to the formation of singlet oxygen or other oxidants [162; 165]. Light is essential for the activation of the disruption process, although the specific role light plays in its activation is uncertain, with many conflicting theories [165; 170; 171].

It is therefore suggested that acifluorfen did possibly inhibit the production of H_2O_2 by the thylakoids, while also affecting them in other ways, thus causing a rise in the net amount of H_2O_2 produced. This effect appears to be concentration-dependent. The suggested explanation compares well to a similar example found in the literature. In the example of a biosensor for the detection of specific classes of herbicides, using their effect on the fluorescence of photosynthetic particles (fluorescence increases with an increase of herbicides) [174], it was reported that the biosensor could be used for the detection of DNOC (a phenolic herbicide) until a concentration of 300 µg/l. The effect of DNOC on the measured fluorescence signal (increase) was attributed to the inhibition of PSII electron transport while the uncoupling effect was considered to be comparably negligible at such low concentrations. However, at higher concentrations, although the PSII inhibition still increased, the uncoupling effect of DNOC tended to become the major parameter, which therefore caused a decrease of the fluorescence signal, thus not allowing for any meaningful detection of the herbicide at higher concentrations.

A similar method of action could therefore be suggested in the presented work, where the opposing actions leading to H_2O_2 formation and inhibition of H_2O_2 formation coexist in the chemiluminescence signal detected. Without further and detailed experiments this cannot be ascertained in any more detail.

As the incubation of the thylakoids with acifluorfen did not result in a meaningful inhibition of their H_2O_2-producing capacity, no further measurements were made, and there are no dose-response curves obtained to plot that would be classified as a calibration curve for the detection of acifluorfen based solely on the inhibition of H_2O_2 production by the thylakoids, and hence reduction of the chemiluminescence signal. It is important however to acknowledge the added effect acifluorfen has on the photosynthetic material itself, as it leads to the exact opposite result than the photosynthesis-inhibiting herbicides do (i.e. production of H_2O_2 rather than inhibition).

4.4.3.7 Chemiluminescence-related measurements made with herbicides

The literature provides very detailed descriptions of the effect of herbicides on target, or other organisms. There was however a clear need to evaluate the possible effect the herbicides used in this work have on the chemiluminescence reaction, as it is the second step of the herbicide detection assay, that provides the physical quantity (light) that is then correlated to the herbicide concentration.

Various combinations of the reagents taking part in the HRP-mediated chemiluminescence reaction between luminol and H_2O_2 were investigated when incubated with herbicides, using a series of different experiments.

For atrazine, diuron, propanil, 2,4-D and paraquat, when the standard chemiluminescence detection of known H_2O_2 concentration samples was performed with the addition of individual herbicides in the H_2O_2 sample, no significant change (increase or reduction) of the chemiluminescence signal detected was observed. Therefore, the herbicides do not interact with any of the components (H_2O_2, luminol, HRP) or affect the standard chemiluminescence reaction thereof. The same absence of an effect was also observed when the aforementioned five herbicides were mixed with luminol and HRP in the absence of H_2O_2.

For acifluorfen however, the standard chemiluminescence reaction in the presence of the herbicide, with or without H_2O_2, appeared to give higher than normal results. This effect is exemplified in Fig. 4.30. This is due to the fact that, as acifluorfen is a phenolic herbicide, it enhances the chemiluminescence reaction. Chlorophenols act as enhancers of the peroxidase-catalysed luminol chemiluminescence reaction. Using the enhancing property of chlorophenols as the detection principle, there is a published example of using this enhancement of the chemiluminescence signal as a means of detecting the said herbicides [87], by measuring the increase in chemiluminescence signal.

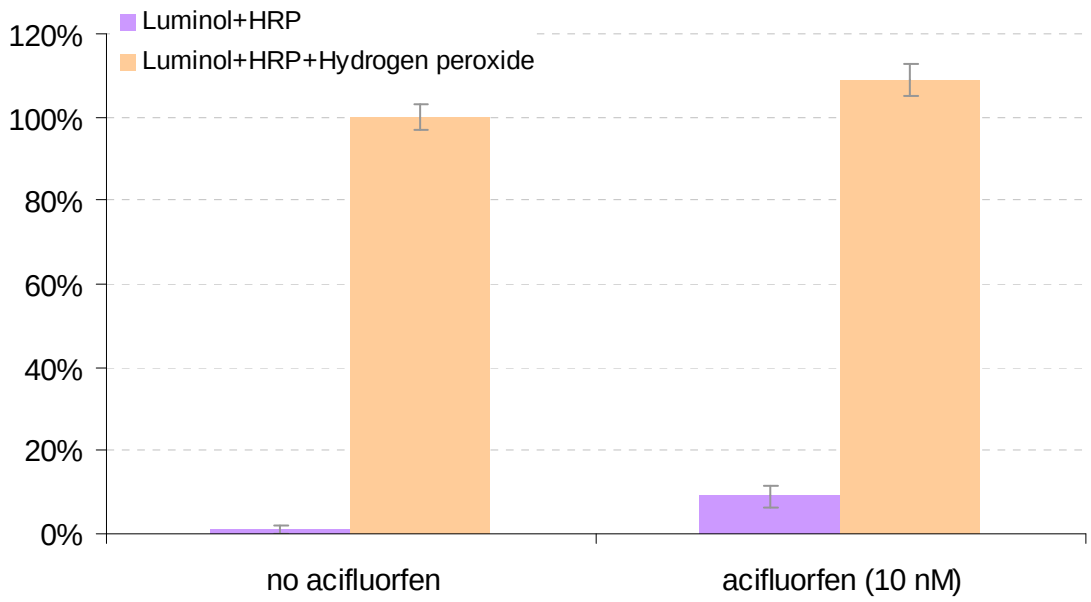

Figure 4.30 Effect of herbicide acifluorfen on the HRP-mediated luminol chemiluminescence reaction with H_2O_2.

For all six herbicides no chemiluminescence signal was detected when a herbicide sample was incubated with a thylakoid sample but not illuminated, effectively reproducing the standard experiments the results of which make up most of Section 4.4.3, but without the illumination step. This means that none of the herbicides effect the production of H_2O_2 by thylakoids without illumination.

4.5 Chlorophyll content and activity measurement of isolated photosynthetic material

4.5.1 Introduction

In order to ascertain whether the isolated chloroplasts and thylakoids contained some of the organelles and molecules necessary for the photosynthetic oxygen evolution, and whether these were photosynthetically active, as well as, importantly, also as a means of allowing for comparative performance assessment of the different isolated thylakoid preparations, it was important to identify common parameters that apply to all different preparations, and to measure and quantify those. This was considered as a way of adjusting all different thylakoid preparations to a common value in order to allow for harmonised conditions over which to compare them.

A parameter that is commonly used as a quantity measured following the isolation of photosynthetic material, according to the literature [6; 44; 175], is the amount of chlorophyll that can be found in such preparations. Therefore, absorbance measurements were taken of the different chloroplast and thylakoid preparations in order to allow such quantification.

Another parameter identified as commonly reported in the literature is the chlorophyll fluorescence [48]. The capacity of a plant for photochemistry is limited and will depend upon a range of factors including stresses caused by environmental conditions. Energy in excess of that used for photochemistry must be effectively dissipated by non-photochemical processes. Such processes include the emission of heat and re-emission of small but diagnostically significant amounts of the absorbed radiation as longer wavelength red/far-red light energy. This re-emission of light is termed chlorophyll fluorescence [176]. The fluorescence of chlorophyll is therefore a known process that has been used extensively in basic as well as applied agricultural and photosynthesis-related research; not only is it a process that has been used to assess the effect of a variety of environmental factors upon

whole plants, such as amount of light, water, gases etc, but also as a method of quantifying chemical moieties that affect in some way the fluorescence of subcellular organelles, more notably in biosensors for the quantitative detection of herbicides [175]. It was therefore deemed necessary to quantify the fluorescence of the different preparations in order to allow for the estimation of photosynthetic activity.

4.5.2 Materials and methods

4.5.2.1 Chlorophyll concentration measurements

In order to calculate the chlorophyll a and b content, a variation of a protocol was used, found in literature [177]. Twenty five microlitres of each chloroplast and thylakoid preparation were mixed with 5 ml of acetone (80%) and then centrifuged. The supernatant was placed in a 1 cm glass cuvette, and absorbance measurements of the supernatant were made at two wavelengths, 663 and 647 nm. The equation then used is as shown:

$[Chl\ (a+b)]\ (mg/l) = (7.15 * A_{663} + 18.71* A_{647})/5$

where A is the absorption at the given wavelengths.

4.5.2.2 Chlorophyll fluorescence measurements

A 200 µl aliquot of the sample to be measured (diluted thylakoid preparations) was placed in a small opaque sample holder. The sample was then dark adapted for 20 min. The chlorophyll fluorescence was measured and analysed using a Handy Plant Efficiency Analyser chlorophyll fluorometer (Hansatech Instruments Ltd., King's Lynn, UK). The instrument is a light detector designed for measurement and analysis of chlorophyll fluorescence. The relative fluorescence or Fv/Fm was automatically calculated and reported as (Fm – Fo)/Fm, where:

- Fo - fluorescence level when plastoquinone electron acceptor pool (Qa) is fully oxidised (in the dark, at the end of dark adaptation period)

- Fm - fluorescence level when Qa is transiently fully reduced (after pulse light illumination)
- Fv - variable fluorescence (Fm-Fo)
- Fv/Fm - maximum quantum efficiency of Photosystem II.

4.5.3 Results and discussion

4.5.3.1 Chlorophyll concentration measurements and adjustments

All chloroplast and thylakoid preparations, prior to illumination experiments for the production, and detection, of H_2O_2, were tested for the amount of chlorophyll they contained, in mg per ml of the final aliquots that were the result of the isolation process. As the isolation protocols employed varied greatly in overall methodologies, amounts of spinach leaves used, reagent volumes throughout the isolation protocols and final isolated thylakoids volumes, this was aimed to allow for a more direct comparison of the results, although the chlorophyll content is only an indication of potential activity. The results can be seen in Table 4.10.

Table 4.10 Absorbance and calculated chlorophyll concentration of the different chloroplast and thylakoid preparations.

Chloroplast and Thylakoid preparation name	Absorbance at 663 nm	Absorbance at 647 nm	Chlorophyll concentration of undiluted thylakoid preparation, mg/ml
Ch0a	1.24	0.72	4.467
Ch0b	1.98	0.85	6.012
Ch1	1.77	0.84	5.674
Ch2	0.68	0.35	2.282
Ch3	1.01	0.52	3.390
Ch4	1.09	0.52	3.505
Ch5	2.01	0.93	6.354

Next, in order to achieve uniformity, and thus comparability, amongst the different chloroplast and thylakoids preparations, the final volumes of all preparations were adjusted to contain the same amount of chlorophyll, prior to

their use in experiments. The adjustments made are shown in Table 4.11. The value of chlorophyll concentration chosen as the one to adjust all chloroplast and thylakoid preparations to, was 0.284 mg/ml. This is the optimal chlorophyll concentration for the highest production and detection of H_2O_2 for isolated thylakoids Ch1, and, as this was the first thylakoid preparation produced and tested, the rest were adjusted according to its chlorophyll concentration.

Table 4.11 Calculated chlorophyll concentration of the different chloroplast and thylakoid preparations, and volume adjustments in order to achieve the desired uniform such concentration in the final 990 µl of a typical chemiluminescence measurement in Chapter 4.

Chloroplast and Thylakoid preparation name	Chlorophyll concentration of undiluted thylakoid preparation, mg/ml	Desired chlorophyll concentration benchmark, mg/ml	Volume of undiluted thylakoid preparation to achieve desired chlorophyll concentration, µl
Ch0a	4.467	0.284	64
Ch0b	6.012	0.284	47
Ch1	5.674	0.284	50
Ch2	2.282	0.284	124
Ch3	3.390	0.284	84
Ch4	3.505	0.284	81
Ch5	6.354	0.284	45

However, as shown in Fig. 4.7 in Section 4.3.3.2, it appears that harmonising the final volume of each thylakoid preparation used in the chemiluminescence assays by adjusting them according to their chlorophyll concentrations resulted in some thylakoid preparations producing less detectable H_2O_2 in those thylakoid concentrations than in other, 'arbitrary' concentrations.

The true reason for the observed behaviour whereas the different thylakoid preparations a) do not contain the same amount of chlorophyll and b) do not produce the same amount of H_2O_2 when volume adjusted to contain the same amount of chlorophyll, is probably the heterogeneity of the thylakoids preparations, due to the different protocols used to deliver them. The different methods of isolation lead to the fact that, as all of the thylakoid preparations do

not simply contain purified chlorophyll, but, realistically, expectably, and even more so, ideally, whole thylakoid particles, adjusting the thylakoid concentration of each thylakoid preparation according to a common chlorophyll concentration is taking into consideration only partially the important element of sample absorbance when H_2O_2 production and chemiluminescence detection is taking place. It appears that the harmonised (according to chlorophyll concentration) thylakoid concentrations resulted in some preparations containing thylakoid concentrations that were inhibiting the H_2O_2 production or detection. The most probable reason for this is believed to be the increased absorbance of some of the thylakoid preparations, in relation to their individual H_2O_2 production yields, thereby inhibiting two-fold the detection of photosynthetically produced H_2O_2; firstly by inhibiting the light from the light source to reach as many thylakoids in order to produce H_2O_2 during the sample illumination, and, secondly, by inhibiting the chemiluminescence-produced light to escape the cuvette and be detected by the light detector during the detection. In a similar way, the exact opposite could have taken place, where adjusting for a chosen chlorophyll concentration could have resulted in thylakoid samples under-producing detectable H_2O_2, as is the case for each thylakoid preparation, as seen in Fig. 4.7, at the part of the curve prior to reaching the individual optimal concentration.

It was thus necessary to reach the final optimal thylakoid concentrations in thylakoid preparations by using experimental means. Therefore, sets of measurements were made for all thylakoid preparations in order to identify the optimal thylakoid (and hence chlorophyll) concentration that would result in the maximum H_2O_2 production and, equally importantly, detection. The results have already been reported in Section 4.3.3.2. As the chloroplast preparations did not produce any H_2O_2 production, or at least the detection thereof, it was not necessary, or indeed possible, to perform such measurements on the isolated chloroplasts. This set of experiments resulted in the optimised concentration / volume as shown in the right-most column in Table 4.12, for each individual thylakoid preparation. It is noted that the thylakoid preparation Ch5 appears to

produce the highest chemiluminescence signal resulting from the produced H_2O_2, from the lowest chlorophyll concentration, when compared to the other four thylakoid preparations, as seen in Fig. 4.7. Assuming that all thylakoid preparations contain thylakoids with the same amount of chlorophyll per thylakoid membrane, this would signify that the thylakoid preparation Ch5 has the most active, intact thylakoids, with the best H_2O_2 production yield.

Table 4.12 Chlorophyll concentration and thus volumes: a) set to a standardised amount (columns 2 and 3), b) set to the amounts optimal for the production and detection of H_2O_2 (columns 4 and 5)

Chloroplast and Thylakoid preparation name	Desired chlorophyll concentration benchmark, mg/ml	Volume of undiluted thylakoid preparation to achieve desired chlorophyll concentration, µl	Final chlorophyll concentration optimised for H_2O_2 production and detection, mg/ml	Final volume of undiluted thylakoid preparation optimised for H_2O_2 production and detection, µl
Ch0a	0.284	64	n/a	n/a
Ch0b	0.284	47	n/a	n/a
Ch1	0.284	50	0.284	50
Ch2	0.284	124	0.171	75
Ch3	0.284	84	0.237	70
Ch4	0.284	81	0.131	37.5
Ch5	0.284	45	0.064	10

4.5.3.2 Chlorophyll fluorescence measurements

One of the most common parameters reported in plant health studies is plant fluorescence, and specifically the Fv/Fm ratio. When a leaf is kept in the dark, all residual energy is processed and the amount of fluorescence is small (Fo); then, when a flash of bright light is shone to the leaf, the fluorescence signal will increase to a maximum, called Fm, as it can not use all of this energy. The difference between the maximum and minimum fluorescence is the variable fluorescence, Fv (Fv = Fm – Fo). The parameter that indicates the proportion of the maximum possible fluorescence, which was used for photosynthesis, is the result of dividing Fv by the maximum Fm. The quantum yield ratio Fv/Fm has for

some years been used to provide a diagnostic measure of the overall efficiency with which a plant is able to utilise light [176]. Values of 0.70 and upwards are considered examples of healthy photosynthetic material. A decline in Fv/Fm in dark-adapted plants is a good indicator of photo-inhibitory damage in plants subjected to stress.

Measurements were made of the chlorophyll fluorescence efficiency of the different isolated chloroplast and thylakoid preparations. For each thylakoid preparation, the chlorophyll fluorescence efficiency of two dilutions was measured, with one being the dilution adjusted for providing a final chlorophyll concentration of 0.284 mg/ml and the second being the dilution that provided the optimal H_2O_2 production and detection in experiments, as reported in Table 4.12. The calculated Fv/Fm ratios can be seen below in Table 4.13.

As it can be seen from the fluorescence efficiencies achieved by different concentrations of thylakoids in Table 4.13, for each thylakoid preparation separately, there is no direct relative correlation between changes in chlorophyll concentration and chlorophyll photosynthetic activity. This is logical, given that the parameter of chlorophyll fluorescence activity that is being measured, i.e. the ratio Fv/Fm, is a relative measurement of the sample's fluorescence pre- and post-illumination. For example, when more than halving the amount of chlorophyll in the sample of thylakoid preparation Ch3, the quantum yield does not respond in such a reaction as the overall proportion remains constant.

Table 4.13 Chlorophyll fluorescence efficiency of the isolated chloroplast and thylakoid preparations. a) set to a standardised amount (columns 2 and 3), b) set to the amounts optimal for the production and detection of H_2O_2 (columns 4 and 5)

Chloroplast and Thylakoid preparation name	Desired chlorophyll concentration benchmark, mg/ml	Corresponding chlorophyll photosynthetic activity (Fv/Fm)	Final chlorophyll concentration optimised for H_2O_2 detection, mg/ml	Corresponding chlorophyll photosynthetic activity (Fv/Fm)
Ch0a	0.284	0.70	n/a	n/a
Ch0b	0.284	0.61	n/a	n/a
Ch1	0.284	0.82	0.284	0.81
Ch2	0.284	0.66	0.171	0.65
Ch3	0.284	0.71	0.237	0.70
Ch4	0.284	0.59	0.131	0.59
Ch5	0.284	0.72	0.064	0.70

However, as has already been highlighted with the fact that the thylakoid dilutions, when chosen to reflect a harmonised chlorophyll concentration (0.284 mg/ml), were not the optimal to also yield the maximum H_2O_2 production, it is therefore not surprising that, when comparing the chlorophyll activity (column 3 in Table 4.13) for all thylakoid preparations against each other, there is no direct relationship. The same can also be said for the photosynthetic activity of the different optimised concentrations of thylakoids; again, the best photosynthetic yields, as far as fluorescence is concerned, are not necessarily achieved by the preparations that appear to have the most chlorophyll (column 4). These observations point towards an experimental unknown, that, as the thylakoid preparations have undergone major, and diverse, isolation procedures, the photosynthetic activity of chlorophyll cannot be directly correlated to its concentration, in the same way it could be assumed for a healthy leaf. What is more, the fact that, in response to identifying the optimal concentration for the optimal H_2O_2 detection some of the chlorophyll concentrations had to be reduced, suggests that the chlorophyll activity ought not to be used as a direct comparative indicator of the potential H_2O_2 production, and detection, of any preparations described in this work.

To conclude, having identified two methods commonly used to report plant health, the use of these methods on the isolated chloroplast and thylakoid preparations revealed that they do not correlate in any way with the H_2O_2 production and detection achieved by said preparations.

4.6 General discussion

To summarise, the work presented in Chapter 4 establishes the development of a bench-top, batch format assay for the detection of certain classes of herbicides, based on the HRP-mediated chemiluminescence reaction of luminol with H_2O_2 produced by illuminated thylakoids following incubation with a herbicide sample.

4.6.1 Production of H_2O_2 by illuminating isolated chloroplasts, and detection thereof using chemiluminescence

An investigation into obtaining detectable H_2O_2 from isolated chloroplasts following illumination was carried out. Two different isolation protocols were used to obtain chloroplasts, but with either, no H_2O_2 was detected. Various treatments of the chloroplasts, pre- and post-illumination, as well as the assaying of their contents or their preparation's supernatant, with or without added H_2O_2, has led to the suggestion that the inability to detect any produced H_2O_2 is not due to the unsuitability of the H_2O_2 detection step (chemiluminescence reaction), but due to the chloroplasts' preparations having a catalase-like active compound that scavenges any produced H_2O_2, if there is any produced.

4.6.2 Production of H_2O_2 by illuminating isolated thylakoids, and detection thereof using chemiluminescence

Following this, a different photosynthetic material organelle, the thylakoid, was obtained, using five different isolation methods, three of which were the most commonly used in the literature and two were variations thereof. All thylakoid

preparations produced H_2O_2 following their illumination, that could be detected and measured with the standard chemiluminescence H_2O_2 assay. The H_2O_2 production was affected by a variety of parameters of the illumination step (intensity, wavelength, length of time), the suspension medium (buffer) and the experimental method (pipette tips holding the thylakoids during illumination) used.

The production of H_2O_2 increased with the time of illumination, for all five preparations. As chemiluminescence signals reporting the produced H_2O_2 increased with the longer illumination times, there were clear differences in the ability of the different thylakoid preparations to produce detectable H_2O_2. This is partly due to the optical density of the thylakoid samples, which, following illumination, were then introduced in the standard HRP-mediated chemiluminescence reaction, which was affected by the absorbance of the chemiluminescence light by the thylakoids. However, for each thylakoid preparation the dilution (reported as chlorophyll concentration) at which they produced the most H_2O_2 while keeping all other experimental variables had been identified, thus making the dilutions and comparison of the different thylakoid preparations based on H_2O_2 production yields. What is more, illumination longer than 10 min appeared to significantly limit the rate of H_2O_2 production, although, without further detailed experiments this cannot be ascertained, as it could instead be due to the scavenging of H_2O_2 following a time lag.

It is important to highlight however that, as the assay for the detection of produced H_2O_2 is performed in a batch method with the H_2O_2-producing sample having to enter the chemiluminescence reaction step, the chemiluminescence signal intensity resulting from the H_2O_2 effectively underreported the amount of H_2O_2 produced, due to the sample's optical density.

The Ch5 thylakoid preparation was the preparation that, for the least amount of thylakoids (reported as chlorophyll concentration) produced the most light after

a 10-min illumination, with all aforementioned parameters optimised. That makes the Ch5 preparation also the one with the most amount of the 'better performing thylakoids' / 'total thylakoids in the preparation irrespective of performance'. Nevertheless, all five different isolated thylakoid preparations were used in the next set of experiments, as a definitive suggestion on whether good overall characteristics on the H_2O_2 production step would also be translated in the lowest LOD for herbicides, could not be ascertained.

Illuminating all five different thylakoid preparations with spectrum- (and intensity) filtered variations of the same light source provided a fascinating account of the behaviour of thylakoids as a whole depending on the illumination wavelength changes, but also between the different preparations. The results showed the effect the different spectral distributions have on the production of H_2O_2. An expectation for the H_2O_2 production to vary accordingly only to the light intensity is not met, as photosynthesis is affected by the differences in wavelengths as well. Differences in H_2O_2 production found between thylakoid preparations can now be partly attributed to their active pigments constitutions (which are unknown, other than chlorophyll).

4.6.3 Detection of herbicides based upon their inhibitory effect on H_2O_2 production by illuminated thylakoids

Incubating all five different thylakoid preparations with increasing concentrations of photosynthesis-inhibiting herbicides did result in clear, correlated reduction of the chemiluminescence signal, which therefore suggests also a correlated reduction of the H_2O_2 production by thylakoids during an illumination step following the incubation step. For all three photosynthesis-inhibiting herbicides, thylakoid preparation Ch5 resulted in the lowest LODs of all five preparations; this suggests that Ch5's seemingly higher proportion of thylakoids that produce a lot of H_2O_2, while containing the least thylakoids overall, did also result in the ability of less herbicide molecules to effect a detectable reduction in their H_2O_2 production. The lower LODs achieved (atrazine: $6.0x10^{-09}$, diuron: $8.0x10^{-08}$, propanil: $1.4x10^{-07}$) are not sufficiently low to meet the E.U. limits of maximum

permissible concentrations of herbicides in waters. Given the wide range of detection achieved (approximately 4-5 orders of magnitude), it is expected that the inability to detect sufficiently low concentrations of herbicides is due to the fact that, with the relatively high concentrations of thylakoids in each measurement, the binding sites for the herbicide molecules are too many for low herbicide concentrations to have a measurable effect on the H_2O_2 production, compared to the blank signal, which, as this is an assay measuring the inhibitory effect of the analyte, is the maximum possible signal obtained rather than 'zero', therefore adding to the difficulty to detect it. The RSD for the detection of photosynthesis-inhibiting herbicides is: 5.7%.

The confidence in the presence of this relationship is increased due to a variety of measurements that were performed with the herbicides, the thylakoids and the chemiluminescence reagents and standard chemiluminescence H_2O_2 assay using different variables of presence or absence of any of the steps (incubation, illumination, chemiluminescence reaction) and of any of the participating components (herbicides, thylakoids, luminol, HRP) in order to identify any unwanted effects.

For non-photosynthesis-inhibiting herbicides, the batch assay gave a variable response, due to the means of action of the herbicides chosen. For paraquat and acifluorfen, the H_2O_2 detected was over the blank, for some concentrations many times over. This of course could be considered a valid method to detect said herbicides, i.e. by measuring their effect on the photosynthetic material, which is an effect different to the inhibition of H_2O_2 production. However, what makes the developed assay a valid method for the detection of photosynthesis-inhibiting herbicides is the fact that the classes categorised as such all have a similar effect on the photosynthetic material, while the non-photosynthesis-inhibiting herbicides vary in their means of action. Interestingly, although 2,4-D was not expected to cause any inhibition of the H_2O_2 production by thylakoids, according to knowledge of its mode of action, a small inhibition was observed, which was concentration dependent. There is no knowledge to the cause of this

however, as no literature reporting the effect of 2,4-D on isolated photosynthetic material was found.

Chapter 5: Design, Testing and Implementation of the Fluidic Chemiluminescence Assay Unit for Hydrogen Peroxide

A major part of the work presented in Chapter 5 has been published, albeit in less detail and depth, in a paper [196], together with parts of the work described in Chapter 4 on the detection of herbicides in a batch assay.

5.1 Introduction – Fluidic sensor unit principles and design

5.1.1 Fluidic assay requirements and considerations

As stated in the aims and objectives of the project (Section 1.2), the central aim of the work presented, is the establishment of a fluidic sensor unit for performing a chemiluminescent bioassay for the detection of herbicides in water, that can be reused and regenerated, itself a key objective for the development of a stand-alone, fully automated, field-based, reusable sensing system.

When altering the properties of 'wet chemistry' batch assays with the aim of converting said assays for use in miniaturised, stand-alone systems with automated methods of introducing and processing samples, performing the assays and being primed for reuse, the most common way of achieving this is to use the principles of flow-based analysis. Hence, the assay for the detection of herbicides in a batch format (presented in Section 4.4) needs to be converted into a fluidic assay. This includes performing the stages of the batch assay, namely the herbicide-induced inhibition of the production of H_2O_2 by thylakoids and its subsequent detection.

In order to achieve the objective of transferring the established herbicide assay from a batch to a fluidic format, the sensor unit needs to allow for the following discreet steps to be performed;

1. the illumination-stimulated production of H_2O_2 by thylakoids, and its inhibition by a herbicide-containing sample
2. the detection of produced H_2O_2 using the HRP-mediated chemiluminescence reaction of luminol/H_2O_2.

What is more, these steps need to be performed in a way that will allow for the sensor unit to be subsequently incorporated into a system that will be able to be used as a stand-alone device with minimal user involvement. To achieve this, the method developed had to therefore take into account the need for the sensor unit to be able to be reused or replaced. There are already developed sensors for the electrochemical detection of herbicides, that inhibit the photosynthetic oxygen evolution that require the physical replacement of the component that incorporates the photosynthetic material in use [8; 9; 48; 140-142; 154]. In all of these prior examples, the photosynthetic material has been immobilised on an electrode's surface. The literature reveals that an individual electrode can sometimes be reused for a limited number of individual measurements, which then requires the user to replace with a new electrode. Hence, this signifies little integration of the key element of the sensor (the electrode with the photosynthetic material) with other elements of the unit, namely the fluidics and detection method. There are no current examples of research performed attempting to allow for the seamless replacement of the reusable element of such a sensor, namely of the photosynthetic material and its support / immobilisation structure. It was therefore decided to investigate this route.

To address the need for reusability, regenerability and suitability for automation, the fluidic assay developed would need to alter some of the components of either / both of the two steps mentioned above into a format that would allow for that improvement. A common trend in research and development for medical and environmental assays is the immobilisation of a component used in an

assay. This allows for better detection limits, automation, as well as, importantly, for the stabilisation of said components, allowing the assay a longer time during which it can be used, following its production. As already mentioned, in herbicide detection fluidic assays, immobilisation methods for the photosynthetic material used have been employed, albeit with the disadvantage that the said methods do not allow for the easy replacement of key components of the sensor.

A novel immobilisation method that is increasingly employed in clinical diagnostics [106; 118] is based on the use of superparamagnetic beads. As it has already been discussed in the literature review, superparamagnetic beads allow for a variety of immobilisation chemistries to be used on a wide array of functionalised chemical-linking groups that can be attached on their surface, and are very good candidates for automation [106]. Importantly, the non-permanent nature of the magnetisation of the beads, means that replacing them is achievable simply by means of appropriate fluidic and magnetic control. Consequently, the use of such beads therefore also means that any material immobilised on the beads will also be removed; the subsequent replacement of the beads with a new lot, means that the sensor / assay in which they are used can be effectively regenerated. This is a novel method of being able to manipulate the movement of the photosynthetic material, achieved by attachment on the beads.

Another characteristic that ought to be taken into consideration when developing the fluidic assay and hence the sensor, is the need for distinct areas where the two assay steps would be taking place. Previous work using the principle of the inhibition of the photosynthetic oxygen evolution by herbicides, used illuminated, immobilised photosynthetic organelles, the effect on which by the herbicides would be measured with electrochemical methods concurrently with the incubation taking place, and were therefore not affected by the light source used to illuminate the organelles [8; 9; 48; 142; 154; 159]. This, however, is a limiting factor of the current work, where the illumination of the thylakoids needs

to precede the detection of chemiluminescence signal. Hence, separate areas need to be utilised for the two steps.

5.1.2 Way forward / approach

All of the above was taken into consideration during the fluidic bioassay development and the method chosen includes both HRP and thylakoids covalently coupled on superparamagnetic beads, using appropriate immobilisation chemistries. The fluidic sensor unit will therefore comprise of a fluidic channel with two "active" regions with:

- thylakoids immobilised on beads, and
- HRP immobilised on beads.

The two “active" regions on the fluidic channel are non-permanent, as, although the thylakoids and HRP are chemically immobilised on superparamagnetic beads, the beads will in turn be magnetically entrapped on the “active” regions. By immobilising the said components on superparamagnetic beads, it is thus possible to (i) magnetically define and control the “active" regions of the sensor unit by using magnets to guide the beads to the preferred area and (ii) de-sensitise a region simply by removing the magnetic field, as superparamagnetic beads have no 'magnetic memory'. This is shown schematically in Figures 5.1 and 5.2.

Using two separate areas for necessary reactions to take place, allows for the 2-step assay to take place in the same fluidic sensor unit, as the beads with thylakoids and the beads with HRP are magnetically entrapped in separate areas of the channel, at different times, allowing a herbicide sample flowing in the channel to first react with the thylakoids by inhibiting the production of H_2O_2 while then, any produced H_2O_2 reacts with the pre-mixed luminol and the immobilised HRP to produce a light signal, detected by a photodetector.

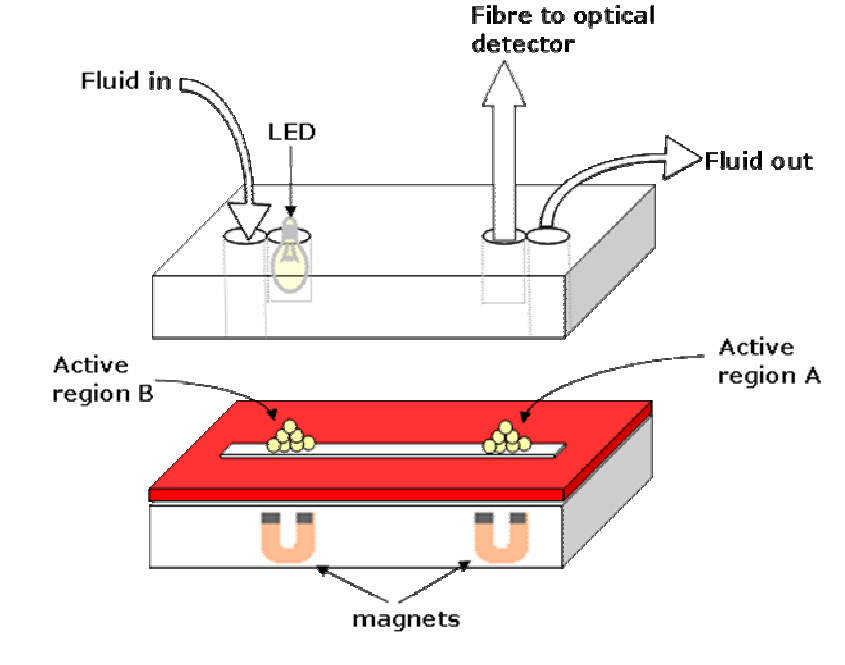

Figure 5.1 Schematic representation of the fluidic sensor unit, semi-exploded view.

The two blocks that sandwich the fluidic channel are shown wide apart. The “active” regions are also shown, with the magnetic beads entrapped into the magnetic fields of the magnets. Not to scale.

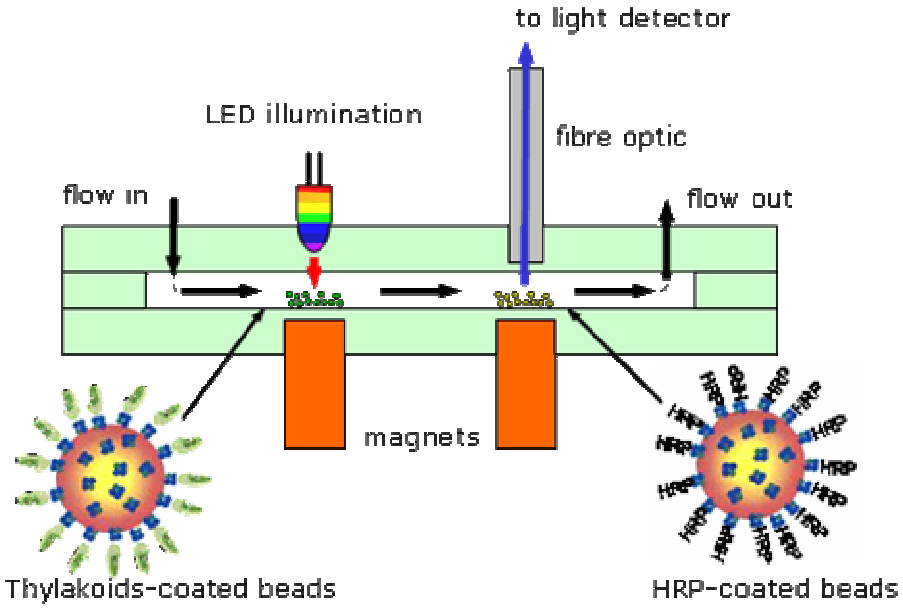

Figure 5.2 Schematic representation of the sensor unit, side view.

The “active” regions are also shown, with the magnetic beads entrapped into the magnetic fields of the magnets. Not to scale.

5.1.3 Fluidic assay setup and method protocol

In order to successfully transfer the batch assay to a fluidic sensor format, the setup for the use of the sensor unit is required to include:

- the fluidic channel
- a flow cell to house the fluidic channel
- pumps to effect the flow of reagents
- a flow-injection port and valve arrangement
- a light source to illuminate the thylakoids and
- a light detector to detect the chemiluminescence reaction light.

The fluidic sensor unit was designed taking into consideration all the requirements and steps of the assay. A method protocol for the use of the fluidic sensor thus includes:

- Beads with immobilised HRP enter the fluidic channel, and are trapped by magnetic forces in region A (as seen in Fig 5.1).
- Beads with immobilised thylakoids enter the fluidic channel, and are trapped by magnetic forces in region B.
- A sample, potentially containing herbicides, pre-mixed with luminol, enters the fluidic channel, and is illuminated, whilst stagnant over the thylakoid-beads (stop-flow technique), on the region B. The illumination will result in a herbicide-dependant production of H_2O_2 by the thylakoids on the beads.
- The sample, now with H_2O_2 potentially produced by the thylakoids, flows towards region A, where the chemiluminescence reaction takes place, and the light produced is collected by the optical fibre and quantified by the detector.
- The removal of the magnetic forces, and the flow of a cleaning buffer, means that all the beads are removed and the sensor is ready to be used again.

Therefore, in the rest of this chapter, results from work performed on the following sub-streams is presented:

- Flow cell fabrication

- HRP immobilisation
- Fluidic assay for H_2O_2 detection using the flow cell described here.

5.2 Fluidic sensor unit fabrication

The fluidic sensor unit was manufactured, following the design and principles described above. It consists of three main parts: a fluidic channel and two blocks that sandwich it.

5.2.1 Fabrication of fluidic sensor unit blocks

The two blocks were designed in detail, and constructed of machined clear Perspex, by Cranfield University at Silsoe's engineering technicians.

Detailed, scaled-down drawings of the blocks can be found in Appendix II. Briefly, the dimensions are height * width * length = 20 mm * 20 mm * 60 mm; Figure 5.3 contains photographs of the two separate blocks.

Figure 5.3 Photographs of the two machined Perspex blocks that will be sandwiching the fluidic channel.
(left: top block, right: lower block)

5.2.2 Fabrication of fluidic sensor unit channel

The fluidic channel effectively functions as a spacer between the two blocks. Various methods were considered and tested for the fabrication of the fluidic

channel; early prototypes of the channel were made from polydimethylsiloxane (PDMS) as well as hand-cut black rubber.

The channels made using the hand-cut method lacked the necessary precision required for more elaborate designs other than a straight channel.

PDMS is the most widely used silicon-based organic polymer. Conventional methods of fabricating microfluidic devices have centred on etching in glass and silicon. Fabrication of microfluidic devices in PDMS by soft lithography provides faster, less expensive routes than these conventional methods to devices that handle aqueous solutions. These soft-lithographic methods are based on rapid prototyping and replica moulding and are more accessible to chemists and biologists working under bench-top conditions than are the microelectronics-derived methods because, in soft lithography, devices do not need to be fabricated in a clean-room [178]. The properties of PDMS that make it a suitable platform for miniaturised biological studies, techniques for fabricating PDMS microstructures, and methods for controlling fluid flow in microchannels have been reviewed [179].

Early attempts to create fluidic channels using PDMS were successful (Fig. 5.4). However, the need for the use of lithography and many intermediate steps before the end channel is fabricated meant that it was a slow method, which did not allow for rapid changes on the designs to take place easily. What is more, previous research using fluidic channels for the detection of chemiluminescence has highlighted that the use of a translucent collagen membrane as the fluidic channel gave chemiluminescence light intensity readings of 10% lower values than in the presence of a white polyamide channel [87]. The explanation provided by the authors was to attribute this to the ability of white membranes to reflect light, resulting in better light collection by the optical fibre.

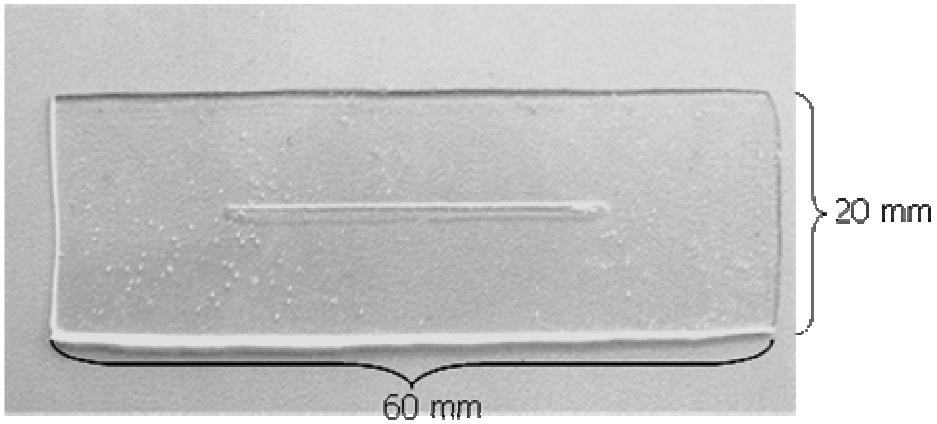

Figure 5.4 An early silicon fluidic channel fabricated.

The preferred method for the fabrication of the fluidic channel is the use of a laser to cut the designed channels from neoprene sheets. A CO_2 laser (30 W, IR, CO_2 Fenix model, by Synrad Inc., USA,) was used for cutting the structures, which allowed for rapid prototyping of the structures, as the whole process was controlled by software (WinMark Pro, Synrad, Inc., USA), coupled with increased accuracy compared to the hand-cutting or the lithographic methods. Alternative channel designs were used in order to optimise the capture and amount of magnetic beads. Examples can be seen the figures below (Fig. 5.5, 5.6); details of their use can be found in the description of the experiments in Section 5.4. As already mentioned, previous research on the use of fluidic channels for the detection of chemiluminescence-produced light has indicated that the colour of the fluidic channel can enhance or limit the collected light [87]. It was therefore decided to make the fluidic channels out of a white neoprene sheet.

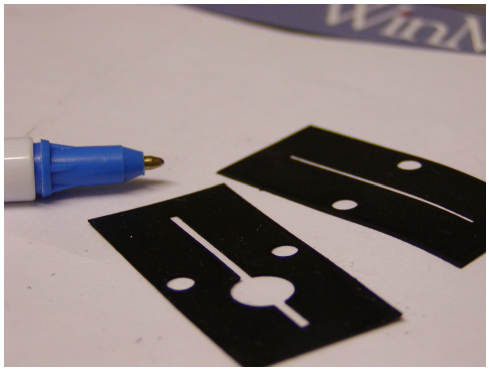

Figure 5.5 Examples of laser-cut channels fabricated.

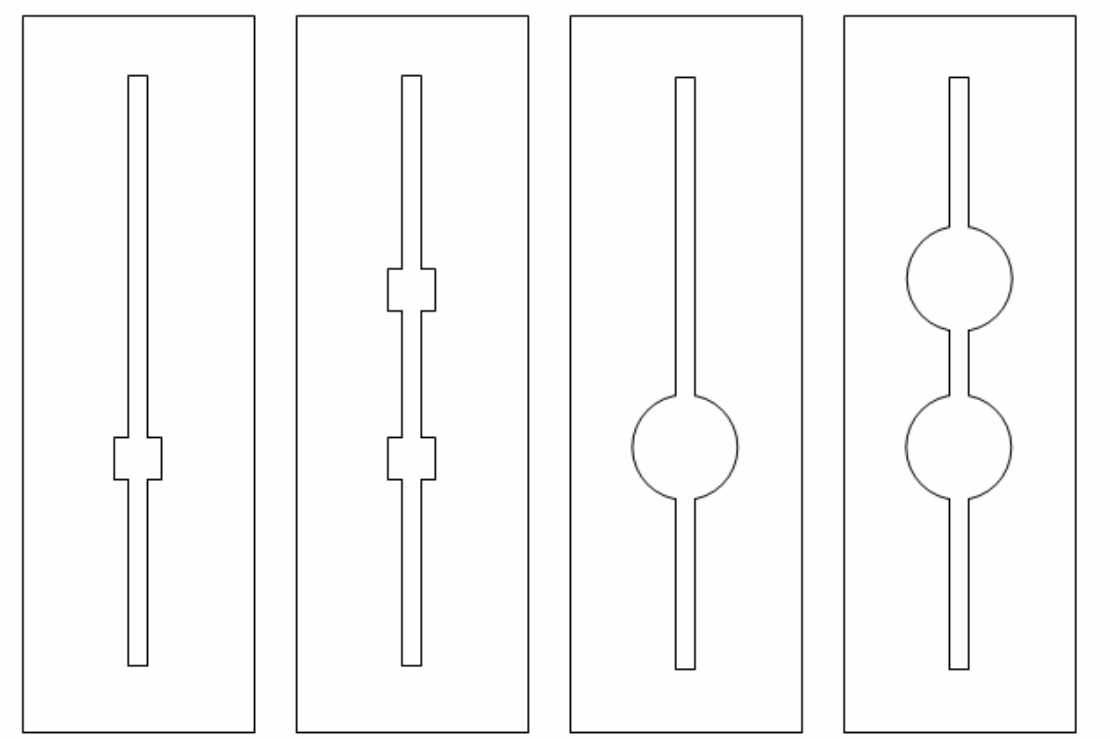

Figure 5.6 Schematic drawings of laser-cut channels fabricated for use with the fluidic sensor.

The regions used for the entrapment of the magnetic beads are the protruding circular and rectangular areas. Not to scale.

5.2.3 Assembly of the fluidic sensor unit components

The two Perspex blocks are kept together with six screws, four are found in the four corners and two in the length of the blocks. The fluidic channel is sandwiched and tightly bound by the two blocks. For the flow of liquids in and out of the channel, standard threaded tubing fittings were used. The tubing and fittings used were from Omnifit Ltd, now Bio-Chem Fluidics (Cambridge, UK). Neodymium magnets were from RS Components Ltd (Corby, UK). The Minipuls3 Peristaltic Pumps were from Gilson (Wisconsin, USA). The injection port valve was from Pharmacia.

Further details of the setup of the system to be used with the fluidic sensor unit can be found in Section 5.4, where detailed descriptions of the setup and methods of its use are given.

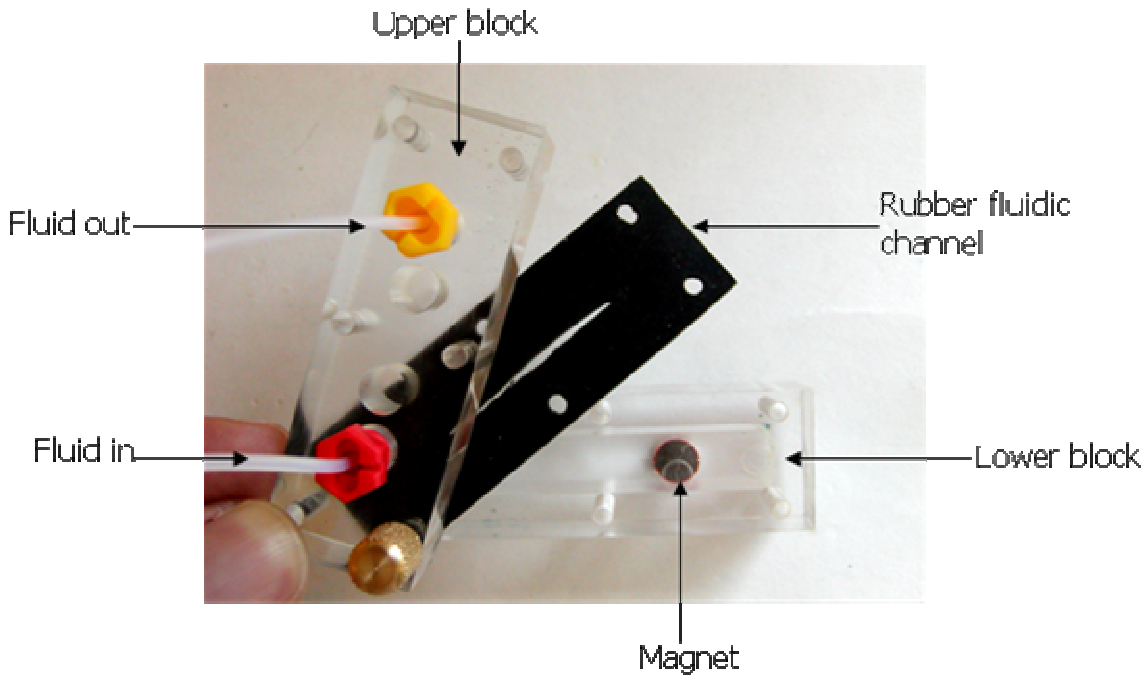

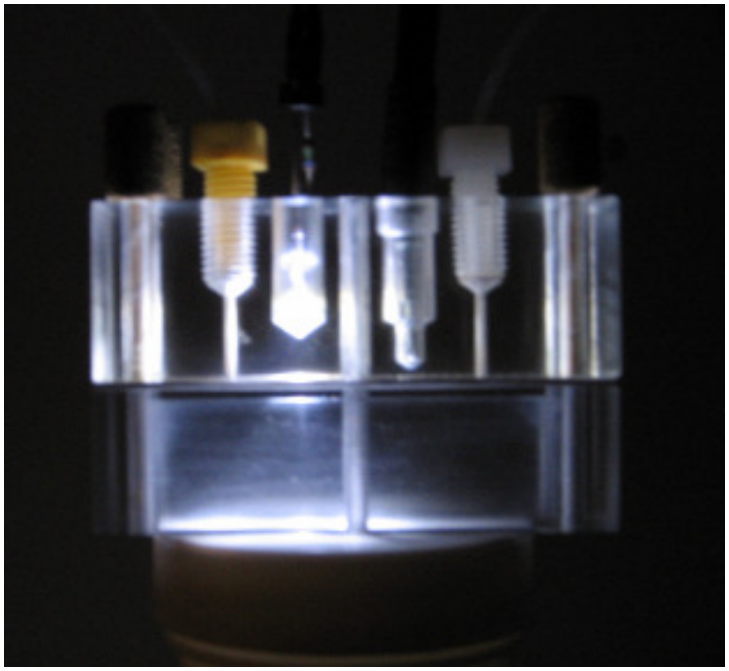

Figure 5.7 Photographs of the micro-system (top and side views).

On the top view, to allow view of the three separate parts (upper block, lower block, channel) they are seen partly rotated. On the bottom view, the LED is switched on.

5.3 Immobilisation of HRP on superparamagnetic beads

5.3.1 Introduction

As Chapter 5 is the collection of the various pieces of work necessary in order to transfer the HRP-mediated luminol chemiluminescence detection of H_2O_2 batch assay into a fluidic format, the work presented in Section 5.3 is focused on the immobilisation of HRP on beads. As mentioned in the Aim and Objectives, part of the objective covering the transfer of the assay into a fluidic format, is the immobilisation of a component of the batch assay. Following the extensive use of immobilised HRP for chemiluminescence assays, as reported in the Literature Review (Section 2.3.4.4 and 2.4.2.5), it was decided to immobilise HRP on the superparamagnetic beads.

Having determined the design needs for the fluidic sensor and hence the components necessary to achieve the successful use of a fluidic assay for the detection of H_2O_2 (Section 5.1), and having fabricated the physical components of the sensor (Section 5.2), work followed on the immobilisation of HRP on superparamagnetic beads, as this is the final key preparation stage in order to then test the H_2O_2 detection chemiluminescence fluidic assay.

The nature of the assay that beads are to be used in, determines whether to coat the beads with protein completely or not. Although in some cases an incomplete coating of the beads with the chosen component is necessary [180], for bead-capture ELISAs and tests, dyed-beads sandwich tests, solid-phase assays, and DNA probes, coating the beads as heavily as possible (a monolayer coating) is desirable [114]. This is also the case for the work presented here, as it is expected that it is best to achieve the maximum and quickest reaction with H_2O_2. In a monolayer coating, the HRP will mediate the reaction of the maximum amount of luminol and H_2O_2, maximising the signal.

The simpler method of physical adsorption of HRP on non-functionalised magnetic beads is possible, but studies have shown that this method results in

a significant decrease in active HRP being immobilised, compared to using chemical covalent linking [181]. Therefore, it was decided to choose a covalent attachment method.

Careful examination of the reading material and information therein provided by magnetic beads manufacturers, presented no preferred option of beads to select, on a scientific basis. Therefore, the bead type chosen for the immobilisation of HRP was the MagaBeads^{TM} from Cortex Biochemicals (now Promega Corp, Winskonsin, USA). The beads are uniform, monosized, superparamagnetic, with a mean diameter of 3.2 µm, composed of highly cross-linked polystyrene with evenly distributed magnetic material (iron oxide). These beads are carboxyl group (-COOH) modified, with a monolayer of carboxyl groups pre-immobilised on their surface.

For the immobilisation of the HRP, the ethyl-dimethyl carbodiimide (EDC) chemistry was used (Fig. 5.8). The carbodiimide is utilised to activate the beads for amide bonding with primary amines. The mechanism and optimisation of carbodiimide mediated amide bond formation is extensively discussed in the literature [182]. A generic protocol was supplied by the distributor (Europa Bioproducts), and immobilisation was performed using this as the basis.

The approximate amount of active immobilised HRP was calculated by measuring the peroxidase activity with the colorimetric assay of 2,2'-Azino-bis(3-ethylbenzthiazoline-6-sulfonic acid) (ABTS) and comparing that of a sample with the response obtained by a series of dilutions of known concentrations of HRP.

ABTS was chosen as it is a chromogenic enzyme substrate specific for peroxidases. The peroxidase-catalysed reduction of H_2O_2 to water is coupled to a one-electron oxidation of ABTS, forming a radical cation. This cation has a brilliant blue-green colour with a peak wavelength at about 410 nm [183]. Other protein assays were considered (Bradford reagent, Bicinchoninic acid, TMB,

Modified Lowry assay, Coomassie), but they are not peroxidase-specific and some are able to detect only larger concentrations of enzymes (about 10 times the estimated maximum in the experiments described here).

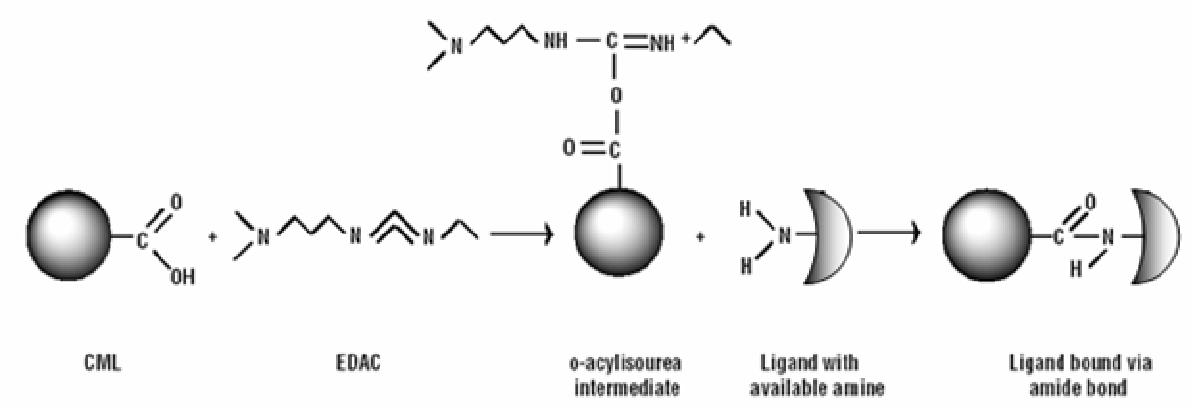

Figure 5.8 HRP immobilisation chemistry using EDC as the intermediate linker between the carboxyl group of the beads and the amine of the HRP.

Following the choice of the immobilisation method to use, HRP was immobilised on superparamagnetic beads. As the protocol provided by the manufacturer of the beads was not HRP-specific, the immobilisation took place many times, each time building on the knowledge and optimised parameters of the previous occasions, aiming to produce a fully optimised protocol.

5.3.2 Materials and methods

5.3.2.1 Materials

HRP (type II, 148 U/mg), HRP (type VI, highly stabilised, 300 U/mg), MES, NaOH, sodium acetate trihydrate, acetic acid (glacial), glycine, hydrogen peroxide (30% w/w), EDC, PBS, phosphate-citrate tablets and ABTS tablets were purchased from Sigma Chemical Co. The 'MagaBeads-Carboxyl Terminated' were supplied from Europa Bioproducts (Cambridge, UK). The buffers (0.1 M sodium acetate, pH 4) and (50 mM MES buffer, pH 6.1) were

prepared using RO water. EDC (100 nM), HRP (1 nM), glycine (0.03% w/v) were prepared freshly before each immobilisation assay, in MES buffer (50 mM, pH 6.1).

5.3.2.2 Immobilisation protocol

For the immobilisation of HRP on the beads, a protocol supplied by Cortex Biochemicals was used, which can be found in Appendix III. Briefly, the protocol required the following key steps:

- Washing and volume adjusting of the beads
- Incubation of beads with EDC
- Incubation of beads with HRP
- Washing
- Blocking the remaining active sites with glycine
- Washing.

The protocol was used as supplied when starting the optimisation process, and, via the detailed optimisation process described in the results, alterations were made. The final protocol resulting from the optimisation process is therefore found in the end of the results, Section 5.3.3.7.

5.3.2.3 HRP activity assay

A standard curve was firstly prepared from the absorbance measured from known HRP concentrations, in order to then compare the results obtained from the immobilised HRP to the reference curve.

For the HRP activity standard curve, one tablet of ABTS (10 mg) was dissolved in 100 ml of phosphate-citrate buffer (50 mM, pH 5) and 25 µl of 30% H_2O_2 was added immediately prior to use. 100 µl of this reagent were added to 100 µl of known HRP samples in wells of a white microtitre plate with a clear bottom. Immediately after initiation of reaction, the absorbance at 405 nm was measured every 1 minute for 10 minutes, using a Dynex Revelations 4.21 microplate reader (Dynex Technologies Ltd., Worthing, UK). The microplate

reader reported both the individual absorbance measurements per minute as well as the rate of the reaction.

When measuring the HRP activity found on immobilised HRP on beads, the ABTS assay was repeated, with a dilution of the beads replacing the known HRP sample.

5.3.3 Results and discussion

With the aim of the work presented in this section being to achieve an optimised HRP immobilisation process, step-by-step changes were made to the original, manufacturer-provided protocol. The optimisation process of the generic immobilisation protocol included varying:

1. the washing steps after the HRP immobilisation,
2. the concentration of EDC during the functionalisation of the carboxyl groups on the beads,
3. the type of HRP used,
4. the addition of a washing step of excess EDC, between the EDC and HRP incubations, and
5. the concentration of HRP during the immobilisation of HRP on bound EDC.

The effect of making these changes was measured with the ABTS HRP-activity assay, thereby measuring whether the changes made to the protocol resulted in an increase to the amount of active HRP bound on the beads.

5.3.3.1 HRP activity assay

In order to quantify the amount of active HRP bound on the beads, the ABTS assay was performed on the resulting beads obtained from each immobilisation optimisation attempt.

Firstly, the standard curve obtained for the activity of known concentrations of HRP using the ABTS assay was plotted, in order to be able to translate the

ABTS activity results obtained from the beads into an approximation of the active amount of HRP bound on the beads.

Therefore, when the immobilisation protocol was used, the resulting HRP immobilised on beads from all the optimisation steps was diluted and the ABTS assay was performed, the results of which were then checked against the standard curve. After finding the corresponding concentration of HRP that was bound on the beads, that was used to calculate the standard activity units of HRP (purpurogallin units), as this is the standard method used in the literature to report HRP activity.

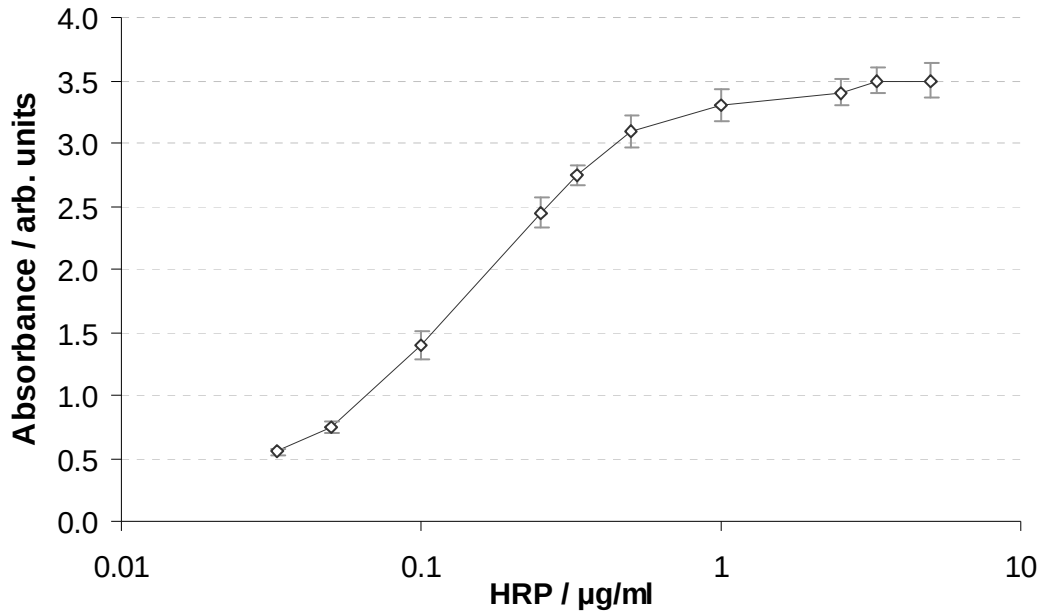

Figure 5.9 Standard curve of HRP activity using the ABTS assay.

5.3.3.2 Optimisation of the sodium acetate washing steps after the HRP immobilisation

The original protocol included a step of washing the beads twice with sodium acetate buffer (0.1 M, pH 4.0) after the HRP immobilisation (step 11 in the original protocol, Appendix III). Given the low pH of the buffer suggested, and

the denaturing effect this could be having on the bound HRP, it was decided to evaluate its effect.

The immobilisation was therefore performed with the sodium acetate wash step (with one and two washes) and without this step altogether. It should be noted that, when the step was omitted, a washing step was carried out nevertheless, using MES buffer (50 mM, pH 6.1) instead, thus bringing the total number of washes of the three variations to the same number, in order to avoid introducing another varying parameter (the number of washes overall) to the experiments. Thus, the resulting beads with immobilised HRP from using all three variations of the protocol were then tested for active HRP bound on the beads, using the ABTS assay.

The results presented in Table 5.1 show that beads with the two sodium acetate washes had less active HRP bound on the beads than the ones washed only with MES, while the variation of the protocol that employed one sodium acetate wash gave intermediate results. Having performed these measurements using two different pH values for the acetate buffer reveals that the acetate buffer and its low pH are having an effect on the activity of HRP bound on the beads.

Table 5.1 Effect of washing the beads with acetate buffer after the immobilisation of HRP on the activity of the final amount of HRP bound on the beads.

	HRP activity per 1 mg of beads (purpurogallin units)	
Number of washing cycles	pH 4.0	pH 5.0
2 sod. acetate washing cycles	0.088	0.092
1 sod. acetate washing cycles	0.092	0.095
No sod. acetate washing cycles	0.100	

Values presented are the average of two replicates.

Protocols for the immobilisation of ligands available from other manufacturers of beads, using EDC as the intermediate, appear to have no similar step of washing the beads post-immobilisation with an acetate buffer at such a low pH [180; 184; 185]. Similarly, previous research on the effect of pH on the immobilisation of HRP on chitosan beads, showed that buffers with pH 4 more than halved the activity of immobilised HRP [186]. A possible explanation given is that the structure of the enzyme is changed due to the fact that such extreme pH values are far beyond the isoelectric point of HRP, which is pH 7.2.

To ensure no reduction in active HRP on the beads, it was therefore decided to remove the step, and substitute it with washing the beads once with MES buffer (50 mM, pH 6.1) instead.

5.3.3.3 Optimisation of the EDC concentration during the carboxyl groups functionalisation step

Following the optimisation of the sodium acetate washing step, the amount of EDC employed during the beads' carboxyl groups functionalisation step was altered in order to identify the optimal conditions.

For the step of binding EDC onto the carboxyl groups of the beads, different concentrations of EDC were tested. The original protocol suggested 100 nmol of EDC per 1 mg of beads, so concentrations above and below this amount were tested.

The results are presented in Table 5.2, with the amount of HRP activity found on the beads post-immobilisation following the same protocol apart from one variable, the EDC concentration. Concentrations above the suggested 100 nmol per 1 mg of beads did not result in an increased amount of active HRP bound and detected with the ABTS assay. This suggests that complete activation of all the carboxyl groups on the beads is achieved by following the amount suggested in the protocol, while also bearing in mind the amount of HRP used

too. Therefore, the amount of EDC used was kept to 100 nmol per 1 mg of beads.

Table 5.2 Effect of EDC concentration during the carboxyl groups activation to the activity of the final amount of HRP bound on the beads.

EDC concentration (nmol per 1 mg of beads)	HRP activity per 1 mg of beads (purpurogallin units)
80	0.090
90	0.095
100	0.100
110	0.100

Values presented are the average of two replicates.

5.3.3.4 Optimisation of the HRP type immobilised on the beads

Following the optimisation of the EDC concentration during the carboxyl groups functionalisation step, the HRP type immobilised on the beads was altered in order to identify the optimal conditions.

Initially, an HRP with a lower hemin content, and therefore activity, was immobilised on the beads (HRP-1, Sigma product code P8250); it is also more prone to deactivation in various environments when they are not favourable (pH, temperature). A different HRP was subsequently used (HRP-2, Sigma product code P2088) which is further purified and also chemically stabilised to protect the primary amines and maintain activity at low pH and higher temperature [41].

Having immobilised both types of HRP on beads while keeping all conditions of the immobilisation the same, the amount of active HRP bound on the beads was measured using the ABTS assay, and was then converted to the standard purpurogallin units. The results can be seen in Table 5.3. Use of the more stable and active type of HRP resulted in better yields of active HRP bound on the beads. What is more, the increase in bound, active HRP is approximately

threefold, while the difference in purpurogallin units of free HRP is twofold. It was therefore decided to substitute the previous type of HRP with the new HRP-2.

Table 5.3 Effect of HRP type during the binding of HRP on the beads to the activity of the final amount of HRP bound on the beads.

Type of HRP	HRP activity per 1 mg of beads (purpurogallin units)
HRP-1	0.100
HRP-2	0.375

Values presented are the average of two replicates.

5.3.3.5 Optimisation of the washing of excess EDC between the EDC and HRP incubation steps

Following the optimisation of the type of HRP used for the immobilisation, the washing of excess EDC step was altered in order to identify the optimal conditions.

Following a protocol suggested by a different carboxyl-modified magnetic beads manufacturer [180], where a clear distinction is made between three different methods of performing the immobilisation of protein on carboxyl-beads via EDC, another refinement of the protocol used was tested, namely the washing of any excess, unbound EDC prior to adding the HRP. In more detail, according to the authors [180] the three variations of the EDC-assisted immobilisation process of the ligand of interest are:

- the "one-step" process of immobilising the target protein is to mix the beads with EDC and the protein at the same time; the greatest disadvantage of this being the fact that EDC binds indiscriminately and may cross-link protein molecules as well as bind to the beads, and results in the formation of denatured proteins, clumped in large groups.
- the "one-and-a-half step" process, as so called by same manufacturer, still uses the mixing of the beads, EDC and the protein altogether, but only

following careful calculation of the amount of EDC required to activate the available amount of carboxyl groups on the beads as well as the amount of protein available.

- the "two-step" process allows the carboxyl groups on the beads to react with EDC, with any unused EDC then washed away, and only then the addition of the protein takes place, allowing for a more complete utilisation of the reagents as well as controlling any undesirable cross-linking.

The protocol provided by the manufacturer of the beads used in the experiments presented here falls into the category of the so-called "one-and-a-half step" process, as, any excess, unbound EDC is not removed prior to the addition of HRP, although the addition of EDC and HRP do not take place simultaneously but in series, which would be partly alleviating the negative effect of the excess EDC. Therefore, a step was added to the protocol, whereas, before the HRP was incubated with the beads, any excess EDC was washed away with MES buffer twice. The activity assay was then performed on the resulting beads.

The results with this alteration showed a significant increase of active HRP bound on the beads, as it can be seen in Table 5.4. This suggests that a significant amount of unbound EDC was previously binding to HRP molecules, while also either somehow preventing the immobilisation of these HRP molecules on bead-bound EDC, or perhaps inactivating the HRP molecules thus hindering their activity. It was therefore decided to retain this alteration to the protocol.

Table 5.4 Effect of presence or absence of excess EDC during the HRP immobilisation on the bound EDC to the activity of the final amount of HRP bound on the beads.

Washing step removing excess EDC	HRP activity per 1 mg of beads (purpurogallin units)
Yes, wash step added	1.200
No washing prior to HRP addition	0.375

Values presented are the average of two replicates.

5.3.3.6 Optimisation of the HRP concentration during the HRP immobilisation step

Following the optimisation of the washing of excess EDC, the HRP concentration during the HRP immobilisation step was altered in order to identify the optimal conditions.

Although, according to the protocol, 10 nmol of protein is suggested as the required amount for an optimal coating of 1 mg of beads, which corresponds to 50 µg of HRP, it was decided to measure the effect other concentrations may have on the amount of HRP finally immobilised on the beads. Therefore, different concentrations of HRP were used during the immobilisation, and the resulting beads with immobilised HRP were tested for the amount of active HRP found using the ABTS activity assay. The active HRP bound on beads, in purpurogallin units, from the different variations of the protocol are found in Table 5.5.

As it can be seen, 50 µg of HRP appear to not have been very close to the optimal amount of HRP necessary for what would be categorised as a complete coating of the beads. Increasing the concentration effected a significant increase of the amount of HRP immobilised on the beads, although from 80 µg/mg and more the activity measured appears to plateau, suggesting that perhaps this is due to the achievement of a complete coating of the beads with HRP.

Table 5.5 Effect of HRP concentration during its immobilisation to the activity of the final amount of HRP bound on the beads.

HRP concentration per 1 mg of beads (µg/mg of beads)	HRP activity per 1 mg of beads (purpurogallin units)
45	1.1
50	1.2
65	1.5
80	2.1
100	2.1

5.3.3.7 Final HRP immobilisation protocol

In order to ascertain that the immobilisation of HRP on the magnetic beads was optimal, and following all the optimisation steps taken as described in Sections 5.3.3.2.-6, the protocol was thus shaped into the following final form. Magnetic beads with 2.1 purpurogallin units per 1 mg of beads were obtained.

HRP immobilisation protocol

1. Mix beads thoroughly by gently mixing and dispense desired quantity in an appropriate sized container.
2. Wash the beads 3 times with 2 ml of MES buffer (50 mM, pH 6.1) each time.
3. Adjust volume of beads to a 10 mg/ml concentration.
4. Add EDC (200 µg/ml, in 50 mM MES, pH 6.1, 100 nmol per 1 mg of beads).
5. Mix gently for 5 minutes at room temperature.
6. Remove excess EDC by washing with 2 ml of MES buffer each time.
7. Add 80 µg of HRP-2 per 1 mg of beads.
8. Mix gently for 2 hours at room temperature.
9. Wash mixture 4 times with 2 ml of MES buffer each time.
10. Add 2 ml of 0.03% glycine in MES buffer and mix gently for 30 minutes.
11. Wash beads 5 times with 2 ml of MES buffer each time.
12. Wash beads 3 times with 2 ml of Tris buffer (10 mM, pH 8.5)

Following the steps presented for the fine-tuning of the immobilisation protocol, the beads with HRP immobilised on them were therefore obtainable in an optimised way to be used with the designed and constructed fluidic cell, for the implementation of the fluidic assay for the detection of H_2O_2.

5.4 Flow assay for the detection of hydrogen peroxide

5.4.1 Introduction

Following the immobilisation of HRP on the magnetic beads, experimental work was undertaken in order to transfer the batch assay for the detection of H_2O_2 into a fluidic format. This was the first step towards fully transferring the herbicides batch assay, which works by inhibiting the H_2O_2 production by thylakoids.

More specifically, the beads with immobilised HRP were used in the fluidic sensor unit, in order to perform the H_2O_2 assay with one reactive component immobilised (HRP), and luminol pre-mixed with the H_2O_2 sample in flow, therefore establishing a flow chemiluminescence assay for H_2O_2. This would then allow for a smoother transfer of the herbicides assay to a fluidic format, having fine-tuned some of the parameters of the assay already.

As described in the fluidic assay method principles (Section 5.1.3), the beads would be magnetically entrapped in the fluidic channel, and standards of H_2O_2 with luminol would be flown through. The chemiluminescence light produced would be detected with a portable detector, collected with an optical fibre.

Albeit, the fluidic assay for the detection of hydrogen peroxide required to be optimised in order to yield for the lowest detectable amount of hydrogen peroxide. Therefore, the first section of the results (Section 5.4.3.1) reports on the optimisation of the chemiluminescence H_2O_2 fluidic assay, followed by the calibration of the assay with the final, optimised conditions, as well as testing of real environmental water samples.

5.4.2 Materials and methods

5.4.2.1 Materials

Chemicals and reagents

Trizma, hydrochloric acid, 5-amino-2,3-dihydrophthalazine-1,4-dione sodium salt (luminol), PBS tablets and hydrogen peroxide (30% w/w) were purchased from Sigma Chemical Co. The Tris-HCl and PBS buffers were prepared using RO water. Luminol (various concentrations) and H_2O_2 (various concentrations) were prepared freshly each day, in Tris-HCl buffer, 10 mM, pH 8.5. The MagaBeads-Carboxyl Terminated beads with a 3.2 µm diameter were from Cortex Biochemicals (now Promega Corp, Winskonsin, USA). The beads with immobilised HRP (2.1 U/mg beads) were prepared as in Section 5.3.

Detection

The customised QP1000-2-VIS/NIR-BX optical fibre was from Anglia Instruments Ltd. (Ely, UK). The detector C5460 APD Module was from Hamamatsu Photonics UK Ltd (Welwyn Garden City, UK). The PCI-1200 multifunction Input/Output data acquisition device and LabVIEW 5.0 was from National Instruments Ltd. (Newbury, UK).

5.4.2.2 Setup and method

The flow assay for the detection of H_2O_2 was performed using the fluidic unit described earlier (Section 5.2). A schematic diagram of the setup used is pictured in Fig. 5.10 below.

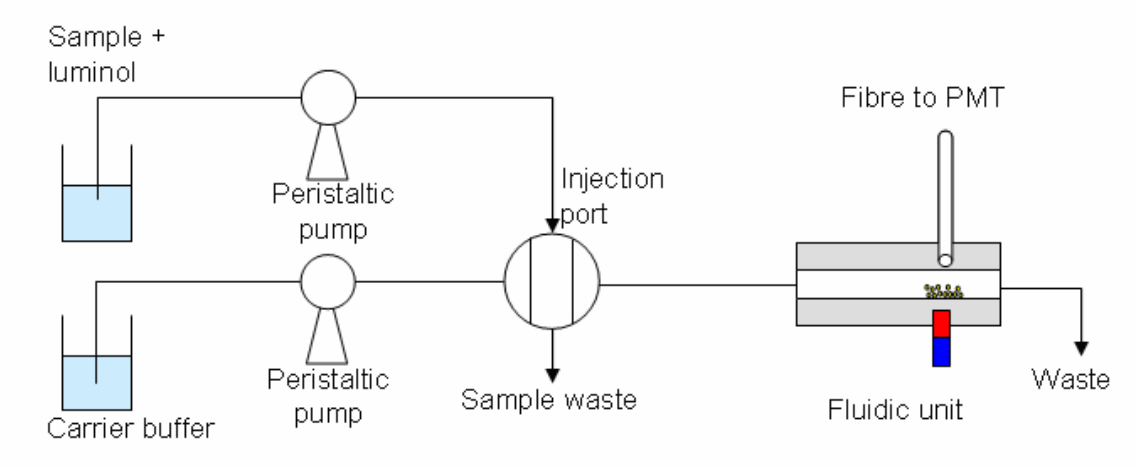

Figure 5.10 Schematic representation of the experimental setup for the H_2O_2 fluidic assay.

The HRP-coated magnetic beads were introduced in the flow cell prior to a measurement taking place. The magnet was used in order to magnetically entrap the beads on the desired position. To achieve a uniform positioning of the beads in the region of the fluidic channel that was directly beneath the position of the optical fibre, careful physical movement of the magnet had to be undertaken in order to spread the beads uniformly. Blu-Tack adhesive was then used to fix the magnet, which allowed for easy removal of the magnet when desired, as also used for other similar work [111]. As described in examples found in the literature [103; 111], after the removal of the beads following a chemiluminescence measurement, the flow cell was washed by flowing PBS buffer (100 mM, pH 7.2), in order to discard the beads completely.

A peristaltic pump was used to deliver the carrier buffer (Tris-HCl, 10 mM, pH 8.5). Inline with the flow was connected an injection port, on the sample loop of which the H_2O_2 sample was pre-mixed with luminol, which was also carried to the flow cell when the valve was switched to the appropriate position. PTFE tubing was used to connect all components in the flow system.

The optical fibre assembly used was a customised, 1000 µm diameter premium-grade fibre. The fibre was terminated with a standard SMA 905 connector on

one end (the end that attaches to the spectrometer), while the other end consisted only of the ferrule without the outer part of the SMA connector, which had been removed by the manufacturer, in order to allow for the fibre to fit closer to the fluidic channel. Light detected by the fibre was then transferred to the detector. The detector module contains an avalanche photodiode, with an effective active photon counting area of 0.78 mm^2. The specific APD module has a higher sensitivity at 420 nm from other series of Hamamatsu APDs. The detector's electrical signal converted from light was acquired via a data acquisition card by a PC, and further analysed and controlled by LabVIEW.

Following the assembly of all the components, the process of performing a single measurement of the H_2O_2 assay was the following:

~the fluidic setup was readied for the assay to be initiated~

- the tubing was washed with PBS buffer (100 mM, pH 7.2)
- a magnet was fixed underneath the active region A, 'viewed' by the optical fibre, aiming to magnetically trap the HRP-coated beads
- the magnetic beads with immobilised HRP were aspirated in the flow cell and magnetically trapped in the designated active region of the channel, directly below the optical fibre
- the tubing was washed with PBS buffer
- the flow of the Tris (carrier) buffer was initiated at varying flow rates
- a plug of the H_2O_2 sample and luminol was injected into the flow
- delivery of the sample plug in the channel area covered by the beads prompted the initiation of the HRP-mediated chemiluminescence reaction of luminol with H_2O_2
- the chemiluminescence light intensity was collected by the optical fibre

- the light signal was transduced to an electrical signal by the detector
- the obtained chemiluminescence intensity signal was recorded and the maximum intensity was used to plot the graphs or input in tables
- the magnet was removed from its fixed position
- the tubing was washed with PBS buffer, thus removing all beads, as well as the sample plug

~the fluidic setup was ready for the assay to be repeated~

5.4.2.3 Water samples collection

Rainwater was collected on two separate raining events, on two separate days. It was collected from outside the Institute of Bioscience and Technology, Cranfield University at Silsoe, Silsoe, MK45 4DT. Water from a small stream located in the countryside situated between the triangle of Silsoe, Flitton and Pulloxhill in Bedfordshire was collected. The three water samples were filtered with a 0.45 µm Whatman filter membrane to remove particles. The water samples collected were analysed on the same day following the collection, as well as with extra H_2O_2 of varying concentrations added. The environmental water samples were used as a replacement of the 50 µl sample used in the optimised fluidic sensor unit for the detection of H_2O_2. Prior to this, 45 µl of a water sample were mixed with 5 µl of luminol, which was diluted from a stock solution in buffer to the appropriate concentration using the water sample as the dilutant, thus making the presence of a buffer in the final 50 µl of water sample negligible.

5.4.3 Results and discussion

5.4.3.1 Optimisation of fluidic assay parameters

There are many parameters and aspects of the fluidic assay that were subject to scrutiny and optimisation, in an attempt to allow for the best conditions to

achieve the desired conditions for the detection of low levels of H_2O_2. The parameters of the fluidic assay that were optimised were the channel's geometry, namely the area that was covered by the HRP-beads, the H_2O_2 sample volume and flow rate and the reagents' concentrations, namely of luminol and HRP.

5.4.3.1.1 Optimisation of the fluidic channel geometry

Firstly, the geometry of the flow channel was optimised. Two designs were tested, a square-shaped with a surface area of 16 mm^2, and a circular-shaped design with a surface area of 78.5 mm^2 (Fig. 5.11). More specifically, in both cases, the differently-shaped area that protrudes from the straight, rectangular channel was used as the area where the beads with the immobilised HRP were magnetically trapped, which was also the area directly below the optical fibre that would collect the light and deliver it to the APD. Altering the size of the area, should result in a different spread of the beads, even when the same amount of beads is used.

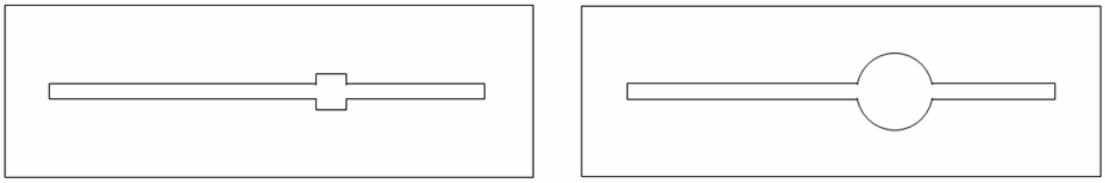

Figure 5.11 Schematic diagrams of the two fluidic channel designs used for the detection of H_2O_2.

The protruding areas were the areas were the magnetic beads with immobilised HRP were magnetically entrapped.

The design of the catchment area played an important part in the chemiluminescence signal detected for the same concentration of H_2O_2 in the sample. It was expected that increasing the area that the beads occupy during the chemiluminescence reaction would be allowing for increased catalysis of the chemiluminescence reaction by more HRP molecules, as more such molecules would have the opportunity to come into contact with H_2O_2 and luminol molecules. What is more, a larger surface area would naturally result in a larger

volume that a potential sample could occupy and therefore increased interaction between more H_2O_2, luminol and HRP.

The results in Table 5.6 present the peak light intensity resulting from the use of the fluidic unit to perform the H_2O_2 fluidic assay, as described in the Materials and Methods, when using the two different designs of the fluidic channel.

Table 5.6 Peak chemiluminescence intensity for three different H_2O_2 concentrations, from the two different active region designs tested.

	Measured chemiluminescence intensity (a.u)		
Area	**10 μM H_2O_2**	**5 μM H_2O_2**	**1 μM H_2O_2**
16 mm^2	455	342	73
78.5 mm^2	1260	727	150

Values presented are the average of three replicates.

As it can be seen from the results, with the same amount of HRP-coated beads in both cases, the flow channel with the circular design resulted in a much higher peak light signal produced by the chemiluminescence reaction. This suggests that a larger surface area, which, as ascertained by visual inspection allows for the better spread of the magnetic beads, appears to be resulting in better interaction between the reactants, with more H_2O_2 being reduced by the HRP-catalysed luminol reaction, from a single sample. Thus, the larger, circular active area fluidic channel was chosen for the H_2O_2 assay.

5.4.3.1.2 Optimisation of the sample volume and flow rate

Following the channel design optimisation, the variables studied and optimised were the sample volume (in this case H_2O_2 sample and luminol) and flow rate. The aim of varying these parameters' values was to identify the conditions that would allow for sharp, narrow 'spikes' from each measurement, with the higher peaks achievable.

In order to identify the range of sample volume values that would not result in the chemiluminescence reaction taking place for longer than needed in order to achieve a flash / spike kinetic, the volume occupied by the circular active region was calculated. Any sample volume value higher than this would be resulting in some form of delayed response that would be effectively resulting in a 'glow' chemiluminescence light production. With the area of the detection region being 78.5 mm^2, and the height of the channel being 1 mm, the volume occupied by the said structure is 78.5 mm^3. Therefore, the theoretical value obtained as the sample volume that would be expected to fill the active region is 78.5 µl. This figure will serve as a possible target volume, around which more volumes were tested, but in fluidic movement of such low volumes this serves only as a theoretical target.

Therefore, the fluidic assay for the detection of a single concentration of H_2O_2 was performed varying these two parameters. The sample volume injected was varied between 30 – 150 µl. The sample flow rate was varied between 50-1500 µl/min.

The difference in peak heights between background / blank and the sample increased with increasing sample volumes up to 50 µl, above which 'glow'-like behaviour was observed, as, the maximum value detected was not achieved momentary, but persisted for the duration of the sample being in the detection zone, that is, the circular area covered by the HRP-beads. This effect is exemplified in Figure 5.12. As it can be seen, for either of the two concentrations, although the signal intensity was not affected negatively, with the same peak value being achieved with a sample of 50 µl or 150 µl, it was unnecessary to obtain the longer kinetic obtained with the larger volume sample, as the peak light intensity was used for the measurements.

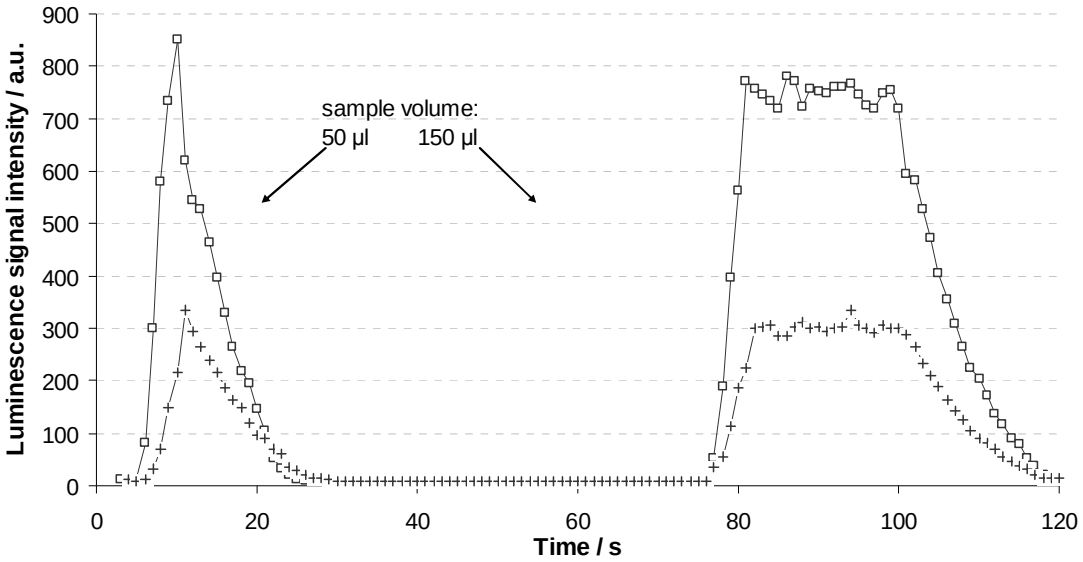

Figure 5.12 The effect of H_2O_2 sample volume on the kinetics of the chemiluminescence reaction with luminol and HRP, for two H_2O_2 concentrations.
(□: 6.5 µM, +: 2 µM).

Altering the flow rate employed when the H_2O_2 sample is passing through the fluidic channel had a great effect on the resulting chemiluminescence signal detected, as seen in Fig. 5.13.

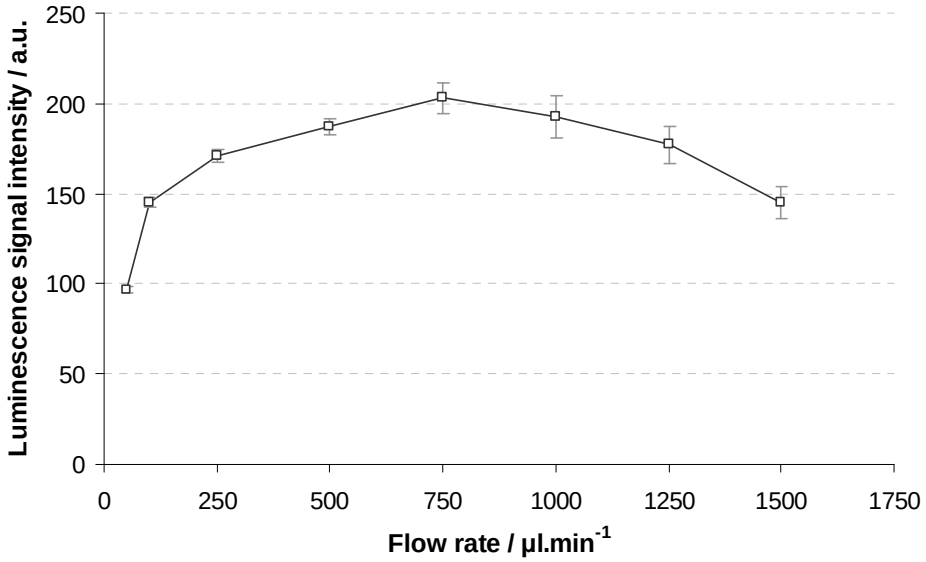

Figure 5.13 The effect of H_2O_2 sample flow rate on the signal intensity of the chemiluminescence reaction with luminol and HRP, for 1 µM H_2O_2.
Values presented are the average of three replicates.

As it can be seen from the results in Fig. 5.13, increasing the flow rate corresponded to an increase of peak chemiluminescence light intensity being obtained, up to a 750 µl/min, while higher flow rates resulted in a decrease. Flow rates higher than the 750 µl/min may have resulted in the dislocation of some magnetic beads, as there was a signal decrease observed, while it was envisaged that sharper peaks could still be achieved. It is suggested in the literature [126] that lower chemiluminescence intensities achieved by higher flow rates of samples containing the substrate while the enzyme is immobilised on the channel, could be the result of the shortening of the contact time between substrate and enzyme. The authors of the same paper also suggest that poor substrate exchange between the stream and the immobilised enzyme could be the cause of the decrease in signal with the lower flow rates.

What is more, there was a notable increase of the deviation of replicate measurements performed for flow rates above 500 µl/min, with a decrease in detection reproducibility. A similar phenomenon was found in the literature, for a chemiluminescence flow assay developed with immobilised enzyme [187]. The authors observed that, although increasing the flow rate produced sharper peaks with higher intensity, the stability of the chemiluminescence emission and detection reproducibility deteriorated, leading to higher RSD values that were not acceptable.

It was found that with a flow rate of 500 µl/min the chemiluminescence signal produced when the H_2O_2 sample was flown through the channel, had the desired sharp, and highest, peak characteristics. As mentioned, due to the high RSD observed with a flow rate of 750 µl/min (RSD=4.9%), even though it produced the highest peak intensities, it was decided to choose the flow rate that nevertheless produced satisfactory peak intensities, but importantly with the added advantage of lower deviation between replicates (RSD=2.8%).

Sample volumes lower than 50 µl, as well as low flow rates, especially in combination, resulted in wider and lower peaks; this is due to the sample

dispersion in the flow process, as visual inspection by using an aqueous dye instead of the sample confirmed.

The more well-formed peaks (height and sharpness) for the H_2O_2 concentration of 1 µM, were achieved with a flow rate of 500 µl/min and sample volume of 50 µl. Therefore, these values would be used for the two parameters, in the finalised fluidic assay for H_2O_2.

5.4.3.1.3 Optimisation of the luminol and HRP concentrations

Having optimised the flow rate and the sample volume for the optimal spike kinetics, as well as the geometry of the channel detection area for the best spread of the immobilised HRP, the concentrations of the chemicals participating in the chemiluminescence detection of H_2O_2 were then optimised, namely the luminol concentration and the immobilised HRP concentration. These were optimised by aiming to obtain the greatest chemiluminescence light intensity peak for a 2 µM H_2O_2 concentration, from each of the combinations of concentrations. Four luminol concentrations and six different HRP-beads concentrations were tested. The results are presented in Table 5.7.

Table 5.7 Peak chemiluminescence light intensity detected for 2 µM H_2O_2, from the cross-combinations of 50 – 200 µM luminol concentrations and 0.1 – 0.35 mg of magnetic beads with immobilised HRP.

	HRP (mg of beads)					
Luminol concentration	**0.1**	**0.15**	**0.2**	**0.25**	**0.3**	**0.35**
200 µM	56	87	103	117	112	124
150 µM	65	113	147	259	265	253
100 µM	114	154	207	305	310	306
50 µM	78	104	157	207	201	217

Values presented are the average of three replicates.

As it can be seen from the results, the concentration of luminol had an effect on the light intensity produced by its reduction of H_2O_2 in the presence of HRP. Higher luminol concentrations appeared to inhibit the said light production, as did low concentrations as well. The optimal was found to be 100 µM luminol.

The amount of beads magnetically entrapped in the fluidic channel's detection region also had an effect on the light intensity produced by the HRP-catalysed reaction of luminol with H_2O_2. Given the optimisation of the flow rate for faster reaction kinetics, the amount of HRP deemed as aiding towards that goal was at the higher end of concentrations tested. However, the higher amounts of beads (and therefore HRP) tested, 0.3 and 0.35 mg, resulted in no further increase of the chemiluminescence signal for 2 µM of H_2O_2, compared to the 0.25 mg of beads. A possible explanation for this appears to be the fact that these higher amounts of beads do not aid in the catalysis of the chemiluminescence reaction any more that the 0.25 mg of beads, due to the fact that a monolayer of beads coating the active circular region where the reaction takes place has probably been achieved by the 0.25 mg of beads, and any further addition of beads results in the beads getting assembled on top of other beads, rather than next to them.

Therefore, 0.25 mg of HRP-coated beads will be used in the fluidic channel, and 100 µM luminol will be used for the detection of H_2O_2 using the final, optimised fluidic assay.

5.4.3.2 Optimised chemiluminescence fluidic assay for the detection of hydrogen peroxide using HRP-coated magnetic beads

Having ascertained the optimal conditions for the desired characteristics of the detection of low H_2O_2 concentrations, namely narrow 'spikes' with the highest peaks, the fluidic sensor was utilised to perform the standard fluidic assay for the detection of H_2O_2, thus achieving the transfer of the batch chemiluminescence H_2O_2 assay into a fluidic format. The assay's Materials and Method are described in Section 5.4.2.2, with the concentrations, channel

design and flow rate and sample volume values were finalised from the optimisation of the assay procedure, in Section 5.4.3.1.

The peak light intensities obtained from chemiluminescence reactions of single H_2O_2 samples were collected. The standard curve and the linear calibration curve of the data have been plotted, seen in Fig. 5.14.

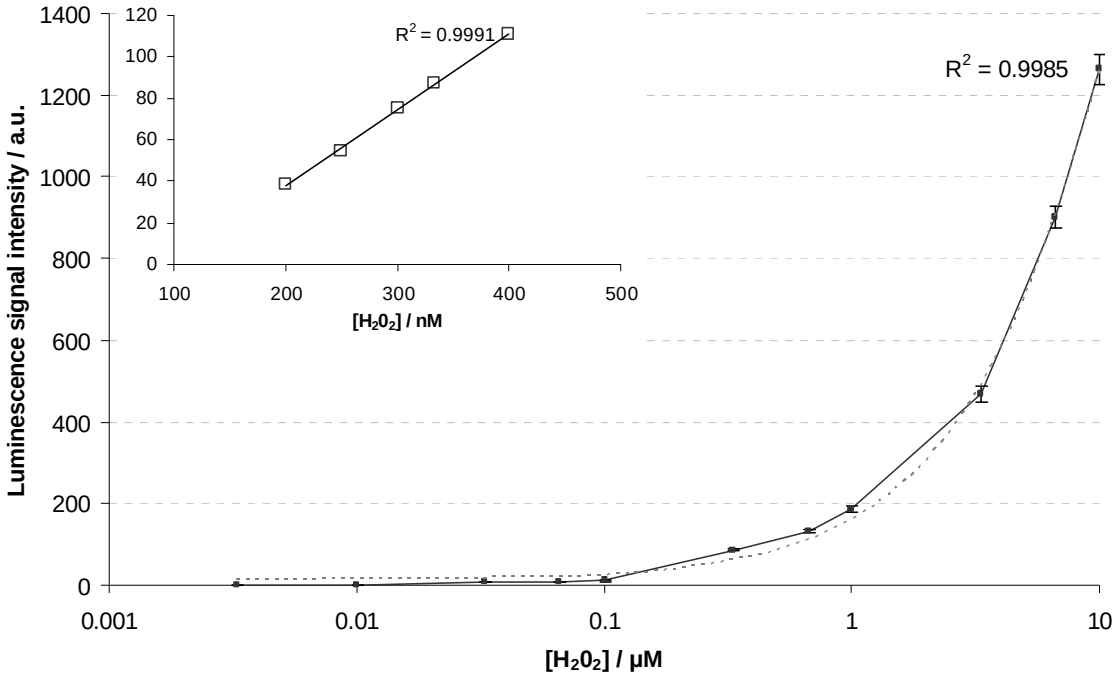

Figure 5.14 Standard curve and linear detection range (inset) for the fluidic assay for the detection of H_2O_2, with HRP immobilised on magnetic beads.
Values presented are the average of four replicates.

The lower limit of detection was calculated to be 107 nM H_2O_2. The RSD for the determination of a $5x10^{-7}$ M H_2O_2 sample was 2.7%, based on four replicates.

Comparison with other published work on the lower detection limits of H_2O_2 using the HRP-mediated luminol chemiluminescence reaction, with HRP immobilised in some way and the assay being run in a flow arrangement reveal not too dissimilar results: 180 nM [129], 130 nM [188], while also some with much more lower LODs: 4 nM [189], 40 pM [190]. Of course, as every fluidic sensor is

different, it is difficult to truly compare the LODs. An interesting note however is the fact that the two published works reporting the much lower LODs use a PMT for the detection of chemiluminescence signal, while the work described here uses an avalanche photodiode.

5.4.3.3 Use of real water samples for the determination of H_2O_2 with the fluidic unit with immobilised HRP

In order to further characterise the developed assay for the detection of H_2O_2, the sample plug containing known concentrations of H_2O_2 and luminol in buffer was replaced by water samples collected from the environment. Three different water samples were tested, two sourced from rain and another from a stream; the collection method and further details described in Section 5.4.2.3. The water samples were tested using the optimised, final method as used for the assay for the detection of H_2O_2 described in Section 5.4.3.2. The results of measuring the H_2O_2 present in the water samples, as well as adding known concentrations of H_2O_2 are presented in Table 5.8.

Table 5.8 Determination and recovery of H_2O_2 in rain and stream water samples.

	H_2O_2 added (µM)	H_2O_2 found (µM)	Recovery (%)
Rainwater 1	0	0.55	N/A
	1	1.60	103.2%
	3	3.64	102.5%
Rainwater 2	0	1.19	N/A
	1	2.27	103.7%
	3	4.30	102.6%
Stream water	0	0.34	N/A
	1	1.31	97.8%
	3	3.24	97.0%

The H_2O_2 measurements were performed with the complete fluidic sensor unit for the determination of H_2O_2. The results presented in the "H_2O_2 found" column are the averages of 3 replicates.

As it can be seen, H_2O_2 was found naturally in all three environmental water samples, with the concentrations found in rainwater being within the range described elsewhere [189]. According to the literature [189], variations in hydrogen peroxide levels are attributed to several factors, with slight elevations being due to an increase in the photochemical production of the precursor hydroperoxyl radicals that form hydrogen peroxide in the troposphere, while decreases in hydrogen peroxide levels are due to washing and dilution effects of the rainwater. Influences from other meteorological factors such as wind speed and direction as well as chemical factors can also affect the concentration of hydrogen peroxide in the atmosphere.

Both rainwater samples increased the detection of H_2O_2 measured with the fluidic sensor unit for the determination of H_2O_2, although by a small proportion, while the stream water caused a reduction in the chemiluminescence signal obtained when known H_2O_2 concentrations were added to the water sample. Overall, the recoveries suggest the interference from the sample matrix on the chemiluminescence signal is small.

5.5 General discussion

Following the development of a set of principles of design and operational mode, the flow sensor unit was designed and fabricated. The aim to demonstrate the potential of the final developed fluidic assay in aiding the reuse and regenerability of the sensor was taken into account; thus, it was decided to employ superparamagnetic beads as the immobilisation support for the biological elements of the bioassay, which would need to be easily and automatically replaced in a field deployment.

The decision to immobilise HRP on superparamagnetic beads in order to aid the final sensor's regenerability was made; this was followed by the immobilisation itself, which was thoroughly optimised in order to achieve the highest possible amount of active HRP on the beads (2.1 purpurogallin units per

1 mg of beads). As the protocol provided by the manufacturer was not specific for HRP immobilisation, following the necessary calculations to identify the concentrations needed, these concentrations, as well as other parameters of the immobilisation protocol, were subject to optimisation in order to identify the optimal concentrations and steps. As perhaps envisaged, the final developed protocol has many differences when compared to the original, generic one.

The fluidic assay for the detection of H_2O_2 using the developed unit and the optimised HRP-coated magnetic beads was itself then optimised in order to yield for the lowest detectable amount of hydrogen peroxide, as well as other desired chemiluminescence signal characteristics. These included varying the fluidic channel geometry for the better spread of the beads, varying the sample volume and flow rate for the higher, sharper, but reproducible signal peaks, and the concentration of luminol and HRP (immobilised on the beads) for the lower H_2O_2 LOD.

The optimised fluidic unit was then used as part of a fluidic sensor for the chemiluminescence detection of H_2O_2 utilising magnetic beads as the immobilisation support material for HRP. The lower LOD for H_2O_2 was 107 nM H_2O_2. The limit of detection is close to the limit achieved with the bench-top batch assay (Section 3.3.2), which was 90 nM.

The matrix effect of the real water samples on the detection of H_2O_2 was identified; rain water caused an increase to the chemiluminescence signal observed compared to the expected by approx. 3%, while water from a stream caused a decrease of the chemiluminescence signal by approx 2.5%.

Chapter 6: Fluidic Chemiluminescent Assay for the Detection of Herbicides

6.1 Introduction

As discussed in the introduction of Chapter 5, in order to achieve the objective of transferring the established herbicide assay from a batch to a fluidic format, the sensor unit is required to allow for the following discrete steps to be performed;

1. the illumination-stimulated production of H_2O_2 by thylakoids, and its inhibition by a herbicide-containing sample
2. the detection of any produced H_2O_2 using the HRP-mediated chemiluminescence of luminol/H_2O_2.

Following the design and fabrication of the flow cell and its testing and usage as part of a fluidic sensor for the detection of H_2O_2, utilising magnetic beads as the immobilisation support material for HRP, Step 2 has thus been established, as reported in Chapter 5. Therefore, in order to achieve the overall aim of establishing a fluidic sensor unit for performing a chemiluminescent assay for the detection of herbicides in water, work was undertaken in order to accomplish Step 1.

The work undertaken and presented in this chapter has been divided in the following sub-sets:

- the immobilisation of thylakoids on magnetic beads,
- the selection of an appropriate miniaturised light source,
- the optimisation of the herbicide detection fluidic assay's parameters,

- the implementation of the complete fluidic assay for the detection of herbicides,
- the testing of the complete assay with real water samples and
- studies on reagent and material stability.

The results of these sub-streams will be presented in the above order in the remaining sections of this chapter.

6.2 Immobilisation of thylakoids on superparamagnetic beads

6.2.1 Introduction and immobilisation protocols review and choice

Examples of the use of immobilised photosynthetic material for the detection of pollutants have been described in Section 5.1.1. The common feature of the sensors that these immobilised materials were employed in, is the immobility of the immobilisation platform; with the chloroplasts, thylakoids or sub-thylakoidal particles immobilised, usually on the surface of a polymer, or within a matrix of a cross-linked gel, the immobilisation step thus renders them immobile, requiring for the appropriate amount of the immobilisation material to be further immobilised on the sensor's biological / transductive interface. This then results in a further component of the sensor needing replacement after one or more measurements; in the case of electrochemical detection this tends to be the whole electrode.

Nevertheless, in order to identify the appropriate immobilisation chemistry to be used for the magnetic beads a literature review was conducted of the methods used to immobilise photosynthetic material on surfaces. Whole cells have been immobilised on filter paper and there entrapped by being covered by a layer of alginate, hardened by $CaCl_2$ [191]. The physical entrapment of algal cells by their filtration through glass or similar microfibre filters has also been used for a flow assay [192]. Published work has described the comparison of four PSII immobilisation methods; gelatine, agarose or calcium alginate gel entrapment and albumin-glutaraldehyde crosslinking [9]. The first three methods resulted in

products that could not be then used due to poor adhesion on the electrode surface or due to the stability of the photosynthetic material being lower than when not immobilised. A research group at the University of Quebec performed detailed exploration in order to identify the immobilisation method that would provide the best support for the thylakoids as well as result in optimal conditions for the electrochemical detection of pollutants [46; 47; 143-146]. Their work suggested that immobilisation of thylakoids in a glutaraldehyde-albumin crosslinked matrix resulting in a sponge-like material to be then fixed on electrode surfaces, was shown to give better detection results than other techniques [145]. From the literature review, it was therefore revealed that the use of glutaraldehyde for the immobilisation of thylakoids on the magnetic beads would potentially yield the more stable and active immobilised thylakoids.

A review of magnetic beads that would be useful for such immobilisation chemistry methods revealed that magnetic beads with amine groups immobilised on their surface could be used (Fig. 6.1). A review of various manufacturers returned a few similar products that could be used, with the following product codes: BM546 [193], 18879-2 [194], CM3540 (from Cortex Biochemicals, discontinued), AM-30-10 [195]. There were no apparent scientifically advantageous characteristics of any specific product hence the choice was made based on pricing and availability in both the UK and Italy.

Three available immobilisation protocols were collected from manufacturers (Appendix IV). Similarities and differences were identified amongst the immobilisation protocols; there are close similarities in the overall procedure described in all of these protocols, which, without exception, follows the following process:

- washing of beads,
- functionalisation of the beads by mixing with glutaraldehyde,
- washing of beads to remove excess glutaraldehyde,
- coupling of ligand of interest,
- washing of beads to remove excess ligand of interest.

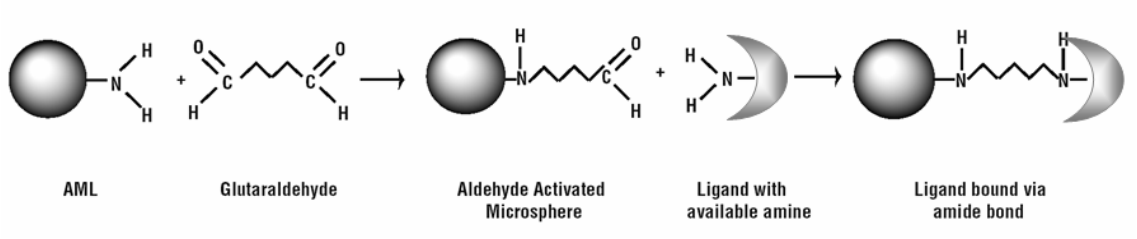

Figure 6.1 Thylakoid immobilisation chemistry using glutaraldehyde as the intermediate linker between the amino group of the beads and the amine of the HRP.

There are however great differences amongst the protocols in the actual values of all relevant parameters such as volume, concentration, time, repetitions of steps, as can be seen in Appendix IV.

The protocols were then forwarded to a partner in the European collaborative project that the work described here was part of (Partner 1A: Dr M.T. Giardi, Institute of Biochemistry and Ecophysiology IBEV, National Council of Research-CNR, Rome, Italy), in order for the partner to perform the optimisation process of the immobilisation of thylakoids on the selected beads. It was a requirement of the project for research partners to collaborate where research experience in specific scientific processes would be best utilised by dividing and sharing of tasks appropriately.

The isolated thylakoid preparation chosen for the immobilisation was the "Ch5", as it allowed for the lower detection limits for the photosynthesis-inhibiting herbicides when assayed in suspension (Section 4.4.3), and also was the thylakoid preparation that produced the highest chemiluminescence signal intensity, and hence H_2O_2, when illuminated for 10 min, compared to the other four preparations (Section 4.3.3.1). It was therefore envisaged that it was the most suitable candidate for the production of a chemiluminescence signal due to its H_2O_2 production that would allow for the quantitative detection of herbicides in the fluidic assay. It should be noted, that, the thylakoid preparation used during the optimisation of the immobilisation by the research partner was a

variation of Thylakoid Isolation Protocol 5 (named Ch5), as described in the literature [196], while the thylakoids used in the subsequent use of the optimised immobilisation protocol for the current work presented was the actual Thylakoid Isolation Protocol 5 (named Ch5), as described in Section 4.3.2.1.5.

The immobilisation protocol used here is hence the result of the project partner's work, and no further changes were made to it, other than substituting the isolated thylakoid preparation employed during the immobilisation to the thylakoid preparation Ch5.

6.2.2 Materials and methods

6.2.2.1 Materials

All chemicals and reagents were purchased from Sigma Chemical Company Ltd. (Gillingham, UK). The PBS, MES and Tricine buffers were prepared, using RO water. Sphero Amino magnetic beads with a 3.6 µm diameter (Catalogue Number: AM-30-10), were manufactured by Spherotech Inc. (Illinois, USA), and obtained from Saxon Europe (Kelso, UK). The thylakoids were isolated using the Isolation protocol 5, in Section 4.3.2.1.5.

6.2.2.2 Immobilisation protocol

The final protocol used for the immobilisation of thylakoids on the magnetic beads was the following:

- Five hundred microlitres of water suspension of magnetic aminopolystyrene-beads (5% w/v) were washed with 1.0 ml of PBS buffer (KH_2PO_4 1.8 mM, KCl 7 mM, NaCl 15 mM, Na_2HPO_4 10 mM, pH 7.2) for three times.
- The pellet was suspended in 1.0 ml of a glutaraldehyde solution (glutaraldehyde dissolved in PBS buffer to a final concentration of 10% w/v).
- The reaction was carried out with continuous mixing at 16℃ for 24 h.
- The microsphere suspension was washed three times with 1.0 ml of PBS buffer to remove the excess of glutaraldehyde.

- Pellet was resuspended in 0.5 ml of 5 mM $MgCl_2$, 0.07 M Sucrose, 15 mM MES buffer, pH 6.5.
- Then, 200 µl of thylakoid membranes ([Chlorophyll] = 2.75 mg/ml) and 300 µl of the same MES buffer were added at 4℃ in the dark.
- To allow the coupling between the glutaraldehyde and the thylakoids, the reaction was carried out at 4℃ for 2 h under continuous mixing.
- Finally, 100 µl of BSA (quenching solution) was added per 400 µl of immobilised thylakoids. The beads were then washed three times with 1 ml of PBS buffer, and then stored in 20 mM Tricine buffer, pH 7.8, 5 mM $MgCl_2$, 70 mM sucrose.

The measurements of photosynthetic activity and chlorophyll concentration of the resulting thylakoid-coated beads were performed as described in Section 4.5.2.

6.2.3 Results and discussion

As a result of the optimisation of the immobilisation process by the project partner, beads were obtained with 0.3 µg of chlorophyll / mg of beads, while the photosynthetic activity, as measured by the chlorophyll fluorescence, was 0.7 [196]. The fluorescence value indicates that the thylakoids immobilised on the beads have retained most of their activity. This is ascertained by the fact that the isolated, non-immobilised thylakoids have a Fv/Fm ratio of 0.72, which suggests that there was no significant reduction in the photosynthetic activity of the thylakoids as a result of the immobilisation. These results however were obtained using the variation of the isolation protocol 5, and thus a variation of thylakoids Ch5.

When the isolated thylakoids immobilised on the beads were obtained by using the isolation protocol 5, there was an increase in the amount of thylakoids immobilised on the beads (0.49 µg of chlorophyll / mg of beads). As the immobilisation protocol used in both occasions was the same, the increase can only be attributed to the thylakoids obtained by the immobilisation protocol 5 having somewhat better qualities for the immobilisation, or, simply, a higher

chlorophyll concentration. However, it is important to remember that the amount of chlorophyll found, in a suspension of isolated thylakoids or subsequently in immobilised thylakoids, does not represent a quality of thylakoids that reflects the H_2O_2 yield produced by the thylakoids, as explained in detail in Section 4.5.3.

The reproducibility of the immobilisation of thylakoids on the beads was calculated, with each full immobilisation experiment being performed with Ch5 thylakoids isolated on the same occasion; therefore the reproducibility of the immobilisation does not also account for the reproducibility of the isolation. The average chlorophyll concentration from three immobilisations was found to be 0.49 ± 0.026 µg of chlorophyll / mg of beads, therefore with an RSD value of 5.4%.

6.3 Selection of an appropriate miniaturised light source

6.3.1 Introduction

Following the successful use of a standard 20 W, 240 V full spectrum halogen lamp as the illumination source of a suspension of thylakoids for the production of H_2O_2, and having optimised the wavelength spectrum that allowed for the optimal production thereof (Section 4.3.3.6), it was necessary to investigate the application of alternative light sources that would provide the light energy for a similar production of H_2O_2 in the fluidic assay, with the thylakoids immobilised on the beads, rather than in suspension. An investigation of the literature revealed that, for the purpose of illuminating photosynthetic material in miniaturised assays, LEDs appeared to be the preferred illumination technology employed [8; 9; 48; 142; 154; 159]. Therefore, an investigation was undertaken, aiming to identify the preferred LED that would be allowing for the optimal illumination conditions, in order to achieve the highest H_2O_2 yield. The work presented here forth was carried out with the isolated thylakoids in suspension using the batch assay, and not immobilised thylakoids, as this allowed for a much quicker turnaround time, while also utilising resources more effectively, as a great

amount of beads with immobilised thylakoids and HRP would be needed to perform all the individual measurements presented.

6.3.2 Materials and Methods

The experiments described in 6.3.3 were HRP-mediated luminol chemiluminescence reactions in cuvettes using a bench-top spectrometer, with the H_2O_2 required for the reaction being provided by illuminated isolated thylakoids. It is therefore a variation of the experimental process described in Section 4.3.3.6, where the results for the different light sources for the cuvette assay are presented, with the main difference being the use of LEDs as the illumination source, instead of the halogen lamp or the laser diode.

The steps followed thus are:

- 330 µl of luminol (100 µM) in Tris-HCl buffer (10 mM, pH 8.5) and 330 µl of HRP (5 Units/ml) in Tris-HCl buffer (10 mM, pH 8.5) were added in a Kartell disposable semi-micro optical polystyrene cuvette (Thermo Fisher Scientific Ltd., Loughborough, UK), in a time window of 1 hour before the experiment to follow, unless stated otherwise.
- The cuvette with 660 µl of luminol and HRP in Tris-HCl buffer (10 mM, pH 8.5) was placed in the sample holding compartment of a Cary Eclipse fluorescence spectrophotometer (Varian UK Ltd., Oxford, UK). The spectrometer was set up, via the use of its bespoke software, to record the intensity of detected light over 60 seconds.
- In order to induce the production of H_2O_2 by the thylakoids, the sample illumination step was undertaken:
    - The isolated thylakoid preparation Ch5, obtained from protocol 5, was diluted in Tris-HCl buffer (10 mM, pH 8.5) in order to form the measuring sample
    - A 330 µl diluted sample was aspirated in a pipette tip attached to an air-displacement pipette
    - The pipette was placed within a plastic hollow tube, internally covered with aluminium foil, opposite an individual LED (as in Fig. 6.2)

- The LED was powered and illumination took place, for 1 min
- When the designated illumination time ended, the LED was switched off.

- Using a PC interface, the spectrometer's detection process was initiated the moment the illumination ended, and 10 seconds later the aliquot containing the previously illuminated chloroplast sample was forcefully pipetted manually in the cuvette, thus resulting in the initiation of any potential chemiluminescence reaction between luminol and H_2O_2, in the presence of HRP.
- At the end of 1 min, the spectrometer would stop recording the intensity of the light detected, and would produce a file containing the light intensity recorded over time, in arbitrary units, every 100 ms, over 1 minute. Microsoft Office Excel 2003 was used to further analyse the data.

LEDs were selected from the widest possible range of wavelengths, illuminating angles and intensities. Information on the identification as well as parameters of individual LEDs can be found in Appendix V.

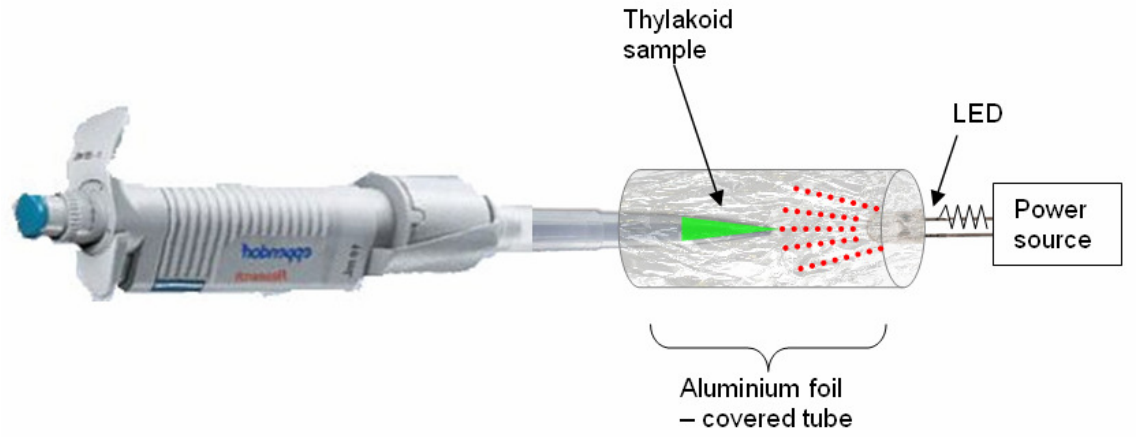

Figure 6.2 Schematic representation of the experimental setup for the illumination of thylakoids by an LED.
Not to scale.

Furthermore, measurements of the spectral qualities of the different LEDs were also made, in order to characterise the LEDs and allow for comparison with

each other, as well as with the optimal light source for the batch assay, the halogen lamp. These measurements were conducted within an experimental setup similar to the one employed for the illumination of the thylakoids (Fig. 6.3), with the thylakoid sample-containing pipette tip being replaced by an optical fibre connected to an S2000 Miniature Fiber Optic Spectrometer from Ocean Optics B.V. (Duiven, The Netherlands). It was connected to a single-strand, 100 µm diameter optical fibre (P100-2, Ocean Optics B.V.) through which the light was collected.

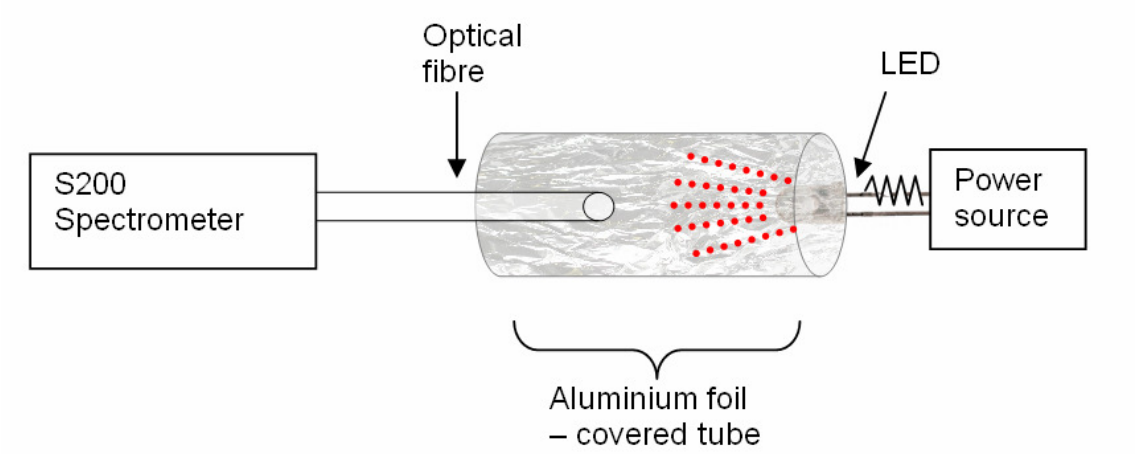

Figure 6.3 Schematic representation of the experimental setup for the measurement of the light intensity output by an LED.

Not to scale. The distance between the tip of the optical fibre and the tip of the LED was 5 cm.

6.3.3 Results

6.3.3.1 Characterisation of the LED light sources

A substantial amount of work was performed on illuminating the thylakoids using LEDs. It was therefore important to understand, characterise and quantify certain parameters of the light emitted by the LEDs.

LEDs are light-emitting semiconductors and are inherently monochromatic devices, with the colour being determined by the band gap between various semiconductor materials utilised in diode construction [155]. When current flows

through the p-n junction of compound semiconductors consisting of GaP (gallium phosphide) or GaAsP (gallium arsenide phosphide), light is emitted as a result of electrons recombining with holes near the p-n junction. The characteristics of LEDs are as follows: low voltage operation, low heat emission, a compact and lightweight design, lack of noise (electron discharge tubes produce noise) and easy control [153].

The diode of white LEDs, like all LEDs, is actually monochromatic, however, the glass cover of the LED is internally coated with a phosphorescent material which, after getting excited by the diode's blue luminescence, phosphoresces. Figure 6.4 shows how the total emission spectrum of a white LED is composed of the blue luminescence as generated by the diode chip and the primarily yellow phosphorescence as generated by the coating [197].

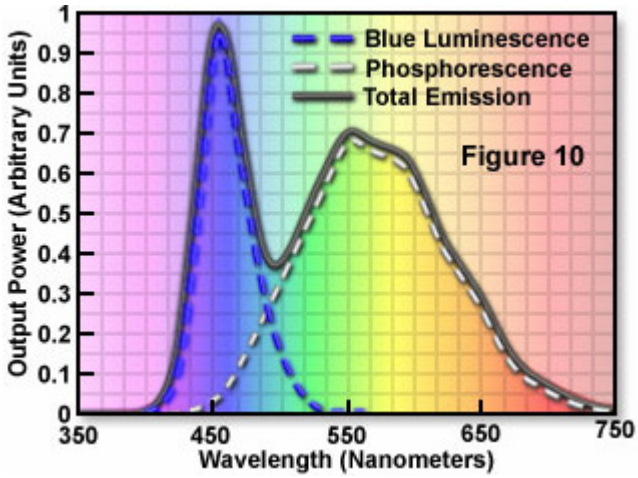

Figure 6.4 White LED emission spectrum.
(from [197])

Similarly to the other light sources, as reported in Section 4.3.3.6.1, the spectral quality of the light emitted by each LED was measured (Fig. 6.5). The light intensity spectral distribution wavelength scan of the different LEDs was performed by placing an optical fibre, connected to a spectrometer, in the area directly in front of the LED, facing towards the source. There was immense variation amongst the wavelength 'fingerprints' of all LEDs, as LEDs of many different peak wavelengths were chosen, which were therefore also of different

colour appearance to the human eye (blue, green, yellow, orange, red and white).

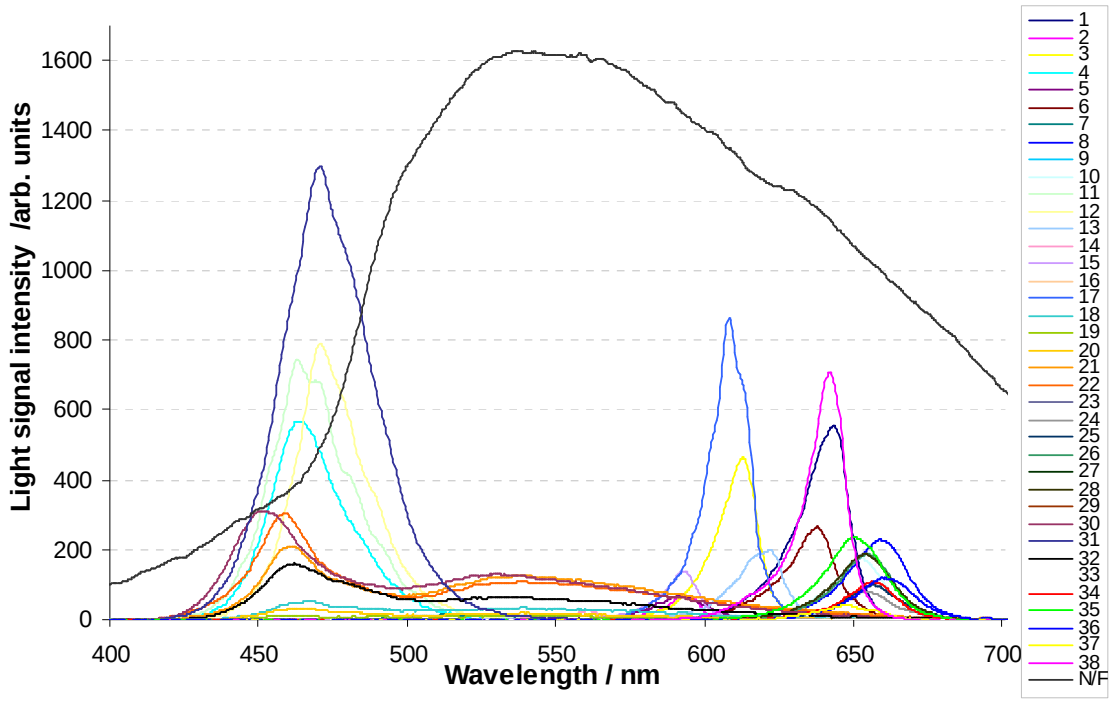

Figure 6.5 Light intensity spectral distribution wavelength scan of different LEDs used to illuminate the thylakoid preparations.

The trace of the non-filtered halogen lamp has been included in the graph to allow visual comparison (N/F). The LED traces are coded 1-38, which are the LEDs' assigned codes for this work.

Based on the measured light intensity over the whole visible light spectrum that the LEDs emit in, as displayed in Fig 6.5, the 'total light output' was measured, by calculating the sum of all the data points over the 400-700 nm spectrum window. The results can be seen in Figure 6.6. It was important to calculate a means of comparing the light intensity output of all the different LEDs, as the wavelengths over which they produced light varied greatly. It was also important to be able to compare the amount of light produced by the LEDs to that of the main halogen lamp light source. Therefore, for the purpose of comparison, the 'total light output' of each LED was also calculated as a proportion of the total light output achieved by the un-filtered halogen lamp light source. From both

graphs in Figures 6.5 and 6.6, it can be seen that amount and spectral characteristics of the light emitted from the LEDs varies greatly.

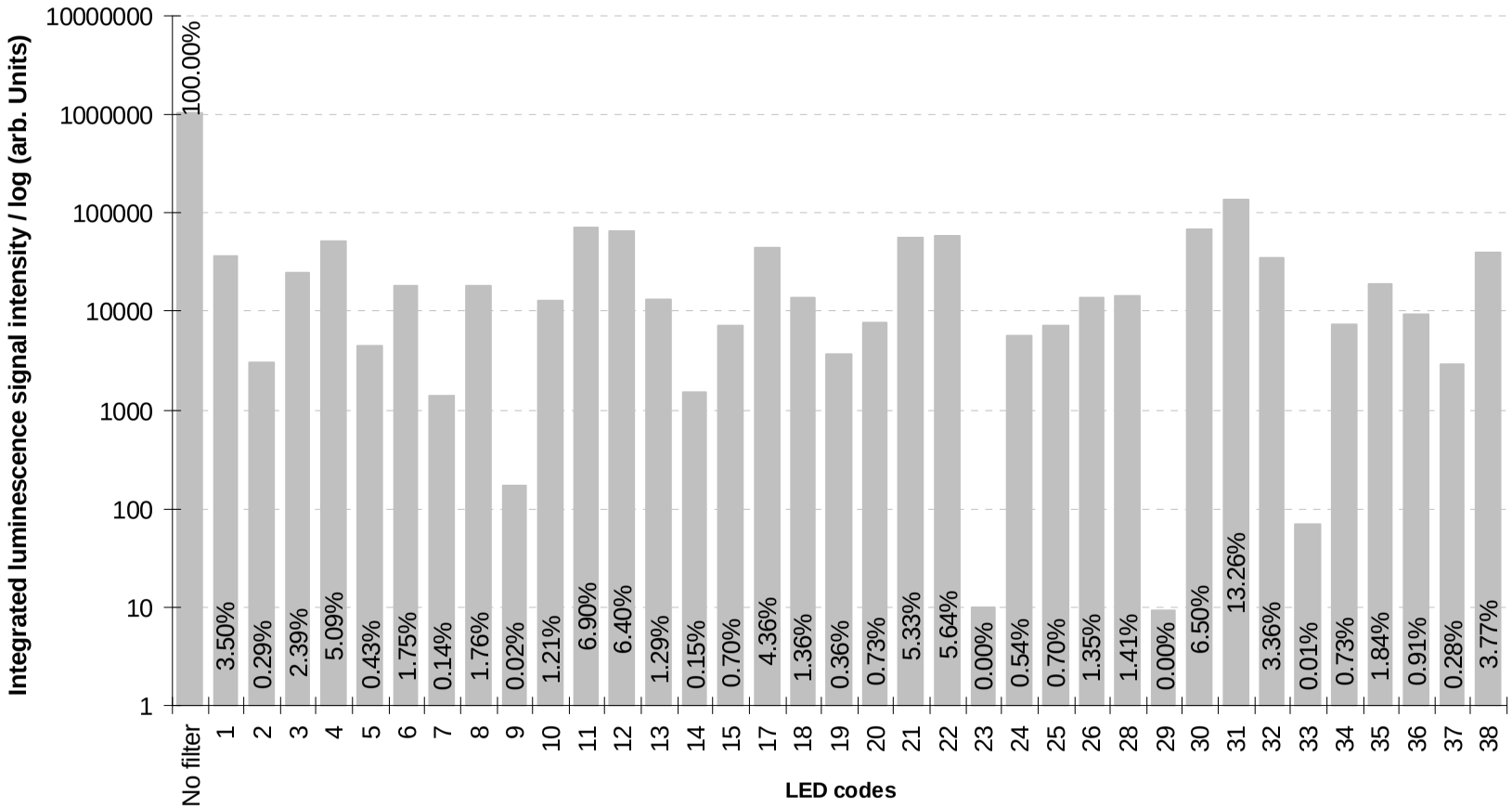

Figure 6.6 The sums of 'total light output', irrespective of wavelength, achieved by the different LEDs over the whole spectrum between 400 and 700 nm.

The sum of 'total light output' achieved by the halogen lamp is included for comparison (left-most column). The percentage on each column depicts the proportion of total light output each LED achieved in comparison to the un-filtered halogen lamp (100%).

6.3.3.2 Effect of LEDs as thylakoid illumination sources on the H_2O_2 production

Radiometry is the measurement of optical radiation, which is electromagnetic radiation within the frequency range between 3×10^{11} and 3×10^{16} Hz. This range corresponds to wavelengths between 0.01 and 1000 µm, and includes the regions commonly called the ultraviolet, the visible and the infrared. Photometry is the measurement of light, which is defined as electromagnetic radiation that is detectable by the human eye. It is thus restricted to the wavelength range from about 360 to 830 nm. Photometry is therefore like radiometry, except that everything is weighted by the spectral response of the eye. Visual photometry uses the eye as a comparison detector, while physical photometry uses either optical radiation detectors constructed to mimic the spectral response of the eye, or spectroradiometry coupled with appropriate calculations to perform the eye response weighting [198].

The standard unit for characterising the light output of man-made light sources is the lumen which is the total luminous power (luminous flux) emitted from the source. The lumen is an SI derived unit for luminous flux. The lumen is derived from the candela and therefore the luminous flux is the product of luminous intensity and solid angle. It is analogous to the unit of radiant flux (watt), differing only in the eye response weighting [198; 199].

Conversely, the candela (cd) is the unit of luminous intensity, which can be defined as the amount of luminous flux (total luminous power emitted from a source and expressed as lumens) per unit solid angle in a given direction. Therefore 1 candela = 1 lumen/steradian [200]. One steradian (sr) is the solid (3-D) angle that, having its vertex in the center of a sphere, cuts off an area on the surface of the sphere equal to that of a square with sides of length equal to the radius of the sphere [198].

If a light source is isotropic, the relationship between lumens and candelas is 1 cd = 4π lm. Isotropic implies a spherical source that radiates the same in all directions, i.e., the intensity is the same in all directions. If a source is not isotropic, it is calculated empirically.

In order to empirically calculate the luminous flux, the two parameters needed are the luminous intensity and the viewing angle, both of which are given in the used LEDs' manufacturers' data sheets.

The viewing angle is typically defined as the angle which encompasses 50% of the maximum intensity. It is also referred to as the spatial or directional pattern of a LED light beam. The expressed degree dictates the width of the light beam and also controls, to some extent, the intensity of a LED. That is because the luminous intensity does not represent the total light output from an LED. Both the luminous intensity and the viewing angle must be taken into account. If two LEDs have the same luminous intensity value, the lamp with the larger viewing angle will have the higher total light output. The viewing angle is a function of the LED chip type and the epoxy lens that distributes the light. The highest luminous intensity (mcd) does not equate to the highest visibility. A higher light output is achieved by concentrating the light in a tight beam.

As the luminous flux takes into account the viewing angle, and based on the theoretical relationship between the luminous intensity and flux, and as only the intensity is provided by the manufacturers of LEDs, it was decided to calculate the flux of all LEDs. The calculated flux for all LEDs used can be found as a separate column in Appendix V.

Thirty eight different LEDs were used to illuminate the thylakoids. These experiments were only performed with one thylakoid preparation (Ch5), which was shown to have produced the lowest detectable concentrations / best detection limits for herbicides (Section 4.4.3), and had been thus also chosen to be the thylakoid preparation to be immobilised on the beads. The illumination of

the thylakoids and subsequent detection of any produced H_2O_2 was performed using the standard illumination method, with the modified illumination setup for LEDs (Section 6.3.2).

The results of the chemiluminescence detection of the produced H_2O_2 can be seen in Fig. 6.7, with each bar representing an individual LED, sorted in chemiluminescence intensity achieved for each emitted colour category of LEDs (blue, green, yellow, orange, red and white). As it can be seen, illumination of the thylakoids with one white LED (code 22) resulted in the highest H_2O_2 production and therefore highest chemiluminescence signal. It was thus decided that the LED named LED22 would be used for experiments for the detection of herbicides by measuring their effect on the production of H_2O_2 by thylakoids immobilised on beads, that are illuminated by said LED.

It is important to highlight the fact that red LEDs did perform quite well in stimulating the production of H_2O_2 by thylakoids. This is in accordance with the fact that red wavelengths are both best absorbed by chlorophyll and result in maximal photosynthesis [153], as discussed in Section 4.3.3.6.3, where the results of H_2O_2 production by the different filters were presented.

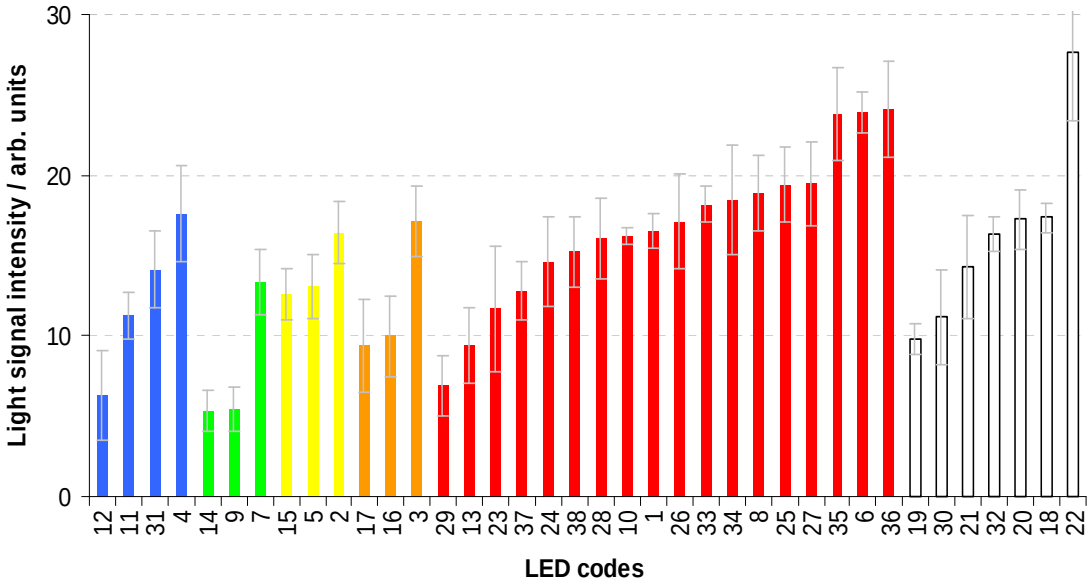

Figure 6.7 Chemiluminescence signal intensity resulting from H_2O_2 produced by thylakoids illuminated by 38 different LEDs.

The luminescence signal, detected by a bench-top spectrophotometer, resulted from the production of light by the cuvette-based chemiluminescence reaction of luminol, HRP and H_2O_2. [HRP] = 5 U.ml-1, [luminol] = 100 µM, in Tris-HCl buffer (10 mM, pH 8.5). The H_2O_2 was previously produced by illuminating diluted thylakoid samples with different LEDs, while aspirated in a pipette tip, for an illumination time of 1 min. The Ch5 thylakoid preparation ([chlorophyll] = 64 µg.ml^{-1}) were diluted in buffer A (10 mM Tris-HCl buffer, adjusted to pH 8.5). Average values and the SDs shown are the results of 3 replicates.

6.3.3.3 Meta-analysis / investigation into LED parameters

In order to understand the effect different parameters of the illumination light produced by the LEDs had on the production of H_2O_2 by the thylakoids, the chemiluminescence-detected H_2O_2 results were also considered against the peak wavelength, the provided luminous intensity, the calculated luminous flux and the measured 'total light output'.

It was expected that parameters identifying the light quality and characteristics of an LED, when compared to the amount of H_2O_2 produced by thylakoids due to their illumination by that LED, may provide with a model that could potentially be used to identify the ideal characteristics of the LED to be used.

The peak wavelength (nm) and the luminous intensity (mcd) were provided by the manufacturers, although the peak wavelength was verified by own measurements. The luminous flux (mlm) was calculated as mentioned above (results in Appendix V), and the 'total light output' (a.u.) was measured and calculated experimentally, with the results presented in Fig. 6.6. The measured 'total light output' (a.u.) differs from the luminous intensity (mcd) provided by the manufacturers, as it was experimentally measured by collecting light emitted by LEDs with an optical fibre at a fixed distance from the LEDs, while no information is provided about the way the luminous intensity (mcd) was measured by the manufacturers.

Figures 6.8 to 6.11 below are the plots of the chemiluminescence signal intensity, resulting from the detection of H_2O_2 produced by thylakoids, against the peak wavelength, the provided luminous intensity, the calculated luminous flux and the measured 'total light output'. The coefficient of determination, R^2, has been calculated and included in the plots of the results.

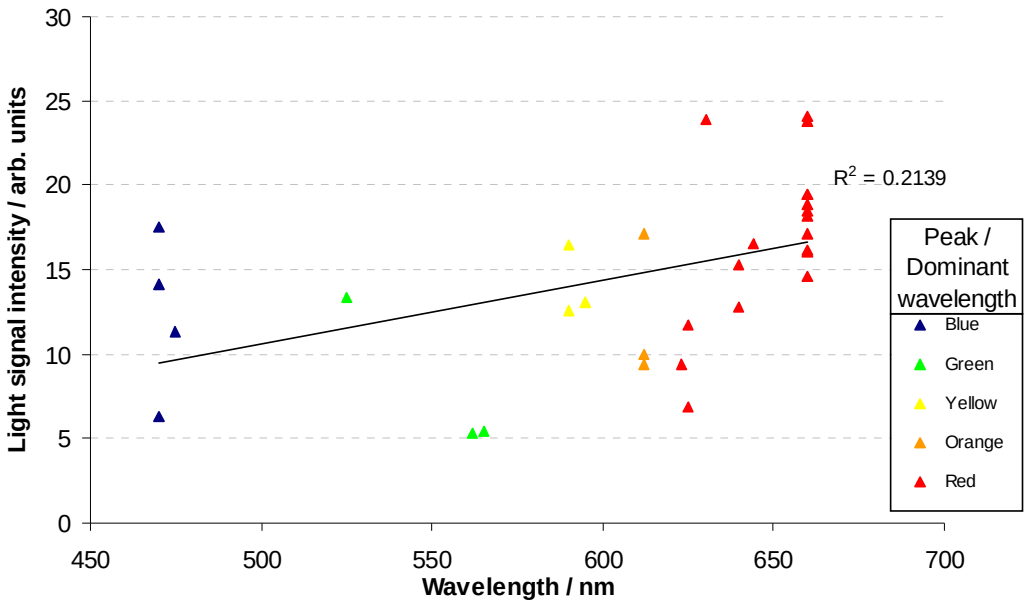

Figure 6.8 Effect of the illumination wavelengths of individual LEDs on the H_2O_2 production by thylakoids when illuminated.
R^2 calculated for all LEDs together.

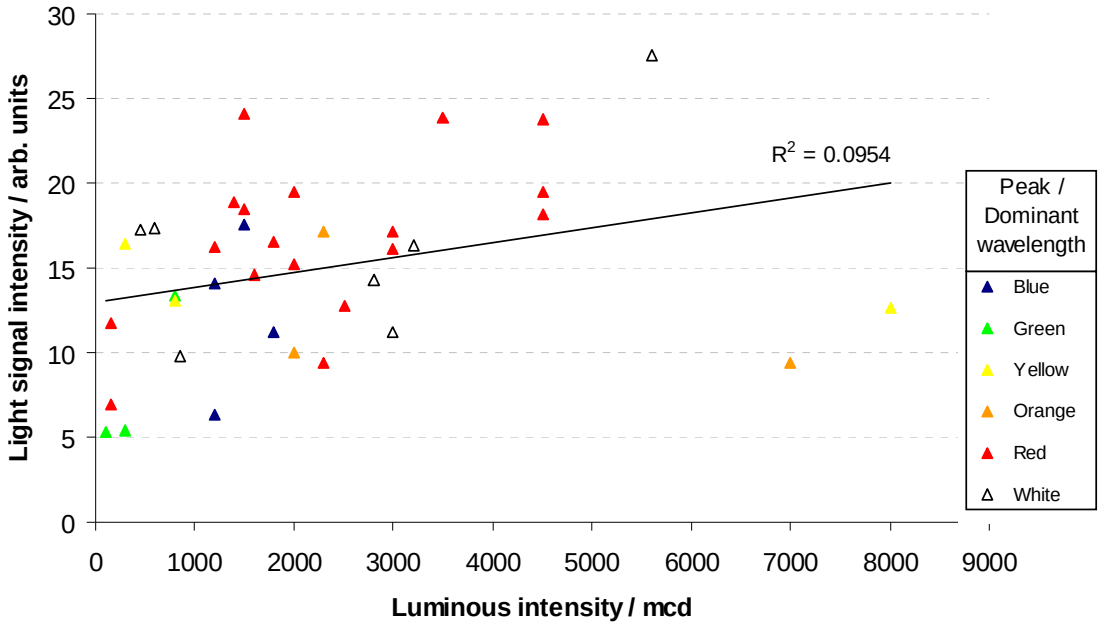

Figure 6.9 Effect of the luminous intensity of individual LEDs on H_2O_2 production by thylakoids when illuminated.

R^2 calculated for all LEDs together.

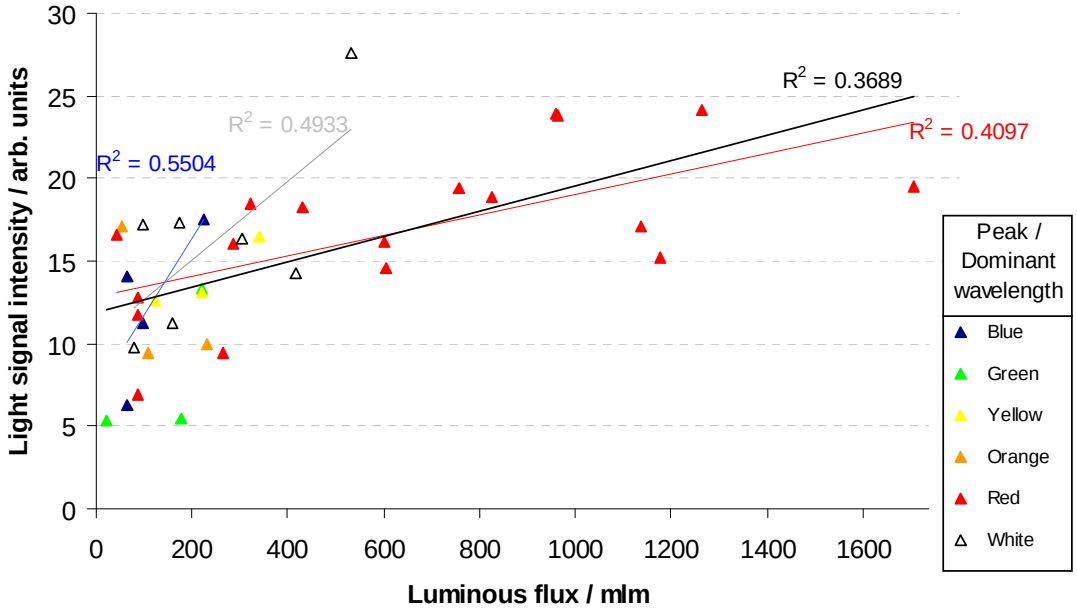

Figure 6.10 Effect of the luminous flux of individual LEDs on the H_2O_2 production by thylakoids when illuminated.

R^2 calculated for all LEDs together (black trace), as well as the red (red trace), blue (blue trace) and white LEDs (light grey trace) separately. It was not possible to calculate the coeffictient for the green, yellow or orange LEDs due to low numbers of individual LEDs used.

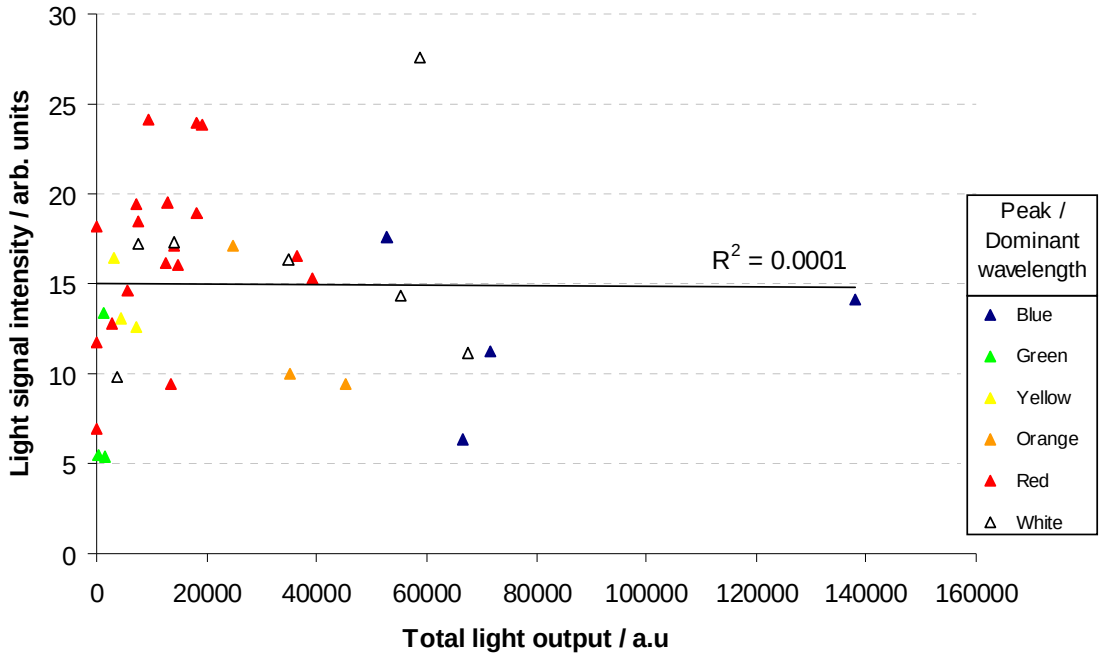

Figure 6.11 Effect of the measured 'total light output' of individual LEDs on H_2O_2 production by thylakoids when illuminated.

R^2 calculated for all LEDs together.

In order to measure the association between the different parameters (peak wavelength, provided luminous intensity, calculated luminous flux and measured 'total light output') and against the detected H_2O_2, correlation analysis was performed on the results obtained, presented in Appendix VI. The correlation coefficient R was calculated using as paired (dependent and independent) variables the above four LED light quality parameters and the detected H_2O_2. This was performed for each group of LEDs according to their primary colour, as well as for all LEDs together. Two separate calculations were performed for all the LEDs together, one with the white LEDs included and one without; this was in order to potentially identify behaviour that may be only seen in the white LEDs, or vice-versa, as the white LEDs, as described in more detail in Section 6.3.3.1, emit light that cannot be described as monochromatic, or near to such. Clearly, that was also why it was not possible to include the peak / dominant wavelength category in any such calculations for the white LEDs, as such one does not exist. An R value between 0.5 – 0.699 was considered to be the result of moderate correlation, a value between 0.7 – 0.899 was considered

to be pointing towards a strong correlation, and a value between 0.9 – 1.0 to be resulting from a very strong correlation. The identified R values falling within those categories have been highlighted in the table in the Appendix VI using colour coding.

Firstly, as it can be seen from the Pearsonian coefficient of determination, R^2, as displayed in the graphs above, there is no strong correlation between the H_2O_2 detected and some of the LEDs' variables, such as the peak wavelength (Fig. 6.8) or the luminous intensity (Fig. 6.9). For the 'total light output' as measured independently for this project, there is no association between said variable and the H_2O_2 produced whatsoever, resulting in a R^2 value of almost zero. For the luminous flux, as calculated by the provided luminous intensity and viewing angle, there appears to be a moderate association between said variable and the H_2O_2 production, with a positive correlation between increasing luminous flux and H_2O_2 produced.

From the R values in Appendix VI, it can be seen that the correlation coefficient R consistently indicates an association between the luminous flux values of LEDs and the H_2O_2 produced; that is observed for LEDs of different colour as well as for all LEDs together. There is generally no other consistent correlation for the different groups of LEDs; that could be attributed to the small sample number for all but the blue, red and white LEDs.

There was a lack of almost any positive association between the measured 'total light output' (a.u.) and the H_2O_2 produced. It would have been expected that the experimentally measured light intensity (a.u.) would be resulting in just as high, if not higher, R values as those obtained for the theoretically calculated flux (mlm), which is a measure of luminous intensity (mcd) when taking the effect of the illumination angle into consideration. This highlights a possible misjudgement in the experimentally measured light intensity values obtained (Fig. 6.5), which were then summed to provide the 'total light output' values (Fig. 6.6).

The reason behind this is believed to be the fact that the standard method used to measure the light intensity introduced an error to the measurement, or, more specifically, to the ability to use the measurements as a means of comparing different LEDs. That is because, although used consistently, using an optical fibre as a means of collecting light from the different LEDs (Fig. 6.3) was not representative of the setup when the LEDs were used to illuminate the thylakoids. The fibre only allowed for what could effectively be described as the detection of light reaching a specific spot in front of the LED, while, when using the LEDs to illuminate the thylakoids, the thylakoids were receiving light emitted by an LED directly, in a varying angle depending on the LED, as well as indirectly, as light was reflected by the aluminium foil that was coating the inside of the tube where the illumination took place. Therefore, the measured light intensity for an LED does not represent well the light that each LED provided for the illumination of the thylakoids.

Therefore, it can be concluded that the statistical analysis of the results did not highlight any of the LED light quality parameters analysed as appropriate for the theoretical identification of the optimal characteristics that an LED should possess in order to be selected as the best performing, as far as H_2O_2 production by thylakoids illuminated in suspension is concerned. It was therefore decided to proceed to the next stage, the further optimisation, and, finally, implementation, of the fluidic assay for the detection herbicides, employing the aforementioned white LED.

6.4 Optimisation of the herbicide detection fluidic assay parameters

6.4.1 Introduction

Following the successful immobilisation of thylakoids on magnetic beads, and the selection of a suitable miniaturised light source to illuminate them, their use as part of an assay for the detection of herbicides in the fluidic unit, based upon the herbicides' inhibitory effect, was the next step to be optimised.

The fluidic assay for the detection of herbicides would be based upon the fluidic assay for the detection of H_2O_2 (Section 5.4.3.2), by extending it to include the step of the H_2O_2 production and inhibition by herbicides, prior to its detection.

Having optimised and finalised the detection of H_2O_2 in the fluidic assay setup employing the use of the HRP-coated beads, as presented in Section 5.4.3.1, there would therefore not be a need to optimise the luminol concentration in flow, the amount of beads with immobilised HRP in the H_2O_2 detection region of the fluidic channel, or of the sample volume and flow rate, at least not during the H_2O_2 detection step.

As already highlighted in Section 4.4.3, where the effect of varying the incubation time of herbicides with thylakoids in suspension was presented, it is expected that the time that the herbicides are in contact with the immobilised thylakoids during the fluidic assay would be altering the inhibition level of the H_2O_2 production, and thus of the chemiluminescence signal that would be used as the parameter to allow for the quantification of the herbicides in a water sample.

What is more, as the sample with a known H_2O_2 concentration, as previously used for the calibration of the fluidic assay for the detection of H_2O_2 (Section 5.4.3.2), would now be replaced with H_2O_2 produced by illuminated thylakoids, it was also necessary to investigate the effect altering the illumination time would be having on the said H_2O_2 production.

Furthermore, the amount of beads with immobilised thylakoids would be varied, in order to identify the quantity that would result in an adequate H_2O_2 production, following illumination.

Therefore, it was decided that it would be required to optimise these parameters in order to gain the best possible conditions for the detection of the lowest possible concentrations of herbicides.

6.4.2 Materials and methods

6.4.2.1 Materials

Chemicals

Trizma, hydrochloric acid, 5-amino-2,3-dihydrophthalazine-1,4-dione sodium salt (luminol), PBS tablets and hydrogen peroxide (30% w/w) were purchased from Sigma Chemical Co. The Tris-HCl and PBS buffers were prepared using RO water. Luminol (100 µM) and H_2O_2 were prepared freshly each day, from stock solutions, in Tris-HCl buffer, 10 mM, pH 8.5. The six herbicides used were all from the PESTANAL®, analytical standard grade from Sigma Chemical Company Ltd. (Gillingham, UK). The MagaBeads-Carboxyl Terminated beads with a 3.2 µm diameter (Catalogue Number: CM3530), were from Cortex Biochemicals (now Promega Corp, Winskonsin, USA). The Sphero Amino magnetic beads with a 3.6 µm diameter (Catalogue Number: AM-30-10) were from Spherotech Inc. (Illinois, USA).

Detection

The customised QP1000-2-VIS/NIR-BX optical fibre was from Anglia Instruments Ltd. (Ely, UK). The detector C5460 APD Module was from Hamamatsu Photonics UK Ltd (Welwyn Garden City, UK). The PCI-1200 multifunction Input/Output data acquisition device and LabVIEW 5.0 was from National Instruments Ltd. (Newbury, UK).

Fluidics

The tubing and fittings used were from Omnifit Ltd, now Bio-Chem Fluidics (Cambridge, UK). Neodymium magnets were from RS Components Ltd (Corby, UK). The Minipuls3 Peristaltic Pumps were from Gilson (Wisconsin, USA). The injection port valve was from Pharmacia.

6.4.2.2 Setup and method

The herbicides were diluted in a variety of concentrations, all in Tris-HCl buffer (10 mM, pH 8.5), as described in Section 4.4.2. The beads with immobilised HRP were prepared as in section 5.3, and stored in Tris-HCl buffer (10 mM, pH 8.5) prior to use. The beads with immobilised thylakoids were prepared as in section 6.2, and stored in Tricine buffer (20 mM, 5 mM $MgCl_2$, 70 mM sucrose, pH 7.8) prior to use.

The fluidic assay for the detection of herbicides was performed using a variation of the fluidic unit described earlier (Section 5.2), and used for the detection of H_2O_2, as presented in Section 5.4. A schematic diagram of the setup used is pictured in Fig. 6.12.

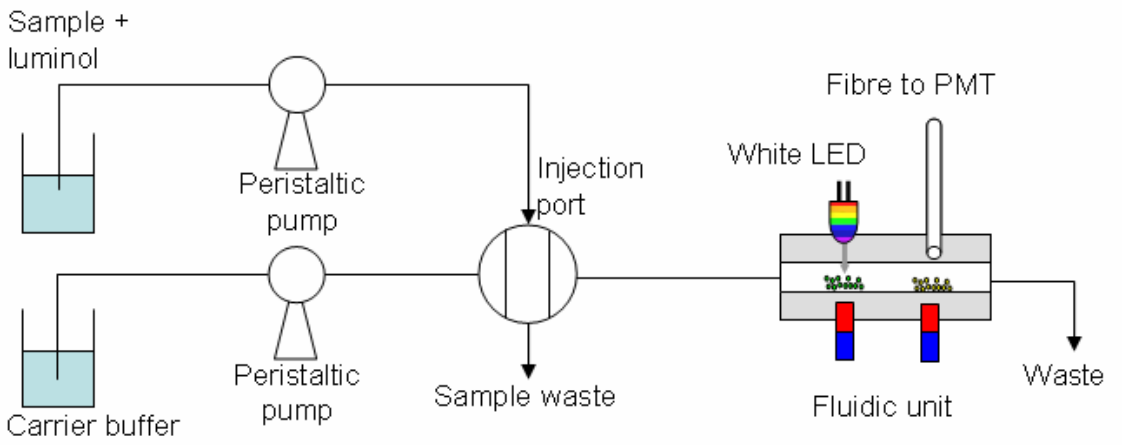

Figure 6.12 Schematic representation of the experimental setup for the fluidic assay for the detection of herbicides.

Following the selection of the fluidic channel design based on the optimised detection of H_2O_2 with HRP-coated beads entrapped in the designated area (Section 5.4.3.1.1), the fluidic channel for the herbicides assay was designed, following the optimised design in Fig. 5.11. A drawing of the channel manufactured can be seen in Fig. 6.13.

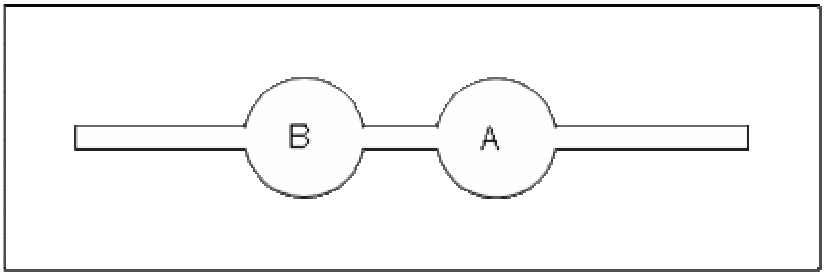

Figure 6.13 Schematic drawing of laser-cut channel fabricated for use with the fluidic sensor for the detection of herbicides.

The regions used for the entrapment of the magnetic beads are: active region A, the area covered with the HRP-coated beads; active region B, the area covered with the thylakoid-coated beads. Not to scale.

The HRP-coated and thylakoid-coated magnetic beads were introduced in the flow cell prior to a measurement taking place. The neodymium magnets were used in order to magnetically entrap the beads on the desired positions, which were the regions of the fluidic channel that were directly beneath the position of the optical fibre for the HRP-coated beads (active region A) and the area directly beneath the position of the LED for the thylakoid-coated beads (active region B). Blu-Tack adhesive was then used to fix the magnets, which allowed for easy removal of the magnets when desired, as also used for other similar work [111]. As described in examples found in the literature [103; 111], after the removal of the beads following a chemiluminescence measurement, the fluidic cell was washed by flowing PBS buffer (100 mM, pH 7.2), in order to discard the beads completely.

Two peristaltic pumps were used to deliver the carrier buffer (Tris-HCl, 10 mM, pH 8.5). Inline with the flow was connected an injection port, on the sample loop of which the herbicide sample was pre-mixed with luminol, which too was carried to the flow cell when the valve was switched to the appropriate position. PTFE tubing was used to connect all components in the flow system.

The optical fibre assembly used was a customised, 1000 µm diameter premium-grade fibre. The fibre was terminated with a standard SMA 905 connector on one end (the end that attaches to the spectrometer), while the other end

consisted only of the ferrule without the outer part of the SMA connector, which had been removed by the manufacturer, in order to allow for the fibre to fit closer to the fluidic channel. Light detected by the fibre was then transferred to the detector. The detector module contains an avalanche photodiode, with an effective active photon counting area of 0.78 mm^2. The specific APD module has a higher sensitivity at 420 nm from other series of Hamamatsu APDs. The detector's electrical signal converted from light was acquired via a data acquisition card by a PC, and further analysed and controlled by LabVIEW.

The LED used to illuminate the thylakoid-coated beads was a white LED, coded LED22 when used in experiments presented in Section 6.3.3, manufactured from MARL Optosource Ltd (Cumbria, UK), Manufacturer Part No: NSPW500BS, and acquired from Farnell Ltd (Leeds, UK).

Following the assembly of all the components, the process of performing a single measurement of the herbicide assay was the following:

~the fluidic setup was readied for the assay to be initiated~

- the tubing and fluidic channel were washed with PBS buffer (100 mM, pH 7.2)
- a neodymium magnet was fixed underneath the active region A, 'viewed' by the optical fibre, aiming to magnetically trap the HRP-coated beads
- the magnetic beads with immobilised HRP (0.25 mg of beads) were aspirated in the flow cell and magnetically trapped in the designated active region A of the channel, directly below the optical fibre
- the tubing was washed with PBS buffer
- a neodymium magnet was fixed underneath the active region B, 'viewed' by the LED, aiming to magnetically trap the thylakoid-coated beads

- varying amounts of the magnetic beads with immobilised thylakoids were aspirated in the flow cell and magnetically trapped in the designated active region B of the channel, directly below the LED
- the flow of the Tris (carrier) buffer was initiated at a flow rate of 0.5 ml/min
- a 50 µl plug of the herbicide sample and luminol was injected into the flow
- arrival of the plug in the channel area covered by the thylakoids-coated beads signalled the initiation of the incubation period
- the flow was stopped for a varying amount of time, in order to allow for the incubation of the herbicide sample with the thylakoids
- following the desired incubation time period, the illumination of the thylakoids was initiated and continued for a varying amount of time, with the flow still stopped
- following the desired illumination time, the LED was switched off, and the flow was then continued, with the plug of the herbicides and luminol now enriched with any produced H_2O_2, subject to the complete inhibition by herbicides
- delivery of the plug in the channel area covered by the HRP-coated beads prompted the initiation of the HRP-mediated chemiluminescence reaction of luminol with H_2O_2
- the chemiluminescence light intensity was collected by the optical fibre
- the light signal was transduced to an electrical signal by the detector
- the obtained chemiluminescence intensity signal was recorded and the maximum intensity was used to plot the graphs or input in tables
- the magnets were removed from their fixed positions
- the tubing was washed with PBS buffer, thus removing all beads, as well as the sample plug

~the fluidic setup was ready for the assay to be repeated~

The above process was followed for the optimisation experiments described in this section, while varying some of the values of parameters included in the process, namely:

- the concentration of thylakoids immobilised on beads
- the herbicide incubation time with the immobilised thylakoids
- the illumination time of the thylakoids.

6.4.3 Results and discussion

6.4.3.1 Optimisation of the concentration of thylakoids immobilised on beads

The chosen isolated thylakoid preparation, Ch5, which allowed for the lower detection limits for the photosynthesis-inhibiting herbicides when assayed in suspension (Section 4.4.3), were also the thylakoid preparation that produced the highest chemiluminescence signal intensity, and hence H_2O_2, when illuminated for 10 min, compared to the other four preparations (Section 4.3.3.1). It was therefore envisaged that it was the most suitable candidate for the production of a chemiluminescence signal due to its H_2O_2 production for the quantitative detection of herbicides in the fluidic assay.

Following the immobilisation of Ch5 thylakoids on magnetic beads (Section 6.2), they were used in the fluidic sensor, in order to quantify the H_2O_2 production following illumination within the fluidic unit by employing the previously chosen LED (Section 6.3). This would allow to determine the 'base' signal, which is the signal that would be produced by a sample containing no herbicides. More importantly, at this stage, the amount of beads with immobilised thylakoids was varied, in order to identify the optimal concentration of thylakoids to be used further for the detection of herbicides.

Therefore, following the magnetic entrapment of the previously determined amount of HRP-coated magnetic beads in the Region A of the fluidic channel, several amounts of thylakoid-coated magnetic beads were magnetically

entrapped in the Region B, and then a sample with no herbicides but only luminol was introduced in Region B, where then the illumination of the immobilised thylakoids on the entrapped beads took place. Following this, the H_2O_2-enriched sample was introduced in the Region A, where the detection of said H_2O_2 took place, due to its consumption in the chemiluminescence reaction with luminol, in the presence of the HRP-coated beads. The results of the chemiluminescence signal peak intensity produced from the H_2O_2 following its production by illuminating the different amount of thylakoid-coated beads can be seen in Fig. 6.14.

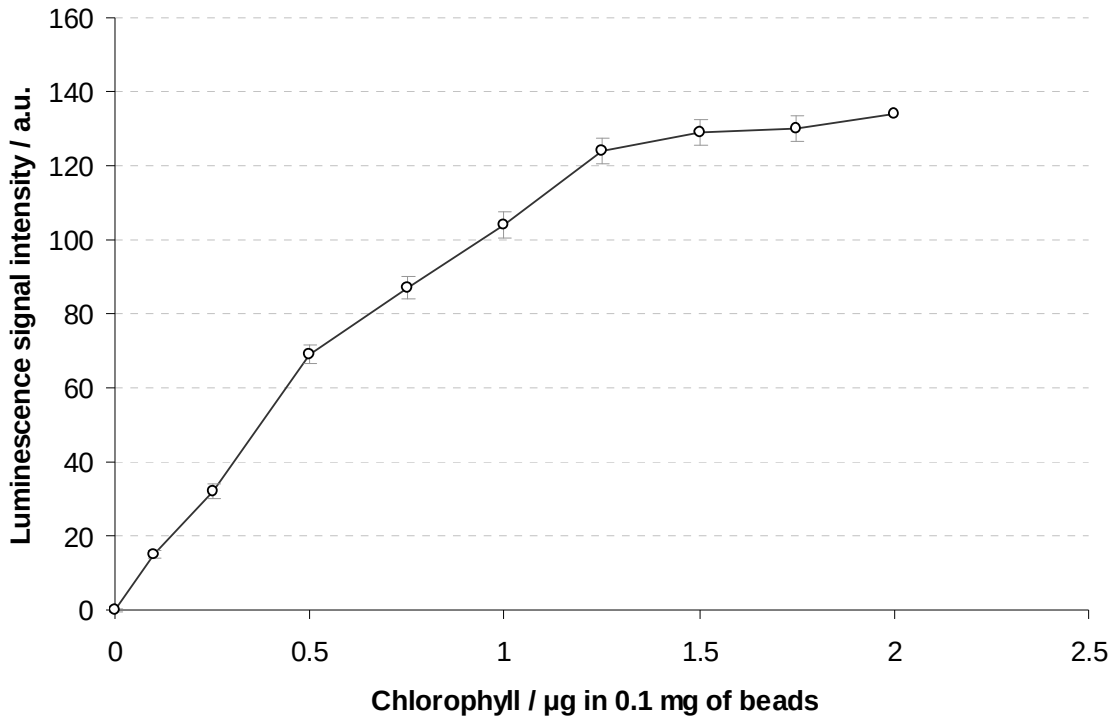

Figure 6.14 Effect of varying the amount of thylakoid-coated magnetic beads, reported as chlorophyll concentration, to the production of H_2O_2 and thus chemiluminescence signal intensity obtained.

Average values and the SDs shown are the results of 3 replicates.

Firstly, the results signify that H_2O_2 is produced by thylakoids immobilised on magnetic beads, possibly in a manner similar to when suspended in solution. As it can be seen, varying the amount of thylakoid-coated magnetic beads during their illumination, and hence H_2O_2 production, had a significant effect on the

chemiluminescence signal intensity produced due to said H_2O_2. More specifically, increasing the amount of beads, as quantified on the x-axis of the graph by the chlorophyll concentration of the different amounts of beads, resulted in an increase of the H_2O_2 production, and therefore chemiluminescence signal intensity. This was not noted for the entire range of the amounts of beads tested; entrapping, illuminating and then measuring the H_2O_2 produced by thylakoid-coated magnetic beads that had the equivalent of 1.25 µg of chlorophyll or more, resulted in very little increase of chemiluminescence signal intensity when compared to the near-linear increase for the lower increments. The only possible explanation for this is that the higher amounts of beads are too closely packed and possibly stacked on each other rather than spread in the designated circular region of the fluidic channel into a monolayer. A similar effect had also been noted when the amount of HRP-coated magnetic beads was being optimised, where, increasing the amount of beads higher than 0.25 mg of HRP-coated beads resulted in a very small chemiluminescence signal increase (Table 5.7). Calculating the amount of thylakoid-coated beads that have a chlorophyll concentration of 1.25 µg, given that the amount of chlorophyll immobilised on the beads is 0.49 µg of chlorophyll / mg of beads suggests that the optimal amount of beads is approximately 0.25 mg, which is the same with the optimal amount of HRP-coated beads for the detection of H_2O_2. As the two different types of beads are magnetically entrapped in regions that have the same dimensions, and that, although the beads perform different roles, the optimised amounts are the same, the possible explanation for reaching a maximum optimal concentration of beads, before then seeing a plateau effect, is thus justified.

It is also important to highlight that the linear increase of H_2O_2 production associated with an increase of the amount of thylakoids, is a relationship that was previously not able to be established, as, in the experiments described in Section 4.3.3, the thylakoids illuminated in varying amounts were in suspension, and thus any produced H_2O_2, and, more specifically, the associated chemiluminescence signal resulting from the detection of said H_2O_2, was

subject to being masked due to the effect that the thylakoids had on the chemiluminescence signal, as explained by a series of measurements in Section 4.3.3.2 and particularly displayed in Fig. 4.9. Previously, increasing the amount of thylakoids being illuminated also resulted in an increase of the sample's absorbance of the chemiluminescence light produced; with the thylakoids immobilised, the H_2O_2 produced following their illumination is then transported to a different region of the sensor for its chemiluminescence detection to be performed, thus eliminating the effect of the sample absorbance.

6.4.3.2 Optimisation of the illumination time of the thylakoid-coated magnetic beads

As presented in Section 4.3.3.1, increasing the time that the thylakoids in suspension are illuminated, resulted in an increase of the H_2O_2 production and hence chemiluminescence detection thereof. It was important to effectively repeat the experiments with the thylakoids immobilised on the magnetic beads and in the fluidic assay format. What is more, as the fluidic assay is based upon the flow of the sample first in the fluidic channel region occupied by the thylakoid-coated beads where the illumination would be taking place, and then in the region of the chemiluminescence detection (for which the optimal flow rate has already been established), this investigation would be allowing for the establishment of the optimal flow rate during the illumination period.

Therefore, following the magnetic entrapment of the previously determined amount of HRP-coated magnetic beads in the Region A of the fluidic channel, and the entrapment of the now established amount of thylakoid-coated magnetic beads in the Region B, then, a sample with no herbicides but luminol was introduced in Region B, where the illumination of the immobilised thylakoids on the entrapped beads took place, for a varying time period. Following this, the H_2O_2-enriched sample was introduced in the Region A, where the detection of said H_2O_2 took place, due to its consumption in the chemiluminescence reaction with luminol, in the presence of the HRP-coated beads. The results of the chemiluminescence signal peak intensity produced

from the H_2O_2 following its production by illuminating the thylakoid-coated beads for a varying period of time can be seen in Fig. 6.15.

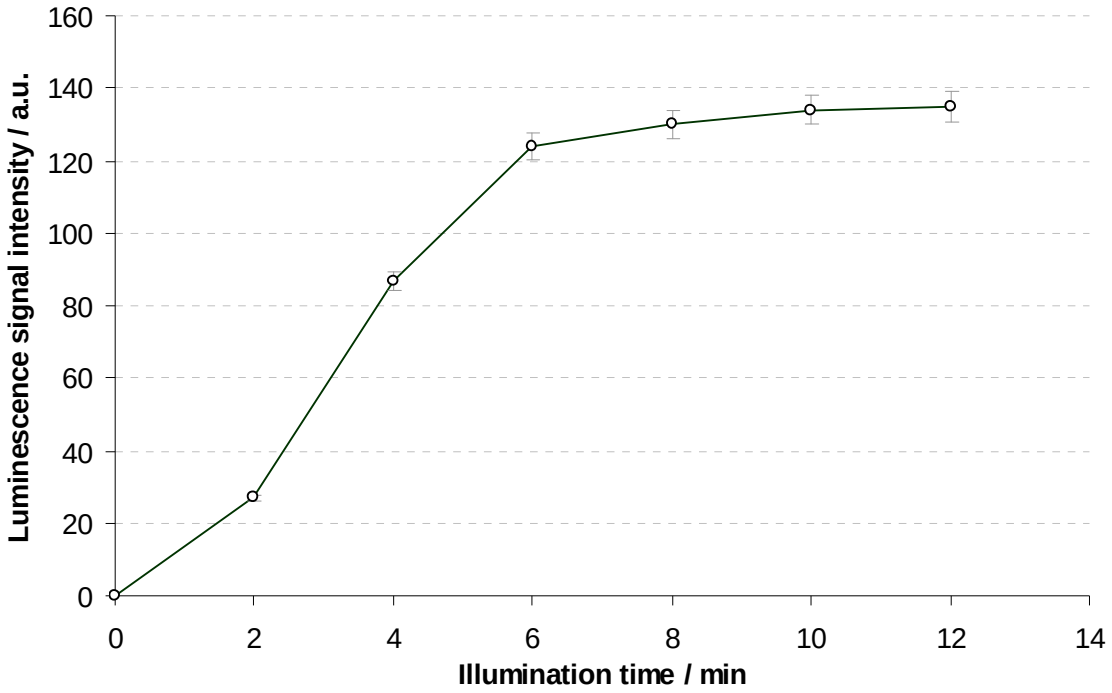

Figure 6.15 Effect of varying the illumination time period of the thylakoid-coated beads to the H_2O_2 production and thus chemiluminescence signal intensity.
Average values and the SDs shown are the results of 3 replicates.

From the results, it appears that, increasing the time for which the thylakoids immobilised on the magnetic beads are illuminated, also increases the H_2O_2 production during that period. For illumination periods longer than 6 minutes, it appears however, that the rate of increased H_2O_2 production per minute of longer illumination period is significantly reduced. The small increase in chemiluminescence signal could possibly even be attributed to an increased diffusion of produced H_2O_2 from the thylakoids towards the sample plug. A similar effect was observed with the thylakoids in suspension, as displayed in Fig. 4.6.

As it is clear from the results, the flow will therefore need to be suspended for the illumination step to take place, for 6 minutes. The possibility of not stopping

the flow or significantly reducing it, would only be possible if a very short illumination time was required. It is also important to state that the signal obtained by illuminating the optimised amount of thylakoid-coated beads for the optimised time is equivalent to 620 nM of H_2O_2. This can be comfortably detected by the H_2O_2 detection step of the fluidic assay, as seen by the curve in Fig. 5.14, but it is a small concentration.

6.4.3.3 Optimisation of the herbicide incubation time

As presented in Section 4.4.3, and in the results shown in Appendix I, increasing the time that the herbicides were in contact with the thylakoids in suspension resulted in an increase of the inhibition of the thylakoids' photosynthetic activity, and therefore H_2O_2 production and hence chemiluminescence detection thereof. It was important to repeat the experiments with the thylakoids immobilised on the magnetic beads and in the fluidic assay format. What is more, as the fluidic assay is based upon the flow of the sample first in the fluidic channel region occupied by the thylakoid-coated beads where the inhibition would be taking place, and then in the region of the chemiluminescence detection (for which the optimal flow rate has already been established), this investigation would be allowing for the establishment of the optimal flow rate during the incubation period.

Therefore, following the magnetic entrapment of the previously determined amount of HRP-coated magnetic beads in the Region A of the fluidic channel, and the entrapment of the now established amount of thylakoid-coated magnetic beads in the Region B, a sample with atrazine and luminol was introduced in Region B, where, following an incubation period, the illumination of the thylakoids immobilised on the entrapped beads took place. Following this, the H_2O_2-enriched sample was introduced in the Region A, where the detection of said H_2O_2 took place, due to its consumption in the chemiluminescence reaction with luminol, in the presence of the HRP-coated beads. The results of the signal peak intensity produced from the chemiluminescence reaction of H_2O_2, following its production by illuminating the thylakoid-coated beads after a

varying incubation period with a herbicide sample (two different atrazine concentrations tested, $1x10^{-8}$ and $6x10^{-8}$), can be seen in Fig. 6.16.

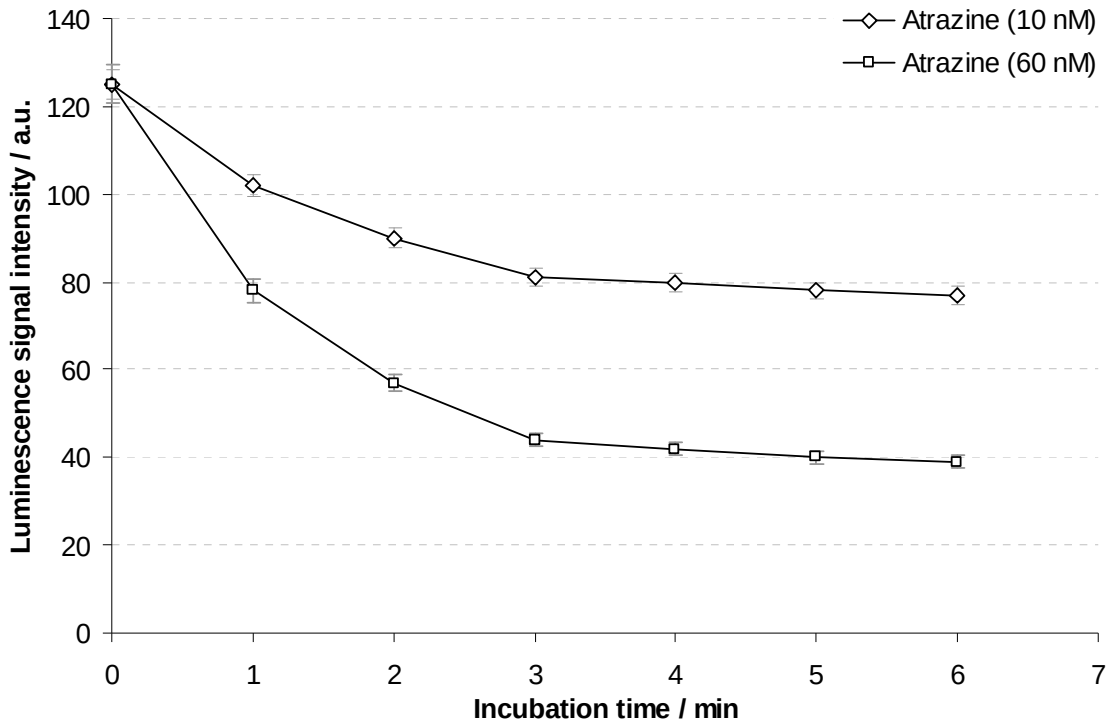

Figure 6.16 Effect of varying the herbicide incubation time period with the thylakoid-coated beads to the H_2O_2 production and thus chemiluminescence signal intensity.

Average values and the SDs shown are the results of 3 replicates.

As it can be seen, for both atrazine concentrations tested, increasing the incubation time of the herbicide sample with the thylakoid-coated beads between 0 and 3 minutes, results in an increased number of herbicide molecules interacting with the thylakoids by binding to the target site in the thylakoids' Photosystem II complexes, thus deactivating more of the H_2O_2 producing ability of the thylakoids. This is measured as a reduction in the chemiluminescence signal intensity detected, which is itself due to the reduced H_2O_2 production. It is also observed that an incubation period longer than 3 minutes does not result in significant further inhibition of the H_2O_2-producing ability. Of course, as the incubation time is then followed by the illumination time, which itself has been optimised to 6 minutes, the overall incubation time

will be longer than the optimised 3 minutes. This, however, as incubation times longer than 3 minutes do not affect their inhibitory effect, does not result in a behaviour that damages the detection of the herbicides.

The flow will therefore be stopped for nine minutes altogether, with the herbicide sample plug suspended in the Region B for that time. A similar method was employed in a HRP-mediated luminol chemiluminescence flow assay for the detection of phenolic herbicides by measuring the increase of the chemiluminescence signal intensity observed due to the enhancing effect of this class of herbicides [87]. In the prior work, in order to allow for the build up of signal, they stopped the sample plug of the flow within the flow cell. The authors call this a 'stop-flow' flow injection analysis technique, suggesting that it can generally be used to increase the sensitivity of measurement by increasing the residence time in the flow cell.

Having optimised various parameters of the fluidic assay for the detection of herbicides, the fluidic assay is ready to be performed for the identification of the working range of herbicide detection, the measurement of the limits of detection and the development of calibration curves.

6.5 Fluidic assay for the detection of herbicides using immobilised thylakoids and HRP on magnetic beads

6.5.1 Introduction

Having established a batch assay for the detection of herbicides, based on the HRP-mediated chemiluminescence reaction of luminol with H_2O_2 produced by illuminated thylakoids following incubation with a herbicide sample, various steps have been taken to transfer the various elements of the assay from a batch to a fluidic format. The HRP-mediated chemiluminescence detection of H_2O_2, based on its reaction with luminol in a fluidic assay format with HRP-coated magnetic beads, has been established and optimised (Chapter 5), while the remaining necessary steps (the immobilisation of thylakoids on magnetic

beads, the selection of a suitable LED to illuminate them, and the optimisation of their interaction with herbicides) have been successfully accomplished (Sections 6.2 – 6.4).

The assembled fluidic sensor, with the optimised materials and methods, had thus been readied for the full experiment set, establishing the fluidic assay for the detection of herbicides. The same three photosynthesis-inhibiting herbicides (atrazine, diuron and propanil) and three non-photosynthesis-inhibiting herbicides (2,4-D, paraquat and acifluorfen) were used, as already assayed in the batch assay (Section 4.4.3).

6.5.2 Materials and methods

6.5.2.1 Materials

The chemicals, detection and fluidics apparati and other materials were all purchased and prepared as described in Section 6.4.2.1.

6.5.2.2 Setup and method

The herbicides, HRP-coated and thylakoid-coated magnetic beads were prepared as described in Section 6.4.2.2. The fluidic assay for the detection of herbicides was performed using the same fluidic unit setup as described in Section 6.4.2.2.

Following the assembly of all the components, and having now optimised various parameters necessary, the process of performing a single measurement of the herbicide assay was the following:

~the fluidic setup was readied for the assay to be initiated~

- the tubing and fluidic channel were washed with PBS buffer (100 mM, pH 7.2)
- a neodymium magnet was fixed underneath the active region A, 'viewed' by the optical fibre, aiming to magnetically trap the HRP-coated beads
- the magnetic beads with immobilised HRP (0.25 mg of beads) were aspirated in the flow cell and magnetically trapped in the designated active region A of the channel, directly below the optical fibre
- the tubing was washed with PBS buffer
- a neodymium magnet was fixed underneath the active region B, 'viewed' by the LED, aiming to magnetically trap the thylakoid-coated beads
- the magnetic beads with immobilised thylakoids (0.25 mg of beads) were aspirated in the flow cell and magnetically trapped in the designated active region B of the channel, directly below the LED
- the flow of the Tris (carrier) buffer was initiated at a flow rate of 0.5 ml/min
- a 50 µl plug of the herbicide sample and luminol was injected into the flow
- arrival of the plug in the channel area covered by the thylakoids-coated beads signalled the initiation of the incubation period
- the flow was stopped for 3 min, in order to allow for the incubation of the herbicide sample with the thylakoids
- with the flow still stopped, following the 3 min herbicide incubation period, the illumination of the thylakoids was initiated and continued for 6 min
- following the illumination period, the LED was switched off, and the flow was then continued, with the plug of the herbicides and luminol now enriched with any produced H_2O_2, subject to the complete inhibition by herbicides
- delivery of the plug in the channel area covered by the HRP-coated beads prompted the initiation of the HRP-mediated chemiluminescence reaction of luminol with H_2O_2

- the chemiluminescence light intensity was collected by the optical fibre
- the light signal was transduced to an electrical signal by the APD detector
- the obtained chemiluminescence intensity signal was recorded and the maximum peak intensity was used to plot the graphs or input in tables
- the magnets were removed from their fixed positions
- the tubing was washed with PBS buffer, thus removing all beads, as well as the sample plug

~the fluidic setup was ready for the assay to be repeated~

6.5.3 Results and discussion

Using the complete fluidic sensor unit to perform the assay for the detection of herbicides, the results obtained for atrazine, diuron and propanil, the three photosynthesis-inhibiting herbicides, are presented in Figures 6.17 to 6.19. A mixture of 50% atrazine and 50% diuron was also tested, and the resulting calibration curve is found in Figure 6.20. These results are followed by the detection results for the three non-photosynthesis-inhibiting herbicides (2,4-D, paraquat and acifluorfen) in Figures 6.21 to 6.23.

6.5.3.1 Detection of photosynthesis-inhibiting herbicides

Following the magnetic entrapment of the 0.25 mg of HRP-coated magnetic beads in the Region A of the fluidic channel, 0.25 mg of Ch5 thylakoid-coated magnetic beads were magnetically entrapped in the Region B, and then a sample with a varying amount of herbicides and luminol was introduced in Region B, where incubated for 3 min, followed by the illumination of the immobilised thylakoids on the magnetically entrapped beads for 6 min. Following this, the now H_2O_2-enriched sample was introduced in the Region A, where the detection of said H_2O_2 took place, due to its consumption in the

chemiluminescence reaction with luminol, in the presence of the HRP-coated beads.

The results of the chemiluminescence signal peak intensities produced from the H_2O_2 following its production by illuminating the thylakoid-coated beads following their incubation with different concentrations of the photosynthesis-inhibiting herbicides can be seen in Figures 6.17-20, expressed as Residual Activity, compared to a sample with no herbicides (100%).

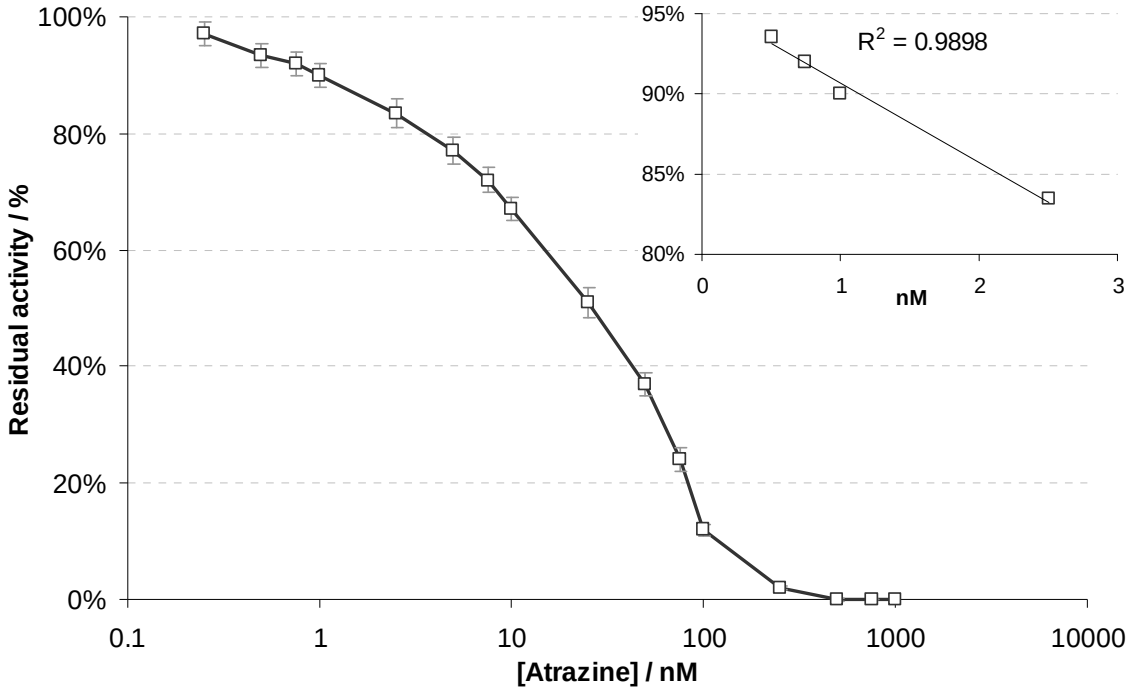

Figure 6.17 Calibration curve for the detection of atrazine, using the fluidic sensor with thylakoids and HRP immobilised on magnetic beads.
Average values and the SDs shown are the results of 3 replicates.

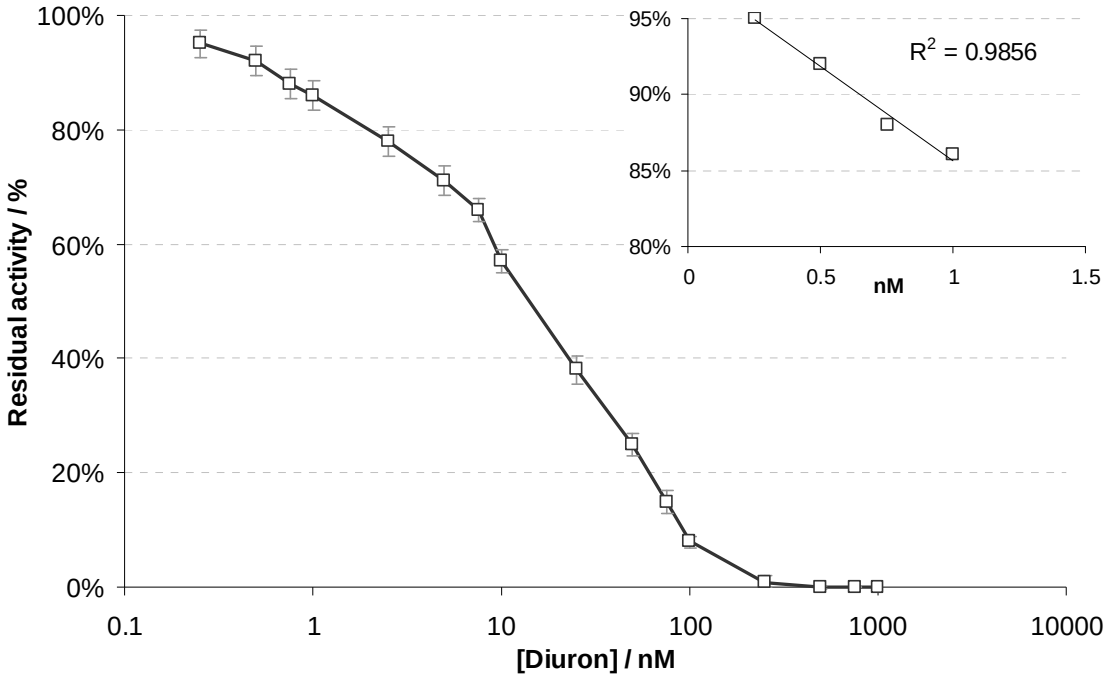

Figure 6.18 Calibration curve for the detection of diuron, using the fluidic sensor with thylakoids and HRP immobilised on magnetic beads.

Average values and the SDs shown are the results of 3 replicates.

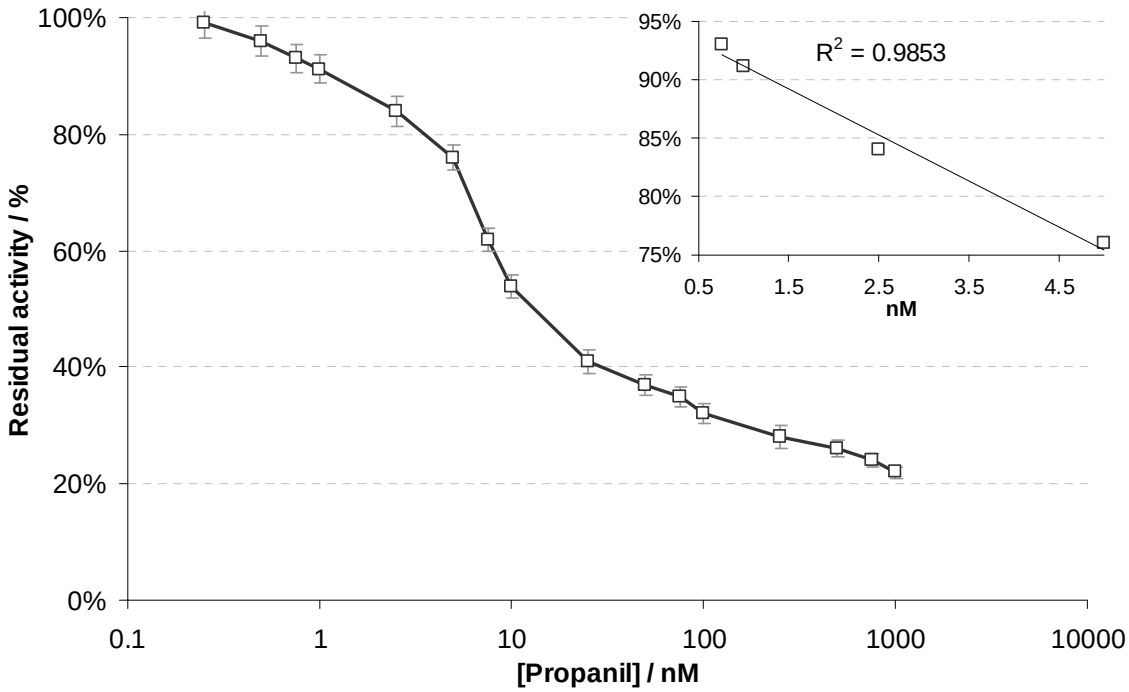

Figure 6.19 Calibration curve for the detection of propanil, using the fluidic sensor with thylakoids and HRP immobilised on magnetic beads.

Average values and the SDs shown are the results of 3 replicates.

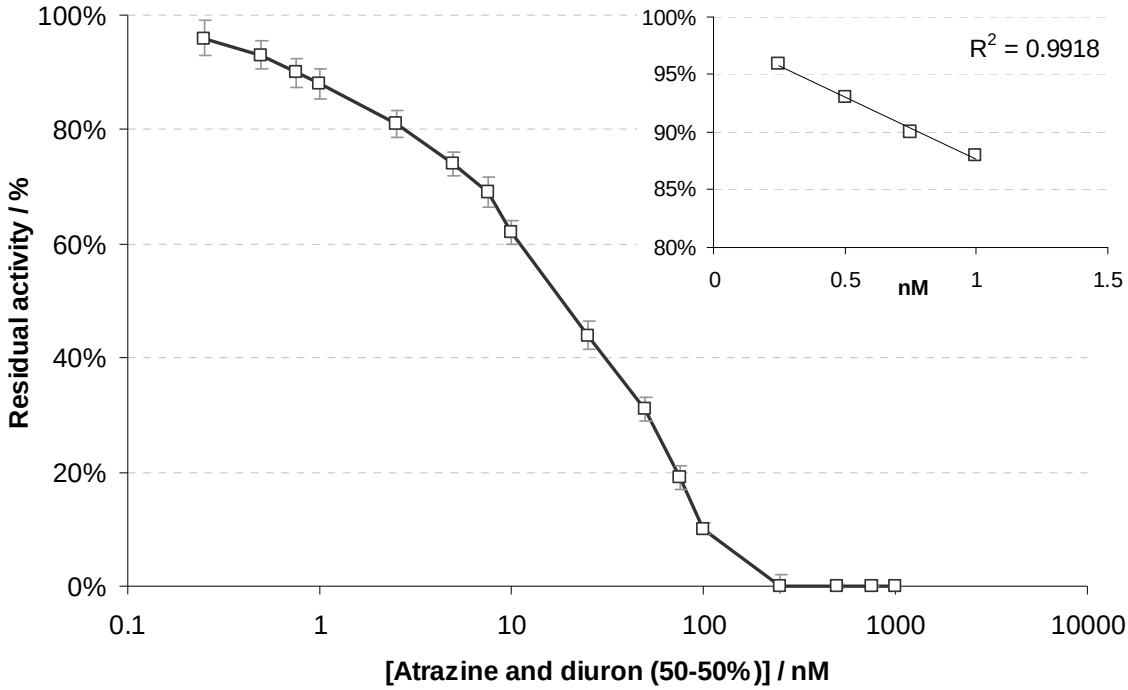

Figure 6.20 Calibration curve for the detection of atrazine and diuron (50-50%), using the fluidic sensor with thylakoids and HRP immobilised on magnetic beads.

Average values and the SDs shown are the results of 3 replicates.

The limits of detection have been calculated, and presented in Table 6.1. As it can be seen, the lower LODs achieved with the fluidic sensor fall close to the region of individual herbicides concentrations that are the highest permissible in EU to be found in drinking and other waters (Table 6.2). More specifically, however, the developed sensor did not achieve the detection of the concentration of an individual herbicide that corresponds to the upper limit of how much of a single herbicide is allowed to be found in drinking water in the EU (0.1 ppb or 0.1 μg/l) for any of the three photosynthesis-inhibiting herbicides tested, although the lower LODs achieved are very close to the target limits. What can also be observed from the two tables, is that the sensor can successfully detect concentrations of herbicides that equal 0.5 μg/l, which is the highest permissible amount of total pesticides to be found in drinking water. That means, if a mixture of any of the three tested photosynthesis-inhibiting herbicides, in whatever proportions, exists in a water sample, the sensor

developed can successfully detect the concentration that the mixture should not go over. This is exemplified by the lower LOD achieved for the 50-50% atrazine and diuron sample, which is lower than the limit it should not exceed (and therefore limit it should be detectable at).

Table 6.1 Limits of detection achieved for the three photosynthesis-inhibiting herbicides and a combination thereof, measured with the fluidic sensor using immobilised thylakoids and HRP.

	Dynamic Range	
Herbicide	Lower LOD (M)	Upper LOD (M)
Atrazine	8.2×10^{-10}	2.5×10^{-07}
Diuron	5.5×10^{-10}	1.0×10^{-07}
Propanil	9.9×10^{-10}	1.0×10^{-08}
Atrazine and diuron (50-50%)	6.5×10^{-10}	2.0×10^{-07}

Table 6.2 Herbicides concentrations that correspond to the surface and drinking water maximum allowances for individual and total pesticides in the E.U.

Herbicide	Concentration that equals 0.1 µg/l (M)	Concentration that equals 0.5 µg/l (M)
Atrazine	4.6×10^{-10}	2.3×10^{-09}
Diuron	4.3×10^{-10}	2.1×10^{-09}
Propanil	4.6×10^{-10}	2.3×10^{-09}
Atrazine+diuron (50-50%)	4.5×10^{-10}	2.2×10^{-09}

It is evident that the detection working range is quite narrow, 2-3 orders of magnitude, compared to the 4 orders or more achieved by the batch assay for the detection of same herbicides. This reduction is believed to be due to the low concentration of thylakoids, and therefore binding sites for the herbicide molecules, compared to the batch assay where the thylakoids were in suspension. A similar effect has been noticed in the literature [103], where lowering the amount of an analyte immobilised on beads, led to a narrower working range. Similarly, in a paper describing the development of an electrode with immobilised PSII [154], it is suggested that lowering the concentration of PSII

particles, compared to previous work, leads to the elimination of the underestimation of low concentrations of herbicides.

Although for atrazine, diuron and their combination, full inhibition of the H_2O_2 production was observed, with propanil, the inhibitory effect of propanil on the production of H_2O_2 by thylakoids appears to be reduced with higher concentrations. As explained in detail in Section 4.4.3, this is not the case; at low concentrations propanil is a strong inhibitor of the photosynthetic process, while at higher concentrations it attacks membranes and at 1 mM it uncouples oxidation from phosphorylation [165; 166], thus causing an increase of the H_2O_2 production.

The RSD for the detection of herbicides is: 3.1%, which is much lower compared to the RSD of 5.7% achieved with the batch assay in Chapter 4.

6.5.3.2 Detection of non-photosynthesis-inhibiting herbicides

Using the complete fluidic sensor unit for the detection of herbicides, the results obtained for 2,4-D, paraquat and acifluorfen, the three non-photosynthesis-inhibiting herbicides, are presented in Figures 6.21 to 6.23.

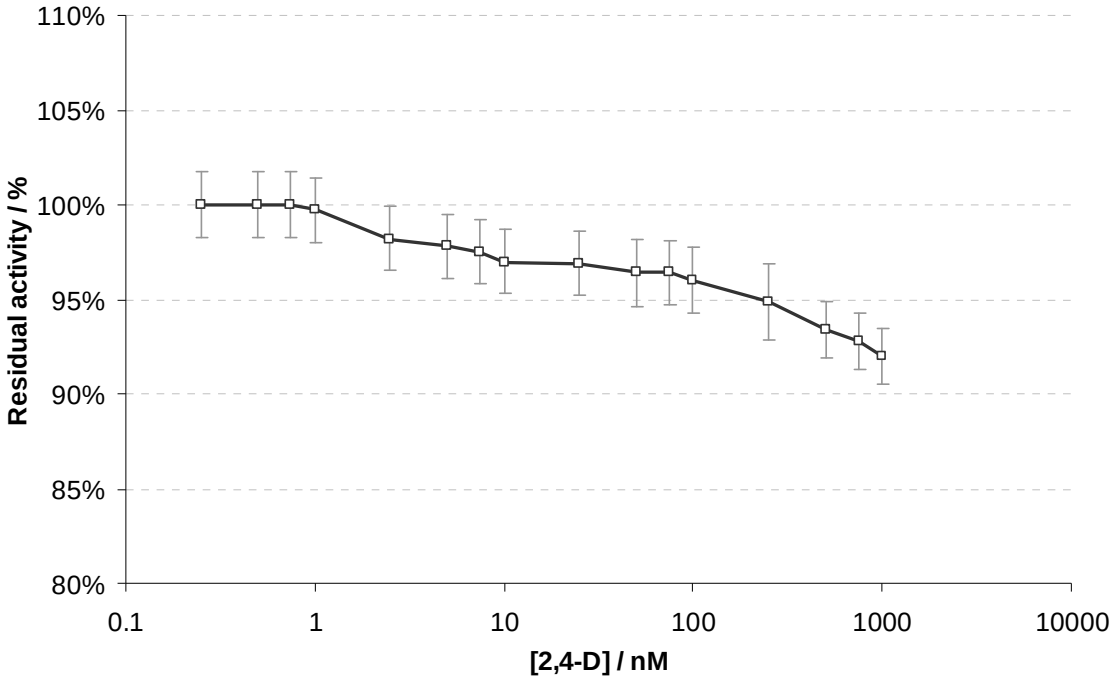

Figure 6.21 Calibration curve for the detection of 2,4-D, using the fluidic sensor with thylakoids and HRP immobilised on magnetic beads.

Average values and the SDs shown are the results of 3 replicates.

As it can be seen, compared to the results obtained using the batch assay (Fig. 4.27), the effect of 2,4-D on the H_2O_2 production by thylakoids has been reduced significantly. As discussed in Section 4.4.3.4, 2,4-D is not expected to effect the ability of thylakoids to undertake their part in the photosynthetic oxygen evolution, and therefore on the production of H_2O_2. Therefore its effect observed with the thylakoids in suspension could not be accounted for, as no knowledge of similar behaviour could be retrieved from the literature. What is however observed with the thylakoids immobilised on the magnetic beads, is that the same effect is not observed to the same degree; previously, 2,4-D concentrations between $1x10^{-7}$ – $1x10^{-4}$ all reduced the H_2O_2 produced by 5-25%, while now the reduction of H_2O_2 production is only between 0-8%.

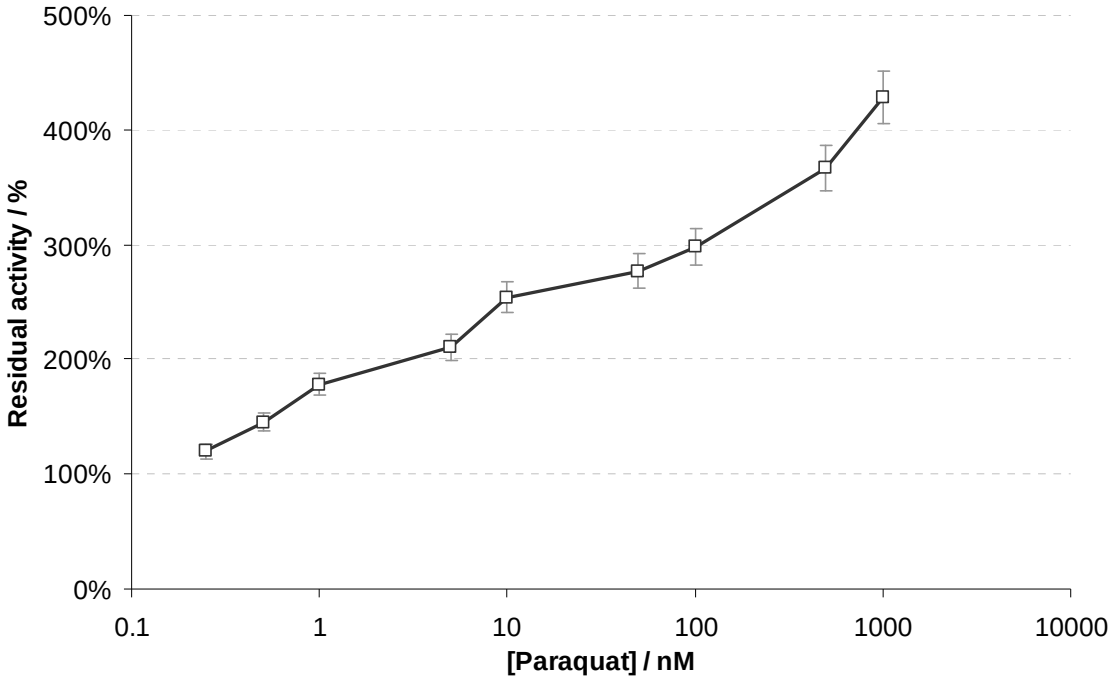

Figure 6.22 Calibration curve for the detection of paraquat, using the fluidic sensor with thylakoids and HRP immobilised on magnetic beads.

Average values and the SDs shown are the results of 3 replicates.

As it can be seen, paraquat had a distinctively different effect on the expected H_2O_2 produced by immobilised thylakoids following illumination, compared to the photosynthesis-inhibiting herbicides. For all concentrations of paraquat tested, there was a large increase in chemiluminescence signal observed, and hence possibly H_2O_2 produced by the thylakoids, when compared to the signal that was achievable by the thylakoids following the illumination without a herbicide incubation step (residual activity = 100%).

As explained in detail in Section 4.4.1.1.6, and already discussed in relevance to the results obtained when testing paraquat-containing samples with non-immobilised thylakoids (Section 4.4.3.6) in the presence of light, paraquat causes the generation of hydrogen peroxide and other free radicals, which explains the increased chemiluminescence signal detected in the work presented here.

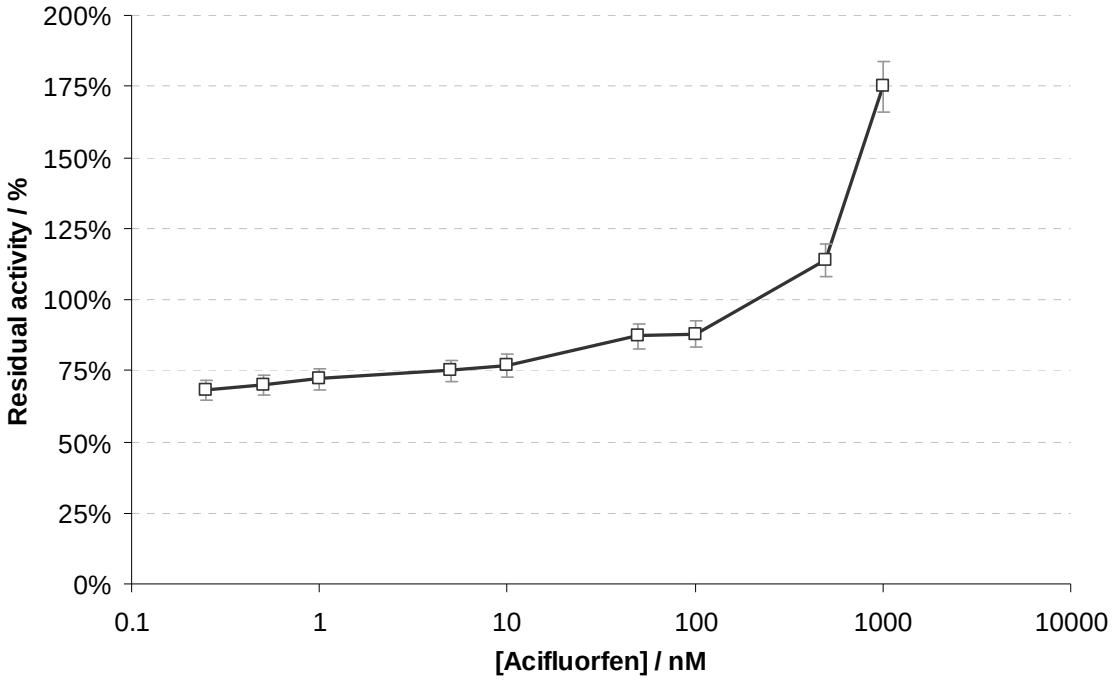

Figure 6.23 Calibration curve for the detection of acifluorfen, using the fluidic sensor with thylakoids and HRP immobilised on magnetic beads.

Average values and the SDs shown are the results of 3 replicates.

As it can be seen, the higher concentrations of acifluorfen tested had a distinctively different effect on the expected H_2O_2 produced by thylakoids following illumination, compared to the photosynthesis-inhibiting herbicides. The increase in chemiluminescence signal observed, when compared to the signal that was achievable by the thylakoids following the illumination without a herbicide incubation step (the 100% signal), was probably effected from all concentrations of acifluorfen tested, but only the highest ones caused a H_2O_2 production that exceeded the base rate of 100%.

As explained in detail in Section 4.4.1.1.7, and in Section 4.4.3.6, the modes of acifluorfen's action are the reason for the obtained results; acifluorfen did inhibit the production of H_2O_2 by the immobilised thylakoids, while also effecting them in other ways, thus causing a rise in the net amount of H_2O_2 produced. This effect appears to be concentration-dependent.

An electrochemical sensor employing photosynthetic PSII particles [9; 48] reportedly displayed good sensitivity to classical herbicides diuron, atrazine and simazine, but significantly reduced sensitivity to phenolic herbicides. The authors attributed this to a very low diffusion rate of the phenolic herbicides in the BSA–glutaraldehyde matrix, while also suggesting that replacing the entrapment gel type restored the inhibitory effect of phenolic herbicides. From the results presented in this and Chapter 4 however, and given the literature reporting the mechanism of action of phenolic herbicides, it can be suggested that, in the case of the mentioned electrochemical biosensor, the authors have misinterpreted their results.

In another example however [174], where a sensor employing PSII for the detection of photosynthesis-inhibiting herbicides is presented, it is acknowledged that "Phenolic herbicides have two modes of action: they are inhibitors of PSII electron transport, and also uncouplers of oxidative phosphorylation and photophosphorylation, due to their protonophoric properties". Furthermore, the authors even suggest that: "In case of herbicides monitoring, precaution should be taken in interpretation of the response particularly if DNOC concentration exceeds …".

6.6 Use of environmental water samples for the determination of herbicides using the fluidic sensor with immobilised HRP and thylakoids

6.6.1 Introduction

In order to further characterise the developed assay for the detection of herbicides, and to investigate the calibration needs of a future instrument based on the fluidic sensor, the sample plug containing known concentrations of herbicides and luminol in buffer was replaced by water samples collected from the environment.

6.6.2 Materials and methods

Two different river water samples were tested, both provided by European project Partner 1B (Dr L Guzzella, Institute for Water Management IRSA, National Council of Research, Via della Mornera 25, 20047 Brugherio, Milan, Italy). Both samples provided were collected from the river Po, and tested for a variety of herbicides with HPLC and GC–MS analyses, the results of which can be seen in Table 6.23. For the purposes of the measurements made with the fluidic sensor for the detection of photosynthesis-inhibiting herbicides, the total amount of pesticides in each sample has been calculated for all the pesticides found as well as only the photosynthesis-inhibiting compounds. As it can be seen, sample 1 has a total amount of pesticides that fall exactly on the maximum limit allowed in drinking water in the E.U. (0.5 µg/l), while two photosynthesis-inhibiting herbicides are near or over the maximum permissible amount of 0.1 µg/l (Diuron and Terbuthylazine). Sample 2 has much lower levels of pesticides overall, and specifically of photosynthesis-inhibiting herbicides.

Table 6.3 Laboratory analysis of individual pesticide concentration of river water samples, and total amounts calculated for all and photosynthesis-inhibiting herbicides (PIH) only.

Compound		Sample 1	Sample 1	Sample 2	Sample 2
Name	**Mode of action**	**All**	**PIH only**	**All**	**PIH only**
2, 6-diethylaniline	PIH	0.02	0.02	0	0
Atrazine	PIH	0.06	0.06	0.008	0.008
Deethylatrazine	PIH	0.05	0.05	0.02	0.02
Deethylterbuthylazine	PIH	0.03	0.03	0.02	0.02
Diuron	PIH	0.12	0.12	0	0
Linuron	PIH	0	0	0	0
Metobromuron	PIH	0	0	0	0
Prometryn	PIH	0	0	0	0
Simazine	PIH	0	0	0.008	0.008
Terbuthylazine	PIH	0.1	0.1	0.02	0.02
Alachor	Phenol	0	-	0.006	-
Metolachlor	Phenol	0	-	0	-
2-methyl 6-ethylaniline	other	0	-	0	-
Butylate	other	0	-	0	-
Molinate	other	0.04	-	0	-
Oxadiazon	other	0.08	-	0.007	-
Thiobencarb	other	0	-	0	-
TOTAL (µg/l)		**0.500**	**0.380**	**0.089**	**0.076**

The water samples were used with the fluidic sensor in order to measure the amount of H_2O_2 contained and the amount of herbicides contained. Therefore, the fluidic sensor was setup as in Section 5.4.3.3 for the H_2O_2 measurements and as in Section 6.5.2.2 for the herbicides measurements.

6.6.3 Results and discussion

6.6.3.1 Calibration method development

The performance of the fluidic assay for the detection of herbicides can be affected by three factors when measuring environmental water samples:

a. the effect of H_2O_2 found in the water sample to the chemiluminescence signal that would otherwise be solely due to the H_2O_2 produced by thylakoids,

b. the effect of the water sample matrix on the detection of H_2O_2, whichever its source,
c. the effect of the water sample matrix on the detection of herbicides in the water sample, probably due to the effect of the matrix on the inhibition of the thylakoids by the herbicides.

Identifying and quantifying these effects can be achieved due to the fact that, as the fluidic sensor has been designed to employ two separate areas and for the herbicide detection assay to be performed in two distinct, independent stages, it is envisaged that, when employed in the field, the assay would therefore be performed in four variations, in order to allow for the measurement of all the effects of the water sample described.

More specifically, the fluidic sensor would be used to:

1. measure the concentration of H_2O_2 found in the water sample,
2. measure the effect of the water sample matrix on the detection of added H_2O_2,
3. measure the concentration of photosynthesis-inhibing herbicides in the water sample, by detecting the reduction in H_2O_2 production by the thylakoids, and
4. measure the effect of the water sample matrix on the herbicide-induced reduction in H_2O_2 production by the thylakoids of added herbicides.

Step 3 is essentially the herbicide detection assay, while steps 1, 2 and 4, are the measurements that need to be performed in order to factor in the effects "a", "b" and "c" from the list above respectively. The calculations thus suggested, in order to adjust the herbicide content reported for the three effects, include the following:

i. Chemiluminescence signal obtained from step 1 is subtracted from chemiluminescence signal obtained from step 3.
ii. The result is adjusted by multiplying with (100% - percentile recovery of H_2O_2 obtained from step 2).

iii. The result is adjusted by multiplying with (100% - percentile recovery of herbicides obtained from step 4).

Calculation i. will remove the chemiluminescence signal due to H_2O_2 inherent in the water sample, from the chemiluminescence signal obtained when measuring the H_2O_2 production by thylakoids, whether inhibited or not by herbicides. As both of these signals are skewed with the effect of the water sample matrix on any chemiluminescence reaction, irrespective of the hydrogen peroxide's source, the chemiluminescence signal value obtained by calculation i. is then weighted by the percentile reduction or increase caused by the sample water matrix on any chemiluminescence signal, which is calculation ii. Then, the resulting chemiluminescence signal value is also weighted by the percentile reduction or increase caused by the sample water matrix on the herbicide reaction with the thylakoids (calculation iii.). The resulting value ought to therefore more accurately reflect the true value of the effect of the concentration of herbicides found in the water sample.

Having devised the necessary steps 1-4 and the calculations necessary to take the factors a.-c. into account, the calibration of the sensor in order to achieve an accurate and true interpretation of a herbicide detection measurement from environmental water samples has been attempted.

6.6.3.2 Determination of herbicides in river water samples

6.6.3.2.1 Step 1 measurement

The standard H_2O_2 detection fluidic assay was performed, as described in Section 5.4.3.2, in order to identify the concentration of H_2O_2 in the water samples, irrespective of herbicide content. Therefore, the sample plug consisting of a water sample collected from the environment with luminol was tested for H_2O_2.

The results of measuring the H_2O_2 present in the water samples are presented in Table 6.4. It should be noted that the reported values for H_2O_2 present in the water samples are not adjusted for the effect of the water sample matrix on the H_2O_2 detection process itself, which can only be achieved following Step 2. As it can be seen, the amount of H_2O_2 present in the both river water samples is very small. This is probably due to the decay of any H_2O_2 present since the sample collection, as a long period of 4 weeks had passed before the samples were used in the measurements described here. There is evidence suggesting that H_2O_2 present in natural waters decays fast within two days from its collection [201]. It should also be noted that both concentrations fall below the fluidic sensor's lower LOD of 107 nM, which has been calculated with a 3xSD, but are still within the instrument LOD, i.e. the concentration that the detector can distinguish from another or from a blank.

Table 6.4 Determination of H_2O_2 in river water samples.

	H_2O_2 added (nM)	Chemiluminescence signal obtained (a.u.)	H_2O_2 found (nM)*
River water sample 1	0	6.2	37
River water sample 2	0	7.9	62

The H_2O_2 measurements were performed with the complete fluidic sensor unit for the determination of H_2O_2. The results presented in the "H_2O_2 found" column are the rounded averages of 3 replicates. *: the amount of reported H_2O_2 found has not been adjusted for the effect of the water matrix on the H_2O_2 chemiluminescence detection, as that can only be achieved following Step 2.

6.6.3.2.2 Step 2 measurement

In order to quantify the effect of the water samples' matrix on the H_2O_2 detection itself, similarly to the experiments presented in Section 5.4.3.3, the standard H_2O_2 detection fluidic assay was performed, with the water samples containing added H_2O_2. The effect of the water samples' matrix on the H_2O_2 detection would then be taken into consideration when reporting the results of measuring the water samples' herbicides based upon the inhibition of the H_2O_2 production

step. The results of measuring the effect of the water samples' matrix on the H_2O_2 detection, presented as percentile recovery, are presented in Table 6.5.

It should be noted that, should the fluidic sensor be used solely for the detection of H_2O_2 in water samples, the chemiluminescence signal obtained from the water samples without any added H_2O_2, would now be adjusted by adding / subtracting the 'Effected matrix change' weighting percentage. As these measurements are only part of the calibration of the fluidic sensor for the detection of herbicides, there is no need to be doing the calculations yet.

Table 6.5 Determination and recovery of H_2O_2 in river water samples.

H_2O_2 added (nM)	Chemiluminescence signal obtained (a.u.)	H_2O_2 found (nM)	Recovery (%)	**Effected matrix change**
River water sample 1				
0	6.2	37	N/A	
300	81.2	321	95.3%	**-4.7%**
River water sample 2				
0	7.9	62	N/A	
300	92.5	352	97.2%	**-2.8%**

The H_2O_2 measurements were performed with the complete fluidic sensor unit for the determination of H_2O_2. The results presented in the "H_2O_2 found" column are the rounded averages of 3 replicates.

As it can be seen, the river water samples did affect the detection of added H_2O_2. Both river water samples caused a decrease in the chemiluminescence signal obtained when known H_2O_2 concentrations were added to the water sample, although by a small proportion. That means that the water sample matrix reduced the 'true' chemiluminescence signal by 4.7% and 2.8% respectively for each sample.

6.6.3.2.3 Step 3 measurement

Next, the river water samples were tested using the optimised, final herbicide detection assay as used for the detection of herbicides described in Section 6.5.3. The results of measuring the effect of the herbicides present in the water samples are presented in Table 6.6.

Table 6.6 Determination of herbicides in river water samples.

	Herbicides added (µM)	Chemiluminescence signal obtained (a.u.)
River water sample 1	0	114
River water sample 2	0	133

The herbicides measurements were performed with the complete fluidic sensor unit for the determination of herbicides. The results presented in the "Chemiluminescence signal obtained" column are the rounded averages of 3 replicates.

If the fluidic sensor was used without the calibration steps for real water samples, the chemiluminescence signals obtained, presented in Table 6.6, would be directly compared to, ideally, a calibration graph for the detection of a mixture of herbicides, the closest to which is presented in Figure 6.20, for a 50-50% mixture of atrazine and diuron. However, as adjusting the signals obtained is necessary in order to obtain a true representation of the amount of herbicides present, the values obtained from this step (Step 3), cannot be directly correlated to a herbicide concentration. Thus, at the moment, without processing the measured chemiluminescence signals, no judgement can be made on what herbicides concentrations the obtained chemiluminescence signals equate to.

6.6.3.2.4 Step 4 measurement and related calculations

In order to quantify the effect of the water samples on the herbicide detection itself, the standard herbicide detection fluidic assay was performed, with the water samples containing added herbicides. The effect of the water samples' matrix on the herbicide detection would then be taken into consideration when reporting the results of measuring the water samples' herbicides based upon the inhibition of the H_2O_2 production step. The results of measuring the chemiluminescence signal obtained when adding herbicides of a known concentration are presented in Table 6.7. A 50-50% mixture of atrazine and diuron was selected as the added herbicide, as it may aid to reflect the fact that an environmental water sample would naturally contain more than a single herbicide.

Table 6.7 Determination of herbicides in river water samples.

	Herbicides added (nM)	Chemiluminescence signal obtained (a.u.)
River water sample 1		
	0	114
	5	97
River water sample 2		
	0	133
	5	101

The herbicides measurements were performed with the complete fluidic sensor unit for the determination of herbicides. The results presented in the "herbicides found" column are the averages of 3 replicates.

In order to identify the effect the water sample matrix is having on the interaction of herbicides with the thylakoids or perhaps the inhibition of the H_2O_2 production by the thylakoids, a set of calculations have to be performed. These will result in the recovery and hence effect the matrix is having, in order to then use the percentile increase or reduction on the results obtained by Step 3, and therefore determine the true amount of herbicides in the water sample. The detailed step-by-step calculations for river water sample 1 are provided, while only a summary of the calculations for river water sample 2 is provided in the main body of text below, while the equivalent, detailed calculations can be found in Appendix VII.

Firstly, calculations i. and ii. are performed on the water sample with no added herbicides.

added 0 nM			
	Step 3 Chemiluminescence signal obtained	114.00	a.u.
	Step 1 Chemiluminescence signal obtained due to H_2O_2 present in water	6.20	a.u.
Calculation i.	Step 3 - step 1 = Chemiluminescence signal calculated, due to herbicide presence only	107.80	a.u.
	Step 2 Effected matrix change (i.e. 4.7% of 107.80 a.u.) = Chemiluminescence signal by which calculation i. result is under-reported	5.07	a.u.
Calculation ii.	Adjusted for matrix under-reporting effect on H_2O_2 detection (i.e. 107.80 + 5.07 a.u.)	112.87	a.u.
	Residual activity (compared to chemiluminescence signal of blank, which is 124 a.u.)	91.02	%
	Equivalent amount of herbicides present	0.66	nM

Then, the same set of calculations is performed on the water sample 1 with added 5 nM of 50-50% atrazine and diuron mixture.

added 5 nM			
	Step 3 Chemiluminescence signal obtained	97.00	a.u.
	Step 1 Chemiluminescence signal obtained due to H_2O_2 present in water	6.20	a.u.
Calculation i.	Step 3 - step 1 = Chemiluminescence signal calculated, due to herbicide presence only	90.80	a.u.
	Step 2 Effected matrix change (4.7% of 90.80 a.u.) = Chemiluminescence signal by which calculation i. result is under-reported	4.27	a.u.
Calculation ii.	Adjusted for matrix under-reporting effect on H_2O_2 detection (i.e. 90.80 + 4.27 a.u.)	95.07	a.u.
	Achieved residual activity (compared to chemiluminescence signal of 124 a.u.)	76.70	%
	Equivalent amount of herbicides present	4.05	nM

The two 'equivalent amounts of herbicides present' are then used to calculate the matrix effect on the interaction of herbicides with the immobilised thylakoids.

added 5 nM			
	Herbicide concentration (known added+ calculated native)	5.66	nM
	Expected residual activity due to 5.66 nM (compared to chemiluminescence signal of 124 a.u.)	72.70	%
	Recovery (comparison of expected vs achieved residual activity)	105.45	%
	Effected matrix change	**5.45**	**%**

Therefore it has been calculated that the water sample matrix causes an over-reporting of the amount of herbicides present by 5.45%.

6.6.3.2.5 Calculating the fully adjusted and calibrated value of herbicides in river water samples

Finally, calculation iii. takes place on the original water sample with the unknown amount of herbicides.

added 0 nM			
Calculation iii.	Chemiluminescence signal by which calculation ii. result is over-reported	6.15	a.u.
	True chemiluminescence signal	106.72	a.u.
	Equivalent amount of herbicides present	**1.45**	**nM**
	Amount of herbicide found by standard methods	**1.78**	**nM**

Water sample 1 was found to have 1.45 nM of a mixture of herbicides. As the amount of herbicides in each river water sample has been provided following the use of standard laboratory methods (Table 6.3), it is possible to compare these with the values obtained following the calibration calculations. As it can be seen, there is a deviation of the calculated herbicides concentration from the one obtained with the standard methods.

For water sample 2, the equivalent amount of herbicides present was calculated to be 0 nM (Appendix VII), which is very close to 0.36 nM as measured with standard methods, which is a value below the lower LOD of the fluidic sensor.

Unfortunately, the process devised of accounting for a multitude of the effects a real water sample matrix can have on the bioassay presented here cannot be compared with similar methods that may have been used for other sensors for the measurement of photosynthesis-inhibiting herbicides, as none have been reported. In published research [6; 48], it is suggested that using real water as a replacement of the carrier buffer: "surprisingly, …, caused a PSII activation. In all tested samples, an activation in the range of 14 - 21% was found". No further work is reported on attempting to detect herbicides in the real water samples.

It will be important to optimise the process of quantifying the environmental water sample effect on each relevant part of the herbicide detection assay and use other scientific methods to ensure the robustness of the method described here by cross-validation. This is very important as the highest concentration of H_2O_2 that can be produced by the thylakoid-coated beads is relatively low compared to the concentrations of H_2O_2 that can be found in water samples. Although the optical detector can detect comfortably and quantitatively reductions to the thylakoids-produced H_2O_2 due to herbicides in samples, when the said sample also contains 'background' H_2O_2 signals that can be significantly higher than the true signal, the possibility for error is high. What is more, the matrix effect on the detection of H_2O_2 that could have otherwise been classed as less significant, is now of great importance as a small percentile change in the background signal, could be as big as the true signal itself.

A caveat should be added on the interpretation and validity of the methodology presented here. There are three occasions during which, based on a proportional difference in the residual activity, i.e. the chemiluminescence signal obtained compared to the blank, an equivalence is calculated of the possible amount of herbicide present in the water sample. This was done a) following

calculation ii. of the water sample with no added herbicides, b) following calculation ii. of the water sample with known added herbicide, and finally, c) following calculation iii. of the original water sample with the unknown amount of herbicides. On each occasion, the chemiluminescence signal (reported as a percentile reduction compared to the 100% of the signal when a blank is used) is compared to the calibration curve signal, and a concentration of herbicide is deduced, by looking at the responding concentration on the curve. However, this method of estimating the amount of herbicide present in the sample would only be appropriate if the relationship between amount of herbicide and the resulting reduction in chemiluminescence signal was linear. Therefore, by employing this method of estimating the amount of herbicide present, it is assumed that the relationship is linear, as the exact equation of the relationship is unknown.

6.7 Reuse, regenerability and stability of the fluidic sensor unit for the detection of herbicides using immobilised thylakoids and HRP on magnetic beads

6.7.1 Introduction

An aim of the work presented in the thesis is to develop a fluidic sensor unit for the detection of specific classes of herbicides. This has been achieved as presented and discussed in Section 6.5. A crucial detail of the aims however, which adds substantially to the novelty of the work, is the use of mobile support for the key substrates and biological material of the two-stage bioassay developed. This has been achieved by using magnetic beads on which HRP and thylakoids have been immobilised. The importance of using the magnetic beads is due to the fact that the fluidic sensor can thus be reused and regenerated, as the beads' handling, namely introduction into the sensor, use and finally discardation can be easily repeated. As the HRP acts as a mediator of the chemiluminescence reaction of luminol with H_2O_2, it is reusable. The literature provides information on the ability to remove bound photosynthesis-inhibiting herbicides from thylakoids, thus allowing for the thylakoids' reuse. The

repeated use of the two types of magnetic beads with immobilised HRP and thylakoids, as well as details of the sensor's regenerability process by the replacement of the beads was investigated further, with results presented in this section. What is more, storage stability studies of some of the components of the fluidic bioassay are presented.

6.7.2 Materials and methods

Chemicals, detection and fluidics apparati and other materials and their use with the fluidic sensor unit, as well as the setup and assay method and steps were as previously described in Section 6.5.2, when measuring herbicides and as described in Section 5.4.2 when measuring H_2O_2. A crucial difference for the reuse studies is the retainment of the magnetic beads after a measurement, either of H_2O_2 or herbicides. For the storage stability studies, the standard fluidic bioassay for the detection of herbicides was performed, with various components having been stored in room temperature of 16℃, a fridge at 4℃, and in freezer at -20℃.

6.7.3 Results and discussion

The ability to reuse the magnetic beads with immobilised HRP and thylakoids was tested, as well as the stability of the magnetic beads when stored, over time.

6.7.3.1 Reuse of HRP-coated beads for the H_2O_2 detection fluidic bioassay

Firstly, the standard fluidic bioassay for the detection of H_2O_2 was performed, with the HRP-coated magnetic beads in the fluidic sensor. The magnetic beads were not removed from the active region A where they were magnetically entrapped during their use for the detection of H_2O_2 after a single measurement, but, following the H_2O_2-containing sample's removal from the fluidic channel, they were used repeatedly for the detection of further H_2O_2-containing samples of the same concentration. Another set of measurements made involved the repeated flow of samples containing no H_2O_2, apart from a 'final' sample

containing H_2O_2 and thus producing a chemiluminescence signal. The results of using the same HRP-coated magnetic beads for a multitude of continuous measurements of 2 µM concentration of H_2O_2 in different samples (series 2 in Figure 6.24), as well as with continuous measurements of no H_2O_2 in different samples apart from the last sample (series 1), can be seen in Figure 6.24.

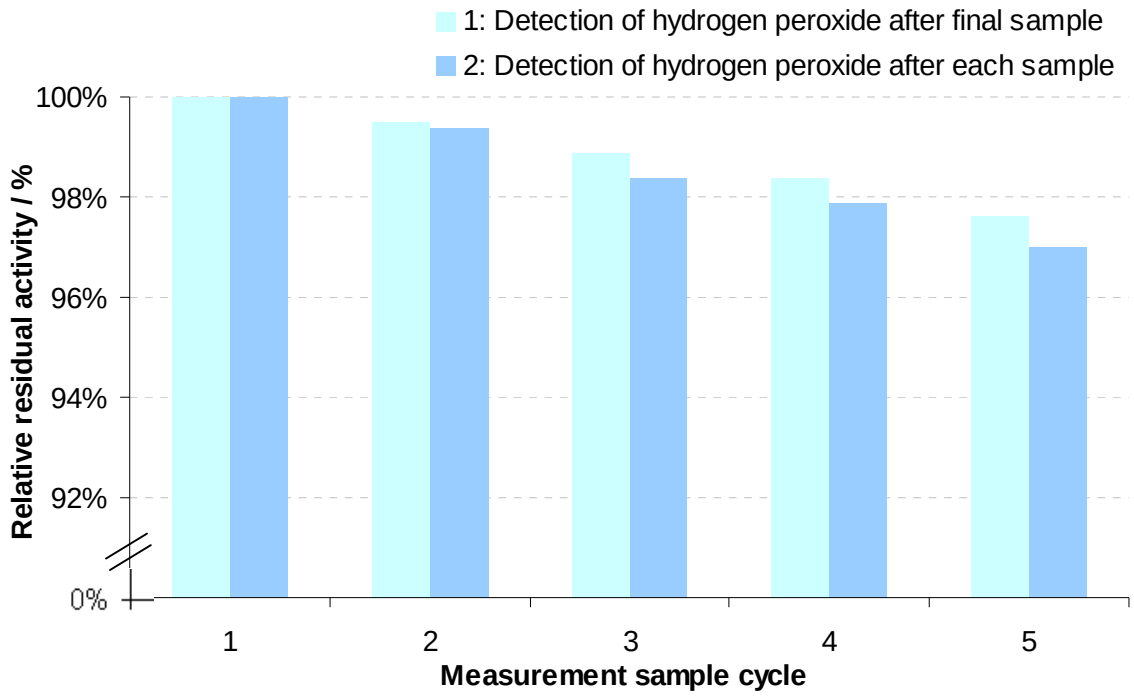

Figure 6.24 Reuse of HRP-coated beads for repeated H_2O_2 detection, with H_2O_2 present in every or specific samples.

As it can be seen from the results, the same 0.25 mg of HRP-coated beads can be reused for a number of repeated measurements of 2 µM H_2O_2 found in a sample; there is, however, a decline in the chemiluminescence signal obtained. Also, a reduction of the chemiluminescence signal expected for the H_2O_2 sample was still identified when only the last of a series of samples contained H_2O_2. By comparing the results of the two sets of experiments this reduction on the detection of H_2O_2 can be attributed to the following reasons: repeatedly flowing a sample with or without H_2O_2 through the channel (series 1) is itself an act that removes either HRP that becomes unbound from beads, or a number of HRP-coated beads themselves, while the rest of the reduction in

chemiluminescence signal as experienced when repeatedly measuring H_2O_2 in samples (series 2) is therefore attributed to a partial irreversible inactivation of the HRP on the beads due to its repeated use as the mediator in the chemiluminescence reaction of luminol and HRP.

It is therefore expected that the HRP-coated beads could be reused for a number of measurements, particularly as the concentration of H_2O_2 produced by the thylakoids, in the absence of herbicides, is relatively low (approximately 620 nM), thus, it would be expected that the irreversible inactivation of HRP (as depicted by series 2) as well as the loss of HRP (as depicted by series 1) would be having a lesser effect when detecting the thylakoid-produced H_2O_2, which would be expected to be even lower if herbicides are present, than with a higher concentration of H_2O_2 that was used in these measurements (2 µM). This study has not been performed as part of the present body of work.

6.7.3.2 Reuse of thylakoids-coated beads for the herbicide detection fluidic bioassay

6.7.3.2.1 Non-photosynthesis-inhibiting herbicides

Following a single measurement of $1x10^{-6}$ M of 2,4-D, of $1x10^{-6}$ M paraquat and of $1x10^{-6}$ M acifluorfen, the thylakoid-coated beads were then tested without a herbicide sample, but only in order to identify the amount of H_2O_2 that can still be produced following the illumination step, i.e. the baseline signal, following the removal of the herbicides. From the results presented in Figure 6.25, by comparing the baseline H_2O_2 production of thylakoids before and after the use of the specific herbicides, it can be seen that paraquat and acifluorfen, due to their method of action and effect on the thylakoids already presented in Section 6.5.3.2, cause a great reduction of the ability of the thylakoids immobilised on the beads to further produce H_2O_2. This is inline with a similar study found in the literature [174], where, following the use of DNOC, a herbicide that belongs to the same family with acifluorfen, damage inflicted on isolated, immobilised photosynthetic material is irreversible. More specifically, the authors report that,

following the rinsing of the biosensor in order to remove DNOC, the signal measured decreased "far below the reference level suggesting that the membrane has been damaged due to the uncoupling effect".

2,4-D has almost no effect, which suggests that the effect of 2,4-D on the thylakoids, as noted in Section 6.5.3.2 and earlier in Section 4.4.3.4, is temporary and does not result due to some partially irreversible binding of the herbicide onto the thylakoids. However, as already mentioned in Section 4.4.3.4, no further insight into the possible cause of the reduction in thylakoid activity due to 2,4-D can be gained from the literature.

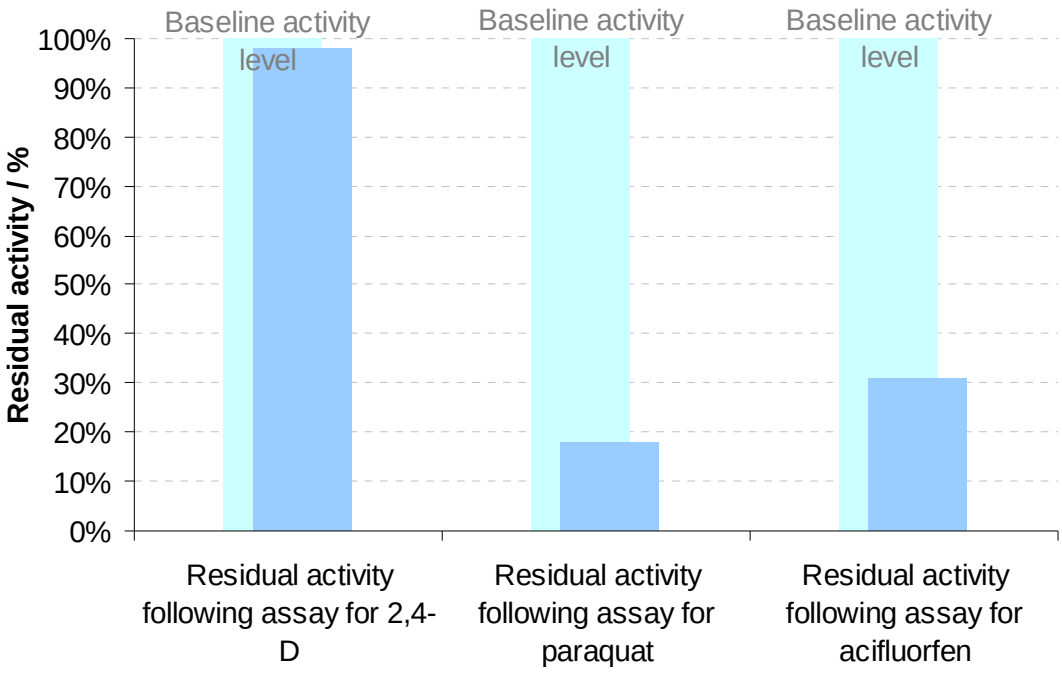

Figure 6.25 Effect on residual ability of immobilised thylakoids on beads to produce H_2O_2 following an incubation and illumination with sample of non-photosynthesis-inhibiting herbicides.

6.7.3.2.2 Photosynthesis-inhibiting herbicides

Sets of measurements similar to those presented in the study of the HRP-coated beads (Section 6.7.3.1) were made for the step of the illumination of thylakoid-coated beads, as well as the step of the inhibition of their ability to

produce H_2O_2 by photosynthesis-inhibiting herbicides. In all of the following experiments, HRP-coated magnetic beads were magnetically entrapped in active region A of the fluidic channel, therefore adding to the decrease in residual activity of the herbicide detection bioassay. This added decrease has not been explicitly accounted for and removed in the results presented here forth.

Firstly, with thylakoid-coated magnetic beads magnetically trapped in active region B of the fluidic channel, samples containing no herbicides were repeatedly flown through the channel, without illuminating any of the samples apart from the last one in a series of samples (series 1 in Figure 6.26). As it can be seen, the maximum signal achieved by the thylakoids following one illumination step but after many assay cycles is reduced. This is probably due to either the dislocation of thylakoids from the magnetic beads, or the removal of some magnetic beads from their entrapment region. It should be noted that the residual activity (95.1% after five cycles) is less than that of a similar measurement performed on the H_2O_2 detection by HRP-coated beads, as presented by series 1 in Figure 6.24 (97.6% after five cycles), suggesting that perhaps the immobilisation of the thylakoids on beads is weaker than the immobilisation of HRP.

Secondly, with thylakoid-coated magnetic beads magnetically trapped in active region B of the fluidic channel, samples containing no herbicides were repeatedly flown through the channel, with an illumination step taking place following each of the samples (series 2 in Figure 6.26). As it can be seen, the maximum signal achieved by the thylakoids following each illumination step after each assay cycle is reduced. This is due to the possible reasons for the reduction in residual activity identified in series 1, as well as due to another reason; as, each time, the signal achieved following the same number of assay cycles is lower for series 2 than for series 1, it is suggested that the illumination of thylakoids, and the associated production of H_2O_2, results in some irreversible inactivation of the thylakoids, accounting for the relative difference

between signals 1 and 2. This is supported by the literature, where it is suggested that repeated illumination of strong light causes not only photoinhibition but also irreversible photodamage in photosynthetic material [152].

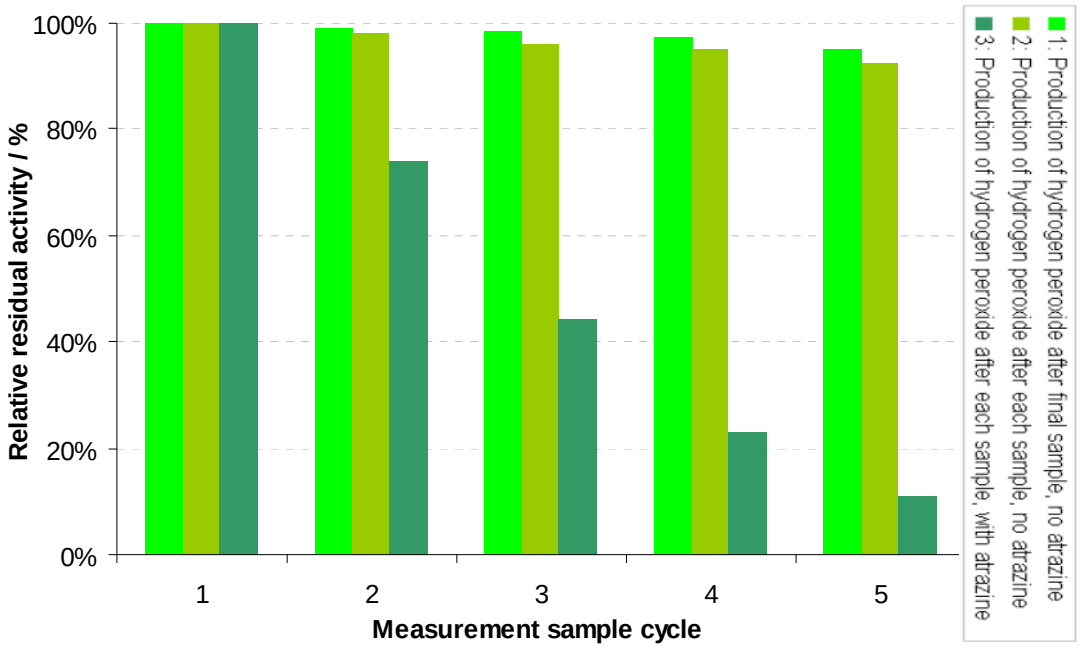

Figure 6.26 Effect of reuse on thylakoids immobilised on beads, with variation on number of assay cycles containing atrazine (5 nM).

Thirdly, the complete bioassay was performed with all necessary steps for the detection of herbicides: with thylakoid-coated beads entrapped in active region B, a sample containing atrazine ($5x10^{-9}$ M) was flown, incubated, and then illuminated. Following the removal of the herbicide-containing sample, another full assay cycle was performed, with a sample containing the same amount of atrazine, and with the same thylakoid-coated beads. This was repeated four times. As it can be seen from series 3 (Fig. 6.26), there is a reduction in the H_2O_2 production by the thylakoids compared to what would be expected for the specific amount of herbicide, i.e. compared to the signal achieved from the first cycle of this experiment. Series 3 is also lower than series 1 or 2, as the related reductions in residual activity found in signals 1 and 2 are essentially incorporated in series 3; the further reduction in series 3 is attributed to some irreversible binding of herbicides on the thylakoids or otherwise effected

irreversible inactivation of the thylakoids due to the herbicides. As it can be seen, following the first measurement of herbicides in a sample, only 74% of activity remains when a second sample of the same herbicide is assayed. That means that the amount of H_2O_2 produced following the second inhibition was 26% lower than that achieved following the first inhibition by the same amount of atrazine in the sample. Therefore, approximately 25% of the thylakoids' ability to be inhibited for a second time is lost. It should be noted that the atrazine concentration used is relatively low, and a different pattern of behaviour may have had emerged if a larger concentration had been used.

The literature provides results of similar studies performed on the reversibility of the inhibitory effect of herbicides following a measurement cycle. Biosensors with immobilised PSII measuring the effect of photosynthesis-inhibiting herbicides with electrochemical means can reportedly have their activity restored after one measurement by 70% [154], and by almost 100% [142]. The two examples do not mention however the concentration of herbicides assayed, which would be expected to have an effect on the reversibility. Another example of a biosensor with immobilised thylakoids measuring the effect of photosynthesis-inhibiting herbicides with electrochemical means can only have 60% of its initial activity restored after one measurement of a $1x10^{-6}$ sample of atrazine. This suggests that when using immobilised thylakoids the reversibility following a measurement of a herbicide sample appears to be achieved to a lesser degree than when using PSII. It should be noted however that none of the examples found in the literature are reporting detailed studies of the likely causes of the relative irreversibility.

The fact that the fluidic sensor presented here retains only a small percentage of its activity following a measurement of a herbicide sample, makes the inherent ability of the magnetic beads to be removed, following a measurement in order to be replaced by a different lot of beads, a key quality of the design and realisation of the method developed for the fluidic sensor.

6.7.3.3 Storage and stability studies

Prepared and stored magnetic beads with immobilised HRP and thylakoids were tested over time in order to identify the period of time over which they can be used adequately with the fluidic bioassay for the detection of herbicides but also H_2O_2, in the case of the HRP-coated beads.

When stored in room temperature (16℃), the HRP-coated beads performed close to their initial activity for the first two days, with even an increase in activity before a decrease, over 1 week, when measuring a 2 μM H_2O_2 sample (Fig. 6.27). The fact that the HRP used was of a high grade, stabilised form, may have attributed to its stability in room temperature. The thylakoid-coated beads however, declined rapidly in baseline activity, as measured by the amount of H_2O_2 produced following the incubation of a herbicide sample (10 nM atrazine), over the same period of time. According to the literature [142], the stability of photosynthetic material is increased at 16℃ compared to the standard 25℃, in which case the deterioration of the thylakoids would have been even greater. An important observation is that the RSD during the first three days for both lots of beads was around 4%, while by the point of the last three measurements it had risen to 8% for the HRP- and 10% for the thylakoid-coated beads. This appears to signify that, during the passage of time in the less favourable conditions offered by a temperature of 16℃, the stability of the immobilised material, or of the immobilisation itself of the material, was much reduced, leading to the normal variations experienced during the handling and use of the beads to be a cause of more deviation in the results from the average.

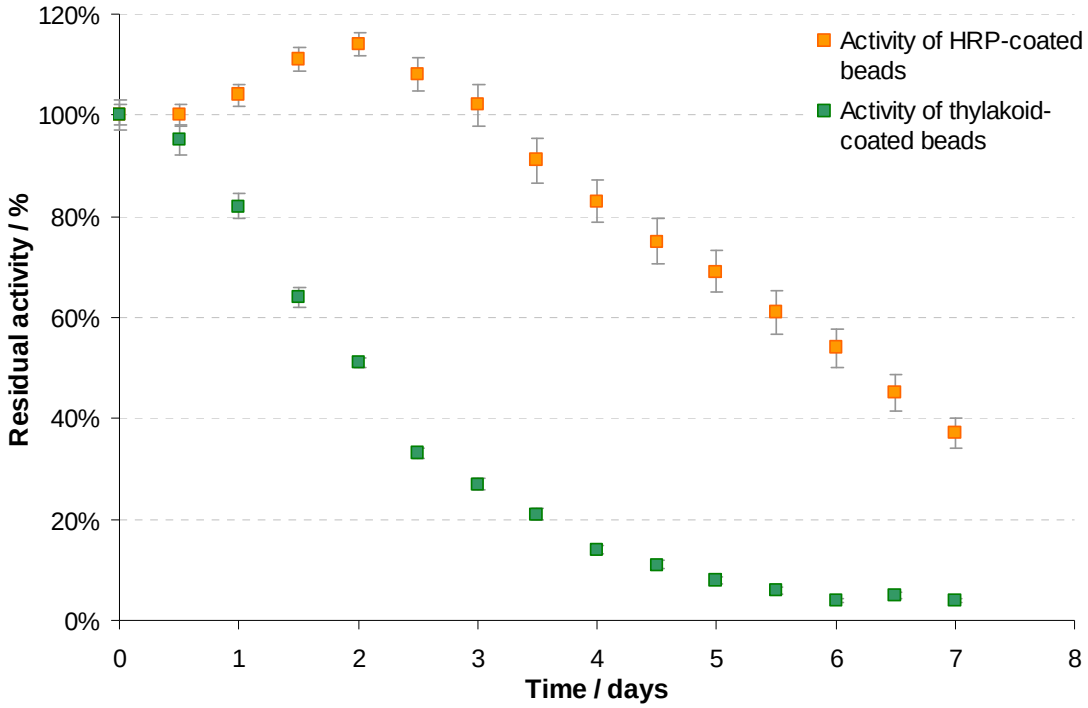

Figure 6.27 Activity of HRP- and thylakoid-coated beads remaining over 7 days stored in room temperature (16℃).

When stored in a fridge at 4℃, the stability of the HRP- and thylakoid-coated beads was longer, as measured by their residual activity, as it can be seen from Fig. 6.28, over 2 weeks. It is thus suggested that the HRP-coated beads are in a usable condition for seven days and the thylakoid-coated beads for three days, which is the point by which both lots of beads reach the point where 90% of activity is remaining. This is in accordance with work presented elsewhere [186], where the usability of immobilised HRP, after storage in a 4℃ environment, remains in similar levels for seven days.

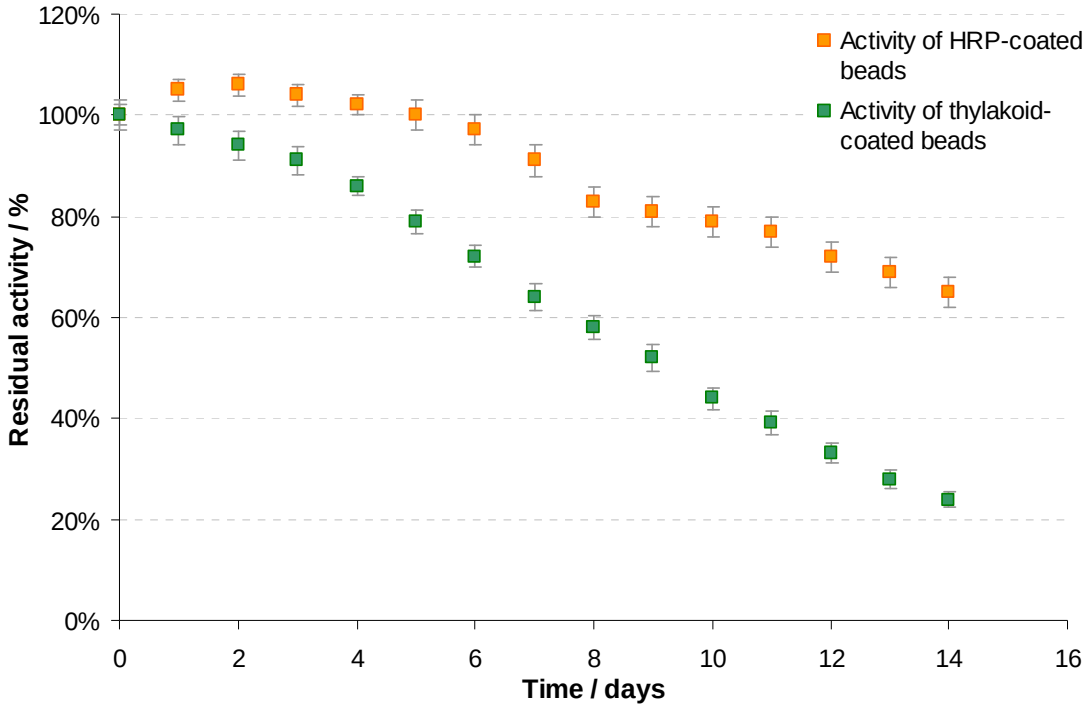

Figure 6.28 Activity of HRP- and thylakoid-coated beads remaining over 14 days stored in a fridge (4℃).

The stability and usability of the coated beads following storage in a -20℃ freezer was also studied. The results of using the two different beads following the storage in the freezer temperature can be seen in Figure 6.29. It was observed that, the HRP-coated beads retained 90% of their activity for 10 weeks at -20℃, while the thylakoid-coated beads had 72 % of their activity present after the same time period. This is similar to the activity found to be retained for immobilised thylakoids on an electrode surface, where approximately 75% was retained after 11 weeks of storage in a -20℃ environment.

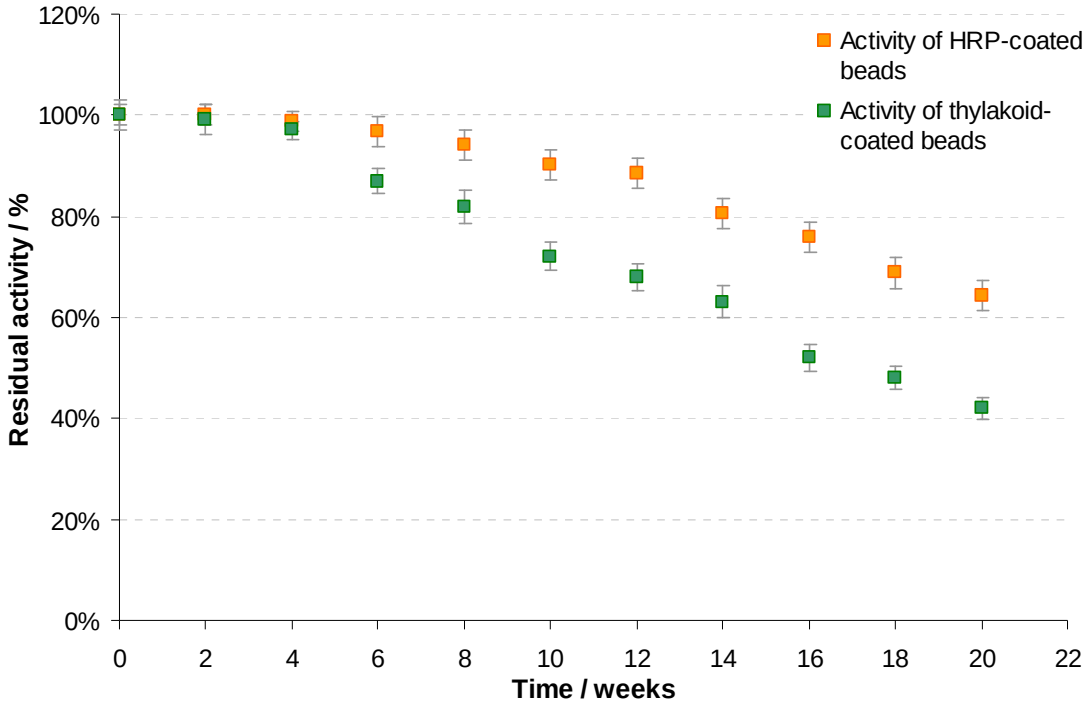

Figure 6.29 Activity of HRP- and thylakoid-coated beads remaining over 20 weeks stored in a freezer (-20℃).

Further studies would need to be performed with combinations of variably stored HRP- and thylakoid-coated beads, specifically when performing the detection of herbicides, in order to gain a fully characterised profile of the time restrictions of the use of the fluidic bioassay as a whole, importantly on the detection limits.

6.8 General discussion

Chapter 6 concluded the practical work performed for this PhD project; all experimental work presented in Chapters 3-5 forms a logical, natural continuum of the steps needed to achieve the final Objective and therefore reach all three Aims of the work.

In order to demonstrate a field-deployable fluidic bioassay for the detection of herbicides that has an inherent attribute to regenerate by using superparamagnetic beads as the immobilisation substrate on which the

biological element of the sensor is immobilised, thus allowing for its introduction, use and removal by using simple flow and magnetic controls, and having achieved many of the individual steps leading to this, as summarise at the Conclusions and Summaries of Chapters 3-5, the following sets of work were performed, as reported in Chapter 6:

- the immobilisation of thylakoids on magnetic beads

As a result of the optimisation of the immobilisation process by the project partner, beads were obtained with 0.3 µg of chlorophyll / mg of beads. When the isolated thylakoids immobilised on the beads were those obtained by using the isolation protocol 5, an increase in the amount of thylakoids immobilised on the beads (0.49 µg of chlorophyll / mg of beads) was achieved. This allowed for an increase in the chemiluminescence signal detected by the production of H_2O_2 by the immobilised thylakoids.

- the selection of an appropriate miniaturised light source

Thirty eight different LEDs were tested in order to identify the one that effected the highest H_2O_2 production, which was successful. Many of the spectral and illumination parameters of all LEDs were taken into consideration, but no highly statistically significant correlation was identified between the parameters and the H_2O_2 production.

- the optimisation of the herbicide detection fluidic assay's parameters

Having optimised and finalised the detection of H_2O_2 in the fluidic assay setup employing the use of the HRP-coated beads, as presented in Section 5.4.3.1, there was no need to optimise the luminol concentration in flow, the amount of beads with immobilised HRP in the H_2O_2 detection region of the fluidic channel, or of the sample volume and flow rate, at least not during the H_2O_2 detection step. Instead, the following aspects of the fluidic assay were optimised:

- the concentration of thylakoids immobilised on beads

Varying the amount of thylakoid-coated magnetic beads during their illumination, and hence H_2O_2 production, had a significant effect on the chemiluminescence signal intensity produced due to said H_2O_2. More specifically, increasing the amount of beads, resulted in an increase of the H_2O_2 production, and therefore chemiluminescence signal intensity. This was not noted for the entire range of the amounts of beads tested; entrapping, illuminating and then measuring the H_2O_2 produced by thylakoid-coated magnetic beads that had the equivalent of 1.25 µg of chlorophyll or more, resulted in very little increase of chemiluminescence signal intensity when compared to the near-linear increase for the lower increments. The only possible explanation for this is that the higher amounts of beads are too closely packed and possibly stacked on each other rather than spread in the designated circular region of the fluidic channel into a monolayer. Therefore, 0.25 mg of beads were identified as the optimal amount. The linear relationship between H_2O_2 production and the amount of thylakoids was established.

- the herbicide incubation time with the immobilised thylakoids

As expected following the results achieved with the batch assay, the incubation time that the herbicides are in contact with the immobilised thylakoids during the fluidic assay altered the inhibition level of the H_2O_2 production, and thus of the chemiluminescence signal that was used as the parameter to allow for the quantification of the herbicides. Increasing the incubation time of the herbicide sample with the thylakoid-coated beads between 0 and 3 minutes, resulted in an increased number of herbicide molecules interacting with the thylakoids by binding to the target site in the thylakoids' Photosystem II complexes, thus deactivating more of the H_2O_2 producing ability of the thylakoids. This was measured as a reduction in the chemiluminescence signal intensity detected, which is itself due to the reduced H_2O_2 production. It was also observed that an incubation period longer than 3 minutes did not result in significant further inhibition of the H_2O_2-producing ability, probably due to reduced interaction of the herbicide molecules with the thylakoids.

- the illumination time of the thylakoids

Increasing the time that the thylakoids in suspension are illuminated, resulted in an increase of the H_2O_2 production and hence chemiluminescence detection thereof. For illumination periods longer than six minutes however, the rate of increased H_2O_2 production per minute of longer illumination period is significantly reduced. A similar effect was observed with the thylakoids in suspension. The lower increase in chemiluminescence signal could possibly even be attributed to an increased diffusion of produced H_2O_2 from the thylakoids towards the sample plug. Therefore, the flow will need to be suspended for the illumination step to take place, for six minutes. It is also important to state that the signal obtained by illuminating the optimised amount of thylakoid-coated beads for the optimised time is equivalent to 620 nM of H_2O_2. This can be comfortably detected by the H_2O_2 detection step of the fluidic assay developed in Chapter 5.

- the implementation of the complete fluidic assay for the detection of herbicides

From the use of the complete fluidic bioassay for the detection of herbicides, the lower LODs achieved with the fluidic sensor fall close to the region of herbicides concentrations that are the highest permissible in EU to be found in drinking and other waters. More specifically however, the developed sensor did not achieve the detection of the concentration of any individual herbicide that corresponds to the upper limit of how much of a single herbicide is allowed to be found in drinking water in the EU (0.1 ppb or 0.1 µg/l) for any of the three photosynthesis-inhibiting herbicides tested, although the lower LODs achieved are very close to the target limits. What can also be observed from the two tables, is that the sensor can successfully detect concentrations of herbicides that equal 0.5 µg/l, which is the highest permissible amount of total pesticides to be found in drinking water.

The LODs achieved compare very comfortably with those of electrochemical sensors with immobilised photosynthetic material:

	Ref. 136	Ref. 242	Ref. 132	Ref. 130
Atrazine (M)	2.5×10^{-9}	$2.0x10^{-9}$	$2.0x10^{-9}$	$1.3x10^{-8}$
Diuron (M)	1.8×10^{-9}	$5.0x10^{-10}$	$5.0x10^{-10}$	$1.5x10^{-8}$

Although for atrazine, diuron and their combination, full inhibition of the H_2O_2 production was observed, with propanil, the inhibitory effect of propanil on the production of H_2O_2 by thylakoids appears to be reduced with higher concentrations, which is actually due to propanil's different mode of action depending on its applied concentration. The RSD for the detection of herbicides was 3.1%, which is much lower compared to the RSD of 5.7% achieved with the batch assay.

- the testing of the complete assay with real water samples

In order to further characterise the developed assay for the detection of herbicides, and to investigate the calibration needs of a future instrument based on the fluidic sensor, the sample plug containing known concentrations of herbicides and luminol in buffer was replaced by water samples collected from the environment. Identifying and quantifying these effects was achieved due to the fact that the fluidic sensor has been designed to employ two separate "active" regions and for the herbicide detection assay to be performed in two distinct, independent stages. The real water matrix did have an effect on the detection of the herbicides present in the water sample, which varied depending on the water sample source, and the stage of the assay. It is important that such a detailed account of the different effects the matrix can have has been devised and taken into consideration, as that would be essential for the use of the sensor in a field-deployed situation.

- studies of beads' reuse and stability

The repeated use of the two types of magnetic beads with immobilised HRP and thylakoids, as well as details of the sensor's regenerability process by the replacement of the beads was investigated further; HRP-coated beads could be reused for at least 5 times with 90% of their activity retained. The fact that the thylakoid-coated beads retain only a small percentage of their activity following a measurement of a herbicide sample, makes the inherent ability of the magnetic beads to be removed, following a measurement in order to be replaced by a different lot of beads, a key quality of the design and realisation of the method developed for the fluidic sensor.

Storage stability studies of the magnetic beads were performed, and although HRP-coated beads could be considered in a state that allowed for their use for a week at 4℃, the thylakoid-coated beads would require storage at lower temperatures. This was already expected, due to similar studies performed with thylakoids immobilised for their use with electrochemical sensors.

Chapter 7: Final discussion, conclusions and future work

7.1 Final Discussion

The four experimental chapters (Chapters 3, 4, 5 and 6) report work that was carried out sequentially and was interdependent. Each chapter has been given a final section called "General discussion", as, for all results presented in each chapter, it was necessary to critically review the findings and implications for subsequent work, in order to progress to the next chapter. Therefore, this section will briefly summarise the general discussions of each experimental chapter, and the relationship each area of work has on the conclusion of this PhD work.

7.1.1 Establishment of a standard bench-top batch assay for the detection of H_2O_2

The chosen standard chemiluminescence assay for the detection of H_2O_2 was established by optimising the concentrations of the reagents (luminol and HRP), as well as other parameters such as the detector's voltage gain, for the most sensitive detection of H_2O_2. The observed LLOD of $9.0x10^{-8}$ agrees with published literature for similar batch assays.

Elements of the actual measurement process were optimised or standardised, such as establishing a specific method for the length of time between activation of the spectrometer's software and introduction of the sample in the cuvette, and the manual nature of the introduction of the sample into a cuvette (pipetting angle). It was important to standardise these as early as possible, as the work performed for the establishment of the standard chemiluminescence batch assay for the detection of H_2O_2 will form the basis of consequently researching the chemiluminescence detection of the probable production of H_2O_2 by photosynthetic material, and inhibition thereof by certain classes of herbicides.

7.1.2 Establishment of the production of H_2O_2 from photosynthetic material

The focus was then placed on attempting to substitute the source of H_2O_2 from standard, known concentrations, to being a product of the illumination of isolated photosynthetic material.

Following the fruitless investigation into obtaining detectable H_2O_2 from isolated chloroplasts following illumination, sub-chloroplastic organelles, the thylakoids, were used with the same aim. It had already been ascertained by various experiments that the inability to detect any produced H_2O_2 by chloroplasts was not due to the unsuitability of the H_2O_2 detection step (chemiluminescence reaction), but due to the chloroplasts' preparations having a catalase-like active compound that scavenges any produced H_2O_2, if there is any produced.

All different thylakoid preparations isolated, produced H_2O_2 following their illumination, that could be detected and measured with the standard chemiluminescence H_2O_2 assay. The H_2O_2 production was affected by a variety of parameters of the illumination step (intensity, wavelength, length of time), the suspension medium (buffer) and the experimental method (pipette tips holding the thylakoids during illumination) used. Thus, the said H_2O_2 production was optimised for these and more parameters in order to achieve the highest yields.

Amongst other findings discussed in more detail in the General Discussion of Chapter 4, it was found that the production of H_2O_2 increased with the time of illumination, for all five preparations. As chemiluminescence signals reporting the produced H_2O_2 increased with the longer illumination times, there were clear differences in the ability of the different thylakoid preparations to produce detectable H_2O_2. This was partly due to the optical density of the thylakoid samples, which, following illumination, were then introduced in the standard HRP-mediated chemiluminescence reaction, which was affected by the absorbance of the chemiluminescence light by the thylakoids. However, for each thylakoid preparation the dilution (reported as chlorophyll concentration) at

which they produced the most H_2O_2 while keeping all other experimental variables had been identified, thus making the dilutions and comparison of the different thylakoid preparations based on H_2O_2 production yields. What is more, illumination longer than 10 min appeared to significantly limit the rate of H_2O_2 production.

Illuminating all five different thylakoid preparations with spectrum- (and intensity) filtered variations of the same light source provided a fascinating account of the behaviour of thylakoids as a whole depending on the illumination wavelength changes, but also between the different preparations. The results showed the effect the different spectral distributions have on the production of H_2O_2. An expectation for the H_2O_2 production to vary accordingly only to the light intensity was not met, as photosynthesis is affected by the differences in wavelengths as well.

All five different isolated thylakoid preparations were used in the next set of experiments, as a definitive conclusion on whether good overall characteristics on the H_2O_2 production step would also be translated in the lowest LOD for herbicides, could not be reached.

7.1.3 Establishment of the chemiluminescence bench-top batch assay for the detection of photosynthesis-inhibiting herbicides

Incubating all five different thylakoid preparations with increasing concentrations of photosynthesis-inhibiting herbicides did result in clear, correlated reduction of the chemiluminescence signal, which therefore suggests also a correlated reduction of the H_2O_2 production by thylakoids during an illumination step following the incubation step. For all three photosynthesis-inhibiting herbicides, thylakoid preparation Ch5 resulted in the lowest LODs of all five preparations; this suggests that Ch5's seemingly higher proportion of thylakoids that produce a lot of H_2O_2, while containing the least thylakoids overall, did also result in the ability of less herbicide molecules to effect a reduction in their H_2O_2 production. The lower LODs achieved (atrazine: $6.0x10^{-09}$, diuron: $8.0x10^{-08}$, propanil:

$1.4x10^{-07}$) are not sufficiently low to meet the E.U. limits of maximum permissible concentrations of herbicides in waters.

The confidence in the presence of this relationship was increased due to a variety of measurements that were performed with the herbicides, the thylakoids and the chemiluminescence reagents and standard chemiluminescence H_2O_2 assay using different variables of presence or absence of any of the steps (incubation, illumination, chemiluminescence reaction) and of any of the participating components (herbicides, thylakoids, luminol, HRP) in order to identify any unwanted effects.

For non-photosynthesis-inhibiting herbicides, the batch assay gave a variable response, due to the means of action of the herbicides chosen.

7.1.4 Establishment of the chemiluminescence fluidic assay for H_2O_2

Following the development of a set of principles of design and operational mode, the flow sensor unit was designed and fabricated. The aim to demonstrate the potential of the final developed fluidic assay in aiding the reuse and regenerability of the sensor was taken into account; thus, it was decided to employ superparamagnetic beads as the immobilisation support for the biological elements of the bioassay, which would need to be easily and automatically replaced in a field deployment.

HRP was immobilised on superparamagnetic beads, which was thoroughly optimised in order to achieve the highest possible amount of active HRP on the beads (2.1 purpurogallin units per 1 mg of beads).

The fluidic assay for the detection of H_2O_2 using the developed unit and the optimised HRP-coated magnetic beads was itself then optimised in order to yield for the lowest detectable amount of hydrogen peroxide, as well as other desired chemiluminescence signal characteristics.

The optimised fluidic unit was then used as part of a fluidic sensor for the chemiluminescence detection of H_2O_2, utilising magnetic beads as the immobilisation support material for HRP. The lower LOD for H_2O_2 was $1.07x10^{-7}$ M (107 nM) H_2O_2.

7.1.5 Establishment of the chemiluminescence fluidic assay for the detection photosynthesis-inhibiting herbicides

The immobilisation of thylakoids on magnetic beads was performed by an E.U. project partner.

An appropriate miniaturised light source was selected, by testing thirty eight different LEDs which gave very different results, in order to identify the one that effected the highest H_2O_2 production.

Parameters of the herbicide detection fluidic assay were optimised, in order to allow for the detection of the lowest possible concentrations; these were the concentration of thylakoids immobilised on beads, the herbicide incubation time with the immobilised thylakoids and the illumination time of the thylakoids.

7.1.6 Implementation of the complete fluidic assay for the detection of herbicides

From the use of the complete fluidic bioassay for the detection of herbicides, the lower LODs achieved with the fluidic sensor fall close to the region of herbicides concentrations that are the highest permissible in EU to be found in drinking and other waters. More specifically however, the developed sensor did not achieve the detection of the concentration of an individual herbicide that corresponds to the upper limit of how much of a single herbicide is allowed to be found in drinking water in the EU (0.1 ppb or 0.1 μg/l) for any of the three photosynthesis-inhibiting herbicides tested, although the lower LODs achieved are very close to the target limits. The assay was successful in detecting

concentrations of herbicides that equal 0.5 µg/l, which is the highest permissible amount of total pesticides to be found in drinking water.

To conclude the work, testing of the complete assay with real water samples as well as studies of beads' reuse and stability were performed, which gave promising results about the ability to accurately measure the effect of the water's matrix, as well as the ability to store the HRP- and thylakoid- coated beads for later use.

7.2 Summary and conclusions

The following conclusions are made for the achievement of the project Aims:

- A bioassay that is potentially field-deployable and addresses issues of reuse and regenerability in a remote working environment has been developed and demonstrated, by using superparamagnetic beads as the support on which the expendible bio-recognition element is immobilised.
- This was demonstrated for a bioassay for the detection of photosynthesis-inhibiting herbicides by measuring their effect on photosynthetic material derived from plant cells.
- Thus, a bioassay platform for the detection of trace organic pollutants in water samples, that can be deployed/used in the field, in order to also meet the commercial / regulatory requirements, has been developed.

To achieve the Aims, the following can be concluded on meeting the project Objectives:

- The production and detection of H_2O_2 from isolated illuminated photosynthetic plant material was demonstrated.
- The concentration-dependent inhibition of production of H_2O_2 from isolated illuminated photosynthetic plant material, by photosynthesis-inhibiting herbicides was demonstrated.
- A fluidic sensor unit that can be reused and regenerated by employing the use of superparamagnetic beads to act as the immobilisation support for the

bio-recognition element of the bioassay, allowing for the repeated introduction, use and discardation of the bio-recognition element was developed.

- A fluidic assay using the principle of the superparamagnetic bead immobilisation, by immobilising HRP on beads that were used for detection of H_2O_2 using the HRP-mediated luminol chemiluminescence reaction with H_2O_2 was demonstrated.
- The herbicide detection batch assay was successfully transferred into the demonstrated fluidic format, thus demonstrating a fluidic assay for the detection of herbicides that can be reused and regenerated and therefore allowing for its subsequent development into a field-based system.

Finally,

- The work was performed within the objectives of the funding E.U. project, by contributing to the successful completion of the E.U. project.

The work performed has achieved to demonstrate the additional novelty parameters:

- Second reported demonstration of light induced production of H_2O_2 by thylakoid preparations with the detection of H_2O_2 by HRP mediated chemiluminescence – thus confirming a controversial first experiment.
- First reported demonstration of concentration-dependent herbicide inhibition of light induced production of H_2O_2 by thylakoid preparations with the detection of H_2O_2 by HRP-mediated luminol chemiluminescence.
- First use of superparamagnetic beads with immobilised photosynthetic material enabling regenerability for their use within a fluidic assay for the detection of herbicides.
- First demonstration of analytically undesirable effects of a range of non-photosynthesis-inhibiting herbicides on an assay for the detection of photosynthesis-inhibiting herbicides.

7.3 Future work

7.3.1 Immediate future work – improvement of the demonstrated sensor

In order to achieve better performance out of the current developed work, the following routes could be followed.

In order to achieve better lower LODs for the detection of herbicides, specifically, to achieve the detection of the maximum allowed concentration set by the E.U., the avalanche photodiode used to detect the light produced by the chemiluminescence reaction could easily be substituted by a photo-multiplier tube. This step alone is estimated to allow for 2 orders of magnitude lower concentrations of hydrogen peroxide being detected, while also increasing the sensitivity, which is more relevant, as the herbicides of interest have an inhibitory effect on the chemiluminescence signal [81; 112].

In order to achieve better reproducibility, an automated system for the sequential introduction of all the reagents and beads should be employed, thus removing the element of human error introduced due to the less-than-perfect ability to control the fluidic aspects of each measurement.

Better regenerability could be achieved by using computer-controlled microelectromagnets for the magnetic entrapment of the thylakoid- and HRP-coated beads.

A wider range of real samples could be tested, in order to build a more comprehensive profile of the matrix effect of such samples, and to further test the devised calibration calculations. Similarly, a wider range of herbicides, whether photosynthesis-inhibiting or not, as well as other pesticides and organic pollutants can be tested.

7.3.2 Longer-term future work – towards a field-based / commercial instrument

The work presented here has taken into consideration the need to carefully approach several characteristics of a sensor, such as sensitivity, stability and reliability, while possible improvements on the sensor's performance on these characteristics have been suggested in the shorter-term future work.

On the other hand, little can be done to make the developed sensor less specific and therefore able to detect a wider range of pollutants. It is also not envisaged to be able to make the sensor more specific, as a wide range of pollutants can have an effect on the biological material used in the assay, the thylakoids. These range from heavy metals to other herbicides and pesticides. The effect many of the non-target molecules have on the thylakoids can be either similar to the inhibition of the H_2O_2 production, or the exact opposite.

Overall, the main body of the future work ought to focus on the transfer of the successful fluidic assay, from a setup where the fluidic sensor unit is used with external, large, support technologies, to a fully-automated fluidic sensor system. This requires considerable amount of work, and expertise in a wide range of the sciences and engineering; it is also the stage at which many (bio)sensors fail to perform as required.

References

1. Langford, T. E. L. (1990), *Ecological effects of thermal discharges,* Elsevier Applied Science.

2. Cole, S., Codling, I. D., Parr, W. and Zabel, T. (1999), Guidelines for managing water quality impacts within UK European marine sites, , UK Marine SAC Project, Wiltshire, UK.

3. European Commission (2000), "European inventory of existing commercial chemicals substances plus; EINECSPlus", *EINECS plus,* [Online], vol. 146A, available at: http://ecb.jrc.it/esis/index.php?PGM=ein.

4. Stenersen, J. (2004), *Chemical pesticides : mode of action and toxicology,* CRC, Boca Raton ; London.

5. Guzzella, L. and Pozzoni, F. (2006), "The Problem of Herbicide Water Monitoring in Europe", in Giardi, M. T. and Piletska, E. V. (eds.) *Biotechnological applications of photosynthetic proteins : biochips, biosensors and biodevices,* Landes Bioscience/Eurekah.com; Springer Science+Business Media, Georgetown, Tex.; New York, N.Y., pp. 73.

6. Rizzuto, M., Polcaro, C., Desiderio, C., Koblizek, M., Pilloton, R. and Giardi, M. T. (2000), "Herbicide monitoring in surface water samples with a Photosystem II based biosensor", *Proceedings of the Second Workshop on Chemical Sensors and Biosensors,* , pp. 346-357.

7. Tadeo, J. (2008), *Analysis of pesticides in food and environmental samples,* CRC; Taylor & Francis distributor, Boca Raton, Fla.; London.

8. Giardi, M. T., Koblízek, M. and Masojídek, J. (2001), "Photosystem II-based biosensors for the detection of pollutants", *Biosensors and Bioelectronics,* vol. 16, no. 9-12, pp. 1027-1033.

9. Koblížek, M., Malý, J., Masojídek, J., Komenda, J., Kučera, T., Giardi, M. T., Mattoo, A. K. and Pilloton, R. (2002), "A biosensor for the detection of triazine and phenylurea herbicides designed using Photosystem II coupled to a screen-printed electrode", *Biotechnology and Bioengineering,* vol. 78, no. 1, pp. 110-116.

10. Tadeo, J. L., Sánchez-Brunete, C. and González, L. (2008), "Pesticides: Classification and Properties", in Tadeo, J. L. (ed.) *Analysis of pesticides in food and environmental samples,* CRC; Taylor & Francis distributor, Boca Raton, Fla.; London, pp. 2.

11. Bjarnason, B., Bousios, N., Eremin, S. and Johansson, G. (1997), "Flow injection enzyme immunoassay of atrazine herbicide in water", *Analytica Chimica Acta,* vol. 347, no. 1-2, pp. 111-120.

12. McHillis, J. C., Rippey, B. and Fitzgerald, S. P. (2001), "Response of an enhanced chemiluminescence assay to selected substances", in Case, J. F., Herring, P. J., Robison, B. H., et al (eds.), *Proceedings of the 11th International Symposium on Bioluminescence & Chemiluminescence,* 2001, California, USA, World Scientific Publishing Co. Pte. Ltd, Singapore, pp. 323.

13. The European Commission (2002)*, Assembly and application of photosystem ii-based biosensors for large scale environmental screening of specific herbicides and heavy metals*, available at: http://cordis.europa.eu/fp5/home.html (accessed August/27).

14. Patel, P. D. (2002), "(Bio)sensors for measurement of analytes implicated in food safety: A review", *TrAC - Trends in Analytical Chemistry,* vol. 21, no. 2, pp. 96-115.

15. Neuman, M. R. (1995), "Biomedical sensors", *The Biomedical Engineering Handbook,* , pp. 725-727.

16. Smith, R. L., Gonzalez, C., Hsueh, Y. -., Kamita, G., Firrao, G. and Collin, S. D. (2001), "Photonic microinstruments for biomolecular sensing and analysis", Vol. 1, pp. 390.

17. Chaplin, M. F. (2000), "Biosensors", in Walker, J. M. and Rapley, R. (eds.) *Molecular Biology and Biotechnology,* 4th ed, Royal Society of Chemistry, Cambridge, pp. 521-554.

18. Sharpe, M. (2003), "It's a bug's life: Biosensors for environmental monitoring", *Journal of Environmental Monitoring,* vol. 5, no. 6, pp. 109N-113N.

19. Pietro, W. J. (1992), "Biosensors", *Kirk-Othmer Encyclopedia of Chemical Tehcnology, 4th Edn.,* vol. 4, pp. 208-221.

20. Davis, J., Vaughan, D. H. and Cardosi, M. F. (1995), "Elements of biosensor construction", *Enzyme and Microbial Technology,* vol. 17, no. 12, pp. 1030-1035.

21. Brazel, C. S. (2002), "Biomedical sensing", in Schwartz, M. (ed.) *Encyclopedia of smart materials,* 1st ed, Wiley, Chichester, pp. 21.

22. Trabelsi, H., Bouabdallah, S., Bouzouita, K. and Safta, F. (2002), "Review of the use of biosensors as analytical tools in the food and drink industries", *Food Chemistry,* vol. 77, no. 2, pp. 237-256.

23. Schuetz, A. J., Winklmair, M., Weller, M. G. and Niessner, R. (1999), "Multianalyte detection with an affinity sensor array", in Roda, A., Pazzagli, M., Kricka, L. J., et al (eds.), *Bioluminescence and Chemiluminescence: Perspectives for the 21th Century,* Septemer 1998, Bologna, John Wiley, Chichester, pp. 67.

24. Brinkley, M. (1993), "A brief survey of methods for preparing protein conjugates with dyes, haptens, and cross-linking reagents", *Perspectives in Bioconjugate Chemistry,* , pp. 59-70.

25. Székács, A., Trummer, N., Adányi, N., Váradi, M. and Szendro, I. (2003), "Development of a non-labeled immunosensor for the herbicide trifluralin via

optical waveguide lightmode spectroscopic detection", *Analytica Chimica Acta,* vol. 487, no. 1, pp. 31-42.

26. Piletskaya, E. V., Piletsky, S. A., El'Skaya, A. V., Sozinov, A. A., Marty, J. -. and Rouillon, R. (1999), "D1 protein - An effective substitute for immunoglobulins in ELISA for the detection of photosynthesis inhibiting herbicides", *Analytica Chimica Acta,* vol. 398, no. 1, pp. 49-56.

27. Rawson, D. M., Willmer, A. J. and Cardosi, M. F. (1987), "The development of whole cell biosensors for on-line screening of herbicide pollution of surface waters", *Toxic. Assess.,* vol. 2, pp. 325-340.

28. Brecht, A., Klotz, A., Barzen, C., Gauglitz, G., Harris, R. D., Quigley, G. R., Wilkinson, J. S., Sztajnbok, P., Abuknesha, R., Gascón, J., Oubiña, A. and Barceló, D. (1998), "Optical immunoprobe development for multiresidue monitoring in water", *Analytica Chimica Acta,* vol. 362, no. 1, pp. 69-79.

29. Botchkareva, A. E., Fini, F., Eremin, S., Mercader, J. V., Montoya, A. and Girotti, S. (2002), "Development of a heterogeneous chemiluminescent flow immunoassay for DDT and related compounds", *Analytica Chimica Acta,* vol. 453, no. 1, pp. 43-52.

30. Bourgeois, W., Hogben, P., Pike, A. and Stuetz, R. M. (2003), "Development of a sensor array based measurement system for continuous monitoring of water and wastewater", *Sensors and Actuators, B: Chemical,* vol. 88, no. 3, pp. 312-319.

31. Bourgeois, W. and Stuetz, R. M. (2002), "Use of a chemical sensor array for detecting pollutants in domestic wastewater", *Water Research,* vol. 36, no. 18, pp. 4505-4512.

32. Stuetz, R. M., Fenner, R. A. and Engin, G. (1999), "Characterisation of wastewater using an electronic nose", *Water Research,* vol. 33, no. 2, pp. 442-452.

33. Trinkel, M., Trettnak, W., Reininger, F., Benes, R., O'Leary, P. and Wolfbeis, O. S. (1996), "Study of the performance of an optochemical sensor for ammonia", *Analytica Chimica Acta,* vol. 320, no. 2-3, pp. 235-243.

34. Dickson, L.G., (2000), *Photosynthesis*, 2008th ed., Microsoft® Encarta® Online Encyclopedia.

35. Barber, J. (1998), "Photosystem two", *Biochimica et Biophysica Acta - Bioenergetics,* vol. 1365, no. 1-2, pp. 269-277.

36. Ort, D.R. and Whitmarsh, J., (1999), *Photosynthesis*, John Wiley & Sons, Chichester.

37. Whitmarsh, J. and Govindjee, (2001), *Photosystem II*, John Wiley & Sons, Chichester.

38. Sigma Aldrich (2008)*, Oxidative Stress*, available at: http://www.sigmaaldrich.com/Area_of_Interest/Life_Science/Cell_Signaling/Scientific_Resources/Pathway_Slides___Charts/Oxidative_Stress.html (accessed 08/25).

39. Mano, J., Ushimaru, T. and Asada, K. (1997), "Ascorbate in thylakoid lumen as an endogenous electron donor to Photosystem II: Protection of thylakoids from photoinhibition and regeneration of ascorbate in stroma by dehydroascorbate reductase", *Photosynthesis Research,* vol. 53, no. 2-3, pp. 197-204.

40. Rhodes, D. and Nadolska-Orczyk, A., (2001), *Plant stress physiology*, John Wiley & Sons, Chichester.

41. Sigma Aldrich. (Gillingham, UK), (2002), *Horseradish peroxidase product P2088* (unpublished Product material information sheet), online.

42. Rouillon, R., Mestres, J. -. and Marty, J. -. (1995), "Entrapment of chloroplasts and thylakoids in polyvinylalcohol-SbQ. Optimization of membrane preparation and storage conditions", *Analytica Chimica Acta,* vol. 311, no. 3, pp. 437-442.

43. Brewster, J. D. and Lightfield, A. R. (1993), "Rapid biorecognition assay for herbicides in biological matrices", *Analytical Chemistry,* vol. 65, no. 18, pp. 2415-2419.

44. Rizzuto, M., Polcaro, C., Desiderio, C., Koblizek, M., Pilloton, R. and Giardi, M. T. (2000), "Herbicide monitoring in surface water samples with a Photosystem-II based biosensor.", in Mazzei, F. and Pilloton, R. (eds.), *Proceedings of the Second Workshop on Chemical Sensors and Biosensors,* 2000, ENEA, Rome, pp. 346.

45. Rao, K. K., Hall, D. O., Vlachopoulos, N., Grätzel, M., Evans, M. C. W. and Seibert, M. (1990), "Photoelectrochemical responses of photosystem II particles immobilized on dye-derivatized TiO2 films", *Journal of Photochemistry and Photobiology, B: Biology,* vol. 5, no. 3-4, pp. 379-389.

46. Carpentier, R., Loranger, C., Chartrand, J. and Purcell, M. (1991), "Photoelectrochemical cell containing chloroplast membranes as a biosensor for phytotoxicity measurements", *Analytica Chimica Acta,* vol. 249, no. 1, pp. 55-60.

47. Carpentier, R., Lemieux, S., Mimeault, M., Purcell, M. and Goetze, D. C. (1989), "A photoelectrochemical cell using immobilized photosynthetic membranes", *Bioelectrochemistry and Bioenergetics,* vol. 22, no. 3, pp. 391-401.

48. Touloupakis, E., Giannoudi, L., Piletsky, S. A., Guzzella, L., Pozzoni, F. and Giardi, M. T. (2005), "A multi-biosensor based on immobilized Photosystem II on screen-printed electrodes for the detection of herbicides in river water", *Biosensors and Bioelectronics,* vol. 20, no. 10 SPEC. ISS., pp. 1984-1992.

49. Zastrizhnaya, O. M., Khorobrykh, A. A., Khristin, M. S. and Klimov, V. V. (1997), "Photoinduced production of Hydrogen peroxide at the acceptor side of photosystem II", *Biochemistry (Moscow),* vol. 62, no. 4, pp. 357-361.

50. Ananyev, G., Wydrzynski, T., Renger, G. and Klimov, V. (1992), "Transient peroxide formation by the manganese-containing, redox-active donor side of Photosystem II upon inhibition of O2 evolution with lauroylcholine chloride", *Biochimica et Biophysica Acta - Bioenergetics,* vol. 1100, no. 3, pp. 303-311.

51. Klimov, V., Ananyev, G., Zastryzhnaya, O., Wydrzynski, T. and Renger, G. (1993), "Photoproduction of hydrogen peroxide in Photosystem II membrane fragments: A comparison of four signals", *Photosynthesis Research,* vol. 38, no. 3, pp. 409-416.

52. Ananyev, G. and Klimov, V. V. (1989), "Interaction of the luminol-peroxidase system with manganese of the water-oxidizing complex of Photosystem II", *Biochemistry (Moscow),* vol. 54, no. 8, pp. 1386-1393.

53. Ananyev, G. and Klimov, V. V. (1989), "Investigation of the photoproduction of "bound" hydrogen peroxide in the donor portion of Photosystem II", *Biochemistry (Moscow),* vol. 54, no. 10, pp. 1587-1597.

54. Johansen, J. (1988), "A possible role for hydrogen peroxide as a naturally occurring electron donor in photosynthetic oxygen evolution", *BBA - Bioenergetics,* vol. 933, no. 3, pp. 406-412.

55. Mehlerb, A. H. (1951), "Studies on reactions of illuminated chloroplasts. II. Stimulation and inhibition of the reaction with molecular oxygen", *Archives of Biochemistry and Biophysics,* vol. 34, no. 2, pp. 339.

56. Mehlerb, A. H. and Brown, A. H. (1952), "Studies on reactions of illuminated chloroplasts. III. Simultaneous photoproduction and consumption of oxygen studied with oxygen isotopes", *Archives of Biochemistry and Biophysics,* vol. 38, no. 1, pp. 365.

57. Guiamét, J. J., Tyystjärvi, E., Tyystjärvi, T., John, I., Kairavuo, M., Pichersky, E. and Noodén, L. D. (2002), "Photoinhibition and loss of photosystem II reaction centre proteins during senescence of soybean leaves. Enhancement of photoinhibition by the 'stay-green' mutation cytG", *Physiologia Plantarum,* vol. 115, no. 3, pp. 468-478.

58. Bader, K. P. and Schmid, G. H. (2000), "Cooperative binding of oxygen to the water-splitting enzyme in the filamentous cyanobacterium Oscillatoria chalybea", *Biochimica et Biophysica Acta - Bioenergetics,* vol. 1456, no. 2-3, pp. 108-120.

59. Rögner, M., Boekema, E. J. and Barber, J. (1996), "How does photosystem 2 split water? The structural basis of efficient energy conversion", *Trends in Biochemical Sciences,* vol. 21, no. 2, pp. 44-49.

60. Sheptovitsky, Y. G. and Brudvig, G. W. (1998), "Catalase-free photosystem II: The O2-evolving complex does not dismutate hydrogen peroxide", *Biochemistry,* vol. 37, no. 15, pp. 5052-5059.

61. Tyystjärvi, E., Riikonen, M., Arisi, A. -. M., Kettunen, R., Jouanin, L. and Foyer, C. H. (1999), "Photoinhibition of photosystem II in tobacco plants overexpressing glutathione reductase and poplars overexpressing superoxide dismutase", *Physiologia Plantarum,* vol. 105, no. 3, pp. 409-416.

62. Krupa, Z. and Baszynski, T. (1995), "Some aspects of heavy metals toxicity towards photosynthetic apparatus - Direct and indirect effects on light and dark reactions", *Acta Physiol. Plant.,* vol. 17, pp. 177-190.

63. Baron, M., Arellano, J. B. and Gorge, J. L. (1995), "Copper and Photosystem II: A controversial relationship", *Physiologia Plantarum,* vol. 94, no. 1, pp. 174-180.

64. Samson, G., Morissette, J. -. and Popovic, R. (1988), "Copper quenching of the variable fluorescence in Dunaliella tertiolecta. New evidence for a copper inhibition effect on PSII photochemistry", *Photochem. Photobiol.,* vol. 48, pp. 329-332.

65. Shioi, Y., Tamai, H. and Sasa, T. (1978), "Inhibition of photosystem II in the green alga Ankistrodesmus falcatus by copper", *Physiol Plant,* vol. 44, pp. 434-438.

66. Yruela, I., Alfonso, M., De Zarate, I. O., Montoya, G. and Picorel, R. (1993), "Precise location of the Cu(II)-inhibitory binding site in higher plant and bacterial photosynthetic reaction centers as probed by light-induced absorption changes", *Journal of Biological Chemistry,* vol. 268, no. 3, pp. 1684-1689.

67. Mohanty, N., Vass, I. and Demeter, S. (1989), "Copper toxicity affects photosystem II electron transport at the secondary quinone acceptor, QB", *Plant Physiol.,* vol. 90, pp. 175-179.

68. Hsu, B. -. and Lee, J. -. (1988), "Toxic effects of copper on photosystem II of spinach chloroplasts", *PLANT PHYSIOL.,* vol. 87, no. 1, pp. 116-119.

69. Rijstenbil, J. W., Derksen, J. W. M., Gerringa, L. J. A., Poortvliet, T. C. W., Sandee, A., van den Berg, M., van Drie, J. and Wijnholds, J. A. (1994), "Oxidative stress induced by copper: Defense and damage in the marine planktonic diatom Ditylum brightwellii, grown in continuous cultures with high and low zinc levels", *Marine Biology,* vol. 119, no. 4, pp. 583-590.

70. Baryla, A., Carrier, P., Franck, F., Coulomb, C., Sahut, C. and Havaux, M. (2001), "Leaf chlorosis in oilseed rape plants (Brassica napus) grown on cadmium-polluted soil: Causes and consequences for photosynthesis and growth", *Planta,* vol. 212, no. 5-6, pp. 696-709.

71. Ouzounidou, G. (1993), "Changes in variable chlorophyll fluorescence as a result of Cu-treatment: Dose-response relations in Silene and Thlaspi", *Photosynthetica,* vol. 29, no. 3, pp. 455-462.

72. Li, E. H. and Miles, C. D. (1975), "Effects of cadmium on photoreaction II of chloroplasts", *PLANT SCI.LETTERS,* vol. 5, no. 1, pp. 33-40.

73. Dodeigne, C., Thunus, L. and Lejeune, R. (2000), "Chemiluminescence as a diagnostic tool. A review", *Talanta,* vol. 51, no. 3, pp. 415-439.

74. Roswell, D. F. and White, E. H. (1978), "The chemiluminescence of luminol and related hydrazides", *Methods in Enzymology,* vol. 57, pp. 409-424.

75. Rongen, H. A. H., Hoetelmans, R. M. W., Bult, A. and Van Bennekom, W. P. (1994), "Chemiluminescence and immunoassays", *Journal of Pharmaceutical and Biomedical Analysis,* vol. 12, no. 4, pp. 433-462.

76. Hallaway, B. J., Sanders, M. A. and O'Kane, D. J. (1994), "Genotoxicity assessment of substrates and products of chemiluminescence reactions", in Campbell, A. K., Kricka, L. J. and Stanley, P. E. (eds.), *Bioluminescence and*

Chemiluminescence: Fundamentals and Applied Aspects. 1994, Cambridge, UK, John Wiley, Chichester, pp. 164.

77. Liu, Y. -. and Cheng, J. -. (2002), "Ultrasensitive chemiluminescence detection in capillary electrophoresis", *Journal of Chromatography A,* vol. 959, no. 1-2, pp. 1-13.

78. Schroeder, H. R., Boguslaski, R. C., Carrico, R. J. and Buckler, R. T. (1978), "Monitoring specific protein-binding reactions with chemiluminescence", *Methods in Enzymology,* vol. 57, pp. 424-445.

79. Rauhut, M. M. (1992), "Chemiluminescence", in Grayson, M. (ed.) *Kirk-Othmer Encyclopedia of Chemical Tehcnology, 4th Edn.* Wiley, New York, pp. 247-248.

80. Seitz, W. R. (1978), "Chemiluminescence detection of enzymically generated peroxide", *Methods Enzymol.,* vol. 57, pp. 445-462.

81. Janasek, D. and Spohn, U. (1999), "Chemiluminometric flow injection analysis procedures for the enzymatic determination of L-alanine, α-ketoglutarate and L-glutamate", *Biosensors and Bioelectronics,* vol. 14, no. 2, pp. 123-129.

82. Rost, M., Karge, E. and Klinger, W. (1998), "What Do We Measure with Luminol-, Lucigenin- and Penicillin-amplified Chemiluminescence? 1. Investigations with Hydrogen Peroxide and Sodium Hypochlorite", *Luminescence,* vol. 13, no. 6, pp. 355-363.

83. Nozaki, O. and Kawamoto, H. (2003), "Reactivation of horseradish peroxidase with imidazole for continuous determination of hydrogen peroxide using a microflow injection-chemiluminescence detection system", *Luminescence,* vol. 18, no. 4, pp. 203-206.

84. Pinheiro, S. M. B., Carvalho Jr., L. B. and Chaves, M. E. C. (1999), "The use of ferromagnetic Dacron as solid-phase in chemiluminescent assays", *Biotechnology Techniques,* vol. 13, no. 12, pp. 919-922.

85. Zhou, G. -., Wang, G., Xu, J. -. and Chen, H. -. (2002), "Reagentless chemiluminescence biosensor for determination of hydrogen peroxide based on the immobilization of horseradish peroxidase on biocompatible chitosan membrane", *Sensors and Actuators, B: Chemical,* vol. 81, no. 2-3, pp. 334-339.

86. Janasek, D. and Spohn, U. (1997), "An enzyme-modified chemiluminescence detector for hydrogen peroxide and oxidase substrates", *Sensors and Actuators, B: Chemical,* vol. 39, no. 1-3, pp. 291-294.

87. Degiuli, A. and Blum, L. J. (2000), "Flow injection chemiluminescence detection of chlorophenols with a fiber optic biosensor", *Journal of Medical Biochemistry,* vol. 4, no. 1, pp. 1.

88. Campíns-Falcó, P., Tortajada-Genaro, L. A. and Bosch-Reig, F. (2001), "A new flow cell design for chemiluminiscence analysis", *Talanta,* vol. 55, no. 2, pp. 403-413.

89. Van Fleet-Stalder, V. and Chasteen, T. G. (1998), "Using fluorine-induced chemiluminescence to detect organo-metalloids in the headspace of phototrophic bacterial cultures amended with selenium and tellurium", *Journal of Photochemistry and Photobiology B: Biology,* vol. 43, no. 3, pp. 193-203.

90. Thorpe, G. H. G., Moseley, S. B., Kricka, L. J., Scott, R. A. and Whitehead, T. P. (1985), "Enhanced luminescence determination of horseradish peroxidase conjugates. Application of Benzothiazole Derivatives as Enhancers in Luminescence Assays on Microtitre Plates", *Analytica Chimica Acta,* vol. 170, no. C, pp. 101-107.

91. Samsonova, J. V., Rubtsova, M. Y., Kiseleva, A. V., Ezhov, A. A. and Egorov, A. M. (1999), "Chemiluminescent multiassay of pesticides with horseradish peroxidase as a label", *Biosensors and Bioelectronics,* vol. 14, no. 3, pp. 273-281.

92. Marquette, C. A. and Blum, L. J. (2000), "Regenerable immunobiosensor for the chemiluminescent flow injection analysis of the herbicide 2,4-D", *Talanta,* vol. 51, no. 2, pp. 395-401.

93. Kricka, L. J. (1991), "Chemiluminescent and bioluminescent techniques", *Clinical Chemistry,* vol. 37, no. 9, pp. 1472-1481.

94. Cooper, W. J., Moegling, J. K., Kieber, R. J. and Kiddle, J. J. (2000), "A chemiluminescence method for the analysis of H_2O_2 in natural waters", *Marine Chemistry,* vol. 70, no. 1-3, pp. 191-200.

95. Ma, Q., Ma, H., Wang, Z., Su, M., Xiao, H. and Liang, S. (2001), "Synthesis of a novel chemiluminescent reagent for the determination of hydrogen peroxide in snow waters", *Talanta,* vol. 53, no. 5, pp. 983-990.

96. Nakamura, H., Tanaka, H., Hasegawa, M., Masuda, Y., Arikawa, Y., Nomura, Y., Ikebukuro, K. and Karube, I. (1999), "An automatic flow-injection analysis system for determining phosphate ion in river water using pyruvate oxidase G (from Aerococcus viridans)", *Talanta,* vol. 50, no. 4, pp. 799-807.

97. Sekharam, M., Cunnick, J. M. and Wu, J. (2000), "Involvement of lipoxygenase in lysophosphatidic acid-stimulated hydrogen peroxide release in human HaCaT keratinocytes", *Biochemical Journal,* vol. 346, no. 3, pp. 751-758.

98. Mueller, S. (2000), "Sensitive and nonenzymatic measurement of hydrogen peroxide in biological systems", *Free Radical Biology and Medicine,* vol. 29, no. 5, pp. 410-415.

99. Lin, J. -., Arakawa, H. and Yamada, M. (1998), "Flow injection chemiluminescent determination of trace amounts of hydrogen peroxide in snow-water using KIO4-K2CO3 system", *Analytica Chimica Acta,* vol. 371, no. 2-3, pp. 171-176.

100. Price, D., Mantoura, R. F. C. and Worsfold, P. J. (1998), "Shipboard determination of hydrogen peroxide in the western Mediterranean sea using flow injection with chemiluminescence detection", *Analytica Chimica Acta,* vol. 377, no. 2-3, pp. 145-155.

101. Zhou, Y., Nagaoka, T., Li, F. and Zhu, G. (1999), "Evaluation of luminol-H2O2-KIO4 chemiluminescence system and its application to hydrogen peroxide, glucose and ascorbic acid assays", *Talanta,* vol. 48, no. 2, pp. 461-467.

102. West, J., Gleeson, J. P., Lillis, B., Alderman, J., Collins, J. K., Lane, W. and Berney, H. (2002), "Annular Magnetohydrodynamic Actuation: A Tool for Chemical Microreactors", *The 16th European Conference on Solid-State Transducers,* Vol. 16, September 15-18, Prague, Czech Republic, IEEE, Czech Republic, pp. 318.

103. Soh, N., Nishiyama, H., Asano, Y., Imato, T., Masadome, T. and Kurokawa, Y. (2004), "Chemiluminescence sequential injection immunoassay for vitellogenin using magnetic microbeads", *Talanta,* vol. 64, no. 5 SPEC. ISS., pp. 1160-1168.

104. Alwarthan, A. A. and A. Aly, F. (1998), "Chemiluminescent determination of pyridoxine hydrochloride in pharmaceutical samples using flow injection", *Talanta,* vol. 45, no. 6, pp. 1131-1138.

105. Hatch, G. P. and Stelter, R. E. (2001), "Magnetic design considerations for devices and particles used for biological high-gradient magnetic separation (HGMS) systems", *Journal of Magnetism and Magnetic Materials,* vol. 225, no. 1-2, pp. 262-276.

106. Sinclair, B. (1998), "To bead or not to bead: Applications of magnetic bead technology", *The Scientist,* vol. 12, no. 13, pp. 17-23.

107. Ramadan, Q., Samper, V., Neuzil, P., Marie, L., Meng, L. T., Kiat, H. C., Qin, Y. S. and Puiu, P. D. (2002), "Optomization of On-Chip Micro-Electromagnets for Biomolecular Separation", Vol. 1, pp. 249.

108. Bangs. (Bangs Laboratories Inc.), (2003), *Technote 102: magnetic microspheres* (unpublished Product technical note), Online, http://www.bangslabs.com.

109. Besse, P. -., Boero, G., Demierre, M., Pott, V. and Popovic, R. (2002), "Detection of a single magnetic microbead using a miniaturized silicon Hall sensor", *Applied Physics Letters,* vol. 80, no. 22, pp. 4199.

110. Deng, T., Whitesides, G. M., Radhakrishnan, M., Zabow, G. and Prentiss, M. (2001), "Manipulation of magnetic microbeads in suspension using micromagnetic systems fabricated with soft lithography", *Applied Physics Letters,* vol. 78, no. 12, pp. 1775-1777.

111. Bronzeau, S. and Pamme, N. (2008), "Simultaneous bioassays in a microfluidic channel on plugs of different magnetic particles", *Analytica Chimica Acta,* vol. 609, no. 1, pp. 105-112.

112. Creager, R., Knoll, D., Shellum, C. and Werness, P., (1996), *Commercialization of a chemiluminescence-based analyzer*, March ed., Canon Communications.

113. Bangs. (Bangs Laboratories Inc.), (1999), *Technote 204: Adsorption to Microspheres* (unpublished Product technical note), Online, http://www.bangslabs.com.

114. Bangs, L. B. and Meza, M. (1995), "Microspheres, part 2: Ligand attachment and test formulation", *IVD Technology Magazine,* .

115. Liakopoulos, T. M., Choi, J. and Ahn, C. H. (1997), "Bio-magnetic bead separator on glass chips using semi-encapsulated spiral electromagnets", Vol. 1, pp. 485.

116. Pamme, N. (2006), "Magnetism and microfluidics", *Lab on a Chip - Miniaturisation for Chemistry and Biology,* vol. 6, no. 1, pp. 24-38.

117. Lee, C. S., Lee, H. and Westervelt, R. M. (2001), "Microelectromagnets for the control of magnetic nanoparticles", *Applied Physics Letters,* vol. 79, no. 20, pp. 3308-3310.

118. Hoyle, N. R. (1994), "The application of electrochemiluminescence to immunoassay-based analyte measurement", in Campbell, A. K., Kricka, L. J. and Stanley, P. E. (eds.), *Bioluminescence and Chemiluminescence: Fundamentals and Applied Aspects.* 1994, Cambridge, UK, John Wiley, Chichester, pp. 28.

119. Choi, J. -., Oh, K. W., Han, A., Okulan, N., Ajith Wijayawardhana, C., Lannes, C., Bhansali, S., Schlueter, K. T., Heineman, W. R., Halsall, H. B., Nevin, J. H., Helmicki, A. J., Thurman Henderson, H. and Ahn, C. H. (2001), "Development and characterization of microfluidic devices and systems for magnetic bead-based biochemical detection", *Biomedical Microdevices,* vol. 3, no. 3, pp. 191-200.

120. Chen, X., Zhang, X. -., Chai, Y. -., Hu, W. -., Zhang, Z. -., Zhang, X. -. and Cass, A. E. G. (1998), "DNA optical sensor: A rapid method for the detection of DNA hybridization", *Biosensors and Bioelectronics,* vol. 13, no. 3-4, pp. 451-458.

121. Cheng, Y., Dubovoy, N., Hayes-Rogers, M. E., Stewart, J. and Shah, D. (1999), "Detection of IgM to hepatitis B core antigen in a reductant containing, chemiluminescence assay", *Journal of Immunological Methods,* vol. 230, no. 1-2, pp. 29-35.

122. Assays Designs Inc, (2000)*, General principles of bio- and chemiluminescence*, available at: http://www.assaydesigns.com/products/catalog/compounds/product_luminescent_process.htm (accessed 12/17).

123. Haviger, A., Ševčíka, J. and Lasovský, J. (2000), "USING OF THE AMPLIFIED LUMINOL CHEMILUMINISCENCE METHOD FOR THE DETERMINATION OF SERUM GLUCOSE", *ACTA UNIVERSITATIS PALACKIANAE OLOMUCENSIS, FACULTAS RERUM NATURALIUM,* vol. 36, pp. 23-31.

124. Oosthuizen, M. M. J., Engelbrecht, M. E., Lambrechts, H., Greyling, D. and Levy, R. D. (1997), "The Effect of pH on Chemiluminescence of Different Probes Exposed to Superoxide and Singlet Oxygen Generators", *Luminescence,* vol. 12, no. 6, pp. 277-284.

125. Nozaki, O., Ji, X. and Kricka, L. J. (1994), "Influence of buffers on the boronate enhance chemiluminescent HRP catalyzed luminol oxidation", in Campbell, A. K., Kricka, L. J. and Stanley, P. E. (eds.), *Bioluminescence and Chemiluminescence: Fundamentals and Applied Aspects.* 1994, Cambridge, UK, John Wiley, Chichester, pp. 48.

126. Rauch, P., Ferri, E. N., Girotti, S., Rauchova, H., Carrea, G., Bovara, R., Fini, F. and Roda, A. (1997), "A chemiluminescent flow sensing device for determination of choline and phospholipase D activity in biological samples", *Analytical Biochemistry,* vol. 245, no. 2, pp. 133-140.

127. Kricka, L. J. and Stanley, P. E. (2002), "Luminescence literature.", *Luminescence : the journal of biological and chemical luminescence,* vol. 17, no. 6, pp. 386-401.

128. Janssen, M. A. (1997), *Development and perspectives of fluorescent receptor assays : a case study with benzodiazepines* (unpublished Bachelors of Pharmacy thesis), University of Groningen, Groningen.

129. Navas Díaz, A., García Sanchez, F. and González García, J. A. (1996), "Hydrogen peroxide assay by using enhanced chemiluminescence of the luminol-H2O2-horseradish peroxidase system: Comparative studies", *Analytica Chimica Acta,* vol. 327, no. 2, pp. 161-165.

130. Preuschoff, F., Spohn, U., Blankenstein, G., Mohr, K. -. and Kula, M. -. (1993), "Chemiluminometric hydrogen peroxide sensor for flow injection analysis", *Fresenius' Journal of Analytical Chemistry,* vol. 346, no. 10-11, pp. 924-929.

131. BrandTech Scientific. (www.brandtech.com), (2007), *Transferpette S operating manual* (unpublished Product manual), online.

132. Elstner, E. F. and Frommeyer, D. (1978), "Production of hydrogen peroxide by photosystem II of spinach chloroplast lamellae", *FEBS Letters,* vol. 86, no. 1, pp. 143-146.

133. Naglak, T. J., Hettwer, D. J. and Wang, H. Y. (1990), "Chemical permeabilization of cells for intracellular product release.", *Bioprocess technology,* vol. 9, pp. 177-205.

134. Tobin, A. K. and Bowsher, C. G. (2004), "Subcellular fractionation of plant tissues: isolation of plastids and mitochondria.", in Cutler, P. (ed.) *Protein Purification Protocols,* Second ed, Humana Press, New Jersey, pp. 53-63.

135. Ford, R. C. and Evans, M. C. W. (1983), "Isolation of a photosystem 2 preparation from higher plants with highly enriched oxygen evolution activity", *FEBS Letters,* vol. 160, no. 1-2, pp. 159-164.

136. Markwell, J. P., Nakatani, H. Y., Barber, J. and Thornber, J. P. (1980), "Chlorophyll-protein complexes fractionated from intact chloroplasts", *FEBS Letters,* vol. 122, no. 1, pp. 149-153.

137. Navarro, J. A., Roncel, M., De la Rosa, F. F. and De la Rosa, M. A. (1987), "Light-driven hydrogen peroxide production as a way to solar energy conversion", *Bioelectrochemistry and Bioenergetics,* vol. 18, no. 1-3, pp. 71-78.

138. Rouillon, R., Piletsky, S. A., Breton, F., Piletska, E. V. and Carpentier, R. (2006), "Photosystem II Biosensors for Heavy Metals Monitoring", in Giardi, M. T. and Piletska, E. V. (eds.) *Biotechnological applications of photosynthetic proteins : biochips, biosensors and biodevices,* Landes Bioscience/Eurekah.com; Springer Science+Business Media, Georgetown, Tex.; New York, N.Y., pp. 166.

139. Fido, R. J., Mills, E. N., Rigby, N. M. and Shewry, P. R. (2004), "Protein extraction from plant tissues", in Cutler, P. (ed.) *Protein Purification Protocols,* Second ed, Humana Press, New Jersey, pp. 21-27.

140. Bettazzi, F., Laschi, S. and Mascini, M. (2005), "Disposable biosensors assembled with thylakoid membranes from spinach leaves for herbicide detection", *Chemia Analityczna,* vol. 50, no. 1, pp. 117-128.

141. Li, J., Wei, X. and Peng, T. (2005), "Fabrication of herbicide biosensors based on the inhibition of enzyme activity that catalyzes the scavenging of hydrogen peroxide in a thylakoid membrane", *Analytical Sciences,* vol. 21, no. 10, pp. 1217-1222.

142. Koblizek, M., Masojidek, J., Komenda, J., Kucera, T., Pilloton, R., Mattoo, A. K. and Giardi, M. T. (1998), "A sensitive photosystem II-based biosensor for detection of a class of herbicides", *Biotechnology and Bioengineering,* vol. 60, no. 6, pp. 664-669.

143. Carpentier, R. and Goetze, D. C. (1993), "Microelectrochemical cell containing chloroplast membranes as a fast bioassay for catalase determination", *Analytica Chimica Acta,* vol. 281, no. 2, pp. 335-339.

144. Purcell, M., Carpentier, R., Bélanger, D. and Fortier, G. (1990), "Immobilized plant thylakoid membranes as a biosensor for herbicides", *Biotechnology Techniques,* vol. 4, no. 5, pp. 363-368.

145. Carpentier, R., Leblanc, R. M. and Mimeault, M. (1987), "Photoinhibition and chlorophyll photobleaching in immobilized thylakoid membranes", *Enzyme and Microbial Technology,* vol. 9, no. 8, pp. 489-493.

146. Mimeault, M. and Carpentier, R. (1988), "Electrochemical monitoring of electron transfer in thylakoid membranes", *Enzyme and Microbial Technology,* vol. 10, no. 11, pp. 691-694.

147. Laberge, D., Rouillon, R. and Carpentier, R. (2000), "Comparative study of thylakoid membranes sensitivity for herbicide detection after physical or chemical immobilization", *Enzyme and Microbial Technology,* vol. 26, no. 5-6, pp. 332-336.

148. Piletskaya, E. V., Piletsky, S. A., Sergeyeva, T. A., El'Skaya, A. V., Sozinov, A. A., Marty, J. -. and Rouillon, R. (1999), "Thylakoid membranes-based test-system for detecting of trace quantities of the photosynthesis-inhibiting herbicides in drinking water", *Analytica Chimica Acta,* vol. 391, no. 1, pp. 1-7.

149. Nakatani, H. Y. and Barber, J. (1977), "An improved method for isolating chloroplasts retaining their outer membranes", *Biochimica et Biophysica Acta,* vol. 461, pp. 510-512.

150. Berthold, D. A., Babcock, G. T. and Yocum, C. F. (1981), "A highly resolved, oxygen-evolving photosystem II preparation from spinach thylakoid membranes. EPR and electron-transport properties", *FEBS Letters,* vol. 134, no. 2, pp. 231-234.

151. Whatley, J. M. (1980), *Light and plant life,* Edward Arnold, London.

152. Endo, T., Shikanai, T., Takabayashi, A., Asada, K. and Sato, F. (1999), "The role of chloroplastic NAD(P)H dehydrogenase in photoprotection", *FEBS Letters,* vol. 457, no. 1, pp. 5-8.

153. Tazawa, S. (1999), "Effects of various radiant sources on plant growth (Part 1)", *Japan Agricultural Research Quarterly,* vol. 33, no. 3, pp. 163-176.

154. Maly, J., Masojidek, J., Masci, A., Ilie, M., Cianci, E., Foglietti, V., Vastarella, W. and Pilloton, R. (2005), "Direct mediatorless electron transport between the monolayer of photosystem II and poly(mercapto-p-benzoquinone) modified gold electrode - New design of biosensor for herbicide detection", *Biosensors and Bioelectronics,* vol. 21, no. 6, pp. 923-932.

155. Davidson, M. W. and Abramowitz, M. (2003)*, Sources of visible light*, available at: http://micro.magnet.fsu.edu/optics/lightandcolor/index.html (accessed 11/29).

156. Davidson, M. W. and Abramowitz, M. (2003)*, Light filtration*, available at: http://micro.magnet.fsu.edu/optics/lightandcolor/index.html (accessed 11/29).

157. Alia, Kondo, Y., Sakamoto, A., Nonaka, H., Hayashi, H., Pardha Saradhi, P., Chen, T. H. H. and Murata, N. (1999), "Enhanced tolerance to light stress of transgenic Arabidopsis plants that express the codA gene for a bacterial choline oxidase", *Plant Molecular Biology,* vol. 40, no. 2, pp. 279-288.

158. Pegau, W. S., Gray, D. and Zaneveld, J. R. V. (1997), "Absorption and attenuation of visible and near-infrared light in water: dependence on temperature and salinity", *Applied Optics,* vol. 36, no. 24, pp. 6035-6046.

159. Malý, J., Klem, K., Lukavská, A. and Masojídek, J. (2005), "Degradation and movement in soil of the herbicide isoproturon analyzed by a photosystem II-based biosensor", *Journal of Environmental Quality,* vol. 34, no. 5, pp. 1780-1788.

160. Sigma-Aldrich Co. (2008)*, Protease Inhibitors*, available at: http://www.sigmaaldrich.com/life-science/metabolomics/enzyme-explorer/learning-center/protease-inhibitors.html (accessed 11/29).

161. Jordan, L. S. and Cudney, D. W. (1987), "Fate of pesticides in the environment : Technical seminar : Selected papers", in Biggar, J. W. and Seiber, J. N. (eds.), *Fate of pesticides in the environment,* 1985 Mar, Sacramento, CA, Agricultural Experiment Station, Division of Agriculture and Natural Resources, University of California, Oakland, Calif., .

162. Ware, G. W. (1983), *Pesticides : theory and application,* Freeman, San Francisco ; Oxford.

163. Ahrens, W. H. (1994), *Herbicide handbook,* 7th ed, Weed Science Society of America, Champaign, Ill.

164. Van Rensen, J. J. S. (1989), "Herbicides interacting with photosystem II", in Dodge, A. D. (ed.) *Herbicides and Plant Metabolism,* First ed, Cambridge University Press, Cambridge, pp. 21-36.

165. Hassall, K. A. (1990), *The biochemistry and uses of pesticides : structure, metabolism, mode of action and uses in crop protection,* 2nd ed, Macmillan, London.

166. Cremlyn, R. J. (1991), *Agrochemicals: Preparation and Mode of Action,* First ed, Wiley, West Sussex, UK.

167. Corbett, J. R., Wright, K. and Baillie, A. C. (1984), *The biochemical mode of action of pesticides,* 2nd ed, Academic Press, London.

168. Hill, R. (1939), "Oxygen evolution by isolated chloroplasts", *Nature,* vol. 103, pp. 81.

169. Dodge, A. D. (1989), "Herbicides interacting with photosystem I", in Dodge, A. D. (ed.) *Herbicides and plant metabolism,* First ed, Cambridge University Press, Cambridge, pp. 37.

170. Rao, D. N. R. and Mason, R. P. (1988), "PHOTOREDUCTION OF SOME NITROBIPHENYL ETHER HERBICIDES TO NITRO RADICAL ANIONS BY β-CAROTENE AND RELATED COMPOUNDS", *Photochemistry and photobiology,* vol. 47, no. 6, pp. 791-795.

171. Matringe, M. and Scalla, R. (1988), "Studies on the Mode of Action of Acifluorfen-Methyl in Nonchlorophyllous Soybean Cells : Accumulation of Tetrapyrroles", *PLANT PHYSIOLOGY,* vol. 86, no. 2, pp. 619-622.

172. Kamrin, M. A. (1997), *Pesticide profiles : toxicity, environmental impact, and fate,* CRC/Lewis Publishers, Boca Raton.

173. Montgomery, J. H. (1997), *Agrochemicals desk reference,* 2nd ed, CRC, Boca Raton.

174. Védrine, C., Leclerc, J. -., Durrieu, C. and Tran-Minh, C. (2003), "Optical whole-cell biosensor using Chlorella vulgaris designed for monitoring herbicides", *Biosensors and Bioelectronics,* vol. 18, no. 4, pp. 457-463.

175. Giardi, M. T., Guzzella, L., Euzet, P., Rouillon, R. and Esposito, D. (2005), "Detection of herbicide subclasses by an optical multibiosensor based on an array of photosystem II mutants", *Environmental Science and Technology,* vol. 39, no. 14, pp. 5378-5384.

176. Hansatech Instruments. (King's Lynn, Norfolk,), (2006), *Handy PEA portable fluorescence measurement system* (unpublished Company product brochure), King's Lynn.

177. Ferus, P. and Arkosiova, M. (1999), "Variability of Chlorophyll Content under Fluctuating Environment", *Acta Fytotechnica et Zootechnica,* vol. 4, pp. 123.

178. McDonald, J. C., Duffy, D. C., Anderson, J. R., Chiu, D. T., Wu, H., Schueller, O. J. A. and Whitesides, G. M. (2000), "Fabrication of microfluidic systems in poly(dimethylsiloxane)", *Electrophoresis,* vol. 21, no. 1, pp. 27-40.

179. Sia, S. K. and Whitesides, G. M. (2003), "Microfluidic devices fabricated in poly(dimethylsiloxane) for biological studies", *Electrophoresis,* vol. 24, no. 21, pp. 3563-3576.

180. Bangs. (Bangs Laboratories Inc.), (2002), *Technote 201: working with microspheres* (unpublished Product technical note), Online, http://www.bangslabs.com.

181. Rubtsova, M. Y., Kovba, G. V. and Egorov, A. M. (1998), "Chemiluminescent biosensors based on porous supports with immobilized peroxidase", *Biosensors and Bioelectronics,* vol. 13, no. 1, pp. 75-85.

182. Nakajima, N. and Ikada, Y. (1995), "Mechanism of amide formation by carbodiimide for bioconjugation in aqueous media", *Bioconjugate Chemistry,* vol. 6, no. 1, pp. 123-130.

183. Childs, R. E. and Bardsley, W. G. (1975), "The steady state kinetics of peroxidase with 2,2' azino di (3 ethylbenzthiazoline 6 sulphonic acid) as chromogen", *Biochemical Journal,* vol. 145, no. 1, pp. 93-103.

184. Polysciences. (Polysciences Inc.), (2003), *BioMag®Plus Carboxyl & BioMag®Plus Carboxyl Protein Coupling Kit* (unpublished Technical data sheet 618), Warrington, PA, USA.

185. Polysciences. (Polysciences Inc.), (2003), *Covalent Coupling of Proteins to Carboxylated Polystyrene Microparticles by the "Carbodiimide" Method* (unpublished Technical data sheet 238C), Warrington, PA, USA.

186. Taniai, T., Sukuragawa, A. and Okutani, T. (2001), "Fluorometric determination of ethanol in liquor samples by flow-injection analysis using an immobilized enzyme-reactor column with packing prepared by coupling alcohol oxidase and peroxidase onto chitosan beads", *Journal of AOAC International,* vol. 84, no. 5, pp. 1475-1483.

187. Yang, Z., Fu, Z., Yan, F., Liu, H. and Ju, H. (2008), "A chemiluminescent immunosensor based on antibody immobilized carboxylic resin beads coupled with micro-bubble accelerated immunoreaction for fast flow-injection immunoassay", *Biosensors and Bioelectronics,* vol. 24, no. 1, pp. 35-40.

188. Li, B., Zhang, Z. and Zhao, L. (2001), "Chemiluminescent flow-through sensor for hydrogen peroxide based on sol-gel immobilized hemoglobin as catalyst", *Analytica Chimica Acta,* vol. 445, no. 2, pp. 161-167.

189. Marle, L. and Greenway, G. M. (2005), "Determination of hydrogen peroxide in rainwater in a miniaturised analytical system", *Analytica Chimica Acta,* vol. 548, no. 1-2, pp. 20-25.

190. Hu, Y., Zhang, Z. and Yang, C. (2007), "The determination of hydrogen peroxide generated from cigarette smoke with an ultrasensitive and highly selective chemiluminescence method", *Analytica Chimica Acta,* vol. 601, no. 1, pp. 95-100.

191. Frense, D., Müller, A. and Beckmann, D. (1998), "Detection of environmental pollutants using optical biosensor with immobilized algae cells", *Sensors and Actuators, B: Chemical,* vol. 51, no. 1-3, pp. 256-260.

192. Naessens, M., Leclerc, J. C. and Tran-Minh, C. (2000), "Fiber optic biosensor using Chlorella vulgaris for determination of toxic compounds", *Ecotoxicology and Environmental Safety,* vol. 46, no. 2, pp. 181-185.

193. Bangs Laboratories (2007)*, BioMag® Product Descriptions*, available at: http://www.bangslabs.com/products/bangs/biomag_products.php#BM546 (accessed 10/22).

194. Polysciences Inc. (2007)*, Amino Superparamagnetic Microparticles, 1-2µm*, available at: http://www.polysciences.com/Catalog/Department/Product/98/categoryId__370/productId__1050/ (accessed 10/22).

195. Spherotech Inc. (2008)*, PARAMAGNETIC PARTICLES*, available at: http://www.spherotech.com/para_par.htm (accessed 10/22).

196. Varsamis, D. G., Touloupakis, E., Morlacchi, P., Ghanotakis, D. F., Giardi, M. T. and Cullen, D. C. (2008), "Development of a photosystem II-based optical microfluidic sensor for herbicide detection", *Talanta,* vol. 77, no. 1, pp. 42-47.

197. Silicon Machines Ltd. (2005)*, About white LEDs*, available at: http://www.ledset.com/electronics/index.htm (accessed 11/29).

198. Palmer, J. M. (2005)*, Radiometry and photometry FAQ*, available at: http://www.optics.arizona.edu/Palmer/rpfaq/rpfaq.htm (accessed 11/29).

199. Marktech Optoelectronics (2008)*, White LEDs*, available at: http://www.marktechopto.com/Engineering-Services/technical-articles.cfm (accessed 11/29).

200. Marktech Optoelectronics (2008)*, Measurement of LEDs*, available at: http://www.marktechopto.com/Engineering-Services/technical-articles.cfm (accessed 11/29).

201. Moffett, J. W. and Zafiriou, O. C. (1990), "An investigation of hydrogen peroxide chemistry in surface waters of Vineyard Sound with H218O2 and 18O2", *Limnology & Oceanography,* vol. 35, no. 6, pp. 1221-1229.

Appendices

Appendix I. Detailed results of the batch assay for the detection of the photosynthesis-inhibiting herbicides, varying the isolated thylakoid preparation, incubation time and concentration of each herbicide.

Legend for all figures:

The luminescence signal, detected by a bench-top spectrophotometer, resulted from the production of light by the cuvette-based chemiluminescence reaction of luminol, HRP and H_2O_2. [HRP] = 5 U.ml-1, [luminol] = 100 µM, in Tris-HCl buffer (10 mM, pH 8.5). The H_2O_2 was previously produced by illuminating diluted thylakoid preparations Ch1 - Ch5 with an un-filtered halogen lamp (20 watts, 350 lumens) at a distance of 10 cm for 5 min, while aspirated in a pipette tip, following an incubation period (0 – 15 min) with herbicide concentrations (0 - $1x10^{-4}$). The Ch1 thylakoid preparation ([chlorophyll] = 284 $\mu g.ml^{-1}$) and the Ch3 thylakoid preparation ([chlorophyll] = 237 $\mu g.ml^{-1}$) were diluted in buffer B (5 mM $MgCl_2$, 15 mM NaCl, 2 mM MES, brought to pH 6.9 with NaOH). The Ch2 thylakoid preparation ([chlorophyll] = 171 $\mu g.ml^{-1}$), the Ch4 thylakoid preparation ([chlorophyll] = 131 $\mu g.ml^{-1}$) and the Ch5 thylakoid preparation ([chlorophyll] = 64 $\mu g.ml^{-1}$) were diluted in buffer A (10 mM Tris-HCl buffer, adjusted to pH 8.5).

H_2O_2 production by isolated thylakoids Ch1 - Ch5, inhibited by atrazine (0 – $1x10^{-4}$) after an incubation period of 1 – 15 min

Thylakoid preparation Ch1

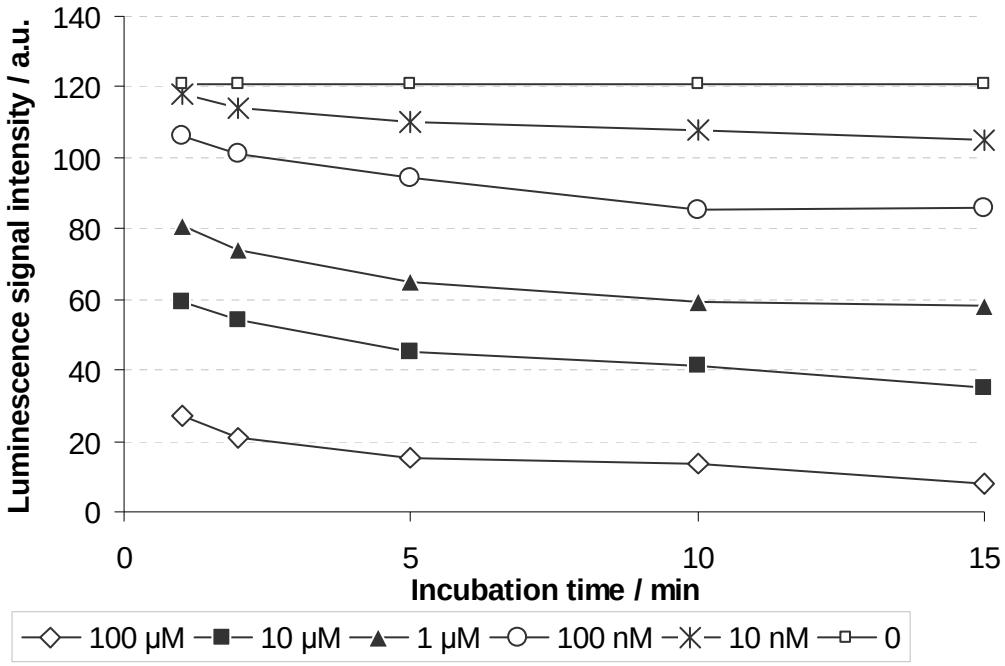

Thylakoid preparation Ch2

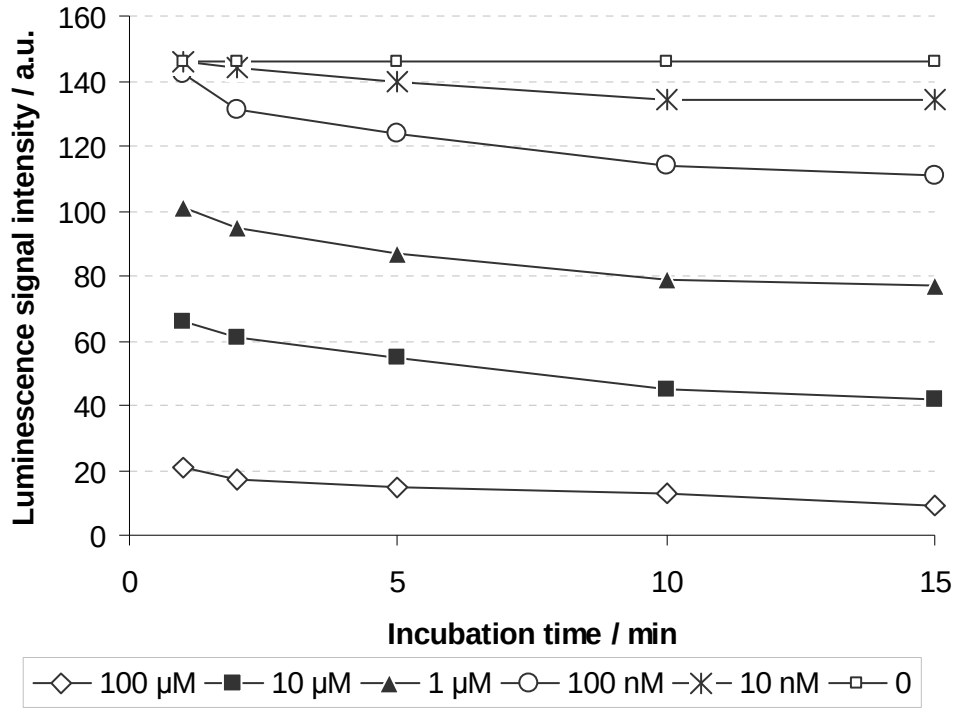

Thylakoid preparation Ch3

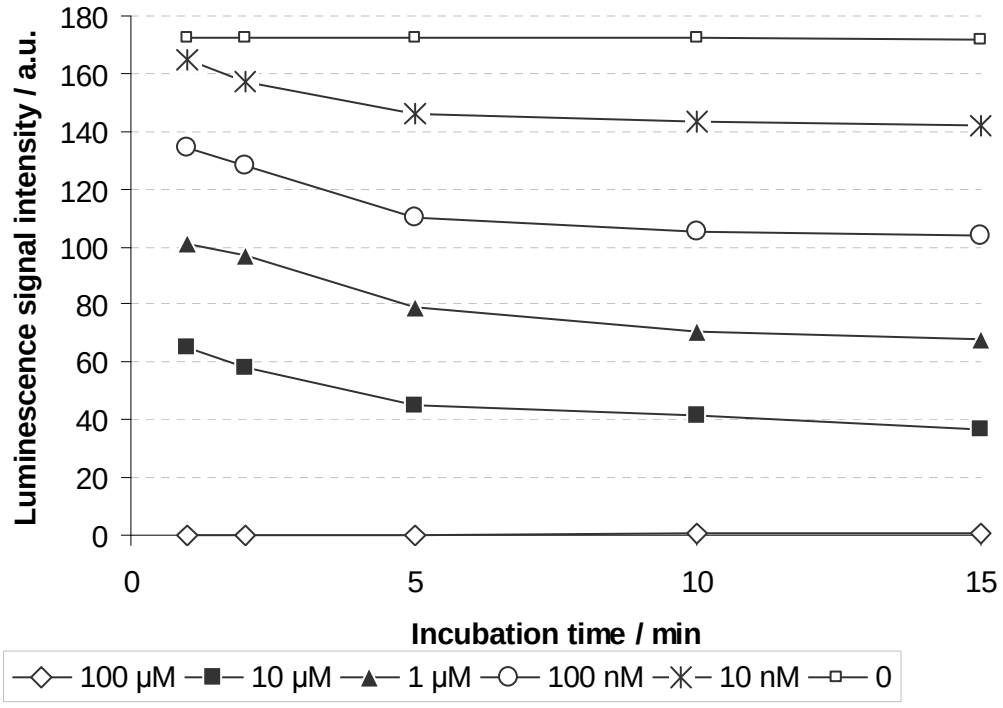

Thylakoid preparation Ch4

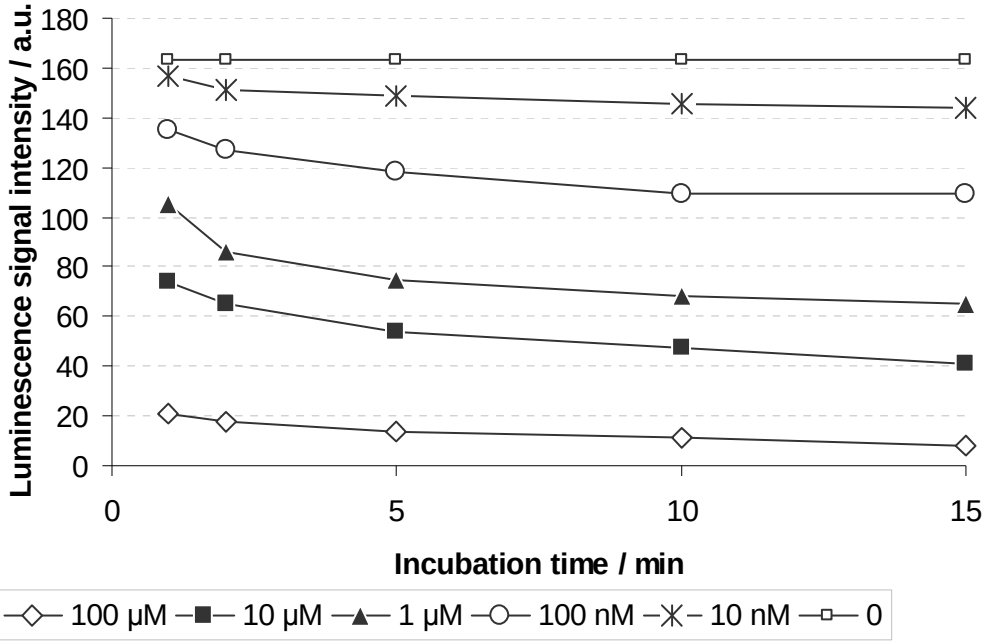

Thylakoid preparation Ch5

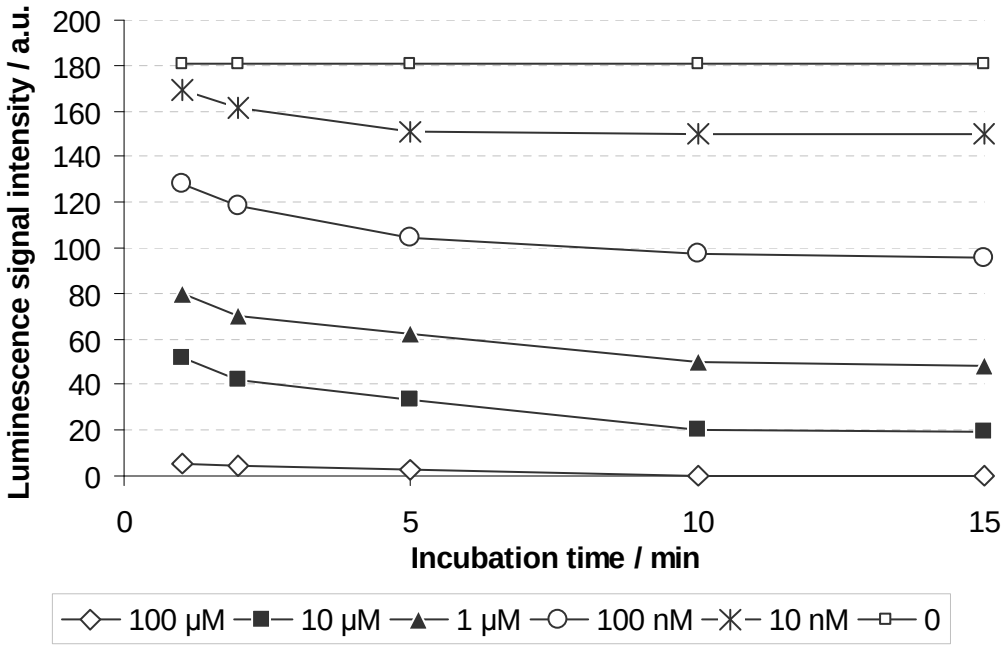

H_2O_2 production by isolated thylakoids Ch1 - Ch5, inhibited by diuron (0 – 1x10^{-4}) after an incubation period of 1 – 15 min

Thylakoid preparation Ch1

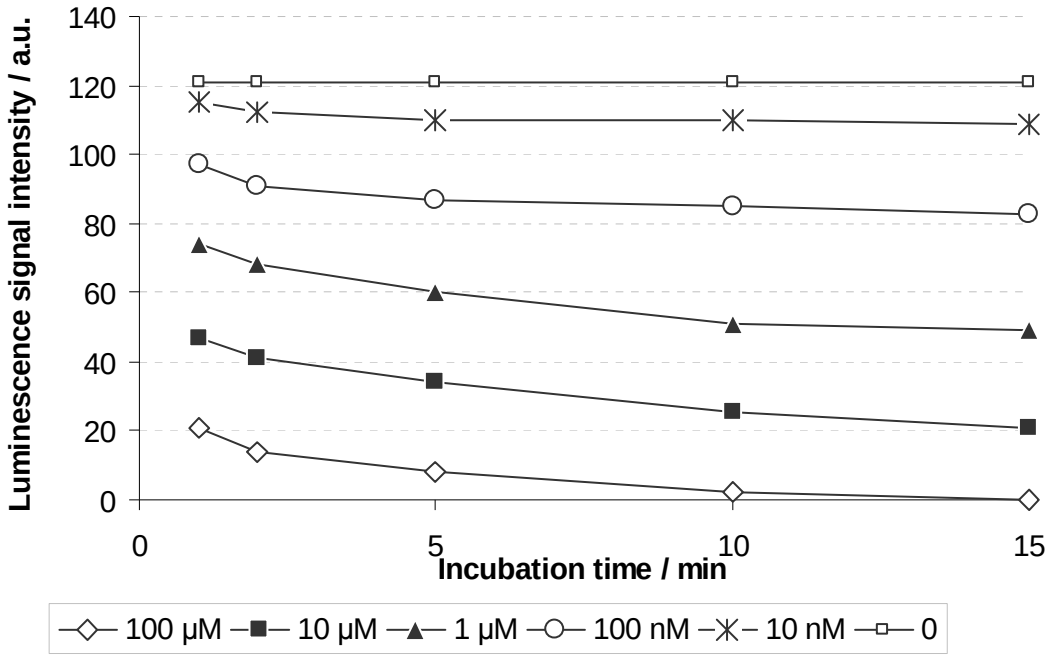

Thylakoid preparation Ch2

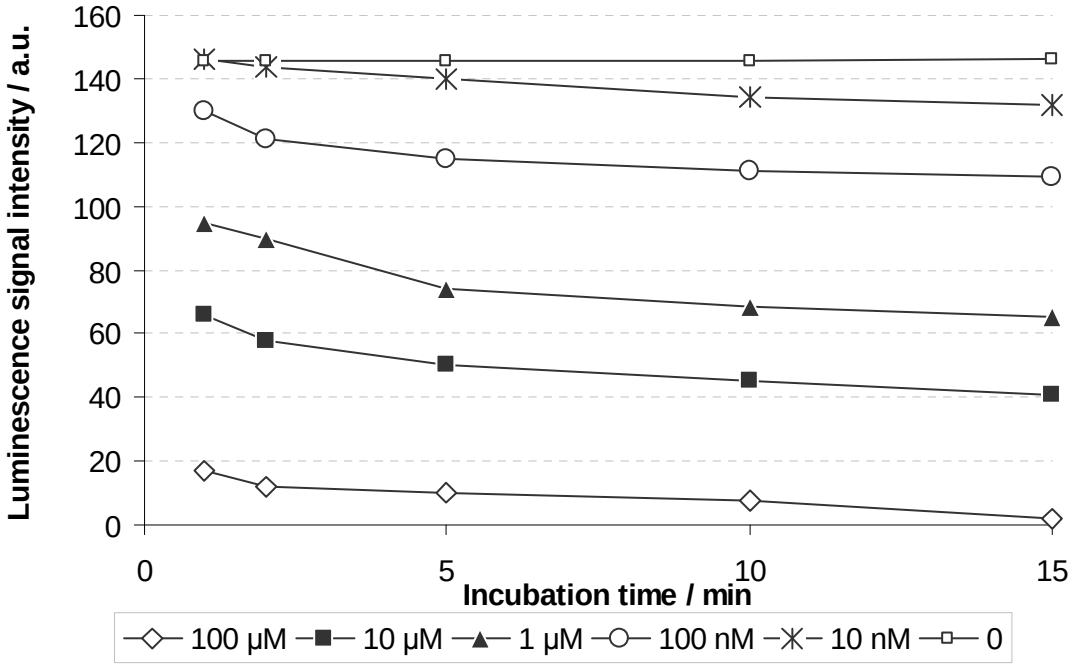

Thylakoid preparation Ch3

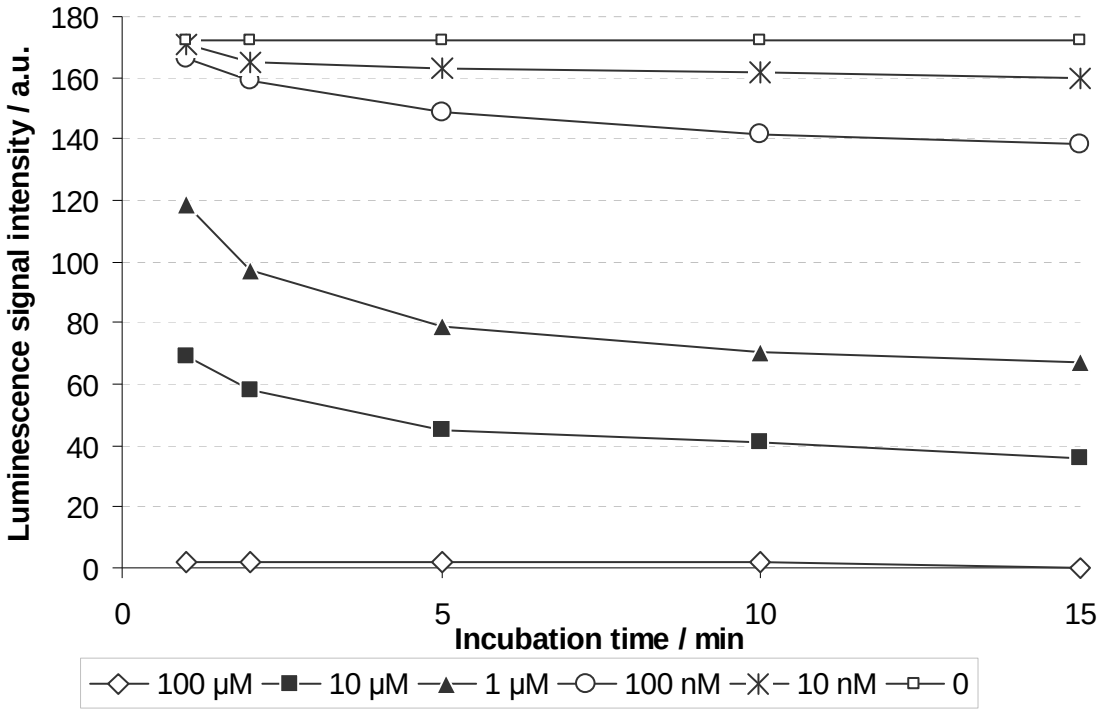

Thylakoid preparation Ch4

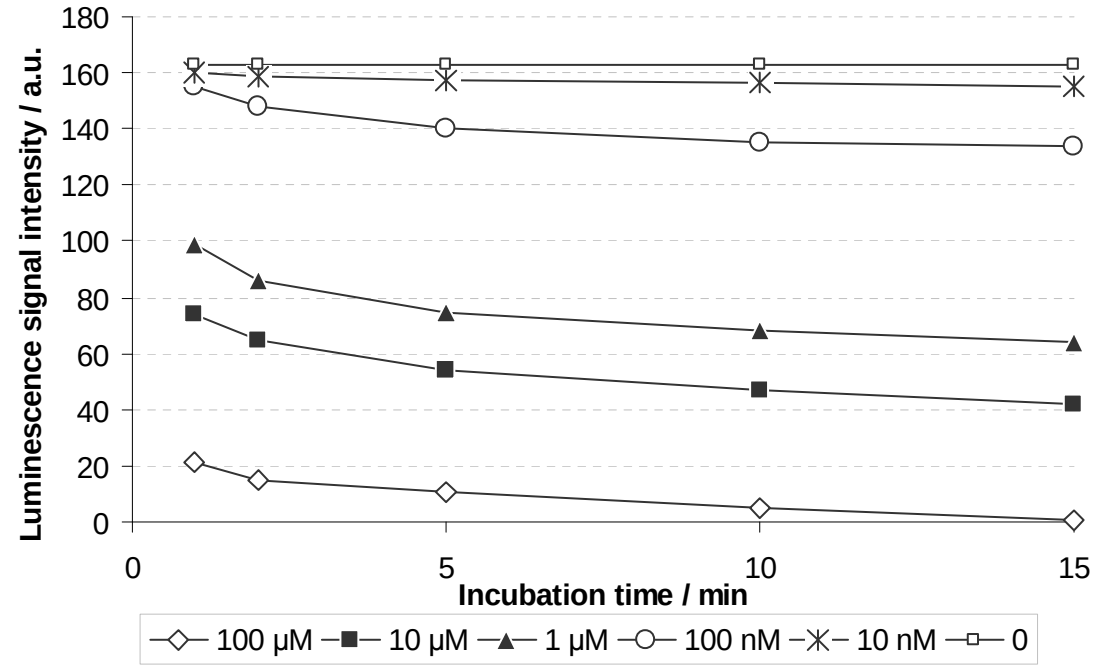

Thylakoid preparation Ch5

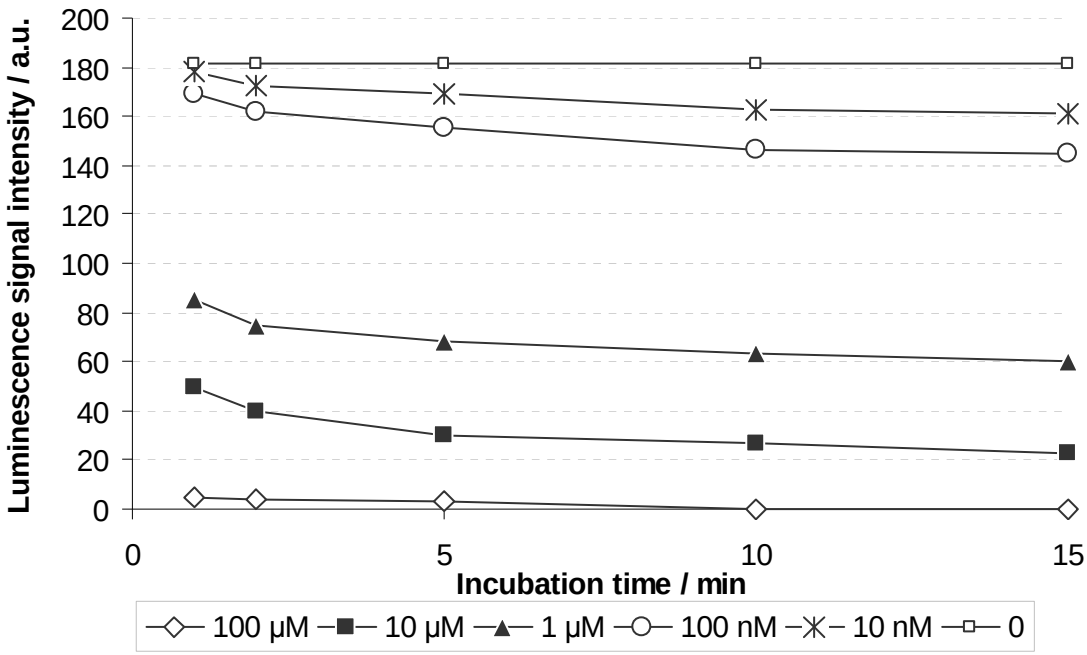

H_2O_2 production by isolated thylakoids Ch1 - Ch5, inhibited by propanil (0 – 1x10^{-4}) after an incubation period of 1 – 15 min

Thylakoid preparation Ch1

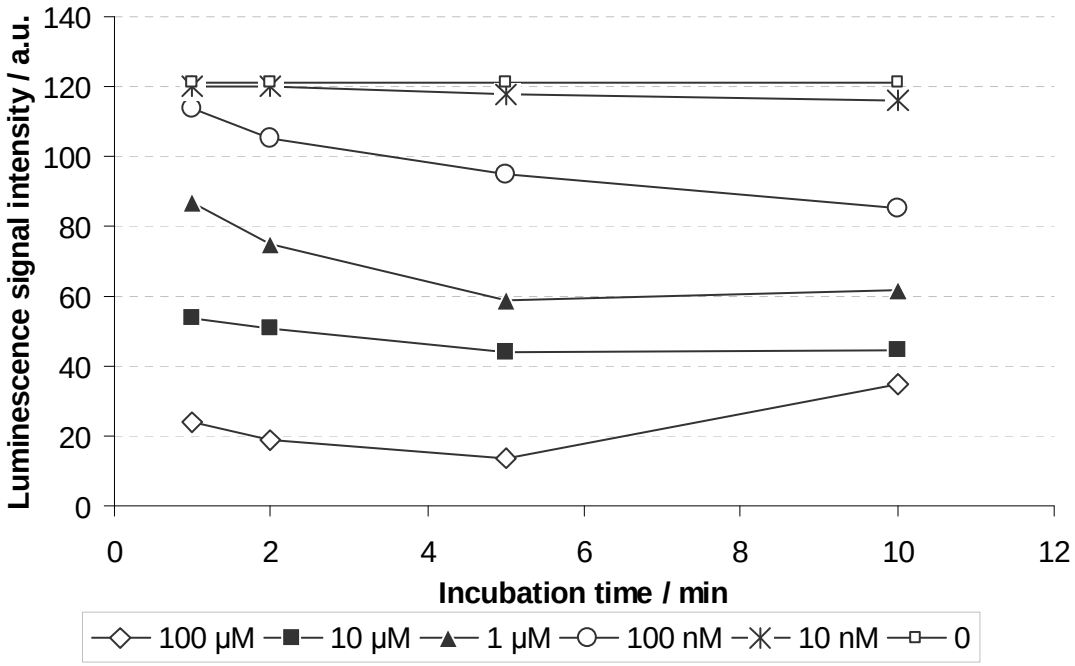

Thylakoid preparation Ch2

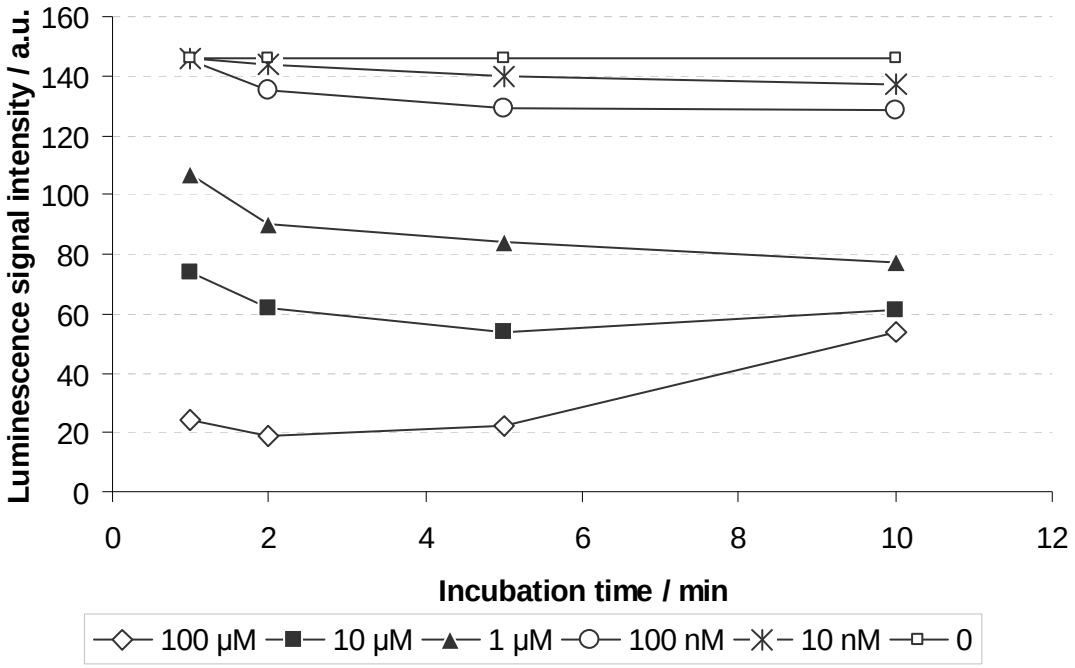

Thylakoid preparation Ch3

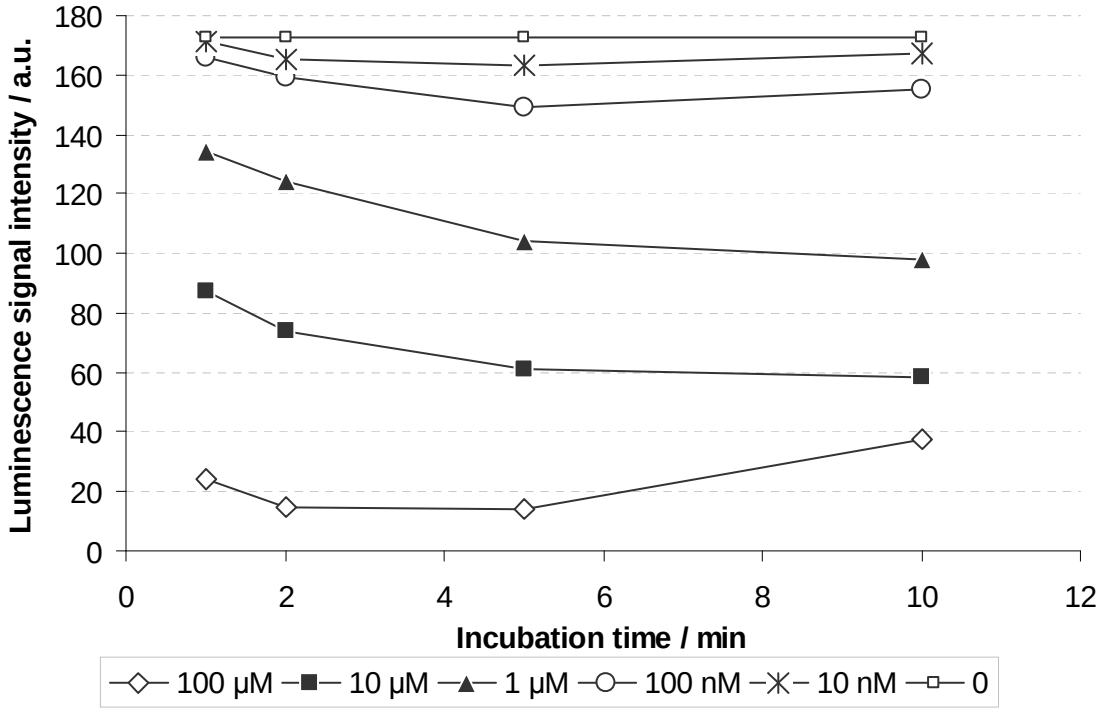

Thylakoid preparation Ch4

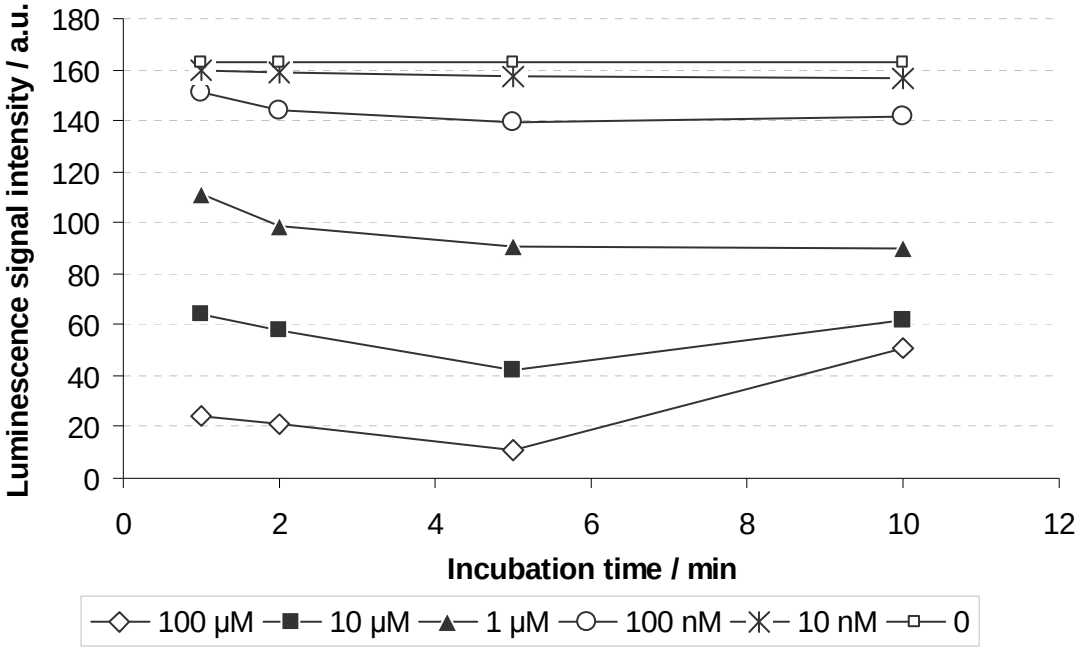

Thylakoid preparation Ch5

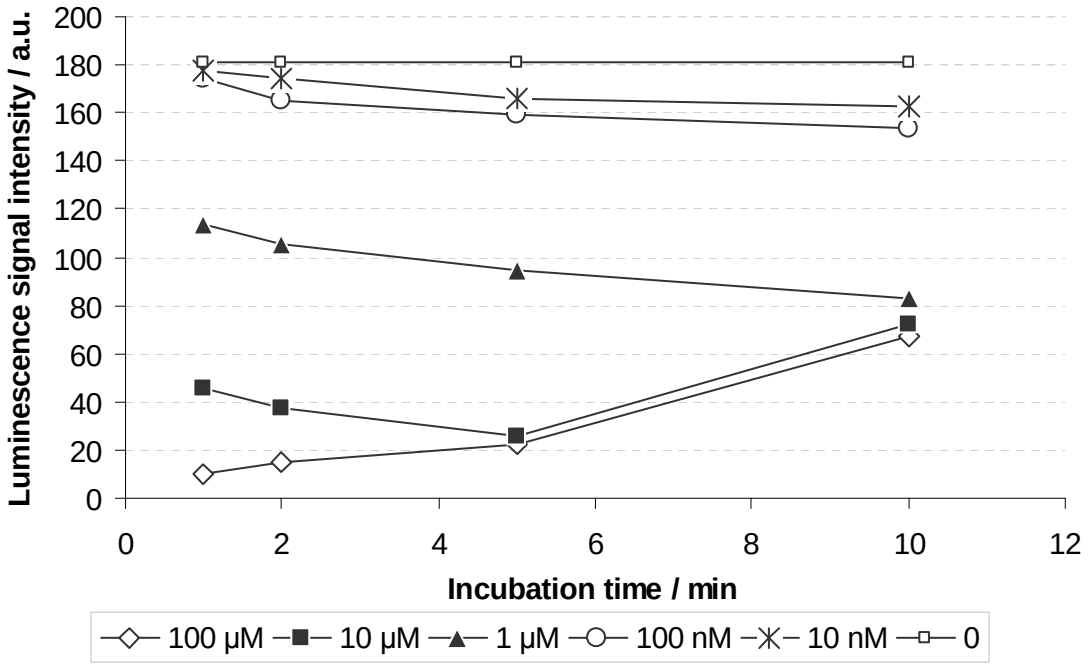

Appendix II. Drawings of the fluidic sensor unit blocks fabricated.

Not to scale.

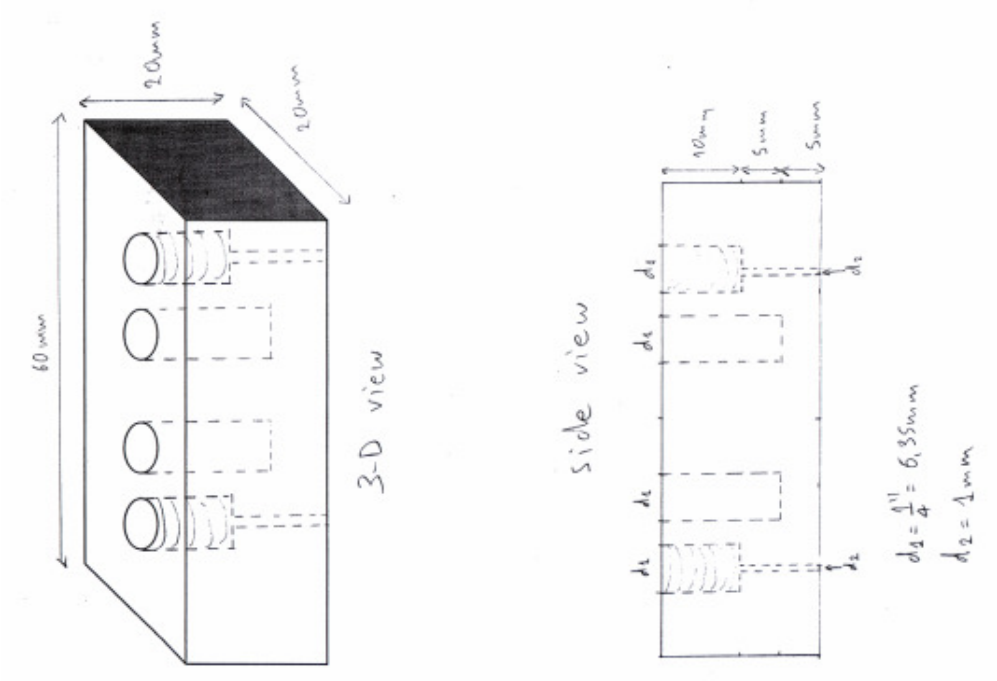

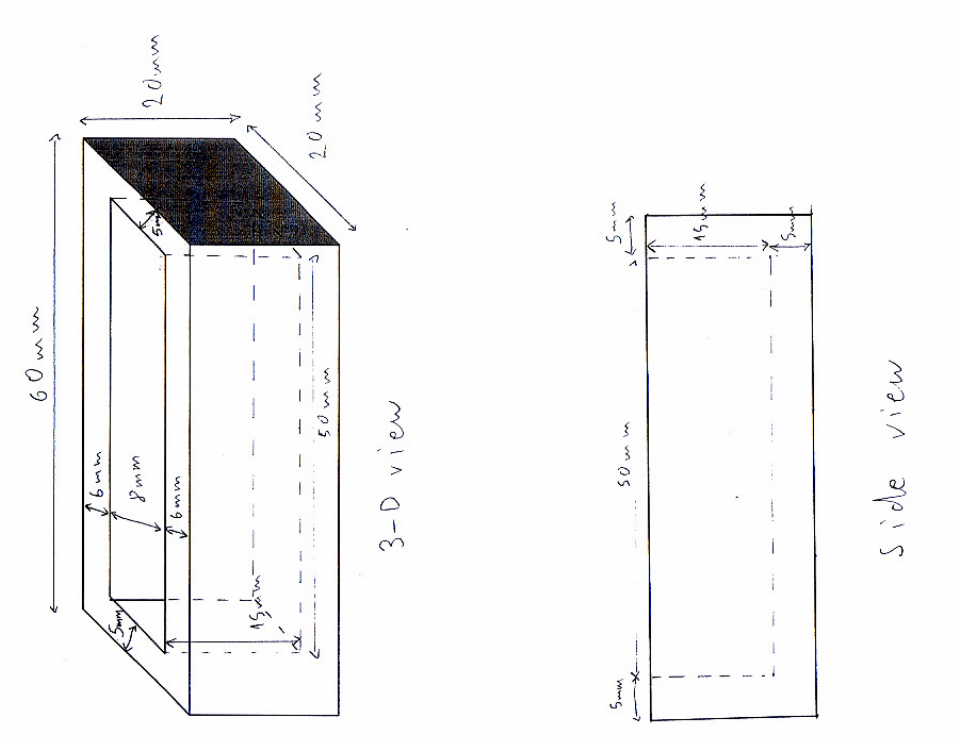

Appendix III. Immobilisation protocol from manufacturer of chosen carboxyl-terminated magnetic beads, used for the immobilisation of HRP.

1. Mix MagaBeads thoroughly by gently mixing and dispense desired quantity for activation in an appropriate sized container.

2. Wash the particles three times with 2 ml of MES buffer (50 mM, pH 6.1) each time, using a magnet to sediment particles between washes.

3. Adjust volume of particles to a 10 mg/ml concentration.

4. Add freshly prepared EDAC (200 μg/ml, of 50 mM MES, pH 6.1, 100 nmol per 1 mg of MagaBeads).

5. Mix gently for five minutes at room temperature.

6. Add 10 nmol of protein in MES buffer (pH 6.1) per 10 mg of MagaBeads.

7. Mix gently for two hours at room temperature.

8. Wash mixture four times with 2 ml of MES buffer each time, using a mag net to sediment particles between washes.

9. It is recommended the remaining active sites of the MagaBeads be blocked in a solution of 0.03% ethanolamine or glycine in MES buffer for thirty minutes at room temperature.

10. Wash the particles four times with 2 ml of MES buffer each time, using a magnet to sediment particles between washes.

11. Wash the particles two times with 2 ml of 0.1 M sodium acetate buffer (pH 4.0) each time, using a magnet to sediment particles between washes.

12. Finally, wash the particles three times with 2 ml of assay buffer of your choice before using.

Appendix IV. Immobilisation protocols from manufacturers of amine-terminated magnetic beads, used for the immobilisation of isolated thylakoids.

Protocol 1. Based on Data Sheet 546, Rev 2. (Bangs Laboratories Inc., USA)

Coupling Procedure for Attaching Proteins to Amine-terminated magnetic beads

Magn.Beads Activation

1. Transfer 10ml of Amine-terminated Magn.Beads (equivalent to 500mg of Magn.Beads) to a 50ml conical tube
2. Add Coupling Buffer to a final volume of 50ml, shake vigorously and magnetically separate perpendicular to gravity until the supernatant is clear (approximately 10 minutes). Aspirate the supernatant, leaving the Magn.Beads as a wet cake on the container wall.
3. Repeat Step 2 three times.
4. Add 20ml of 5% glutaraldehyde to the wet cake and shake vigorously.
5. Rotate at room temperature for 3 hours.
6. Magnetically separate perpendicular to gravity and aspirate the unreacted glutaraldehyde.
7. Repeat Step 2 four times.

Coupling of Protein

8. Add 25-100mg of protein to 10ml of Coupling Buffer.
9. Add the above protein solution to the glutaraldehyde-activated Magn.Beads from Step 7. Shake vigorously and rotate 16-24 hours at room temperature.
10. Magnetically separate and remove supernatant.
11. Add 50ml of Glycine Quenching Solution and shake vigorously. Rotate 30 minutes at room temperature.

Protocol 2. Based on Technotes 205 (Bangs Laboratories Inc., USA)

Immobilisation of thylakoids on aminated polystyrene beads

1. Take 250 µl of Amine-terminated beads (equivalent to 12.5 mg of beads) from your original 10 ml.
2. Add them to 5 ml wash buffer. Mix for 1 min.
3. centrifuge:
    a. Place aliquot of microspheres in appropriate centrifuge tube.
    b. Centrifuge the microspheres at G force 1,200 for 15 minutes to clear the supernatant.
    c. Remove and discard supernatant.
    d. Resuspend the microspheres in same buffer.

e. Sonicate with a sonic bath for 1 minute, or simply vortex with mixer

4. Repeat washing steps 2 more times.
5. At end of final (third) wash, don't resuspend in 5 ml of previous wash buffer, but in 5 ml of 10% Glutaraldehyde in wash buffer, ensuring that beads are completely suspended.
6. Rotate at room temperature for 2 hours (with Rotamixer)
7. Wash 3 times (as steps 2-3 above).
8. At the end of third wash, resuspend pellet in 3 ml coupling buffer appropriate for thylakoids cross-linking with glutaraldehyde.
9. Add the above protein solution to the glutaraldehyde-activated beads from step 8. Shake vigorously and rotate 2 hours at 4℃ temperature.
10. Centrifuge
11. Remove supernatant, and resuspend beads pellet in 5 ml of quenching / blocking solution (5 ml coupling buffer with 30-40 mM glycine with 0.05-1% (w/v) BSA), and mix gently for 30 minutes
12. Centrifuge, remove supernatant, and resuspend microsphere pellet in storage buffer to desired storage concentration (often 10 mg/ml).
    Wash buffer: MES
    Coupling buffer: Tricine (20mM), sucrose (70mM), pH 7.8

Protocol 3. From Technical data sheet 238G (Polysciences Inc., USA)

Procedure to prepare 8% Glutaraldehyde in PBS Solution

1. Pipette 10.0ml of Phosphate buffered saline (PBS) into bottle 2.
2. Using ampoule cracker, open 10ml ampoule of 25% Glutaraldehyde.
3. Pipette 5ml of 25% Glutaraldehyde into bottle 2.
4. Mix well, store at 4°C
   NOTE: Glutaraldehyde can be unstable at a pH of 7.4 and may slowly start to polymerize. Please inspect the 8% Glutaraldehyde, PBS solution prior to each use. If turbid or cloudy discard and prepare a fresh solution.

Procedure for Coupling

1. Place 0.5ml of a 2.5% aqueous suspension of beads in an Eppendorf centrifuge tube (1.5 -1.9ml capacity).
2. Add enough PBS (Component A) to fill the tube and cap tightly.
3. Centrifuge for 6 minutes in a microcentrifuge.
4. Remove supernatant carefully using a Pasteur pipette. Discard supernatant.
5. Resuspend pellet in PBS as follows:
   a). Fill tube halfway and cap tightly
   b). Vortex until pellet is completely dispersed
   c). Fill tube close to capacity and cap
   NOTE: When term "resuspend pellet" is used, refer to Step 5 above
6. Centrifuge for 6 minutes and discard supernatant.
7. Repeat steps 5 and 6 once.
8. Resuspend pellet in 0.5ml of 8% glutaraldehyde in PBS (Component B).
9. Mix for 4 to 6 hours at room temperature on a rocker table, rotary shaker, or any other kind of shaker which provides end-to end mixing.
10. Centrifuge for 6 minutes and discard supernatant.
11. Repeat Steps 5 and 6 twice.
12. Resuspend pellet in 1ml of PBS.
13. Add 200-400 micrograms of protein to be coupled.
14. Leave overnight at room temperature with gentle end-to-end mixing.
15. Centrifuge for 10 minutes. Using a Pasteur pipette, transfer the supernatant completely into a small graduated cylinder or graduated centrifuge tube. Note the volume of the supernatant and save it for protein determination.
    NOTE: If protein determination is done spectrophotometrically, make sure that the supernatant is completely free of turbidity. This can be achieved by centrifuging the supernatant for an additional 10 minutes. The amount of protein added in step 13 minus the amount in the supernatant represents the amount bound to the microparticles.
16. Resuspend pellet in 1ml of 0.2M ethanolamine (Component C) and mix gently for 30 minutes at room temperature. This step serves to block unreacted sites on the microparticles.
17. Centrifuge for 6 minutes and discard supernatant.
18. Resuspend pellet in 1 ml of BSA solution (Component D) and mix gently for 30 minutes and room temperature. The BSA will block any remaining nonspecific protein binding sites.
19. Centrifuge for 6 minutes and discard supernatant.
20. Resuspend pellet in 0.5ml to 1ml of storage buffer (Component E).

Appendix V. Identification and light emission details of the LEDs used for the illumination of thylakoids.

Project / thesis code	Manufacturer's individual or product series code	Manufacturer	Seller	Principal emission colour	Peak wavelength (nm)	Luminous intensity (mcd)	50% power / viewing angle (degrees)	Calculated Luminous flux (mlm)
1	TLRH160	Toshiba	RS	red	644	1800	10	43
2	TLYH262	Toshiba	RS	yellow	590	300	70	340
3	TLOH160	Toshiba	RS	orange	612	2300	10	55
4	L-7104QBC-D	Kingbright	RS	blue	470	1500	25	223
5	L-7104SYC-E	Kingbright	RS	yellow	595	800	34	220
6	L-7104SEC-H	Kingbright	RS	orange	630	3500	34	961
7	L-7104VGCK	Kingbright	RS	green	525	800	34	220
8	L934SRCG	Kingbright	RS	red	660	1400	50	824
9	L934SGC	Kingbright	RS	green	565	300	50	177
10	LURR3000G3	N/A	RS	red	660	1200	46	600
11	E1L55-3B0A2	Toyoda Gosei	Farnell	blue	475	1800	15	97
12	L-7113QBC-D	Kingbright	RS	blue	470	1200	15	64
13	TLSH157P	Toshiba	RS	red	623	2300	22	265
14	TLPGA158P	Toshiba	RS	green	562	100	30	21
15	TLYH180P	Toshiba	RS	yellow	590	8000	8	122
16	TLOH157P	Toshiba	RS	orange	612	2000	22	231
17	TLOH180P	Toshiba	RS	orange	612	7000	8	107
18	L-53MWC	Kingbright	Farnell	white	n/a	600	35	174

Project / thesis code	Manufacturer's individual or product series code	Manufacturer	Seller	Principal emission colour	Peak wavelength (nm)	Luminous intensity (mcd)	50% power / viewing angle (degrees)	Calculated Luminous flux (mlm)
19	L-53MWC	Kingbright	Farnell	white	n/a	850	20	81
20	L-53MWC	Kingbright	Farnell	white	n/a	450	30	96
21	NSPW500	MARL	Farnell	white	n/a	2800	25	417
22	NSPW500	MARL	Farnell	white	n/a	5600	20	534
23	L-793ID	Kingbright	Rapid	red	625	150	50	88
24	L-793SRC	Kingbright	Rapid	red	660	1600	40	606
25	L-793SRC	Kingbright	Rapid	red	660	2000	40	758
26	L-793SRC	Kingbright	Rapid	red	660	3000	40	1137
27	L-793SRC	Kingbright	Rapid	red	660	4500	40	1705
28	L-813SRC	Kingbright	Rapid	red	660	3000	20	286
29	L-813	Kingbright	Rapid	red	625	150	50	88
30	WT5111A	X-opto	Rapid	white	n/a	3000	15	161
31	UB5111A	X-opto	Rapid	blue	470	1200	15	64
32	L-7114QWC-D	Kingbright	Rapid	white	n/a	3200	20	305
33	L-1513SRC-F	Kingbright	Rapid	red	660	4500	20	430
34	L-53SRC-DV	Kingbright	Rapid	red	660	1500	30	321
35	L-53SRC-F	Kingbright	Rapid	red	660	4500	30	963
36	L-53SRD-H	Kingbright	Rapid	red	660	1500	60	1263
37	L-2523SURC-E	Kingbright	Rapid	red	640	2500	12	86
38	L-1613SURC-E	Kingbright	Rapid	red	640	2000	50	1177

Appendix VI. Pearson's correlation analysis performed on the different LED parameters and against the detected H_2O_2,

	peak wavelength (nm)	*luminous intensity (mcd)*	*luminous flux (mlm)*	*total light output (a.u.)*	*H_2O_2 signal*
peak wavelength (nm)	1				
luminous intensity (mcd)	0.870	1			
luminous flux (mlm)	-0.132	0.373	1		
total light output (a.u.)	-0.185	-0.463	-0.583	1	
H_2O_2 signal	-0.145	0.233	0.742	0.094	1

	peak wavelength (nm)	*luminous intensity (mcd)*	*luminous flux (mlm)*	*total light output (a.u.)*	*H_2O_2 signal*
Peak wavelength (nm)	1				
luminous intensity (mcd)	-0.940	1			
luminous flux (mlm)	-0.615	0.848	1		
total light output (a.u.)	-0.490	0.163	-0.385	1	
H_2O_2 signal	-0.997	0.964	0.675	0.420	1

	peak wavelength (nm)	*luminous intensity (mcd)*	*luminous flux (mlm)*	*total light output (a.u.)*	*H_2O_2 signal*
peak wavelength (nm)	1				
luminous intensity (mcd)	-0.449	1			
luminous flux (mlm)	-0.058	-0.866	1		
total light output (a.u.)	-0.167	0.956	-0.975	1	
H_2O_2 signal	-0.397	-0.642	0.939	-0.839	1

	peak wavelength (nm)	*luminous intensity (mcd)*	*luminous flux (mlm)*	*total light output (a.u.)*	*H_2O_2 signal*
peak wavelength (nm)	1				
luminous intensity (mcd)	#DIV/0!	1			
luminous flux (mlm)	#DIV/0!	-0.282	1		
total light output (a.u.)	#DIV/0!	0.838	0.288	1	
H_2O_2 signal	#DIV/0!	-0.514	-0.678	-0.899	1

	peak wavelength (nm)	*luminous intensity (mcd)*	*luminous flux (mlm)*	*total light output (a.u.)*	*H_2O_2 signal*
peak wavelength (nm)	1				
luminous intensity (mcd)	0.361	1			
luminous flux (mlm)	0.441	0.462	1		
total light output (a.u.)	0.006	0.146	0.287	1	
H_2O_2 signal	0.596	0.531	0.640	0.252	1

White	*peak wavelength (nm)*	*luminous intensity (mcd)*	*luminous flux (mlm)*	*total light output (a.u.)*	*H_2O_2 signal*
luminous intensity (mcd)		1			
luminous flux (mlm)		0.866	1		
total light output (a.u.)		0.820	0.671	1	
H_2O_2 signal		0.596	0.702	0.234	1

All - white	*peak wavelength (nm)*	*luminous intensity (mcd)*	*luminous flux (mlm)*	*Total light output (a.u.)*	*H_2O_2 signal*
peak wavelength (nm)	1				
luminous intensity (mcd)	0.244	1			
luminous flux (mlm)	0.519	0.207	1		
Total light output (a.u.)	-0.636	0.012	-0.190	1	
H_2O_2 signal	0.462	0.243	0.669	-0.086	1

All	*peak wavelength (nm)*	*luminous intensity (mcd)*	*luminous flux (mlm)*	*Total light output (a.u.)*	*H_2O_2 signal*
luminous intensity (mcd)		1			
luminous flux (mlm)		0.237	1		
Total light output (a.u.)		0.139	-0.157	1	
H_2O_2 signal		0.309	0.607	-0.010	1

Moderate correlation	Strong correlation	Very strong correlation

The correlation coefficient R was calculated using as paired (dependent and independent) variables all of the above four LED light quality parameters and the detected H_2O_2. This was performed for each group of LEDs according to their primary colour, as well as with all LEDs together. Two separate calculations were performed for all the LEDs together, one with the white LEDs included and one without. An R value between 0.5 – 0.699 was considered to be the result of moderate correlation, a value between 0.7 – 0.899 was considered to be pointing towards a strong correlation, and a value between 0.9 – 1.0 to be resulting from a very strong correlation.

Appendix VII. Step-by-step calculations of the environmental water matrix effect on the detection of herbicides, for river water sample 2 (calibration Step 4 onwards).

Firstly, calculations i. and ii. were performed on the water sample with no added herbicides.

Added 0 nM			
	Step 3 Chemiluminescence signal obtained	133.00	a.u.
Calculation i.	Step 1 Chemiluminescence signal obtained due to H_2O_2 present in water	7.90	a.u.
	Step 3 - step 1 = Chemiluminescence signal calculated, due to herbicide presence only	125.10	a.u.
Calculation ii.	Step 2 Effected matrix change (2.8%) = Chemiluminescence signal by which calculation i. result is under-reported	3.50	a.u.
	Adjusted for matrix under-reporting effect on H_2O_2 detection	128.60	a.u.
	Residual activity (compared to chemiluminescence signal of 124 a.u.)	103.71	%
	Equivalent amount of herbicides present	-0.25	nM

Then, the same set of calculations is performed on the water sample 2 with added 5 nM of 50-50% atrazine and diuron mixture.

added 5 nM			
	Step 3 Chemiluminescence signal obtained	101.00	a.u.
Calculation i.	Step 1 Chemiluminescence signal obtained due to H_2O_2 present in water	7.90	a.u.
	Step 3 - step 1 = Chemiluminescence signal calculated, due to herbicide presence only	93.10	a.u.
Calculation ii.	Step 2 Effected matrix change (2.8%) = Chemiluminescence signal by which calculation i. result is under-reported	2.60	a.u.
	Adjusted for matrix under-reporting effect on H_2O_2 detection	95.71	a.u.
	Achieved residual activity (compared to chemiluminescence signal of 124 a.u.)	77.20	%
	Equivalent amount of herbicides present	3.90	nM

The two 'equivalent amounts of herbicides present' are then used to calculate the matrix effect on the interaction of herbicides with the immobilised thylakoids.

added 5 nM			
	Herbicide concentration (known added+ calculated native)	4.75	nM
	Expected residual activity due to 4.75 nM (compared to chemiluminescence signal of 124 a.u.)	74.70	%
	Recovery (comparison of expected vs achieved residual activity)	103.35	%
	Effected matrix change	**3.35**	**%**

Therefore it has been calculated that the water sample matrix causes an over-reporting of the amount of herbicides present by 3.35%.

Finally, calculation iii. takes place on the original water sample with the unknown amount of herbicides.

added 0 nM			
Calculation iii	Chemiluminescence signal by which calculation ii. result is over-reported	4.31	a.u.
	True chemiluminescence signal	124.29	a.u.
	Equivalent amount of herbicides present	**0.00**	**nM**
	Amount of herbicide found by standard methods	**0.36**	**nM**

Talanta 77 (2008) 42–47

Contents lists available at ScienceDirect

Talanta

journal homepage: www.elsevier.com/locate/talanta

Development of a photosystem II-based optical microfluidic sensor for herbicide detection

Dimitrios G. Varsamis[a,*], Eleftherios Touloupakis[b], Pietro Morlacchi[c], Demetrios F. Ghanotakis[b], Maria Teresa Giardi[c], David C. Cullen[a]

[a] Cranfield Health, Cranfield University, Cranfield, Bedfordshire, MK43 0AL, UK
[b] Department of Chemistry, University of Crete, 71003 Voutes-Heraklion, Crete, Greece
[c] Institute of Crystallography, National Research Council (CNR), Via Salaria km 29.300, 00016 Monterotondo Scalo, Rome, Italy

ARTICLE INFO

Article history:
Received 26 November 2007
Received in revised form 27 May 2008
Accepted 29 May 2008
Available online 17 June 2008

Keywords:
Microfluidic
Herbicide
Photosynthesis
Environment
Chemiluminescence

ABSTRACT

Herbicides are highly toxic for both human and animal health. The increased application of herbicides in agriculture during the last decades has resulted in the contamination of both soil and water. Herbicides, under illumination, can inhibit photosystem II electron transfer. Photosynthetic membranes isolated from higher plants and photosynthetic micro-organisms, immobilized and stabilized, can serve as a biorecognition element for a biosensor. The inhibition of photosystem II causes a reduced photoinduced production of hydrogen peroxide, which can be measured by a chemiluminescence reaction with luminol and the enzyme horseradish peroxidase. In the present work, a compact and portable sensing device that combines the production and detection of hydrogen peroxide in a single flow assay is proposed for herbicide detection.

1. Introduction

The detection of environmental hazardous chemicals using sensor technology has been rising in demand [1–3]. Chemicals such as herbicides, fungicides and insecticides may exist in harmful levels and pose an environmental threat. Even low levels of contaminants can cause adverse effects on humans, plants, animals and ecosystems. The application of herbicides has increased appreciably during the past few decades, resulting in the massive pollution of water and soil. About 40% of herbicides (derivatives of phenylurea, triazine, diazine and phenolic types) that are currently in use inhibit the light reactions of photosynthesis (photosynthetic herbicides); usually by targeting photosystem II (PSII)-dependent electron flow [4].

At present, the modern methods of herbicide detection are HPLC, GC–MS and bioassays. These methods require expensive equipment, shipment of samples to the laboratories and highly qualified personnel for the analysis [5,6].

Photosystem II is a multisubunit complex located in the thylakoid membranes of algae, cyanobacteria and higher plants. It uses light energy to catalyze a series of electron transfer reactions resulting in the splitting of water into molecular oxygen and protons. Isolated thylakoid membranes produce the superoxide free radical ion and hydrogen peroxide as a product of the dismutation of O^{2-} [7]. This reaction is stimulated by autooxidizable electron acceptors of photosystem I and occurs in the presence of the natural electron acceptor system, ferredoxin and NADP, following the reduction of NADP [8].

Triazine, diazines, phenolic and urea herbicides are the ones with the highest effect on chloroplasts. These compounds inhibit photosynthetic process by binding to the D1 protein of photosystem II [9]. Photosynthetic herbicides block electron transport by the displacement of the bound plastoquinone called QB from its binding site on the D1 protein [10]. This protein is an essential part of the PSII reaction centre and together with the homologous protein D2 binds all the prosthetic groups involved in the main PSII electron transfer pathway [11,12].

Immobilized chloroplasts and thylakoids have been used to detect herbicides either by testing inhibition of the Hill reaction, inhibition of DCPIP photoreduction or change in chlorophyll fluorescence [2,13–16]. These observations have initiated interest in

Abbreviations: ABTS, 2,2′-azino-di-(3-ethyl benzthiazoline-6-sulphonic acid); CCD, charged coupled device; DCPIP, 2,6-dichlorophenolindolphenol; EDC, 1-ethyl-3-(3-dimethylaminopropyl) carbodiimide; HRP, horseradish peroxidase; LED, light emitting diode; LOD, limit of detection; MES, 2-morpholinoethanesulfonic acid; NADP, nicotinamide adenine dinucleotide phosphate; PBS, phosphate buffered saline; PTFE, polytetrafluoroethylene.

* Corresponding author. Tel.: +44 1234 758300.
E-mail address: d.g.varsamis.s02@Cranfield.ac.uk (D.G. Varsamis).

0039-9140/$ – see front matter © 2008 Elsevier B.V. All rights reserved.
doi:10.1016/j.talanta.2008.05.060

developing biological sensors to detect low levels of herbicides in water and soil using PSII.

Magnetic particles have been utilized extensively in diagnostics and other research applications for the capture of biomolecules and cells. Many assays and separations have been adapted to a magnetic bead format to take advantage of the benefits of microspheres and magnetic separation [17–21]. The most reported biosensing configurations based on beads are biosensors and bioreactors integrated into bead injection analytical systems [22–24].

In this study, we describe the production and preliminary characterization of an optical (chemiluminescence) PSII microfluidic sensing device for herbicide monitoring. The proposed detection principle is the chemiluminescence-based monitoring of the concentration of photosynthetically produced H_2O_2, which can be disrupted by herbicides.

The photosystem II complex and the HRP enzyme are immobilized on magnetic beads, which are in turn magnetically entrapped. The sensor unit is able to perform the assays and optically stimulate photosystem II within the unit and detect the HRP-catalyzed chemiluminescence of luminol/hydrogen peroxide. The system combines the production and detection of hydrogen peroxide in a single flow assay by combining all the individual steps in a compact and portable device.

2. Experimental

Polystyrene amino-magnetic beads (5% (w/v); 3.35 μm of diameter) were purchased from Spherotech Inc. (USA). The Carboxyl Terminated Beads (10% (w/v); 3.2 nm of diameter, made of polystyrene copolymer/iron oxide, 55:45) were from Europa Bioproducts (UK). All reagents are of analytical grade and were purchased from Sigma Chemical Co. All buffers were prepared using nanopure water.

2.1. Micro-system principles and design

The detection principle used in this system is chemiluminescence-based monitoring of the concentration of photosynthetically produced H_2O_2, which can be disrupted by herbicides. The sensor unit is able to perform the assays and optically stimulate photosystem II within the unit and detect the enzyme-mediated chemiluminescence of luminol/hydrogen peroxide. The sensor comprises of a short fluidic channel with two "active" regions including: (i) immobilized PSII and (ii) immobilized HRP to catalyze luminol/hydrogen peroxide chemiluminescence. Initial design consists of a flow channel constructed of machined Perspex sandwiching a laser-cut elastomer spacer/flow channel in which regions of appropriate reagents will be magnetically entrapped (Fig. 1).

The sensor consists of: (i) a pump in order to force the sample mixed with luminol through the sensor (after pre-concentration and sample "clean-up" if necessary), i.e. a simple flow-injection arrangement; (ii) a light source and delivery optics to illuminate the PSII region, an Agilent HMLP-C117 "high brightness LED" (peak wavelength 645 nm, with luminous intensity 300 mcd) and (iii) a suitable detector module and collection optics for the detection of chemiluminescence from the hydrogen peroxide detection region, e.g. a photomultiplier tube (PMT) or a staircase avalanche photodiode (SAPD) modules to detect luminescence of luminol at about 431 nm.

2.2. μ-Fluidic system fabrication

The micro-system was manufactured in-house at Cranfield University, following the design and principles described. The

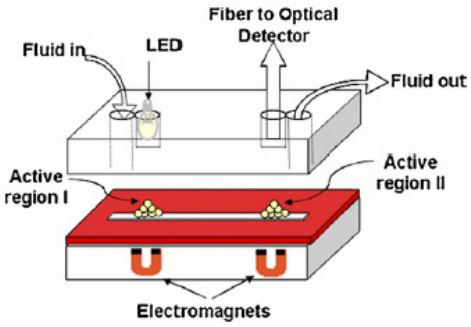

Fig. 1. Schematic representation of the micro-system, with the two Perspex blocks that sandwich the fluidic channel (in red) wide apart. The "active" regions are also shown, with the magnetic beads immobilized into the magnetic field of the magnets. (For interpretation of the references to color in this figure legend, the reader is referred to the web version of the article.)

sandwiching blocks were machined from Perspex (polymethylmethacrylate), while fluidic channels were made from silicon elastomer using a mask as well as black rubber. Each Perspex block has the following dimensions: $H \times W \times L = 20\,\text{mm} \times 20\,\text{mm} \times 60\,\text{mm}$.

The fluidic channel has a height of only 2 mm (for the silicone channel) and 0.3 mm (for the rubber channel). For the rubber fluidic channels, a CO_2 laser was used for cutting the structures, which allowed rapid prototyping of μ-fluidic gaskets/structures, coupled with increased accuracy compared to the silicone ones. Alternative channel structures were used in order to optimize capture and functional activity of HRP-coated magnetic beads. Currently, the fluidic channels are 300 μm thick and 1000 μm wide.

2.3. Particle-based biochemistry

The two "active" regions, PSII and HRP, which are actually non-permanent, are immobilized on magnetic beads, which are in turn immobilized (magnetically) on the "active" regions. The unit was designed taking into consideration all the steps of detection in advance. A protocol of the steps includes the following.

Beads with attached HRP enter the fluidic channel, and are immobilized by magnetic forces on the region II. Beads with attached PSII enter the fluidic channel, and are immobilized by magnetic forces on the region I. A water sample (pre-mixed with luminol) enters the fluidic channel, and is illuminated, on the region I. The sample with H_2O_2 produced by PSII flows towards region II, where the chemiluminescence reaction takes place, and the light produced is, through the optical fiber, detected by the detector. The removal of the magnetic forces and the flow of buffer/water result in the removal of the beads, and the sensor can be used again.

2.4. Luminol chemiluminescence batch H_2O_2

Different concentrations of luminol and HRP were added to 1 ml polystyrene cuvettes, and were placed in the detection region of the spectrophotometer. A sample of Tris–HCl buffer, 10 mM, pH 8.5 with various H_2O_2 concentrations was manually pipetted. To ensure that the crucial first few seconds of the reaction were monitored, the recording of light was started before the addition of the sample, while the ambient light was maintained at the minimum possible.

The chemiluminescence was transduced to an electric signal by a portable SD2000 CCD luminometer (Ocean Optics, Netherlands) or a bench-top VARIAN spectrophotometer. The chemiluminescence intensity profiles were recorded and the maximum intensity was used to plot the graphs.

For samples of thylakoids producing H_2O_2, the procedure was similar. Aliquots of thylakoid membranes were diluted accordingly with Tris–HCl buffer, 10 mM, pH 8.5 and introduced in a glass pipette by aspiration. The glass pipette was then illuminated. Luminol (30 mM), HRP (150 U ml^{-1}) and H_2O_2 (30 μM–3 M) were prepared freshly in Tris–HCl buffer, 10 mM, pH 8.5, and were pipetted in a polystyrene cuvette, that was placed in the appropriate location in or next to the light-reading apparatus. Once the illumination of the glass pipette containing the thylakoids was terminated, its contents were rapidly transferred into the cuvette, to allow instantaneous mixing. The reaction of the H_2O_2, produced by the thylakoids during the illumination, with luminol and the HRP, resulted in the characteristic light which is the product of this reaction. The light-reading apparatus was used to measure the light produced from the very start of this process.

2.5. Immobilization of HRP on magnetic beads

For the immobilization of HRP on the beads, a protocol supplied by Cortex Biochemicals was used (http://www.cortexbiotech.com), with some modifications. One milliliter of MagaBeads-Carboxyl Terminated was washed twice in 10 ml of MES buffer (50 mM, pH 6.1). Volume of particles was adjusted to a 10 mg ml^{-1} concentration. Then a same volume of EDC (100 nM) was added and allowed to react for 15 min at room temperature with continuous mixing. The microsphere particles were washed twice in phosphate–citrate buffer and resuspended in 5 ml of the same buffer. Five milliliters of HRP (1 nM) were added and allowed to react at room temperature for 2 h with constant mixing. The remaining active sites of the MagaBeads were blocked in a solution of 0.03% (w/v) glycine in MES buffer for 30 min at room temperature. The particles were washed four times with 2 ml of MES buffer each time, using a magnet to sediment particles. After a final washing with 2 ml sodium acetate buffer, 0.1 M, pH 4.0, the microspheres were ready to use.

Two types of HRP were used such as HRP-1 (type II, 148 U mg^{-1}) and HRP-2 (type VI, a highly purified and stabilized, 300 U mg^{-1}). EDC (100 nM), HRP (1 nM), glycine (0.03%, w/v) were prepared just before each immobilization assay, in MES buffer, 50 mM, pH 6.1. HRP-1 and HRP-2 were purchased from Sigma Chemical Co.

For the HRP activity assay, one tablet of ABTS was dissolved in 100 ml of 50 mM phosphate–citrate buffer and 25 μl of 30% H_2O_2 was added. One hundred microliters of ABTS–H_2O_2 were added to 100 μl of sample in each well of a white microtitre plate with a clear bottom. Immediately after initiation of the reaction, absorbance at 405 nm was measured every 10 min.

2.6. Flow assay for hydrogen peroxide with HRP immobilized on magnetic beads

The flow system (Fig. 1) consisted of one peristaltic pump, delivering a 10 mM luminol and a H_2O_2 sample pre-mixed at a continuous flow rate of 2.5 ml min^{-1}. Luminol and H_2O_2 were freshly prepared every day in Tris–HCl buffer, 10 mM, pH 8.5. PTFE tubing (0.8 mm i.d.) was used to connect the flow system components. Firstly, the beads (1 mg) were flown in the flow system by a peristaltic pump. A permanent magnet was used to attract the beads as they were flowing, thus immobilizing them in a specific area of the channel, underneath the area "viewed" by the optical fiber (50 μm of diameter, for detection in wavelength: 200–800 nm) (Avantes, Netherlands). The magnet was not moved during the experiment, in order to ensure that the beads were not carried away by the continuing flow. The reaction was initiated once the pre-mixed luminol–H_2O_2 reached the area of the flow channel that was covered with the beads. The chemiluminescence was transduced to an electric signal by a SD2000 portable CCD luminometer (Ocean Optics, Netherlands). The chemiluminescence intensity profiles were recorded and the maximum intensity was used to plot the graphs.

2.7. Thylakoid membranes isolation protocol

Thylakoid membranes were isolated from fresh spinach leaves (*Spinacea oleracea* L.) using the procedure described by Touloupakis et al. [15]. One hundred grams of leaves were washed with distilled water, dried on filter paper and homogenized in 200 ml of extraction buffer containing 20 mM Tricine, pH 7.8, 300 mM sucrose, 5 mM $MgCl_2$, 1 mM EDTA and 0.2% (w/v) bovine serum albumin (BSA). The homogenate was filtered through six layers of cheesecloth and centrifugated at 7500 × *g* for 20 min. The pellet was suspended in a buffer containing 50 mM Tricine, pH 7.8, 70 mM sucrose, 5 mM $MgCl_2$ and centrifugated at 7500 × *g* for 20 min. Finally, the obtained pellet (thylakoid membranes) was resuspended in a buffer containing 50 mM Tricine, pH 7.8, 70 mM sucrose and 5 mM $MgCl_2$. Aliquots at [Chl] = 3 mg ml^{-1} were placed in Eppendorf tubes and kept at −80 °C. The total chlorophyll content was calculated according to Porra [25].

2.8. Immobilization of thylakoid membranes on magnetic, amine polystyrene beads

Five hundred microliters of water suspension of magnetic aminopolystyrene beads (5%, w/v) were washed with 1.0 ml of PBS buffer (KH_2PO_4 1.8 mM, KCl 7 mM, NaCl 15 mM, Na_2HPO_4 10 mM, pH 7.2) for three times. The pellet was suspended in 1.0 ml of a glutaraldehyde solution (glutaraldehyde dissolved in PBS buffer to a final concentration of 10% (w/v)). The reaction was carried out with continuous mixing at 30 °C for 24 h. The microsphere suspension was washed three times with 1.0 ml of PBS buffer to remove the excess of glutaraldehyde. Pellet was resuspended in 0.5 ml of 15 mM MES, pH 6.5 (wash/coupling buffer). Then, 200 μl of thylakoid membranes ([chlorophyll] = 2.75 mg ml^{-1}) and 300 μl of 15 mM MES, pH 6.5, 70 mM sucrose, 5 mM $MgCl_2$ were added at 4 °C in the dark. To allow the coupling between the thylakoids and glutaraldehyde, the heterogeneous reaction was carried out at 4 °C for 2 h under continuous mixing. Finally, 100 μl of BSA (quenching solution) was added to 400 μl of immobilized thylakoids. The beads were washed three times with 1.0 ml of PBS buffer in order to remove the excess glutaraldehyde.

2.9. Fluorescence efficiency

The stability of the photosynthetic material, before and after immobilization in beads, was tested by measuring changes in fluorescence yield with a 650 nm light every 10 min after a dark period. Under exciting light, the fluorescence yield rapidly rises and then slowly decreases. The F_v/F_m ($F_m - F_0)/F_m$ parameter is the maximum quantum yield of PSII and reflects the potential quantum efficiency of PSII as a sensitive indicator of plant photosynthetic performance [26]. All fluorescence measurements were performed by using the Plant Efficiency Analyser (Hansatech Instruments Ltd., UK) at room temperature.

3. Results and discussion

3.1. Chemiluminescence batch assay for H_2O_2 produced by thylakoid membranes

Luminescent signal is seen with illuminated thylakoid membrane preparations. The signal is proportional to the light intensity

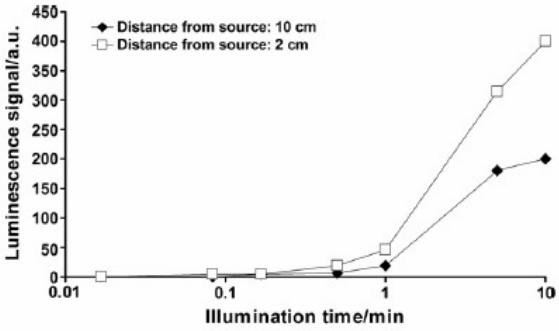

Fig. 2. Light produced by the chemiluminescence reaction of light-induced hydrogen peroxide from thylakoids illuminated for different times and distances. [HRP] = 20 U ml^{-1}, [luminol] = 100 μM, [chlorophyll] = 3.15 mg ml^{-1} with bench-top detector, at pH 8.5.

and duration. The effect of illumination time and distance on luminescence emission is shown in Fig. 2. The same signal is absent in the presence of DCPIP, hydroquinone or catalase, all of which act as either hydrogen peroxide inhibitors or mediators of the electron transport in the photosynthetic cycle. The presence of the latter group of additives means that the electrons never reach the hydrogen peroxide producing complex of the thylakoid, therefore, inhibiting any signal. At the same time, H_2O_2 spiked samples, i.e. thylakoid samples illuminated normally with added known hydrogen peroxide concentrations, give an additive luminescence response, suggesting that the hydrogen peroxide is not consumed by a catalase-type activity in the thylakoid preparation.

Both atrazine and diuron herbicides cause concentration-dependent inhibition of the chemiluminescent signal, and hence the H_2O_2 production by illuminated thylakoids (Fig. 3). The limits of detection (LODs) for these herbicides are: 3.0E−08 for atrazine and 1.0E−08 for diuron. An example of individual luminescence assay for diuron can be seen in Fig. 4.

3.2. Chemiluminescence batch assay for H_2O_2

For the detection of H_2O_2, four concentrations of luminol (10 mM, 1 mM, 100 μM and 50 μM) and four concentrations of HRP (50 U ml^{-1}, 10 U ml^{-1}, 5 U ml^{-1} and 1 U ml^{-1}) were tested in all possible combinations. At higher concentrations of H_2O_2 (mM

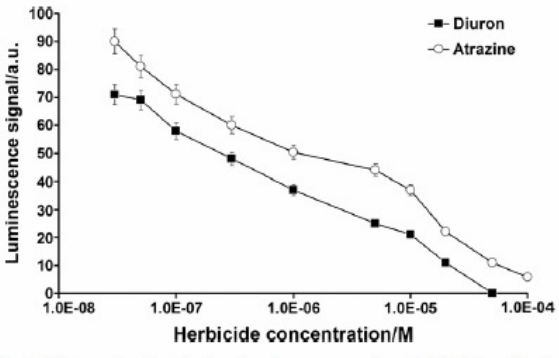

Fig. 3. Light produced by the chemiluminescence reaction of light-induced hydrogen peroxide from illuminated thylakoids in the presence of diuron or atrazine, with [HRP] = 20 U ml^{-1}, [luminol] = 100 μM, [chlorophyll] = 3.15 mg ml^{-1} with bench-top detector, at pH 8.5.

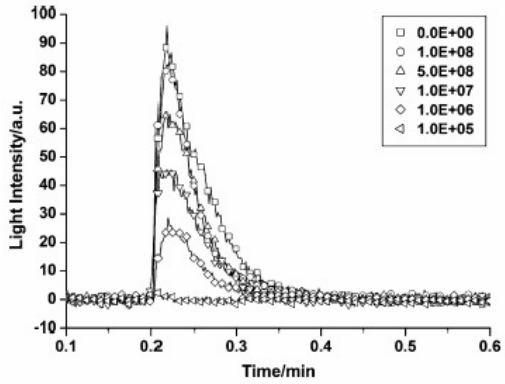

Fig. 4. Light produced by the chemiluminescence reaction of light-induced hydrogen peroxide from illuminated thylakoids in the presence of diuron, with [HRP] = 20 U ml^{-1}, [luminol] = 100 μM, [chlorophyll] = 3.15 mg ml^{-1} with bench-top detector, at pH 8.5.

region), the reaction acts like a typical "glow-type" chemiluminescence reaction expanding over minutes. At concentrations lower than micromolar, the result is typically a flash for less than 1 s. Having identified the peak light production of luminol at 431 nm, measurements of light intensity over time were performed, at a wavelength of 431 ± 20 nm. Such a large "window" was chosen in order to allow the maximum detectable light and, as the reaction is performed in the dark, any light detected would only be from the chemiluminescence reaction.

Calibration curves for all the previously mentioned combinations were plotted, and the LODs were calculated as 5σ values. Calibration curves were obtained for both the maximal light output and the integrated light output (data not shown). Among all the calibrations, the most sensitive detection was in the sample employing luminol 100 μM and HRP 5 U ml^{-1}, with an LOD: 1.34E−06 (data not shown).

3.3. Immobilization of thylakoid membranes on magnetic beads

Thylakoid membranes were immobilized on magnetic beads. Activity of immobilized thylakoid membranes was determined by fluorescence induction analysis. The F_v/F_m parameter represents the maximum quantum yield of PSII. The F_v/F_m parameter of the photosynthetic material, before the immobilization in beads, was 0.7. At 25 °C the observed half-life of thylakoid membranes activity was 53 h (Fig. 5). The data in Fig. 5 represent the average of three experiments with a relative standard devi-

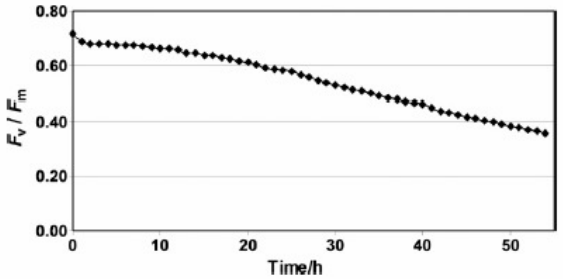

Fig. 5. Fluorescence induction analysis of immobilized thylakoid membranes on magnetic beads. Activity is monitored as F_v/F_m ratio in function of time in storage in the dark at 25 °C.

ation of 6.67. From a chlorophyll calculation it was found that the amount of the immobilized photosynthetic material was 0.3 μg (chlorophyll) mg^{-1} beads.

3.4. Immobilization of HRP on magnetic carboxyl-modified beads

HRP (HRP-1 and HRP-2) were immobilized in active form on magnetic carboxyl-modified beads. The amount necessary to achieve a complete activation of all the carboxyl groups on the beads was 100 nmol of EDC per 1 mg of beads. The optimized immobilization protocol included several washing steps (especially between the EDC and the HRP incubations) and different washing buffers. A step of washing the beads with sodium acetate buffer, 0.1 M, pH 4.0, after the HRP immobilization was included. To evaluate the effect of this, two different routes were taken, one with and one without the sodium acetate buffer washes. It should be noted that, for experimental integrity, the beads that were not washed with sodium acetate were instead washed with MES buffer, which was the buffer used for the washes throughout the experiment, thus bringing the total washes of the two routes to the same number. After the different washing steps, both bead lots were washed three times with the buffer of choice, in this case phosphate–citrate, which was the one favored by the ABTS assay protocol. The beads with the sodium acetate washes had slightly lower HRP activity than the ones washed only with MES. More specific, the rate of activity was lower for the sodium acetate (0.132 OD min^{-1}) compared to the MES buffer (0.150 OD min^{-1}) although the overall substrate conversion at the end of 10 min of the two bead lots was the same (data not shown). Throughout the immobilization procedure, all the in-between washes were also assayed with ABTS, in order to ensure that the multiple washing steps were actually washing out any excess of unbound HRP, and that the final product did not have any residual free HRP (data not shown).

Initially, an HRP with a lower hemin content and therefore activity was used (HRP-1). This HRP-1 was more prone to deactivation in various environments. A different HRP was then used (HRP-2) which is further purified and chemically stabilized to protect the primary amines and to maintain activity at low pH and higher temperature. Using HRP-1, 1 mg of beads had HRP activity equal to 0.1 purpurogallin units according to the ABTS assay (1 unit will oxidize 1 μmol of ABTS per minute at 25 °C, pH 5.0). With HRP-2, 1 mg of beads had activity equal to 0.375 units. A final alteration of the protocol was the washing out of the excess EDC, before the HRP was incubated with the beads. That was performed by following the protocol suggested by Mueller, whereby the excess unbound EDC would bind to HRP that would otherwise be immobilized to the beads [27]. The results with this alteration showed a dramatic increase in activity; 1 mg of beads had 1.2 units. According to the marked difference in the resulting activities between the two HRPs, as indicated by the ABTS assay, only HRP-2 was used in all the experiments shown either in free-form or immobilized.

The theoretical maximum number of HRP molecules bound to a bead can be calculated assuming a monolayer cubic close packing of HRP on the bead surface. The "monolayer coating" assumption is reasonable since the formation of a multilayer enzyme coating may take place, in fact, as a consequence of protein crosslinking. This requires the activation of the carboxyl groups of the enzyme; with the coating chemistry employed here however, only the carboxyl groups of the beads are activated, minimizing the possibility of a multilayer. In the case of the 3.2 μm of diameter beads, with the spherical diameter of HRP to be 4.6 nm, the theoretical maximum value of 441.67×10^3 HRP molecules per bead is obtained [28]. From further calculations, it was found that the amount needed for a monolayer for 3×10^9 beads, which is the amount of beads in 1 mg, would be 88 μg HRP, which is double the amount suggested by the protocol and used through the experiments. As for the immobilization experiments only half the amount of HRP was used, thus it can be assumed that only a partial monolayer has been achieved.

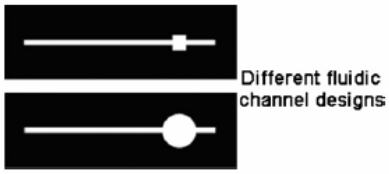

Fig. 6. The rubber channels employed in the experiments. The region used for the entrapment of the magnetic beads is the circular area (channel B) and the rectangular area (channel A).

Different storage buffers were also tested. The activity of free HRP prepared and stored for 1 week was greatly reduced while the activity of HRP immobilized on beads irrespective of the used buffer as a storage medium remained roughly unchanged.The activity of free HRP prepared and stored for 1 week

3.5. Flow assay for hydrogen peroxide with HRP immobilized on magnetic beads

Beads with immobilized HRP were magnetically entrapped in the fluidic device, in order to perform the H_2O_2 assay with luminol pre-mixed with the sample in flow. The light produced was detected with a portable detector.

Samples of different H_2O_2 and luminol concentrations were premixed just prior to the experiments with a T-mixer. Two different fluidic channels were used for the experiments, as shown in Fig. 6. The circular area of channel B is the area covered by the beads, and attracted by the magnet (area = 200 mm^2). For flow channel A, the rectangular area, 16 mm^2 covered by beads was smaller. In both cases 1 mg of beads was used, so the only difference was in the spreading of the beads and not the actual amount of HRP.

The light produced by the reaction was measured and the results are shown in Fig. 7. The channel B, allowing the beads to spread over a larger surface area, allowing for more HRP to be employed in the reaction, gave an increased response, as well as a lower LOD of 100 μM, compared to channel A, that had the beads stacked on a smaller area, as the HRP on the beads was not fully used, as a lot of the beads were covered by others, not allowing the luminol–H_2O_2 to reach them. Therefore, the key to the maximization of the possible chemical interaction between the H_2O_2, luminol and HRP lied in the ability to spread out the HRP bound on the beads in a two-dimensional plane.

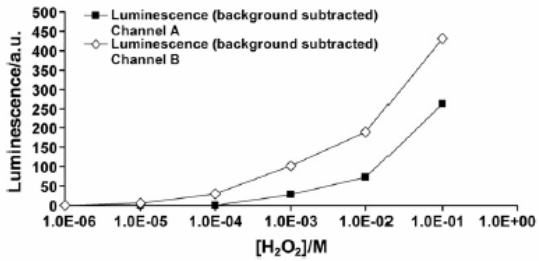

Fig. 7. Light output from different concentrations of H_2O_2. [luminol] = 10 mM at pH 8.5, with buffer 100 mM Tris–HCl. The HRP was immobilized on beads and 1 mg of beads were accommodated in two different channels. In channel A the beads were immobilized on area of 16 mm^2, in channel B they employed a surface area of 200 mm^2.

4. Conclusions

There is a growing interest for the generation of rapid, inexpensive assays to screen for the presence of herbicides. In this work, we have developed photosystem II-based optical microfluidic sensor for herbicide detection. The sensor is easy to handle and sensitive enough to provide preliminary environmental analysis screening the samples that require more detailed laboratory analyses.

The production of hydrogen peroxide by thylakoid membranes extracted from higher plants was investigated and detected under illumination with concentrations increasing in a time- and light intensity-dependent manner. The presence of herbicides in the thylakoid samples reduces the hydrogen peroxide measured in a concentration-dependent manner.

Thylakoid membranes and HRP were immobilized on magnetic beads, which were in turn magnetically immobilized in the device. The luminol–HRP–H_2O_2 chemiluminescence reaction was investigated in respect to H_2O_2 as the reactant of interest, and a calibration curve was obtained.

The integration of the two-step reaction has been achieved by designing and constructing a microfluidic device, which consists of a flow channel constructed of machined Perspex sandwiching a laser-cut elastomer spacer/flow channel in which regions of appropriate reagents are immobilized.

The sensor unit is able to perform the herbicide assays; optically stimulate photosystem II within the unit and detect the HRP-catalyzed chemiluminescence of luminol/hydrogen peroxide, which can be disrupted by herbicides.

The large number of approved active ingredients in agriculture (approximately 600 chemicals) makes difficult to obtain accurate and actual information on herbicide application in different countries. The real samples are present in a complex mixture containing active ingredients and their metabolites [29]. Our preliminary results indicate that use of real water matrix (control not containing herbicides) does not inhibit PSII activity and in some cases can induce an activation by 5–21% measured as oxygen evolution (data not shown). Therefore, the developed biosensor can be applied in real samples and better reflect the real physiological impact of active compounds because even low concentrations of pollutants affect living organisms by altering physiological processes. A deep study on real samples is in progress and will be presented in a future publication.

Acknowledgments

This work was supported by the EU Contract No. QLK3-CT-2001-01629 and by MIUR project.

References

[1] M.T. Giardi, E. Piletska (Eds.), Biotechnological Applications of Photosynthetic Proteins: Biochips, Biosensors and Biodevices, Landes Bioscience Springer, 2006.
[2] M.T. Giardi, L. Guzzella, P. Euzet, R. Rouillon, D. Esposito, Environ. Sci. Technol. 39 (2005) 5378.
[3] J.H. Lee, R.J. Mitchell, B.C. Kim, D.C. Cullen, M.B. Gu, Biosens. Bioelectron. 21 (2005) 500.
[4] C.B. Vicentini, D. Mares, A. Tartari, M. Manfrini, G. Forlani, J. Agric. Food Chem. 52 (2004) 1898.
[5] V. Pacakova, K. Stulik, J. Jiskra, J. Chromatogr. A 754 (1996) 17.
[6] R.J. Bushway, L.B. Perkin, L. Fukal, R.O. Harrison, B.S. Ferguson, Arch. Environ. Contam. Toxicol. 21 (1991) 365.
[7] C. Danna, C. Bartoli, F. Sacco, L. Ingala, G.E. Santa-Maria, J.J. Guiamet, R.A. Ugalde, Plant Physiol. 132 (2003) 2116.
[8] V. Klimov, G. Ananyev, O. Zastryzhnaya, T. Wydrzynski, G. Renger, Photosynth. Res. 38 (1993) 409.
[9] D.E. Moreland, Z. Naturforsch. 48c (1992) 121.
[10] K. Pfister, K.K. Steinback, G. Gardner, C.J. Arntzen, Proc. Natl. Acad. Sci. U.S.A. 78 (1981) 981.
[11] I.S. Booij-James, W.M. Swegle, M. Edelman, A.K. Mattoo, Plant Physiol. 130 (2002) 2069.
[12] M.T. Giardi, E. Pace, Trends Biotechnol. 23 (2005) 257.
[13] M. Koblitzek, J. Maly, J. Masojidek, J. Komenda, T. Kucera, M.T. Giardi, A.K. Mattoo, R. Pilloton, Biotechnol. Bioeng. 78 (2002) 110.
[14] D. Laberge, R. Rouillon, R. Carpentier, Enzyme Microb. Technol. 26 (2000) 332.
[15] E. Touloupakis, L. Giannoudi, S.A. Piletsky, L. Guzzella, F. Pozzoni, M.T. Giardi, Biosens. Bioelectron. 20 (2005) 1984.
[16] D. Merz, M. Geyer, D.A. Moss, H.J. Ache, Fresen. J. Anal. Chem. 354 (1996) 299.
[17] M. Gijs, Microfluid. Nanofluid. 1 (2004) 22.
[18] R.J.S. Derks, A. Dietzel, R. Wimberger-Friedl, M.W.J. Prins, Microfluid. Nanofluid. 3 (2007) 141.
[19] J.W. Choi, K.W. Oh, J.H. Thomas, W.R. Heineman, H.B. Halsall, J.H. Nevin, A.J. Helmicki, H.T. Henderson, C.H. Ahn, Lab Chip 2 (2002) 27.
[20] C. Elkin, H. Kapur, T. Smith, D. Humphries, M. Pollard, N. Hammon, T. Hawkins, Biotechniques 32 (2002) 1296.
[21] G.P. Hatch, R.E. Stelter, J. Magn. Magn. Mater. 225 (2001) 262.
[22] M. Mayer, J. Ruzicka, Anal. Chem. 68 (1996) 3808.
[23] A. Guënther, U. Bilitewski, Anal. Chim. Acta 300 (1995) 117.
[24] A.R. Varlan, J. Suls, P. Jacobs, W. Sansen, Biosens. Bioelectron. 10 (1995) 15.
[25] R. Porra, J. Photosynth. Res. 73 (2002) 149.
[26] K. Maxwell, G.N. Johnson, J. Exp. Bot. 51 (2000) 659.
[27] S. Mueller, Free Radical Biol. Med. 29 (2000) 410.
[28] T. Deng, G.M. Whitesides, M. Radhakrishnan, G. Zabow, M. Prentiss, Appl. Phys. Lett. 78 (2001) 1775.
[29] L. Guzzella, F. Pozzoni, G. Giuliano, Environ. Pollut. 142 (2006) 344.